

NEW MACROCYCLIC GLYCOPEPTIDE ANTIBIOTIC FOR CHIRAL HPLC STATIONARY
PHASES AND IONIC LIQUIDS IN ANALYTICAL CHEMISTRY

by

XIAOTONG ZHANG

Presented to the Faculty of the Graduate School of
The University of Texas at Arlington in Partial Fulfillment
of the Requirements
for the Degree of

DOCTOR OF PHILOSOPHY

THE UNIVERSITY OF TEXAS AT ARLINGTON

May 2011

Copyright © by Xiaotong Zhang 2011

All Rights Reserved

ACKNOWLEDGEMENTS

I would like to thank Dr Daniel W. Armstrong, my research supervisor, for his excellent guidance, valuable advice, and mentoring over the past five years. Without his kind acceptance of me to his group, I would not have had such a happy and fruitful PhD career. I was always inspired by his passion for scientific research.

I also want to thank Dr. Lovely and Dr. Dias for their help and service on my committee. It has been a great honor to have you serve on my committee.

I need to thank my fellow group members Junmin, Xinxin, BaoYe, Chunlei, Ping, Renee, Violet, Koko, Zach, Eranda, Sophie, Qing, Yasith, Sarantha, Jonathon, Edra, Eva, Nilusha, Tharanga, Dilani, Aruna, for their help and friendship. Special thanks to Barbara, who took care of chemical orders and paper work for me over these years.

Finally, I would like to thank my wonderful parents and my grandma for their unconditional support. I also want to express my special gratefulness to Lulu and Nina for their support and care to me as well. I regret that I could not spend much time with those who love me.

April 13, 2011

ABSTRACT

NEW MACROCYCLIC GLYCOPEPTIDE ANTIBIOTIC FOR CHIRAL HPLC STATIONARY PHASES AND IONIC LIQUIDS IN ANALYTICAL CHEMISTRY

Xiaotong Zhang, PhD

The University of Texas at Arlington, 2011

Supervising Professor: Daniel W. Armstrong

The main focus of this dissertation is on the development of new chiral stationary phases for HPLC and GC and the application of ionic liquids in analytical chemistry. They will be discussed separately in two parts.

Enantiomeric separations continue to be of great interest to the pharmaceutical industry. It is because drug molecules of opposite chirality often possess distinctive effects in biological environments. Direct chromatography is one of the major techniques used to address the challenge of enantiomeric analysis. Macrocyclic glycopeptides are a very useful class of chiral selectors for HPLC stationary phases because of their broad enantioselectivity. A study of a new macrocyclic glycopeptide antibiotic, dalbavancin, as chiral selector for HPLC will be described in part one. Two stationary phases based on dalbavancin were synthesized via two different binding strategies and compared against with commercial teicoplanin column.

The application of Ionic liquids in analytical chemistry is growing rapidly due to their valuable properties such as wide liquid temperature range, high thermal stability, inflammability etc. Several techniques based on ionic liquids are maturing into commercialized products. In part two, the synthesis, physical properties, and the use as ion pairing reagent for anion

detection in ESI-MS of linear tricationic ionic liquids will be presented. In chapter 7, a study of new chiral GC columns using ionic liquids as matrices and methylated ionic cyclodextrin as chiral selector will be discussed.

TABLE OF CONTENTS

ACKNOWLEDGEMENTS.....	iii
ABSTRACT.....	iv
LIST OF ILLUSTRATIONS.....	xii
LIST OF TABLES.....	xiv
Chapter	Page
PART ONE: NEW MACROCYCLIC GLYCOPEPTIDE ANTIBIOTIC FOR CHIRAL HPLC STATIONARY PHASES	
1. INTRODUCTION.....	2
1.1 Introduction to chiral chromatography.....	2
1.2 Chiral stationary phases for gas chromatography.....	4
1.2.1 Amino acids based stationary phases.....	4
1.2.2 Metal-ligand complex based stationary phases.....	5
1.2.3 Cyclodextrin derivatives based stationary phases.....	6
1.2.4 Other types of chiral stationary phases.....	8
1.3 Chiral stationary phases for liquid chromatography.....	9
1.3.1 Linear polysaccharide chiral stationary phases.....	9
1.3.2 Macrocyclic glycopeptide chiral stationary phases.....	11
1.3.3 Cyclodextrin chiral stationary phases.....	13
1.3.4 Other types of chiral stationary phases.....	15
2. EVALUATION OF DALBAVANCIN AS CHIRAL SELECTOR FOR HPLC AND COMPARISON WITH TEICOPLANIN BASED CHIRAL STATIONARY PHASE.....	16
2.1 Abstract.....	16
2.2 Introduction.....	16

2.3 Materials and methods	18
2.3.1 Materials	18
2.3.2 Methods	19
2.3.2.1 Preparation of the D1 CSP	19
2.3.2.2 Preparation of the D2 CSP	19
2.3.2.3 Chromatographic condition	20
2.4 Results and discussion.....	20
2.4.1 The structure of dalbavancin	20
2.4.2 Chromatographic evaluation	22
2.4.2.1 Comparison of CSPs in the normal phase mode.....	23
2.4.2.2 Comparison of CSPs in the polar organic mode	25
2.4.2.3 Comparison of CSPs in the reversed phase mode...26	
2.5 Conclusion.....	43
 PART TWO: IONIC LIQUIDS IN ANALYTICAL CHEMISTRY 	
3. GENERAL INTRODUCTION TO IONIC LIQUIDS AND THEIR APPLICATIONS IN ANALYTICAL CHEMISTRY	45
4. EVALUATION OF FLEXIBLE LINEAR TRICATIONIC SALTS AS GAS-PHASE ION PAIRING REAGENTS FOR THE DETECTION OF DIVALENT ANIONS IN POSITIVE MODE ESI-MS	48
4.1 Abstract.....	48
4.2 Introduction	49
4.3 Experiment section	52
4.4 Results and discussion.....	53
4.5 Conclusion	63
5. LINEAR TRICATIONIC ROOM-TEMPERATURE IONIC LIQUIDS: SYNTHESIS, PHYSIOCHEMICAL PROPERTIES, AND ELECTROWETTING PROPERTIES	65
5.1 Abstract	65

5.2 Introduction	65
5.3 Experimental section	68
5.3.1 Materials	69
5.3.2 Procedure for the synthesis of the core structure 1- (Bromodecyl)-3-(bromodecyl)imidazolium Bromide Salt (1a)	70
5.3.3 Procedure for the synthesis of the core structure 1- (Bromohexyl)-3-(bromohexyl)imidazolium Bromide Salt (1b)	70
5.3.4 Procedure for the synthesis of the core structure 1- Bromopropyl)-3-(bromopropyl)imidazolium Bromide Salt (1c)	71
5.3.5 Procedure for the synthesis of LTILs 2a-d, 3a-d, and 4a-d	71
5.3.6 Glass transition temperature/melting point	75
5.3.7 Density	76
5.3.8 Refractive Index	76
5.3.9 Viscosity	76
5.3.10 Thermal stability analysis	76
5.3.11 Electrowetting experiments	77
5.4 Results and discussion	78
5.5 Conclusion	87
6. IONIC CYCLODEXTRINS IN IONIC LIQUID MATRICES AS CHIRAL STATIONARY PHASES FOR GAS CHROMATOGRAPHY	88
6.1 Abstract	88
6.2 Introduction	88
6.3 Experimental	91
6.3.1 Materials	91
6.3.2 Methods	91
6.3.3 Equipment	95
6.4 Results and discussion	95
6.4.1 Optimization of the stationary phase composition	96

6.4.1.1 Optimization of the chiral selector	96
6.4.1.2 Optimization of the matrix.....	99
6.4.2 Improvement over the first ionic liquid containing cyclodextrin-based CSPs	99
6.4.3 Comparison of the BIM-BPM-I CSP to the corresponding commercial CSP	109
6.5 Conclusions	114
7. GENERAL SUMMARY	115

APPENDIX

1. ¹ H AND ¹³ C NMR SPECTRA OF 1-BROMODECYL-3-BROMODECYL IMIDAZOLIUM BROMIDE SALT (1a)	117
2. ¹ H AND ¹³ C NMR SPECTRA OF 1-BROMOHEXYL-3-BROMOHEXYL IMIDAZOLIUM BROMIDE SALT (1b)	122
3. ¹ H AND ¹³ C NMR SPECTRA OF 1-BROMOPROPYL-3-BROMOPROPYL IMIDAZOLIUM BROMIDE SALT (1c)	127
4. ¹ H AND ¹³ C NMR SPECTRA OF 1-(1'-METHYL-3'-DECYLIMIDAZOLIUM)-3- (1''-METHYL-3''-DECYLIMIDAZOLIUM) IMIDAZOLIUM TRI [BIS(TRIFLUOROMETHANESULFONYL)IMIDE] (2a)	132
5. ¹ H AND ¹³ C NMR SPECTRA OF 1-(1'-BUTYL-3'-DECYLIMIDAZOLIUM)-3-(1''-BUTYL-3''- DECYLIMIDAZOLIUM)IMIDAZOLIUM TRI [BIS(TRIFLUOROMETHANESULFONYL)IMIDE] (2b)	138
6. ¹ H AND ¹³ C NMR SPECTRA OF 1-(1'-BENZYL-3'-DECYLIMIDAZOLIUM)-3- (1''-BENZYL-3''-DECYLIMIDAZOLIUM) IMIDAZOLIUM TRI [BIS(TRIFLUOROMETHANESULFONYL)IMIDE] (2c)	144
7. ¹ H AND ¹³ C NMR SPECTRA OF 1-DECYLTRIPROPYLPHOSPHONIUM-3- DECYLTRIPROPYLPHOSPHONIUM IMIDAZOLIUM TRI [BIS(TRIFLUOROMETHANESULFONYL)IMIDE] (2d)	150
8. ¹ H AND ¹³ C NMR SPECTRA OF 1-(1□-METHYL-3□-HEXYLIMIDAZOLIUM)-3-(1''-METHYL-3''- HEXYLIMIDAZOLIUM)IMIDAZOLIUM TRI [BIS(TRIFLUOROMETHANESULFONYL)IMIDE] (3a)	157
9. ¹ H AND ¹³ C NMR SPECTRA OF 1-(1□-BUTYL-3□-HEXYLIMIDAZOLIUM)-3-(1''-BUTYL-3''-	

HEXYLIMIDAZOLIUM)IMIDAZOLIUM TRI [BIS(TRIFLUOROMETHANESULFONYL)IMIDE] (3b)	162
10. ¹ H AND ¹³ C NMR SPECTRA OF 1-(1-BENZYL-3-HEXYLIMIDAZOLIUM)-3- (1-BENZYL-3-HEXYLIMIDAZOLIUM)IMIDAZOLIUM TRI [BIS(TRIFLUOROMETHANESULFONYL)IMIDE] (3c)	167
11. ¹ H, ¹³ C AND ³¹ P NMR SPECTRA OF 1-(HEXYLTRIPROPYLPHOSPHONIUM)-3- (HEXYLTRIPROPYLPHOSPHONIUM)IMIDAZOLIUM TRI [BIS(TRIFLUOROMETHANESULFONYL)IMIDE] (3d)	173
12. ¹ H AND ¹³ C NMR SPECTRA OF (1-METHYL-3-PROPYLMIDAZOLIUM)-3- (1-METHYL-3-PROPYLMIDAZOLIUM)IMIDAZOLIUM TRI [BIS(TRIFLUOROMETHANESULFONYL)IMIDE] (4a)	180
13. ¹ H AND ¹³ C NMR SPECTRA OF (1-BUTYL-3-PROPYLMIDAZOLIUM)-3-(1-BUTYL-3- PROPYLMIDAZOLIUM)IMIDAZOLIUM TRI [BIS(TRIFLUOROMETHANESULFONYL)IMIDE] (4b)	185
14. ¹ H AND ¹³ C NMR SPECTRA OF (1-BENZYL-3-PROPYLMIDAZOLIUM)-3-(1-BENZYL-3- PROPYLMIDAZOLIUM)IMIDAZOLIUM TRI [BIS(TRIFLUOROMETHANESULFONYL)IMIDE] (4c)	191
15. ¹ H, ¹³ C AND ³¹ P NMR SPECTRA OF 1-PROPYLTRIPROPYLPHOSPHONIUM-3-PROPYLTRIPROPYLPHOSPHONIUM IMIDAZOLIUM TRI[BIS(TRIFLUOROMETHANESULFONYL)IMIDE] (4d)	196
REFERENCES	203
BIOGRAPHICAL INFORMATION	219

LIST OF ILLUSTRATIONS

Figure	Page
1.1 The structure of Chirasil-Val stationary phase	5
1.2 The structure of Chirasil-Metal	6
1.3 The structure of immobilized cyclodextrin stationary phase	8
1.4 Structures and trademark names of the most popular cellulose and amylose columns	11
1.5 Structures of macrocyclic glycopeptide antibiotics (a) vancomycin, (b) teicoplanin, (c) restocetin A, (d) teicoplanin aglycone	13
1.6 Structures of six most popular commercial cyclodextrin stationary phases	14
2.1 The structure of the macrocyclic glycopeptide dalbavancin	21
2.2 The structure of the macrocyclic glycopeptide teicoplanin	21
2.3 Representative chromatograms of two analytes on the T1 and D2 CSPs in the normal phase mode: heptane/ethanol 80/20 v/v; flow rate 1ml/min	24
2.4 Representative chromatograms of two analytes on the T1 and D2 CSPs in the polar organic phase mode: 100% methanol; flow rate 1ml/min	26
2.5 Representative chromatograms of two analytes on the T2 and D2 CSPs in the reversed phase mode: 20mM NH ₄ NO ₃ buffer/methanol 1/1 v/v; flow rate 1ml/min	28
3.1 Structures of common cations and anions of ionic liquids	45
4.1 Structures of the tricationic ion pairing reagents used in this analysis	51
4.2 Comparison of the detection of sulfate in the positive mode using tricationic ion-pairing reagents D3 (I) and E2 (II)	59
4.3 Proposed fragmentation pattern for a typical SRM experiment using trication D3	60
5.1 Plot of contact angle vs voltage according to Young's and Lippmann's equation	68
5.2 Structures of linear tricationic ionic liquids	69

5.3 Electrowetting experimental setup.....	78
5.4 Electrowetting curves of (a) linear tricationic ionic liquids with C6 linkage chains and (b) linear tricationic ionic liquids with C6 linkage chains overlaid normal to the maximum θ_0 value.....	84
5.5 Structures of rigid core tricationic ionic liquids	85
5.6 Electrowetting curves of (a) benzylimidazole-substituted linear and rigid type tricationic ionic liquids and (b) benzylimidazolesubstituted linear and rigid type tricationic ionic liquids overlaid normal to the maximum θ_0 value	86
6.1 Structures of ionic permethyl β -cyclodextrins used in this study. A. BIM-BPM-A, B. TPP-BPM-A.....	93
6.2 Structures of the ionic liquid matrices used for the dissolution of chiral selectors.	94
6.3 Separation of α -ionone on (a) BIM-BPM-I plus MIM2PEG3-2NTf2 and (b) BIM-BPM-I plus TPP2C12-2NTf2 and (c) TPP-BPM-I plus MIM2PEG3-2NTf2 and (d) TPP-BPM-I plus TPP2C12-2NTf2	96
6.4 Examples of separations achieved on BIM-BPM-I, BIM-BPM-TfO, and BIM-BPM-NTf2 containing columns.....	98
6.5 Examples of compounds showing improved separation on the BIM-BPM-I column compared to on the Chiraldex BPM column	111
6.6 Comparison of compound peak shapes obtained on the Chiraldex BPM column and the BIM-BPM-I column	112
6.7 Comparison of compound peak shapes obtained on neat polysiloxane column (Rtx-5) and neat MIM2PEG3-2NTf2 column.	113

LIST OF TABLES

Table	Page
2.1 Chromatographic data for the normal phase resolution of racemic compounds on D1, D2, T1 and T2 columns	29
2.2 Chromatographic data for the polar organic phase resolution of racemic compounds on D1, D2, T1 and T2 columns	32
2.3 Chromatographic data for the reversed phase resolution of racemic compounds on D1, D2, T1 and T2 columns	36
4.1 Limits of detection for divalent anions with linear tricationic reagents.....	55
4.2 Comparison of LODs in the SIM positive and SRM positive modes	62
5.1 Physiochemical properties of linear tricationic ionic liquids.....	82
5.2. Electrowetting properties of linear tricationic ionic liquids	83
6.1 Performance improvement of the new IL phase gained over its 2001 predecessor	101
6.2 Performance comparison of neutral BPM stationary phases based on the monocationic IL (BMIM-Cl) and a dicationic IL (MIM2PEG3-2NTf2)	102
6.3 Enantioseparation of 56 compounds on BIM-BPM-I column and ChiralDex BPM column	103

PART ONE: NEW MACROCYCLIC GLYCOPEPTIDE ANTIBIOTIC FOR CHIRAL HPLC
STATIONARY PHASES

CHAPTER 1

INTRODUCTION

1.1 Introduction to chiral chromatography

Chirality (handedness) is the property of an object that is non-superimposable upon its mirror image. This is attributed to the lack of an internal plane of symmetry in the structure. A chiral molecule and its mirror image are referred to as a pair of enantiomers. Tetrahedral carbon atoms connected to four different groups are the most common chiral centers for a molecule. In addition to asymmetric carbon atoms, stereogenic centers can also be based on atoms such as tetrahedral nitrogen, sulfur and phosphorus. Enantiomers have identical physical and chemical properties in an achiral environment, but are distinctive in a couple of aspects. The first and most well-known different behavior observed is that a pure sample of an enantiomer can rotate plane-polarized light in the same magnitude but in opposite direction as that of its mirror form. However, the most important differences between enantiomers are their reactivity in biological environments. Biomolecules such as receptor proteins or enzymes in living organisms are chiral and they have different binding interactions with enantiomers. This usually results in markedly different biological responses. It is very common that a chiral molecule is potent in treating a certain disease while its enantiomer is impotent or even toxic. Thus, chirality has become a major concern for pharmaceutical industry. It is necessary for researchers to get the pure form of each pair and individually evaluate their pharmacokinetic, pharmacodynamic and toxicological properties in the drug development process.¹⁻³ As a result, these data have been required by the U.S. FDA since 1992⁴ for marketing of new chiral drugs. Besides drug research and development and the regulatory process, chiral considerations are also integral parts of the agrochemical industry since enantiomerically pure pesticides are found to be more effective and environmental friendly.

In this context, producing and analyzing chiral synthetic intermediates and final target compounds have become a more intriguing challenge to chemists. After decades of extensive efforts, a variety of different stereoselective separation technologies have been developed. Among them, direct enantioselective chromatography has grown to be a well established and widely used technology to meet the needs of preparation and analysis in academia and industry. For analytical scale, enantiomeric separation is dominated by chiral chromatography especially chiral high performance liquid chromatography (HPLC) and chiral gas chromatography (GC). Chiral GC is featured by high efficiency, sensitivity and speed of separation.⁵ It is mainly used for enantiomeric excess measurements for chiral drug intermediates, pesticides, fungicides, herbicides, pheromones, essential oil, flavors and fragrances with low to moderate molecular weight.⁶⁻⁸ Due to the fact that chiral GC requires analytes to be able to transfer to the gas phase and it is commonly operated at high temperature, its applications are limited to racemates that are volatile and thermally stable. On the other hand, volatility and thermal stability of an analyte is no longer a prerequisite for chiral HPLC since HPLC operates at ambient temperature and analytes are transferred in liquid solvent. Therefore, chiral HPLC has wider applicability. In addition, with the wide choices and combinations of chiral stationary phases, additives and mobile phases that have been developed over the past several decades, chiral HPLC is established as the most used method for enantiomeric separations. Also, analytical scale HPLC can be easily scaled up to the preparative dimension from gram to kilogram levels, which makes it a more important technique than chiral GC. It should be noted that asymmetric synthesis is the ultimate way of producing large quantities of enantiomeric pure drug product. However, preparative enantioselective chromatography is an important option in early drug development due to its fast method development process for resolving racemates and the ability to obtain both enantiomers in one step. Great advances have been made in the development of preparative separation techniques and instrumentation. Supercritical fluid chromatography (SFC)⁹ and simulated moving bed (SMB)¹⁰ technique are growing rapidly and become the major

chromatographic methods for large scale enantiomer production in the pharmaceutical industry. After all, the great success of chiral chromatography emanates from the discovery of several major classes of chiral selectors with broad enantioselectivity and their development into effective chiral stationary phases. These achievements enabled enantiomeric separation to be carried out in a simple and robust fashion. This chapter will summarize the main types of chiral stationary phases that are utilized in the practice of modern chiral GC and chiral HPLC.

1.2 Chiral stationary phases for gas chromatography

As mentioned beforehand, chiral gas chromatography has narrower applicability than chiral liquid chromatography due to its restrictions to analytes of high volatility and thermal stability. However, chiral GC still plays a complementary and particular useful role for the separation of non-aromatic compounds which cannot be easily resolved and detected by HPLC-DAD (diode array detector). It also offers many advantages including high efficiency, easy sample preparation when coupled with head-space to detect fragrances. Several classes of chiral stationary phases have been developed since the first enantiomeric separation was obtained on an amino acid based phase in 1966 by Gil-Av *et al.*¹¹ They can be divided generally into three types: amino acid analogs, metal-ligand complexes and cyclodextrin derivatives. Each will be discussed in detail in the following section.

1.2.1 Amino acids based stationary phases

As the first example of enantiomer discrimination by chiral gas chromatography, a glass capillary column coated with *N*-trifluoroacetyl-L-isoleucine ester was used for the enantiomeric separation of racemic *N*-trifluoroacetyl amino acid esters in 1966.¹¹ This breakthrough has led to further study in the mechanism of enantiomeric discrimination and development of new chiral stationary phases based on amino acids derivatives. The following work of using a coated neat dipeptide phase based on valine revealed that the second amide group is crucial for chiral

recognition by providing additional hydrogen bonding interaction with analyte.¹² However, these early chiral GC stationary phases shared the same weaknesses such as low thermal stability and high bleeding, which prevented them from being used for real analysis. It took scientists ten years since the advent of first successful chiral separation on GC to make the first commercial chiral GC column (Chirasil-Val™) featuring excellent chromatographic properties for the enantiomeric separation of several classes of chiral compounds over a wide temperature range 0-250 °C.¹³ Its structure is shown in Fig. 1.1. The improved thermal stability is achieved by linking the valine ester chiral selector to a copolymer of dimethylsiloxane and (2-carboxypropyl) methylsiloxane with proper viscosity. Its low bleeding property also enables the coupling of mass spectrometer for detection to the column.¹⁴ Even three decades after its birth, Chirasil-Val is still one of the most used columns for the chiral separation of trifluoroacetylated amino acid esters.

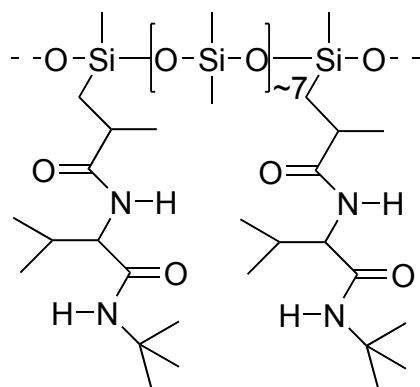


Figure 1.1 structure of Chirasil-Val stationary phase¹³ based on L-valine

1.2.2 Metal-ligand complex based stationary phases

Chiral metal-ligand complexes were proven to be capable of performing enantiomeric separation on GC as well by Schurig in 1977.¹⁵ In this work, the chiral alkane 3-methylcyclopentane was separated on a 200m capillary column coated with dicarbonylrhodium(I) 3-trifluoroacetyl-(1R)-camphorate in squalane solution. In the following work, enantiomeric

separations of oxygen-, nitrogen- and sulfur-containing racemates were successfully performed by columns coated with manganese(II), cobalt(II) and nickel(II) bis [(3-heptafluorobutanoyl)-(1R)-camphorate]] in squalane or dimethylpolysiloxane.¹⁶⁻¹⁹ It was proposed that the enantiomer possessing stronger lone pair or π -electron complexing interaction with the π -orbitals of central metal atom tends to retain longer on the column, which results in chiral discrimination. Later, improved column thermal stability was obtained by immobilizing the chiral metal ligand complex to a siloxane polymer (Chirasil-Metal).²⁰⁻²² Its structure is illustrated in Fig. 1.2. However, poor efficiency caused by severe tailing and low enantioselectivity prevent chiral metal-ligand type chiral GC stationary phases from being widely used for enantiomeric separation.

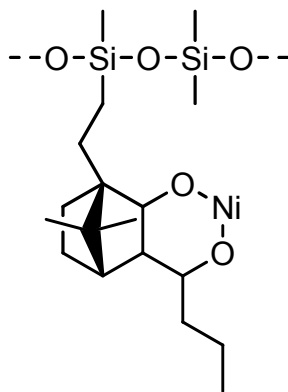


Figure 1.2 Structure of Chirasil-Metal²⁰ based on Ni(II) (1S,2S,3S,4S)-3-((S)-1-hydroxybutyl)-7,7-dimethylbicyclo[2.2.1]heptan-2-ol

1.2.3 Cyclodextrin derivatives based stationary phases

Cyclodextrins (CDs) are a class of natural cyclic oligosaccharides with 6 to 8 D-glucose units linked by α -1,4-glucosidic bonds. They are referred to as α -(6 units), β -(7 unites), γ -(8 unites) cyclodextrin respectively. Cyclodextrin derivative based stationary phases dominate the enantioselective GC field and account for 90% of enantiomeric GC separation.²³ It is the most important class of GC chiral stationary phases today.

The first chiral CD stationary phase employed native α -CD as the chiral selector for the separation of α - and β -pinene and *cis*- and *trans*-pinane. Due to its high melting point,

underivatized α -CD was dissolved in formamide²⁴ solution first and then coated onto Celite which is packed into the glass column prior to coating.²⁴ The breakthrough of CD based chiral stationary phases took place after liquid derivatized CD columns were developed. This type of stationary phases utilized either neat alkylated CD derivatives possessing low melting point²⁵ or methylated CDs dissolved in polysiloxanes²⁶ as coatings. Armstrong *et al.* synthesized more polar CD derivatives possessing hydroxypropyl or trifluoroacetyl groups.²⁷ They were also directly coated to GC column and exhibited excellent resolving power to a wide variety of structural types and classes of compounds. It was proposed that homogeneity of the derivative, the number of polar functional groups (e.g., hydroxyls), and the overall molecular weight of the compound are the three factors determining the physical state of a CD derivative. For CD stationary phases dissolved in polysiloxanes, it has been found that the enantioselectivity does not necessarily increase with the concentration of the CD derivative. The optimum concentration for permethylated β -CD and derivatives with high molecular masses were found to be 30% and 50% respectively.⁵

Chirasil-Dex was the first bonded CD chiral stationary phase and was introduced by Schurig *et al.* in the early 1990's.²⁸ Permethylated β -cyclodextrin was attached to dimethylpolysiloxane through a mono-6-octamethylene spacer. Extended operating temperature range (-20-220°C) and improved robustness were obtained. Polar analytes were able to elute at lower temperatures, and thus pre-derivatization for polar compounds could be avoided. Meanwhile, Armstrong *et al.* demonstrated a different way to immobilize CDs to polysiloxanes backbone.^{27, 29} In this work, CD first reacted with allyl bromide and was subjected to permethylation in the second step. The derivatized CD was linked to polysiloxanes through the double bond on the allyl group. The structure of the stationary phase is shown in Fig. 1.3. The following study of variant wall-immobilized cyclodextrin phases revealed that wall-immobilization can increase stationary phase stability but can also change enantioselectivity and efficiency

significantly. In addition, bulky analytes were found to be better separated on these bonded phases.³⁰

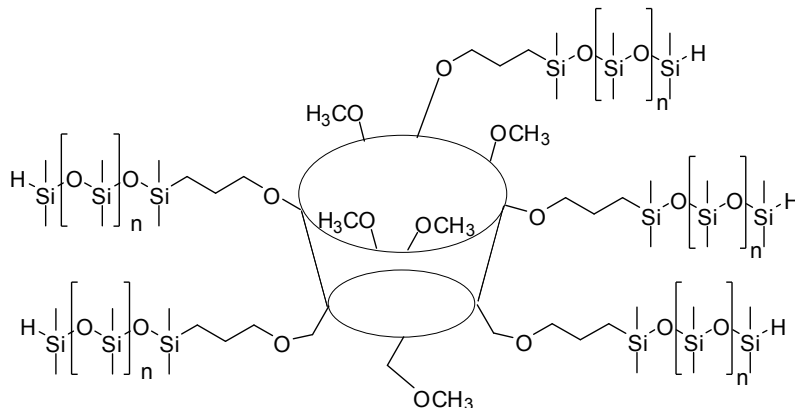


Figure 1.3 Structure of immobilized cyclodextrin stationary phase²⁹

So far, the chiral discrimination mechanism of CD derivatives based GC stationary phases is still under study. It has been suggested that multimodal recognition is likely to take place during the chiral separation process involving inclusion complexation, hydrogen-bonding, dispersion forces, dipole-dipole interaction, electrostatic interactions and hydrophobic interactions.⁵

1.2.4 Other types of chiral stationary phases

Stationary phases based on linear polysaccharides have been also developed and studied. Due to the lack of the ability to form inclusion complex with analytes, these stationary phases can only separate a fraction of racemates that can be resolved on CD derivatives based column.³¹ Two new classes of stationary phases based on chiral ionic liquids^{31,32} and cyclofructans³³ have emerged recently. In comparison, CD derivative series columns still provide the most general applicability for enantiomeric separation.

1.3 Chiral stationary phases for liquid chromatography

Chiral liquid chromatography accounts in large part for the commercial and industrial success of enantiomeric separation. It provides the most general applicability for all kinds of enantiomers based on the establishment of more than one hundred commercial chiral stationary phases. Nowadays, combinations of 10 or fewer of the most popular chiral stationary phases are able to separate the majority of enantiomer of interest. Plus, these analytical stationary phases can be easily extended to preparative scale separations to obtain kilogram or greater amounts of highly enantiomerically pure products per day when coupled with SMB or SFC. Therefore, it is essential to have the knowledge about existing LC chiral stationary phases of variant types and their properties. In the following content, several most popular types of chiral liquid chromatography phases will be discussed.

1.3.1 Linear polysaccharide chiral stationary phases

Cellulose and amylose are the most abundant naturally occurring chiral polymers. They are unbranched linear polymers of optical active D-glucose linked with 1, 4-glycosidic bonds. The main difference is the anomeric configuration: amylose's glucose units are linked with α -(1,4) glycosidic bonds, whereas cellulose's glucose units are linked by β -(1,4) glycosidic bonds. Unlike small chiral molecules, these chiral macromolecules exhibit hierarchically ordered chirality originating from (i) molecular chirality in single glucose unite, (ii) helically twisted polymer backbone, (iii) supramolecular chirality resulting from the alignment of adjacent polymer chains forming ordered regions.³⁴ Such structural peculiarities provide polysaccharide based chiral stationary phases with superior chiral recognition abilities.

Polysaccharides were first reported to be used as chiral selectors in chiral liquid chromatography in 1973.³⁵ Hesse *et al.* used microcrystalline cellulose triacetate as a polymeric packing material. Later, plain crosslinked beads of polysaccharide derivatives were also employed as chiral stationary phase without support. What limited the use of the first generation

polysaccharide stationary phases are their poor mechanical stability and modest applicability. In 1984, Okamoto *et al.* coated cellulose and amylose derivatives (phenylcarbamate and phenylesters) onto the surface of macroporous silica beads as a thin film of about 20wt%.³⁶ This type of coated polysaccharide stationary phases showed exceptional chiral recognition properties, wide applicability and high efficiency. Therefore, their practical usefulness in chiral separations has made them the major workhorses in the chiral HPLC field. It needs to be mentioned that they are not compatible with common organic solvents such as dichloromethane, chloroform, tetrahydrofuran, ethyl acetate, acetone, toluene and 1,4-dioxane. Immobilized polysaccharides HPLC column became commercially available in the mid 2000's.^{37,38} The bonded polysaccharides based stationary phases were prepared via intermolecular polycondensation and exhibit greatly improved mechanical stability and solvent compatibility while maintaining excellent enantioselective property. Due to their universal solvent compatibility, wide applicability and high loading capacity, immobilized polysaccharide phases are also frequently used in large-scale separations such as SMB chromatography. Some studies have shown that the immobilized versions are inferior in enantioselectivity compared to their corresponding coated version in traditional alkane-alcohol normal phase condition. However, the loss in the selectivity can be compensated by using non-standard solvents such as dichloromethane and chloroform which typically provide higher enantioselectivity. The most recent advancement of this cellulose and amylose type stationary phases involves using smaller supporting silica particles (from 5 μ m to 3 μ m) for the purpose of improving the efficiency. The most popular cellulose and amylose based stationary phases are listed in Fig 1.4.

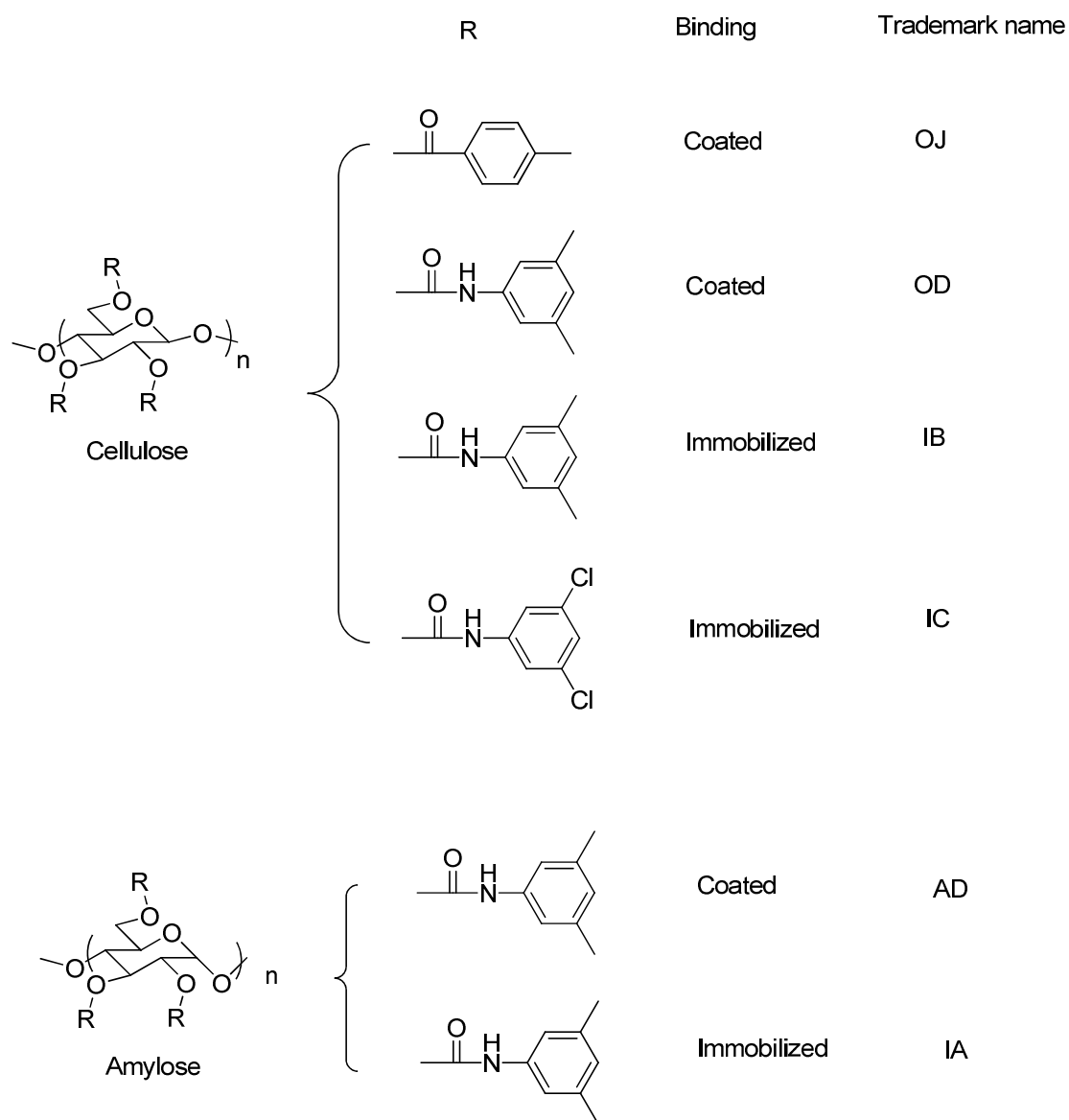


Figure 1.4 Structures and trademark names of the most popular cellulose and amylose columns

1.3.2 Macrocyclic glycopeptide chiral stationary phases

Macrocyclic glycopeptide chiral stationary phases are the second most important class of commercial chiral stationary phase for liquid chromatography, next to the polysaccharides type. Vancomycin was first bonded to silica gel and evaluated as chiral

stationary phase for HPLC by Armstrong *et al.* in 1994 and showed promising enantioselectivity.³⁹ Subsequently, a number of macrocyclic antibiotic molecules of the vancomycin family were also exploited as chiral stationary phases and found to be complementary to each other.⁴⁰⁻⁴⁴ A wide variety of racemates with different structures and functional group can be separated on these phases in different modes including normal, polar organic and reverse phase mode. Chiral stationary phases based on teicoplanin, vancomycin, restocetin A and teicoplanin aglycon are now commercially available, the structures of which are depicted in Figure 1.5. These stationary phases have complementary enantioselectivity to each other. If partial separation of a racemate is obtained on one of these columns, it is often found that a baseline separation can be achieved on one of the other antibiotic columns under the same chromatographic condition.⁴⁵ It also needs to be emphasized that Teicoplanin based stationary phases provide the highest enantioselectivity for underivatized primary and secondary amino acids among all commercial chiral stationary phases.⁴⁶ They are also preferred for preparative scale separation of native amino acids due to the fact that separation can be simply carried out without adding any buffer to the mobile phase system. Generally speaking, Teicoplanin based stationary phases have broader applicability than the rest of the family. In addition, antibiotic chiral stationary phases are also frequently used in separating chiral and achiral metabolites based on their specialty in differentiating polar compounds.

The structures of macrocyclic glycopeptides are relatively complex. The enantiorecognition mechanism is still not clear because there are numerous stereogenic centers and functional groups on these chiral selectors. However, it is believed that a combination of hydrogen bonding, π - π complexation, dipole-dipole stacking, inclusion and steric interaction, and ionic attraction are responsible for the chiral recognition process.

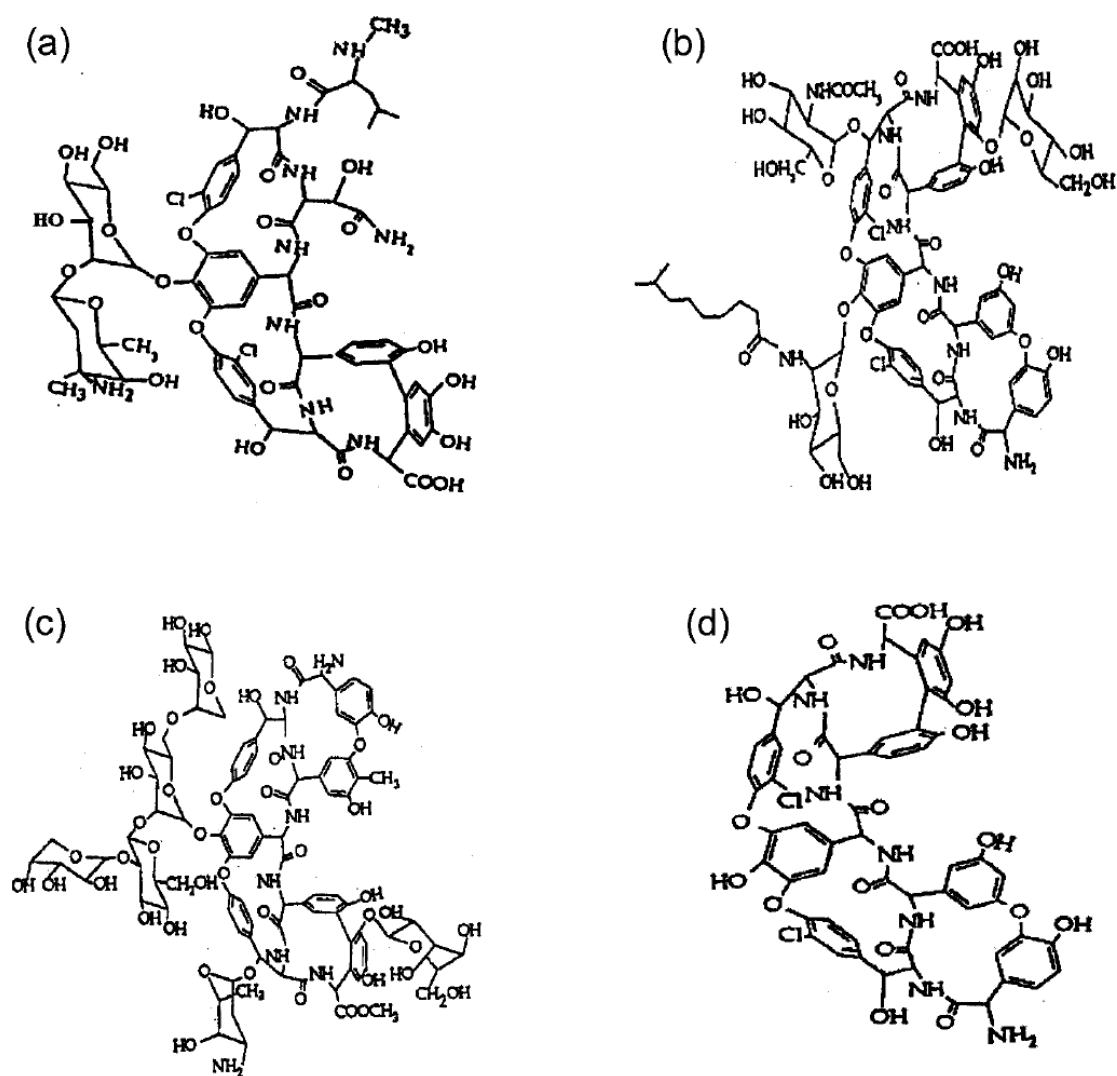


Figure 1.5 Structures of macrocyclic glycopeptide antibiotics (a) Vancomycin, (b) Teicoplanin, (c) Restocetin A, (d) Teicoplanin aglycone. Reprinted from reference 45.

1.3.3 Cyclodextrin chiral stationary phases

Both native cyclodextrins and their derivatives are powerful chiral selectors for liquid chromatography. A plethora of cyclodextrin-based stationary phases of different derivatization groups and binding chemistry have been developed since the first cyclodextrin chiral stationary phase was first introduced by Armstrong *et al.* in 1984.⁴⁷ All of them can be operated in three mobile phase modes. And their distinctive enantioseparation profiles in different modes suggest

different chiral recognition mechanisms. In the reversed phase mode, an inclusion complex is first formed driven by hydrophobic interaction between the hydrophobic part of the guest molecule and cyclodextrin cavity. Hydrogen bonding, steric and π - π interaction that take place on the rim of cyclodextrin are also important for enantioselectivity. In the polar organic mode, the chiral discrimination occurs mostly at the mouth of cyclodextrin. It is because the cavity of the chiral selector is blocked by organic mobile phase molecule such as acetonitrile which is in great excess and thus the central cavity of the cyclodextrin is not accessible to the analyte to form inclusion complex.⁴⁷

Among all the commercial available cyclodextrin based chiral stationary phases, cyclobond I RSP, DMP, RN and SN are most widely used due to their relatively wide enantioselectivity. Their structures are shown in Fig 1.6.

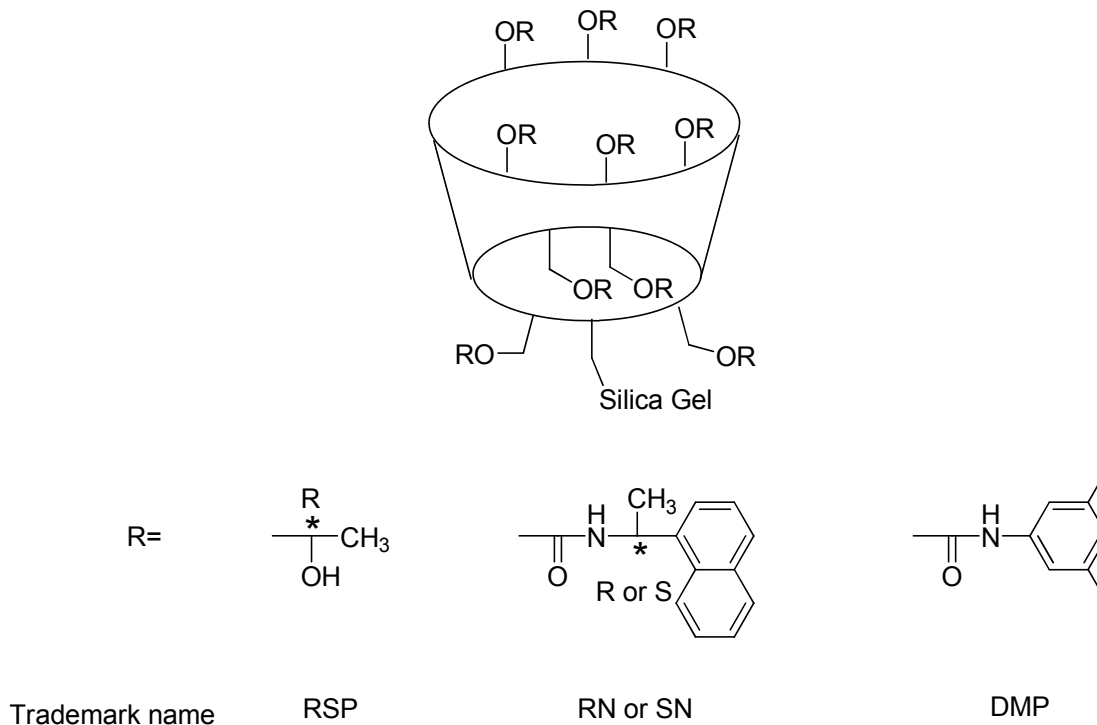


Figure 1.6 Structures of six most popular commercial cyclodextrin stationary phases

1.3.4 Other types of chiral stationary phases

Although most chiral molecules can be resolved by the combination of the aforementioned three types of HPLC chiral stationary phases, there are several other classic chiral stationary phases that are still useful in certain aspect. Protein based chiral stationary phases were one of the earliest commercial chiral columns.⁴⁸ However, their importance keeps declining because of their low loading capacity and poor robustness. They are now more often employed in protein and drug binding study rather than enantiomeric separation. Chiral crown ether based chiral stationary phases are effective in separating compounds containing primary amine group. The chiral crown ether selector can form inclusion complex with the analyte via primary amine group under acidic reverse phase condition.⁴⁹ Pirkle-type (or brush type) stationary phases are used specifically in normal phase. It requires π - π donor-accepter interaction between chiral selector and solute for chiral reorganization. Poly-Whelko-O which is based on polysiloxane has shown good enantioselectivity and high efficiency in SFC.⁵⁰ Chiral ion-exchanger is considered as a subcategory under Pirkle-type. The difference lies in that small molecules containing ionizable group are used as chiral selectors instead of neutral compounds for Pirkle type. Chiralpak QN-AX is so far the only commercialized chiral stationary phase of this type. It is based on a quinine derivative and acts as a weak anion exchanger.

The most important class which has emerged recently is cyclofructan derivatives based chiral stationary phases. They were developed by Armstrong *et al.* in 2009.^{51, 52} The derivatized cyclofructan chiral stationary phases showed broad enantioselectivity to a wide variety of chiral molecules. Therefore, several cyclofructan derivatives based stationary phases have been commercialized in 2010. It needs to be noted that LARIHC CF6-P demonstrated excellent enantioselectivity to chiral primary amine in particular and it works in aqueous solvents and supercritical fluids. It is the chiral stationary phase of choice for chiral primary amines.

CHAPTER 2
EVALUATION OF DALBAVANCIN AS CHIRAL SELECTOR FOR HPLC AND COMPARISON
WITH TEICOPLANIN-BASED CHIRAL STATIONARY PHASES

The experiments were done by me, Ye Bao and Ke Huang.

2.1 Abstract

Dalbavancin is a new compound belonging to the macrocyclic glycopeptide family. It was covalently linked to 5 μm silica particles by using two different binding chemistries. Approximately two hundred and fifty racemates including (A) heterocyclic compounds; (B) chiral acids; (C) chiral amines; (D) chiral alcohols; (E) chiral sulfoxides and sulfilimines; (F) amino acids and amino acid derivatives; and (G) other chiral compounds were tested on the two new chiral stationary phases (CSP) using three different mobile phases. As dalbavancin is structurally related to teicoplanin, the same set of chiral compounds was screened on two commercially available teicoplanin CSPs for comparison. The dalbavancin CSPs were able to separate some enantiomers that were not separated by the teicoplanin CSPs and also showed improved separations for many racemates. However, there were other compounds only separated or better separated on teicoplanin CSPs. Therefore, the dalbavancin CSPs are complementary to the teicoplanin CSPs.

2.2 Introduction

Macrocyclic antibiotics were first introduced as a new class of chiral selectors for enantioseparations by HPLC and capillary electrophoresis in 1994.⁵³ The ANSA family (rifamycin B and SV)^{54,55} and glycopeptides group (vancomycin, ristocetin and teicoplanin⁵⁶⁻⁶⁰)

were demonstrated to have the most advantageous structures for enantiomeric separations. There are many structurally related oligophenolic glycopeptides belonging to the later group which have proven to be useful. Thus far, vancomycin, ristocetin, teicoplanin, A82846B,⁶¹ LY307599,⁶² avoparcin,⁶³ and A40926⁶⁴ of the macrocyclic glycopeptide family, have been evaluated as chiral selectors. These chiral selectors can be further divided into two groups according to the number of fused rings in the aglycone part of their structure. In comparison, vancomycin types have a three ring aglycone, while the teicoplanin-type glycopeptides have one more ring in the aglycone which makes it “semi-rigid”. They all show great selectivity over a wide range of chiral molecules including amino acids, carboxylic acids and neutral compounds. Their excellent enantioselective separation capability have been attributed to the richness of different functional groups in their structures such as aromatic rings with and without chloro-substituents, ionizable phenolic moieties, amino groups, amide groups, carboxylates and carbohydrate moieties. Therefore, many kinds of intermolecular interactions, such as π - π and dipole-dipole interactions, hydrophobic interactions and hydrogen bonding, can be involved in the chiral recognition via association with these functional groups.⁶⁵

Although all the macrocyclic glycopeptides are within the same family of compounds, small changes in their structure can result in significant differences in their enantioselective abilities. For example, α -amino acids are better separated on the teicoplanin aglycone based CSP, that is produced by cleaving all the carbohydrate moieties from Teicoplanin.⁶⁶ In the case of A40926, there are only a few small structural variations compared to teicoplanin. However, it is found that some compounds can only be separated or better separated on the HPLC chiral stationary phase based on A40926, while the teicoplanin column separates a larger total number of racemates.⁶⁴

Dalbavancin is a new semisynthetic lipoglycopeptide derived from A40926, a naturally occurring glycopeptide produced by actinomycete *Nonomuraea* species.⁶⁷ It has enhanced activity against gram-positive bacteria and unique pharmacokinetics compared with existing drugs in its class.⁶⁸ In this work, two CSPs were prepared by binding dalbavancin to two different 5 μm spherical silica gels respectively as to mirror the synthesis and makeup of the Chirobiotic T and T2 columns. They are designated as the D1 and D2. Their enantioseparation capabilities were evaluated with 250 pairs of enantiomers containing different functional groups. These analytes were also screened on the commercial teicoplanin CSPs (i.e. Chirobiotic T and Chirobiotic T2) for comparison. These two CSPs are designated as the T1 and T2.

2.3 Materials and methods

2.3.1 Materials

All the racemic analytes tested in this study were purchased from Sigma-Aldrich. All HPLC grade solvents were obtained from VWR (Bridgeport, NJ). HPLC grade Kromasil silica gel (particle size 5 μm , pore size 100 \AA , and surface area 310 m^2/g) was obtained from Akzo Nobel (EKA Chemicals, Bohus, Sweden). LiChrospher Si(100) silica gel (particle size 5 μm , pore size 100 \AA , and surface area 400 m^2/g) was purchased from Merck (Darmstadt, Germany). All organosilane compounds were obtained from Silar Laboratories (Wilmington, NC). These include: (3-aminopropyl) dimethylethoxysilane, (3-aminopropyl) triethoxysilane, [2-(carbomethoxy) ethyl] trichlorosilane, [1-(carbomethoxy)ethyl] methyldichlorosilane, (3-isocyanatopropyl) triethoxysilane, and (3-glycidoxypropyl) triethoxysilane. Dalbavancin was the generous gift of Pfizer(Washington, MO).

2.3.2 Methods

2.3.2.1 Preparation of the D1 CSP

One gram of dried dalbavancin (0.53 mmol) was dissolved in 55 ml anhydrous DMF in a 250 ml 3-neck round flask with mechanical stirring. Then triethylamine (0.72 ml, 5.16 mmol) and 3-(triethoxysilyl)propyl isocyanate (0.865 ml, 3.50 mmol) were added into the solution at room temperature under argon protection. The solution was heated to 95 °C for 5 h and cooled to 60 °C. The dried Kromasil silica (3.50 g, 5 μm, 100 Å) was added into the solution. The mixture was heated to 105 °C overnight and then cooled to room temperature and filtered. The CSP was washed by methanol, methanol/water (50/50, v/v), pure water, and methanol (50 ml for each solvent), and dried in oven at 100 °C overnight. Elemental analysis showed it has 8.0% carbon loading.

2.3.2.2 Preparation of the D2 CSP

The D2 stationary phase was prepared as previously described for the teicoplanin CSP. Five gram of Lichrospher silica gel was first dried at 150 °C under vacuum, and then it is heated in toluene to reflux to remove azeotropically all residual water. It is followed by adding 2.5 mL of 3-aminopropyl triethoxysilane and the reaction mixture was heated to reflux for 4h. The modified silica gel was filtered and washed with toluene, methanol and dichloromethane and dried at 90 °C overnight. Elemental analysis showed the derivatized silica gel has 4.0% carbon loading. A 2.5 mL portion of 1,6-diisocyanatohexane (15 mmol) was added to an ice-bath-cooled slurry of 2.5 g of 3-aminopropyl- Lichrospher in 50 mL of anhydrous toluene. Next, the mixture was heated at 70 °C for 2 h. After cooling, the supernatant toluene phase was removed under an argon atmosphere. The excess reactant was removed by dry toluene washing. A suspension of 1 g of Dalbavancin (0.53 mmol) in 100 mL of dry pyridine was added dropwise to the wet activated silica. Next, the mixture was heated at 70 °C for 12 h with stirring under an argon atmosphere. After cooling, the Dalbavancin bonded silica was washed with

50mL portions in the sequence pyridine, water, methanol, acetonitrile and dichloromethane. It was dried under vacuum. Elemental analysis showed it has 11.0% carbon loading (increased by 7.0%).

2.3.2.3 Chromatographic condition

CSPs were slurry packed into 250*4.6mm stainless steel columns at 600 bar. Evaluation of the columns was conducted on HP 1090 HPLC system with a DAD detector and autosampler. Detection wavelengths were selected at 220 nm, 230 nm and 254 nm. The injection volumes were 5 μ l. All sample concentrations were ~1 mg/ml. Separations were carried out under isocratic conditions at flow rate of 1 mL/min at 25°C. The mobile phases were premixed and degassed under vacuum for 10 minutes. The column dead times were tested by injection of solution of 1,3,5-tri-tert-butylbenzene in 100% methanol.

2.4 Results and discussion

2.4.1 *The structure of dalbavancin*

Dalbavancin is a second generation glycopeptide antibiotic molecule (see Fig. 2.1). The major difference between dalbavancin and teicoplanin are: (a) different phenyl rings are chloro-substituted (see ring 2 and 3, Figs. 2.1 & 2.2) ; (b) the β -D-N-acety-glucosamine unit of teicoplanin (see ring 5, Figs. 2.1 & 2.2) is replaced by a simple hydroxyl group; (c) the primary hydroxyl group of N-acyl-glucosamine unit of teicoplanin has been oxidized to a carboxylic acid, which can generate an anion; (d) the primary amine group on the aglycone portion of teicoplanin is a secondary amine substituted by methyl group;(e) the carboxylic group close to phenyl ring 7 is converted to an amide group connected with three methylene groups and it has a dimethylamino group at the end (in dalbavancin); and (f) dalbavancin has 10 carbons in the carbon chain of β -D-N-acyl-glucosamine while teicoplanin only has 9. The last difference noted above is the least likely to affect enantioseparation since one more methylene

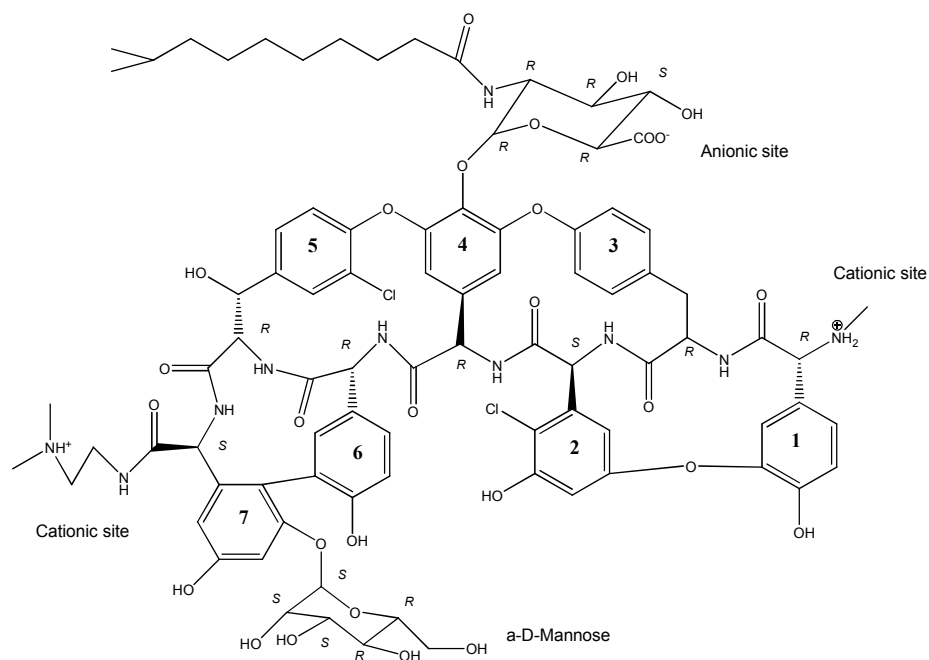


Figure.2.1 The structure of macrocyclic glycopeptide dalbavancin

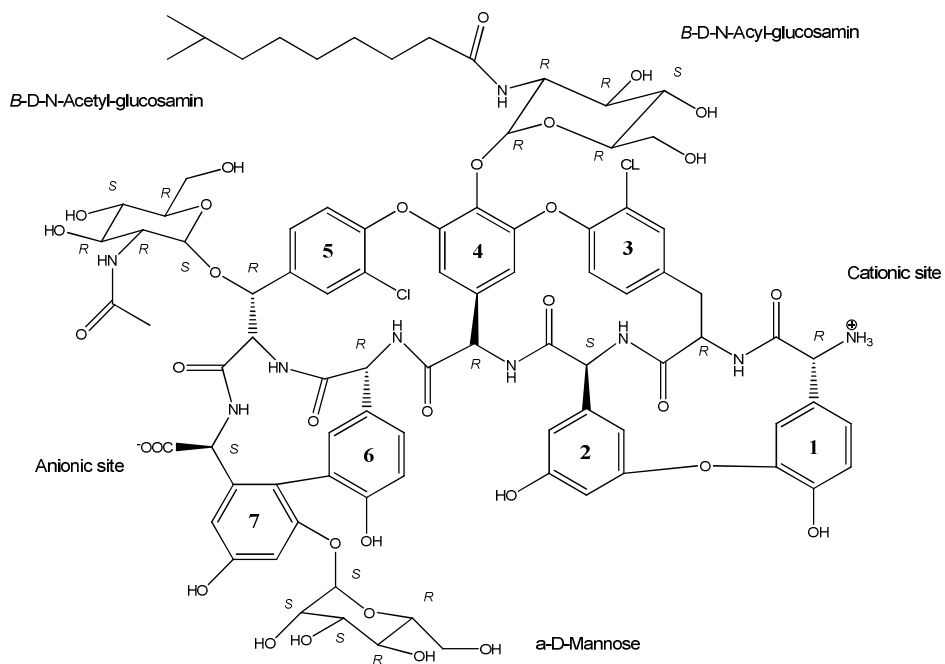


Figure 2.2 The structure of macrocyclic glycopeptide teicoplanin

group does not provide any additional interactions that are beneficial to chiral recognition. Previous studies by our group has shown that the teicoplanin carbohydrate units play an important role in chiral recognition in that it helps in the separation of non-amino acid compounds. However, they also decrease the separation of many α -amino acid enantiomers.⁶⁹ Thus, the elimination of the β -*D*-*N*-acetyl-glucosamine unit in dalbavancin can substantially affect its enantioselectivity. The other changes made to carboxylic groups, hydroxyl group and amino groups can also contribute to differences in the enantioselectivity of dalbavancin relative to teicoplanin. Dalbavancin has one tertiary amine and secondary amine respectively, and one carboxylic group on the β -*D*-*N*-acyl-glucosamine (Figs. 2.1 & 2.2). Whereas teicoplanin has only one carboxylic group connected to the aglycone and one primary amino group. As amine and carboxylic acids group are ionizable in aqueous solution and can interact via electrostatic interactions with charged analytes, these changes could lead to different chiral recognition abilities especially in the reversed phase.

2.4.2 Chromatographic evaluation

The four columns, D1, D2, T1 and T2 were evaluated in three mobile phase modes: the normal phase, polar organic, and reversed phase modes. In the normal phase mode, a mixture of 20% ethanol and 80% heptane were used as mobile phase. In the polar organic mode, 100% methanol was evaluated. In the reversed phase mode, methanol and water were mixed at the ratio of 1 to 1, and 0.1% NH_4OAc was used as buffer to adjust to pH 4.2. In order to compare the behavior of the different CSPs, results presented were obtained with the same mobile phase compositions for all of the CSPs. However, these conditions are not necessarily optimal for all the enantiomeric separations. Better separations can be obtained in specific cases if the mobile phase compositions and organic modifiers are optimized. Other compounds for which standards are not available have not yet be determined.

Approximately 250 compounds were injected on these columns. These analytes include (A) heterocyclic compounds; (B) chiral acids; (C) chiral amines; (D) chiral alcohols; (E) chiral sulfoxides and sulfilimines; (F) amino acid and amino acid derivatives; and (G) other chiral compounds. To simplify the presentation, Table 2.1, Table 2.2 and Table 2.3 list only the chromatographic results obtained when an enantiomeric separation was achieved.

2.4.2.1 Comparison of CSPs in the normal phase mode

Table 2.1 lists the separations achieved on the four columns when used in the normal phase mode. The number of successful enantioseparations achieved on D1, D2, T1 and T2 is 16, 17, 17 and 15 respectively. Interestingly, D2 always gives much greater retention for most of the analytes than the other three columns. Conversely, D1 has the least retention for most compounds. In the case of 2-azabicyclo [2.2.1]-hept-5-en-3-one, the retention factor (k) on D2 is three times as great as it is on D1. According to elemental analysis results of the CSPs, the carbon loading of D2 is higher than D1 by 3%. This can be caused either by more chiral selector loading or more unreacted linkages. And both of these factors can contribute to longer retention of analytes. Also, the additional ureic group of the D2 linkage can interact with analytes and increase the retention time. However, longer retention does not necessarily result in better resolution of racemates. Among the racemates that both D1 and D2 can separate, 6 are better separated on D2 and 4 are better separated on D1 according to the separation factors (α). The enantiomeric separations of 2,6-bis(4-isopropyl-2-oxazolin-2-yl)pyridine, DL-3,4-dihydroxyphenyl- α -propylacetamide, cis-4,5-diphenyl-2-oxazol-idinone, phenyl vinyl sulfoxide were only achieved on the D1 CSP in the normal phase mode. While methyl trans-3-(4-methoxyphenyl) glycidate and 5-hydroxymethyl-2(5H)-furanone enantiomers were separated on the D2 CSP only. Thus, it is obvious that the binding chemistry not only affects the retention factors, but it also changes the enantioselectivity in some cases. The influences of the nonchiral spacers on chiral separation were first studied for β -cyclodextrin chiral stationary phases.⁷⁰

Other studies have been done by several research groups.^{56,71-74} It was found that different types of chiral selectors favor linkages with different nature and length. However, for macrocyclic glycopeptide chiral selectors, each binding methods has its own advantages, and sometimes unique selectivities.

Teicoplanin-based columns can separate five compounds which the dalbavancin-based CSPs did not. 2-Carboethoxy- γ -phenyl- γ -butyrolactone was barely separated by T1 and T2. But its separation was greatly improved to baseline on the D2 CSP. Among the total 29 compounds separated by these four columns in the normal phase mode, nineteen compounds are better or only separated by the dalbavancin based CSPs. There are no obvious structural differences between the solutes separated by one CSP versus another CSP. Representative chromatograms of analytes separated on the macrocyclic glycopeptide CSPs are shown in Fig.

2.3.

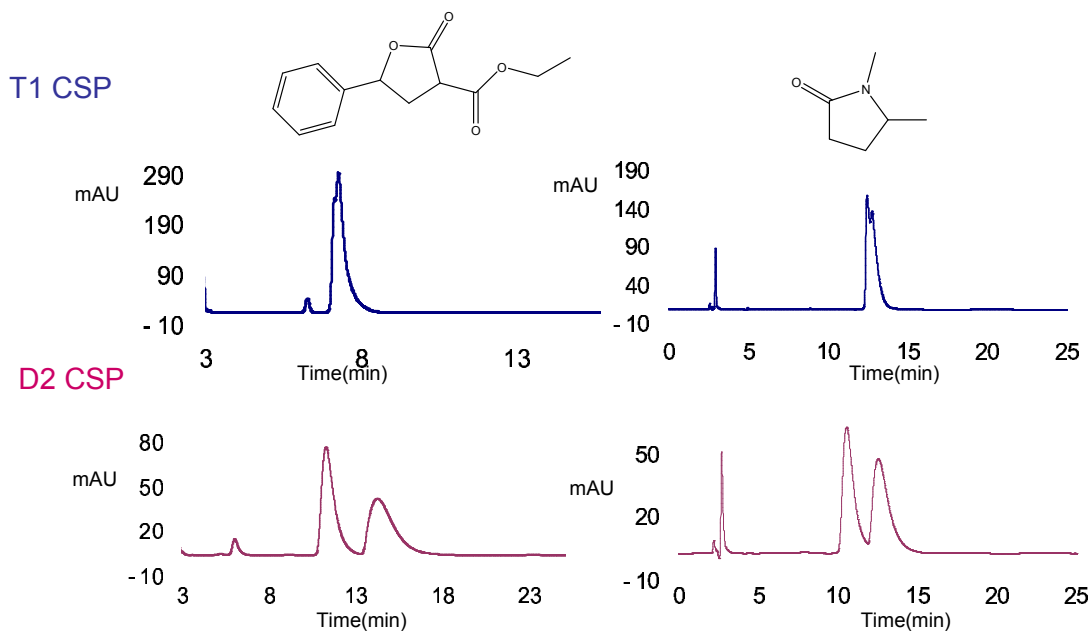


Figure 2.3 Representative chromatograms of two analytes on the T1 and D2 CSPs in the normal phase mode: heptane/ethanol 80/20 v/v; flow rate 1ml/min

2.4.2.2 Comparison of CSPs in the polar organic mode

Methanol is used as mobile phase for the polar organic mode because it can elute analytes faster than acetonitrile for teicoplanin type CSPs.⁵⁶ A total of 13, 17, 18 and 18 racemates have been separated on D1, D2, T1 and T2 respectively. These analytes include carboxylic acids, amine, alcohol and neutral compounds. The results are listed in Table 2 and representative chromatograms are shown in Fig. 4. According to the enantioselectivity factors, three enantiomers are best separated on the D1 CSP, including one that was separated only on this CSP, 12 solutes were best separated by the D2 CSP including 4 that were separated only on this stationary phase, ten racemates were best separated by the T1 column including 4 that were separated only by this CSP, ten analytes were best separated by the T2 CSP including 9 that were separated only by this CSP. There are five compounds can be separated by all of the four CSPs. All of them are neutral molecules containing a hetero-five-member-ring in the structure. For the compound 5-(4-hydroxyphenyl)-5-phenylhydantoin, both the D1 and D2 CSPs gave much higher enantioselectivities and resolutions than those of T1 and T2 CSPs. The enantioselectivity factors for D1 and D2 are 1.95 and 4.07 respectively, and their resolutions correspond to 2.5 and 7.0 respectively, which indicates the excellent chiral resolving capabilities of dalbavancin. Interestingly, the separation results changed significantly if a small alteration is made to the analyte's structure. For example, the only structural difference between 5-(3-hydroxyphenyl)-5-phenylhydantoin and 5-(4-hydroxyphenyl)-5-phenylhydantoin is position of the phenolic group. However, the previous baseline separation (R_s 7.0) achieved on D2 for 5-(4-hydroxyphenyl)-5-phenylhydantoin was downgraded to a partial separation (R_s 1.3) on D2 for 5-(3-hydroxyphenyl)-5-phenylhydantoin. The substantial decline in the enantiomeric selectivity and resolution indicates that the position of phenol group is very important for chiral recognition. Some of the compounds separated in the polar organic mode can also be separated in the normal phase mode. For example, enantiomers of 2-carbethoxy- γ -phenyl- γ -butyrolactone can be separated on all of the four CSPs and was baseline separated by D2. However, it was only

partially separated on D2 in the polar organic mode (R_s 0.7). This is because the analyte does not retain long enough to interact with the chiral selectors in the polar organic mode.

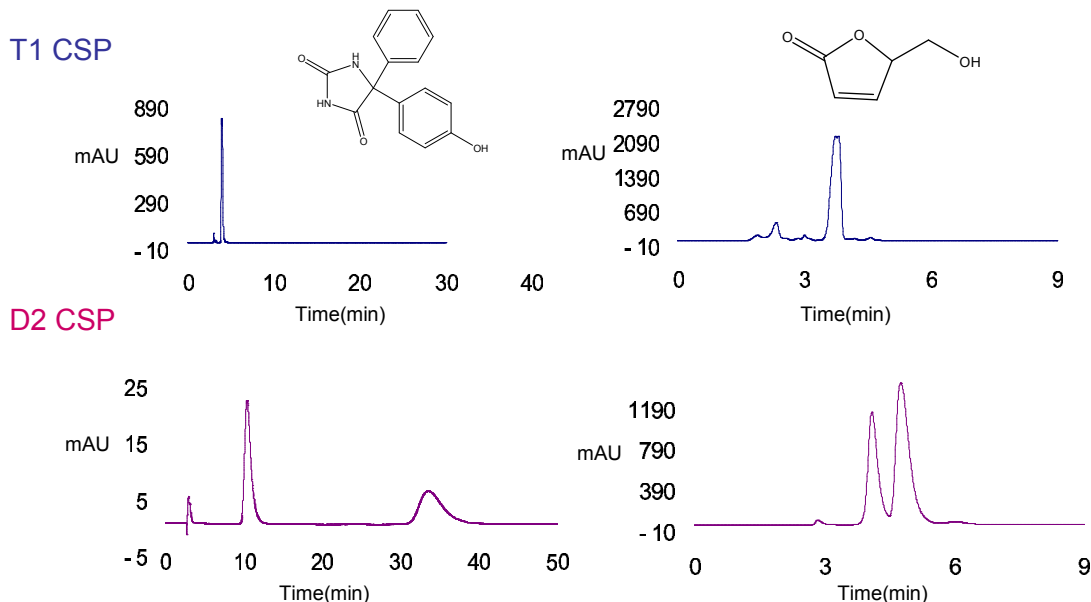


Figure 2.4. Representative chromatograms of two analytes on the T1 and D2 CSPs in the polar organic phase mode: 100% methanol; flow rate 1ml/min

2.4.2.3 Comparison of CSPs in the reversed phase mode

Previous studies have revealed that reversed phase separations are among the most successful for the glycopeptide CSPs. Clearly, dalbavancin and teicoplanin CSPs follow this trend (see Fig. 5). 54 racemates have been separated by these four columns together. The results are listed in Table 3. Twenty three racemic solutes can be separated on both dalbavancin and teicoplanin CSPs. This suggests that these two chiral selectors have somewhat analogous chiral recognition capabilities due to their similar structures. Fourteen racemates were only separated on the dalbavancin columns. This also demonstrates that these two classes of CSPs are complimentary to each other. Atrolactic acid hemihydrate was baseline separated by D1 ($\alpha = 1.82$, $R_s = 2.4$) and D2 ($\alpha = 5.05$, $R_s = 4.9$) CSPs, but it was not

separated on either of the teicoplanin based columns. These differences in enantioselective Gibbs energy correspond to 0.3 kcal/mol for D1, 0.9 kcal/mol for D2 and 0 kcal/mol for T1 and T2. In this particular example, the dalbavancin columns are much more effective. Interestingly, many of the analytes that are only separated on dalbavancin based CSPs have a free carboxylic group in their structure, such as N-(α -methylbenzyl)phthalic acid monoamide, α -methoxyphenylacetic acid, 3-oxo-1-indancarboxylic acid, 2-phenoxypropionic acid, 2-phenylpropionic acid, β -phenyllactic acid and 1,2,3,4-tetrahydro-3-isoquinolinecarboxylic acid hydrochloride. This improved enantioselectivity towards carboxylic acids may be partly attributed to the tertiary amino group coupled to dalbavancin via an amide linkage (Fig. 2.1). In aqueous solution at pH 4.2, this group is protonated and carries a positive charge. This cationic site can interact with deprotonated carboxylic anions through charge-charge interactions which is an important process in chiral recognition. In contrast, the teicoplanin based CSPs (i.e. T2) only separated one of the tested amino acids, DL- α -aminophenyl-acetic acid and one of the tested carboxylic acids, 2-(2-chlorophenoxy)-propionic acid ($R_s=0.4$). Although there is one cationic site on native teicoplanin, it can be converted to a carbamate group when bonded to silica gel. Thus, the teicoplanin chiral selector only has one anionic site after linked to silica gel. The poorer enantioselectivity of teicoplanin to some of the carboxylic acids in this study should be partially due to the lack of cationic sites on the teicoplanin molecule.

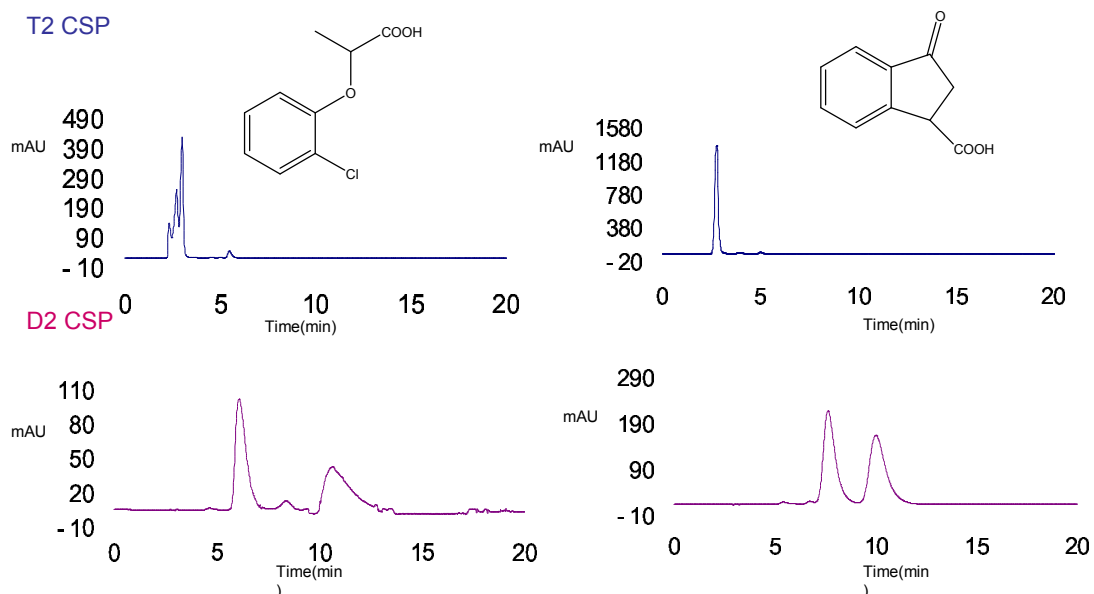


Figure. 2.5 Representative chromatograms of two analytes on the T2 and D2 CSPs in the reversed phase mode: 20mM NH_4NO_3 buffer/methanol 1/1 v/v; flow rate 1ml/min

Table 2.1 Chromatographic data for the normal phase resolution of racemic compounds on D1, D2, T1 and T2 columns

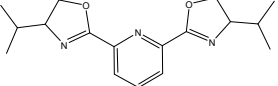
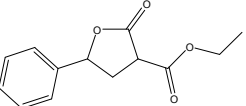
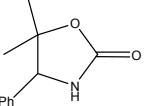
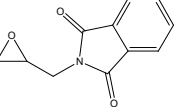
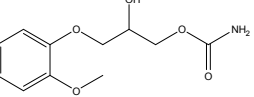
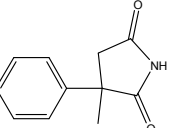
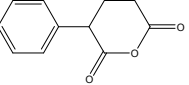
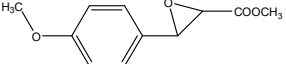
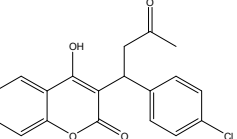
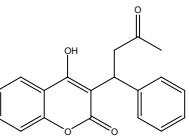
Compound name	Structure	CSPs	80% Heptane/20% Ethanol		
			k_1	α	R_s
2,6-Bis(4-isopropyl-2-oxazolin-2-yl)pyridine		D1	1.04	1.18	1.0
2-Carboethoxy-gamma-phenyl-gamma-butyrolactone		D1	1.34	1.13	0.9
		D2	2.90	1.35	1.5
		T1	1.47	1.03	0.5
		T2	1.15	1.07	0.5
5,5-dimethyl-4-phenyl-2-oxazolidinone		D1	3.93	1.38	1.4
		D2	10.72	1.57	1.8
		T2	4.19	1.44	1.4
N-(2,3-Epoxypropyl)-phthalimide		D2	2.28	1.12	0.9
		T1	1.99	1.07	1.0
Guaiacol glyceryl ether carbamate		T1	7.72	1.05	0.5
alpha-Methyl-alpha-phenyl-succinimide		D1	2.02	1.11	0.9
		D2	4.52	1.44	2.2
		T1	2.37	1.23	1.5
		T2	2.40	1.21	1.4
2-Phenylglutaric anhydride		T1	3.27	1.06	0.5
Methyl trans-3-(4-methoxyphenyl) glycidate		D2	1.07	1.58	1.8
3-(alpha-Acetyl-4-chlorobenzyl)-4-hydroxycoumarin		D1	0.88	1.39	1.4
		D2	0.85	1.21	0.7
		T2	0.89	1.21	1.2
Warfarin		D1	0.83	1.44	1.5
		D2	1.91	1.17	0.8
		T2	0.89	1.17	1.0

Table 2.1 Continued

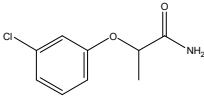
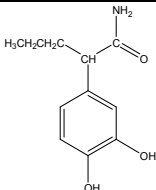
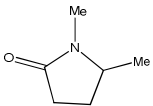
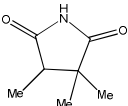
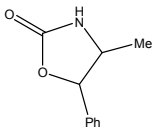
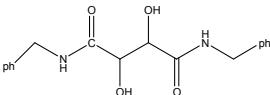
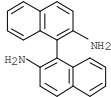
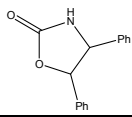
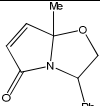
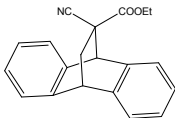
Compound name	Structure	CSPs	80% Heptane/20% Ethanol		
			k_1	α	R_s
2-(3-chlorophenoxy)propionamide		D1	1.49	1.13	1.0
		D2	2.97	1.36	2.2
		T1	2.21	1.09	1.2
		T2	2.18	1.12	1.3
DL-3,4-dihydroxyphenyl- α -propylacetamide		D1	7.43	1.07	0.6
1,5-Dimethyl-2-pyrrolidinone		D2	2.62	1.26	1.3
		T1	3.31	1.03	1.4
α,α -Dimethyl- β -methylsuccinimide		D1	1.05	1.33	1.5
		D2	2.10	1.51	2.5
		T1	1.69	1.10	1.4
		T2	1.55	1.16	1.3
1,5-Dimethyl-4-phenyl-2-imidazolidinone		D1	1.57	1.26	1.4
		D2	4.86	1.65	3.6
		T1	3.24	1.70	2.3
		T2	2.78	1.11	1.0
N,N' -Dibenzyl-tartramide		T1	6.41	1.04	0.5
2,2'-Diamino-1,1'-binaphthalene		D2	5.03	1.05	0.5
		T2	3.40	1.16	1.3
cis-4,5-Diphenyl-2-oxazolidinone		D1	4.52	1.66	2.6
2,3-Dihydro-7 α -methyl-3-phenylpyrrolo[2,1-b]oxazol-5(7 α H)-one		T1	2.29	1.04	0.8
		T2	1.90	1.05	0.5
Ethyl 11-cyano-9,10-dihydro-endo-9,10-ethanoanthracene-11-carboxylate		D2	1.03	1.17	0.8
		T1	0.72	1.05	0.5

Table 2.1 Continued

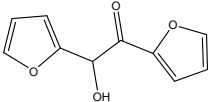
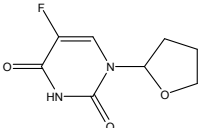
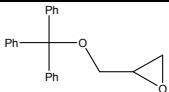
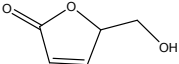
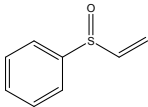
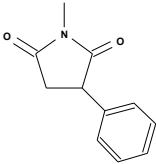
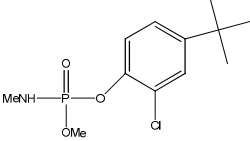
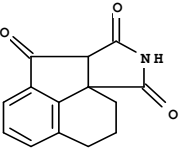
Compound name	Structure	CSPs	80% Heptane/20% Ethanol		
			k_1	α	R_s
furoin		D1	2.61	1.04	1.0
		D2	6.45	1.28	1.3
		T1	3.28	1.22	2.3
		T2	3.88	1.20	1.8
Ftorafur		D1	7.58	1.33	1.4
		T1	15.90	1.17	0.9
Glycidyl trityl ether		T2	0.24	1.15	0.5
5-hydroxymethyl-2(5H)-furanone		D2	7.77	1.27	1.5
Phenyl vinyl sulfoxide		D1	1.41	1.09	0.8
Phensuximide		D2	2.55	1.12	0.9
		T1	2.28	1.11	1.4
		T2	2.13	1.22	1.6
Ruelene		D2	0.79	1.09	0.5
		T2	0.66	1.71	1.2
3a,4,5,6-Tetrahydro-succinido[3,4-b]acenaphthen-10-one		D1	5.93	1.44	1.8
		T1	6.79	1.25	1.4
		T2	0.59	1.94	0.9

Table 2.2 Chromatographic data for the polar organic phase resolution of racemic compounds on D1, D2, T1 and T2 columns

Compound name	Structure	CSPs	100% MeOH		
			k_1	α	R_s
Chlorthalidone		D2	0.44	1.28	0.7
2-Carboethoxy-gamma-phenyl-gamma-butyrolactone		D2	0.13	1.51	0.7
5,5-dimethyl-4-phenyl-2-oxazolidinone		D1	0.22	1.38	1.0
		T2	0.13	2.03	1.4
alpha-Methyl-alpha-phenyl-succinimide		D2	0.23	1.30	0.7
(cis)-(±)-3,3a,8,8a-Tetrahydro-2H-indeno[1,2-d]oxazol-2-one		D1	0.84	1.98	3.0
		D2	2.74	1.96	2.7
		T1	1.02	1.23	1.0
		T2	0.70	1.15	0.9
2-(4-Nitrophenyl)propionic acid		T2	0.17	1.35	0.7
4-Methyl-5-phenyl-2-oxazolidinone		D1	0.26	2.36	2.5
		D2	0.53	4.24	5.5
		T1	0.28	2.79	4.4
Alprenolol		T2	3.46	1.25	2.7
DL-alpha-Aminophenyl-acetic acid		T2	0.30	3.77	1.3
2-Azabicyclo[2.2.1]hept-5-en-3-one		D1	0.24	1.20	0.8
		D2	0.61	1.19	0.9

Table 2.2 Continued

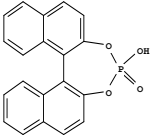
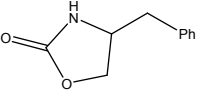
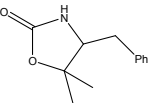
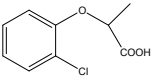
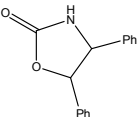
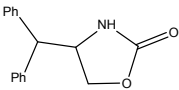
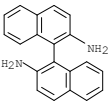
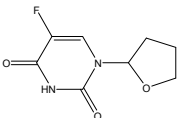
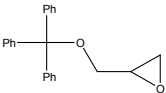
Compound name	Structure	CSPs	100% MeOH		
			k_1	a	R_s
1,1'-Binaphthyl-2,2'-diyl hydrogenphosphate		T1	0.21	1.87	3.2
4-Benzyl-2-oxazolidinone		D1	0.61	1.16	0.9
		D2	2.07	1.08	0.5
		T1	0.72	1.29	1.5
		T2	0.39	1.23	0.9
4-Benzyl-5, 5-dimethyl-2-oxazolidinone		D1	0.29	1.20	0.8
		D2	0.65	1.78	2.3
		T1	0.36	2.73	4.8
		T2	0.15	1.84	1.4
DL-2-(2-Chlorophenoxy)-propionic acid		T2	0.04	3.85	1.3
cis-4,5-Diphenyl-2-oxazolidinone		D1	0.22	1.62	1.4
		T1	0.25	1.75	3.2
		T2	0.21	1.71	1.5
4-(Diphenylmethyl)-2-oxazolidinone		D1	0.38	1.45	1.2
		D2	1.08	1.47	1.5
		T1	0.41	1.55	1.6
2,2'-Diamino-1,1'-binaphthalene		T2	0.24	1.10	0.5
Ftorafur		D1	0.29	1.20	0.8
		T1	0.50	1.08	0.6
Glycidyl trityl ether		T1	0.09	1.23	0.5

Table 2.2 Continued

Compound name	Structure	CSPs	100% MeOH		
			k_1	α	R_s
5-(4-hydroxyphenyl)-5-phenylhydantoin		D1	0.51	1.95	2.5
		D2	2.59	4.07	7.0
		T1	0.36	1.08	0.5
		T2	0.68	1.44	1.4
5-(3-hydroxyphenyl)-5-phenylhydantoin		D2	1.51	1.32	1.3
		T1	0.32	1.11	0.6
		T2	0.49	1.23	0.9
Hydrobenzoin		T1	0.09	1.22	0.5
DL-Homocysteine thiolactone hydrochloride		T2	3.06	1.19	1.8
4-Hydroxy-2-pyrrolidinone		D2	0.60	1.37	1.3
5-(Hydroxymethyl)-2-pyrrolidinone		D2	0.68	2.06	2.9
		T1	0.50	1.19	1.4
5-hydroxymethyl-2(5H)-furanone		D2	0.42	1.54	1.4
		T1	0.29	1.08	0.5
Iopanoic acid or(3-[3-Amino-2,4,6-triiodophenyl]-2-ethyl-propanoic acid		D1	0.26	1.23	0.9
Methoxyphenamine		D2	0.50	1.78	2.2
		T1	0.31	1.27	1.2
		T2	0.34	1.23	0.8
Mephesisin		T1	0.09	1.32	0.6

Table 2.2 Continued

Compound name	Structure	CSPs	100% MeOH		
			k_1	a	R_s
Metanephrine hydrochloride		T2	1.83	1.29	1.0
2-Phenoxypropionic acid		T2	0.02	6.80	1.2
5-Phenyl-2-(2-propynyl-amino)-2-oxazolin-4-one		D1	0.27	1.88	1.3
		D2	0.46	3.81	3.0
		T1	0.31	1.46	0.9
Bamethane		T2	3.88	1.19	1.5
3a,4,5,6-Tetrahydro-succininido[3,4-b]acenaphthen-10-one		D1	0.30	1.14	0.7
		D2	0.81	1.24	0.9
		T1	0.31	1.16	1.0
		T2	0.33	1.19	0.7

Table 2.3 Chromatographic data for the reversed phase resolution of racemic compounds on D1, D2, T1 and T2 columns

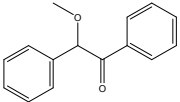
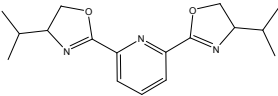
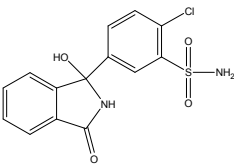
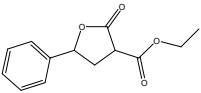
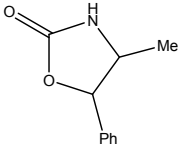
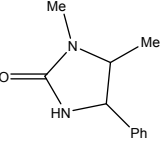
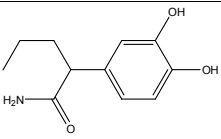
Compound name	Structure	CSPs	NH ₄ OAc Buffer 50%/ MeOH 50%		
			K ₁	A	R _s
Benzoin methyl ether		D2	6.25	1.29	1.4
2,6-Bis(4-isopropyl-2-oxazolin-2-yl)pyridine		D2	1.74	1.58	2.3
		T2	0.79	1.94	3.0
Chlorthalidone		D2	1.86	1.41	1.3
		T1	0.45	1.12	0.8
		T2	0.93	1.06	0.5
2-Carboethoxy-gamma-phenyl-gamma-butyrolactone		D2	5.21	1.11	0.8
1,5-dimethyl-4-phenyl-2-imidazolidinone		D2	2.80	1.21	1.4
		T1	0.57	1.05	0.5
		T2	2.06	1.10	0.9
1,5-dimethyl-4-phenyl-2-imidazolidinone		D2	2.80	1.21	1.4
		T1	0.57	1.05	0.5
		T2	2.06	1.10	0.9
3,4-dihydroxyphenyl-2-propylacetamide		D2	2.19	0.90	0.6

Table 2.3 Continued

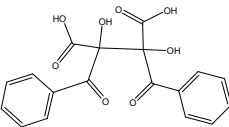
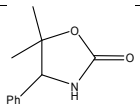
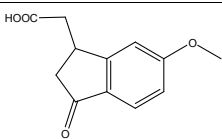
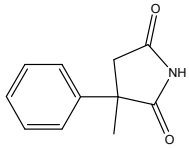
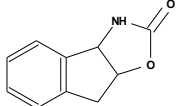
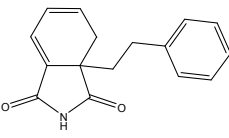
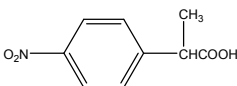
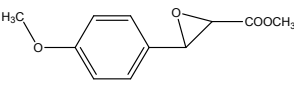
Compound name	Structure	CSPs	NH ₄ OAc Buffer 50%/ MeOH 50%		
			K ₁	A	R _s
2,3-Dibenzoyl-DL-tartaric acid		D2	3.01	1.10	0.5
5,5-dimethyl-4-phenyl-2-oxazolidinone		D1	0.75	1.84	1.2
5-Methoxy-1-indanone-3-acetic acid		D2	1.41	1.10	0.6
alpha-Methyl-alpha-phenyl-succinimide		D2	1.20	1.23	1.2
		T1	0.49	1.13	1.0
		T2	0.69	1.12	0.8
3,3a,8,8a-Tetrahydro-2H-indeno[1,2-d]oxazol-2-one		D1	1.52	1.61	1.5
(1-phenethyl)phthalimide		D2	4.81	1.10	0.8
		T1	0.89	1.07	0.8
		T2	2.38	1.06	0.5
2-(4-Nitrophenyl)propionic acid		D1	1.29	1.30	1.4
		D2	3.33	1.17	1.0
Methyl trans-3-(4-methoxyphenyl)glycidate		D2	1.49	1.10	0.6

Table 2.3 Continued

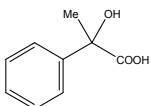
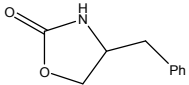
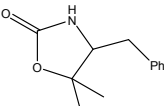
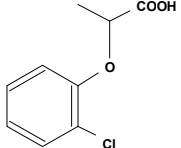
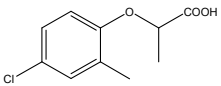
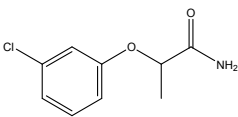
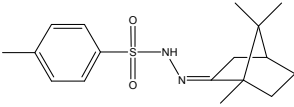
Compound name	Structure	CSPs	NH ₄ OAc Buffer 50%/ MeOH 50%		
			K ₁	A	R _s
Atrolactic acid hemihydrate		D1	0.80	1.82	2.4
		D2	0.59	5.05	4.9
4-Benzyl-2-oxazolidinone		T1	8.50	1.03	0.9
		T2	1.29	1.30	1.5
(-/+)-4-Benzyl-5,5-dimethyl-2-oxazolidinone		D1	1.46	1.31	1.5
		T1	1.00	3.57	5.9
2-(2-Chlorophenoxy)propionic acid		D1	1.00	1.42	1.2
		D2	1.10	2.43	2.4
		T2	0.04	0.62	0.4
2-(4-chloro-2-methylphenoxy)propionic acid		D1	1.21	1.33	1.2
		D2	1.63	1.64	2.0
2-(3-chlorophenoxy)propionamide		D2	1.42	1.18	1.0
		T2	0.77	1.04	0.4
(±)Camphor p-tosyl hydrazon		T1	0.97	1.14	1.0

Table 2.3 Continued

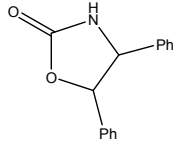
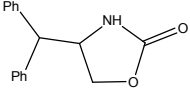
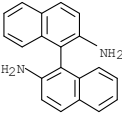
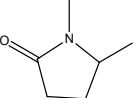
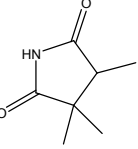
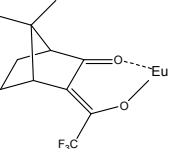
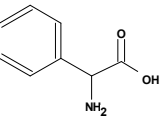
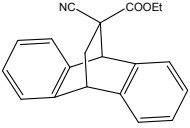
Compound name	Structure	CSPs	NH ₄ OAc Buffer 50%/ MeOH 50%		
			K ₁	A	R _s
cis-4,5-Diphenyl-2-oxazolidinone		D1	1.63	1.23	1.3
		T1	0.87	1.42	2.9
		T2	1.94	1.44	2.7
4-(Diphenylmethyl)-2-oxazolidinone		D1	2.28	1.20	1.2
		T1	1.31	1.59	1.8
		T2	2.06	1.22	1.3
2,2'-Diamino-1,1'-binaphthalene		T1	1.01	1.11	1.0
1,5-Dimethyl-2-pyrrolidinone		D2	0.35	1.16	0.6
		D2	0.37	1.52	1.4
alpha,alpha-Dimethyl-beta-methylsuccinimide		T1	0.30	1.07	0.5
		T2	0.29	1.14	0.6
Europium tris[3-(trifluoromethylhydroxymethylene)](-) camphorate		D2	2.09	1.33	0.8
DL-alpha-Aminophenylacetic acid		T2	0.50	5.05	4.6
Ethyl 11-cyano-9,10-dihydro-endo-9,10-ethanoanthracene-11-carboxylate		D2	4.66	1.04	0.5
		T2	2.07	1.07	0.6

Table 2.3 Continued

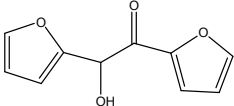
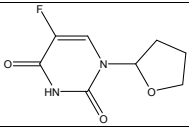
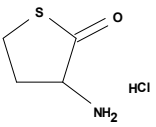
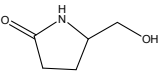
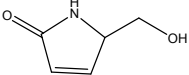
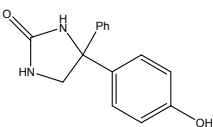
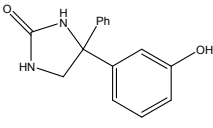
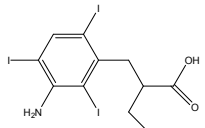
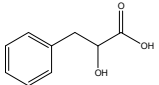
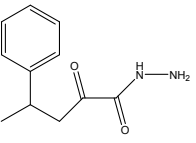
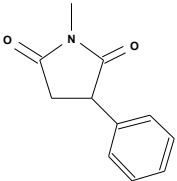
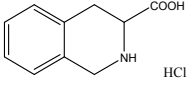
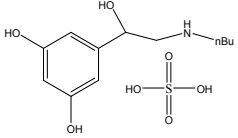
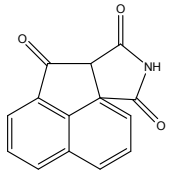
Compound name	Structure	CSPs	NH ₄ OAc Buffer 50%/ MeOH 50%		
			K ₁	A	R _s
furoin		D2	0.73	1.09	0.5
		T2	0.42	1.07	0.4
Ftorafur		T1	0.94	1.08	0.9
DL-Homocysteine thiolactone hydrochloride		D2	0.67	1.15	0.8
		T2	1.40	1.04	0.5
5-(Hydroxymethyl)-2- pyrrolidinone		D2	0.24	1.99	1.4
5-hydroxymethyl-2(5H)- furanone		D2	0.31	1.79	1.4
		T2	0.15	1.20	0.5
5-(4-hydroxyphenyl)-5- phenylhydantoin		D1	3.00	1.48	1.8
		T1	1.27	1.17	1.2
5-(3-hydroxyphenyl)-5- phenylhydantoin		D1	2.36	1.18	1.2
		T1	1.15	1.15	1.2
		T2	4.11	1.36	1.5
Iopanoic acid or(3-[3-Amino- 2,4,6-triiodophenyl]-2-ethyl- propanoic acid		D1	1.94	1.16	0.9

Table 2.3 Continued

Compound name	Structure	CSPs	NH ₄ OAc Buffer 50%/ MeOH 50%		
			K ₁	A	R _s
4-Isobutyl- α -methylphenylacetic acid		D1	1.91	1.08	0.7
(±)2,3-O-Isopropylidene 2,3-dihydroxy-1,4-bis(disphenylphosphino)butane		D2	4.67	1.21	1.0
Methoxyphenamine		D2	1.68	2.00	1.2
		T2	9.30	1.03	0.4
N-(α -Methylbenzyl)phthalic acid monoamide		D1	0.71	1.66	2.0
α -Methoxyphenylacetic acid		D1	0.66	1.07	0.5
3-Oxo-1-indancarboxylic acid		D2	1.64	1.50	1.5
2-Phenoxypropionic acid		D2	0.57	2.73	3.3
2-Phenylpropionic acid		D2	1.10	1.10	0.5
5-Phenyl-2-(2-propynylamino)-2-oxazolin-4-one		D1	0.86	1.69	1.5
Phenyl vinyl sulfoxide		D2	1.08	1.25	1.3
		T1	0.52	1.13	1.0
		T2	0.56	1.27	1.4

Table 2.3 Continued

Compound name	Structure	CSPs	NH ₄ OAc Buffer 50%/ MeOH 50%		
			K ₁	A	R _s
DL-beta-Phenyllactic acid		D1	0.41	1.14	0.6
(±)-5-(alpha-Phenethyl)semioxamide		D2	0.70	1.07	0.5
		T2	0.50	1.13	0.7
Phensuximide		D2	1.01	1.31	1.4
		T2	1.00	1.31	1.4
1,2,3,4-Tetrahydro-3-isoquinolinecarboxylic acid hydrochloride		D1	0.73	1.65	1.5
Terbutaline hemisulfate salt		T2	5.63	1.22	3.1
3a,4,5,6-Tetrahydro-succinido[3,4-b]acenaphthen-10-one		D1	1.06	1.30	1.2
		T1	0.93	1.42	5.0

2.5 Conclusion

Two dalbavancin-based CSPs were made using two different linkages to silica gel. Their enantiomeric separation capabilities have been investigated by comparison of the separations achieved on Chirobiotic T and T2 commercial columns. The structural differences in the chiral selectors and linkages between the four CSPs presented in this work do not make one superior to another. All of them can separate some racemic solutes that cannot be separated by the other CSPs tested. It is as expected that they show similar enantiomeric separation abilities to many analytes since their structures are very closely related. However, dalbavancin based CSPs exhibits enhanced enantioselectivities to carboxylic acids, where the additional cationic site of the chiral selector may play an important role during the chiral recognition process. Thus, it is obvious that these four CSPs are complementary to one another. If a racemate is poorly separated on one CSP, it is possible the other related CSPs will produce an enhanced separation. This is the principal of complementary separation that was model for the class of chiral selectors. Future work will involve the detailed study of elution order of enantiomers and binding linkage effects on dalbavancin based CSPs.

PART TWO: IONIC LIQUIDS IN ANALYTICAL CHEMISTRY

CHAPTER 3
GENERAL INTRODUCTION TO IONIC LIQUIDS AND THEIR APPLICATIONS IN
ANALYTICAL CHEMISTRY

Ionic liquids (ILs) are salts that melt below 100°C. Room temperature ionic liquids (RTIL) are defined as salts that are liquid at room temperature (25°C). ILs are composed of cations and anions just like inorganic salts such as sodium chloride. Cations are typically based on bulky organic cations such as imidazolium, pyridinium, pyrrolidinium, phosphonium, and ammonium. Anions are relatively simpler in structure and could be either inorganic ions (such as Cl⁻, Br⁻, BF₄⁻, PF₆⁻) or organic ions (such as trifluoromethylsulfonate [CF₃SO₃]⁻, bis[(trifluoromethyl)sulfonyl]imide [(CF₃SO₂)₂N]⁻ (or NTf₂⁻), trifluoroethanoate [CF₃CO₂]⁻). Structures of cations and anions that are commonly used in IL are listed in figure 3.1. The high conformational flexibility and low symmetry of the cations or anions lead to inefficient packing in the solid state which results in low melting points for these materials.⁷⁵ More importantly, the physical and chemical properties can be easily altered by tuning the combination of cations and anions.

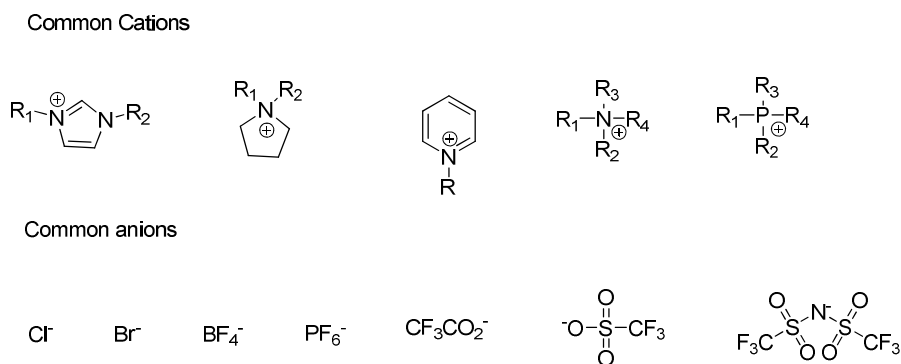


Figure 3.1 Structures of common cations and anions of ionic liquids

The history of IL can be traced back to 1914 when Walden found that ethylammonium nitrate was a liquid at room temperature.⁷⁶ However, this moisture sensitive salt did not trigger much interest in developing IL until the first air-water-stable based ILs were synthesized by Wilkes *et al.* in 1992.⁷⁷ These imidazolium based ILs have improved stability and wider liquid ranges and thus allowed scientists to further explore the potential applications of ILs in different aspects of chemistry. ILs were first applied in organic synthesis as substituents for traditional organic solvents especially for two phase catalysis reactions.⁷⁸ They can also be used as reaction media for all kinds of reactions such as metal complex synthesis, catalytic hydrogenation,⁷⁹ asymmetric synthesis,⁸⁰ etc.

Besides organic chemistry, ILs are valuable in various subdisciplines of analytical chemistry. i) Extractions. ILs such as butylmethylimidazolium (BMIM) BF₄⁻⁸¹ demonstrated great potential for liquid-liquid extractions in part because they possess good extraction power while their vapor pressures are negligible. Extractions of metal ions, small organic molecules and large molecules such as protein and DNA have all been performed successfully with ILs.⁸² The application of ILs in liquid phase microextraction (LPME) and solid phase microextraction (SPME) have also been exploited.⁸³ (ii) Chromatography. ILs are desirable coating materials for GC stationary phases due to their unique properties including low volatility, high viscosity, good thermal stability, and variable polarities. A plethora of GC achiral stationary phases based on a wide range of ILs of different structures and properties have been developed and studied. Among them, a cross-linked ionic liquid based stationary phase showed high selectivity and high thermal stability.⁸⁴ GC columns coated by dicationic RTILs with poly(ethyleneglycol) (PEG) linkages⁸⁵ and RTILs containing phosphonium⁸⁶ are particularly thermally stable at high temperatures. It needs to be noted that several IL-based GC stationary phases developed by Armstrong are now commercially available, which is indicative of the practical use of ILs in separation science. As for liquid chromatography, ILs can be either used as additive in mobile phases^{87, 88} or be used as stationary phases after immobilized onto silica gel.⁸⁹ (iii) MS. One of

the most successful applications of IL in analytical chemistry is their use as ion pair reagents for anion detection in positive ion mode of ESI-MS.⁹⁰ Improvements in anion detection limits of several orders of magnitude were reported. Typically, a dicationic IL can pair with a singly charged anion to form a complex possessing an overall positive charge. Monitoring the anion-dication complex in the positive mode, at higher mass range, is more sensitive than detecting anions in the negative mode. It is because the corona discharge is more prevalent in the negative mode of detection and thus the signal to noise ratio in the negative mode are always lower as a result of the unstable ion current and high background noise. It needs to be mentioned that a liquid state for the ionic component is not required since ILs function just as common organic salts. MALDI-MS is another new application of ILs. IL matrixes are capable of minimizing polymer degradation and improving accuracy of molecular weights determination.⁹¹ Improved reproducibility for biomolecules were also achieved with IL matrices, which allows quantitative analysis without using internal standards.⁹²

Research in ILs is still growing rapidly and their applications will continue to expand into more fields in analytical chemistry. In the following chapters, application of newly developed ILs in mass spectrometry and gas chromatography will be discussed in detail.

CHAPTER 4

EVALUATION OF FLEXIBLE LINEAR TRICATIONIC SALTS AS GAS-PHASE ION-PAIRING REAGENTS FOR THE DETECTION OF DIVALENT ANIONS IN POSITIVE MODE ESI-MS

In this work, ion pairing reagents were designed and synthesized by me and Eranda. The MS detection is done by Zachery.

4.1 Abstract

Anion analysis is of great importance to many scientific areas of interest. Problems with negative mode ESI-MS prevent researchers from achieving sensitive detection for anions. Recently, we have shown that cationic reagents can be paired with anions, such that detection can be done in the positive mode, allowing for low limits of detections for anions using ESI-MS. In this analysis, we present the use of 16 newly synthesized flexible linear tricationic ion-pairing reagents for the detection of 11 divalent anions. These reagents greatly differ in structure from previously reported trigonal tricationic ion-pairing agents, such that they are far more flexible. Here we present the structural features of these linear trications that make for good ion-pairing agents as well as show the advantage of using these more flexible ion-pairing reagents. In fact, the limit of detection for sulfate using the best linear trication was found to be 25 times lower than when the best rigid trication was used. Also, MS/MS experiments were performed on the trication-dianion complex to significantly reduce the detection limit for many dianions. Limits of detection in this analysis were as low as 50 fg.

4.2 Introduction

Anion analysis is of great importance to environmental researchers, biochemists, food and drug researchers, and the pharmaceutical industry, all of which are continually in need of facile, sensitive analytical techniques that can be used to both detect and quantitate trace anions.⁹³⁻¹¹² Often, the anions of interest exist in complex matrixes such as blood, water, and urine.^{94, 98, 100, 113, 104-106} For this reason, separation techniques are routinely coupled with anion detection. Currently, some of these techniques utilize flow injection analysis or ion chromatography,^{109-112, 114-116} with detection frequently obtained through the use of ion selective electrodes, conductivity, or spectroscopic techniques.¹¹⁷⁻¹²¹ Yet, these detection methodologies lack either universality or specificity.¹²¹ For many analytes, ESI-MS has provided broad specificity and lower detection limits. Given the anion's inherent charge, it is not surprising that negative ion electrospray ionization mass spectrometry (ESI-MS) has come to the forefront as a general analytical approach that can be directly coupled with liquid chromatography (LC) if desired. Unfortunately, for most types of analytes, the negative ion mode often results in poorer limits of detection (LOD) than the preferred positive ion mode.^{122, 123} Because of high negative voltages, the negative ion mode is more prone to corona discharge than the positive mode. This causes the negative mode to have an increased chance for arcing events and ultimately more noise resulting in unsatisfactory LODs.¹²² Corona discharge in the negative mode can be controlled by using halogenated solvents and substituting more alkylated alcohols (i.e., butanol or isopropanol) for methanol.^{124,125} Ideally, LC-ESI-MS methodologies would use more common solvents, such as, methanol, water, and acetonitrile. Furthermore, it would be more practical to do all ion detection in the more stable and sensitive positive ion mode. Recently, we have developed a method for the detection of singly charged anions in positive mode ESI-MS using only water/methanol solvents.¹²⁶ This technique involves the addition of a low concentration of a dicationic ion pairing reagent to the mobile phase. The dication pairs with the singly charged anion, resulting in a complex possessing an overall plus one charge, which can be detected in

the positive ion mode. The benefits of this technique include (a) the use of more practical solvents, (b) substantial increases in the sensitivity, (c) ease of use, (d) the ability to detect anions that fall below a trapping mass spectrometer's low mass cutoff region, and (e) detection of the complex at a much higher mass-to-charge region where there is far less chemical noise. To fully take advantage of factor e alone, it is best to choose a relatively high-molecular weight pairing agent that will result in a complex of a single positive charge. Subsequently, the dicationic ion-pairing agent was used to determine the LODs for over 30 singly charged anions.¹²⁶ Also in this work, it was shown for the first time that MS/MS can often be used to further lower the LODs of these anions. Overall, this analysis showed the true ultrasensitivity of ion-pairing by producing the lowest reported LODs for several anions by any known technique.¹²⁶ The effectiveness of over 20 dicationic ion-pairing agents was evaluated in order to determine the structural properties that allow for low LODs.¹²⁷ A major finding in this study was that flexibility of the dication seemed essential for good sensitivity. Therefore, the best dicationic ion-pairing reagents cited were those which possessed a flexible alkyl chain that linked the two cationic moieties. Recently, the ion-pairing technique was extended to the use of tricationic reagents for the detection of divalent anions.¹²⁸ The essential tricationic reagents were found to bind divalent anions, and monitoring the complex in the positive ion mode was a more sensitive detection method than monitoring the naked doubly charged anions in the negative mode. However, the tricationic reagents used had a somewhat rigid trigonal structure (for a representative structure see the bottom of Figure 4.1), which may be an undesirable feature of an ion-pairing agent from a sensitivity standpoint.

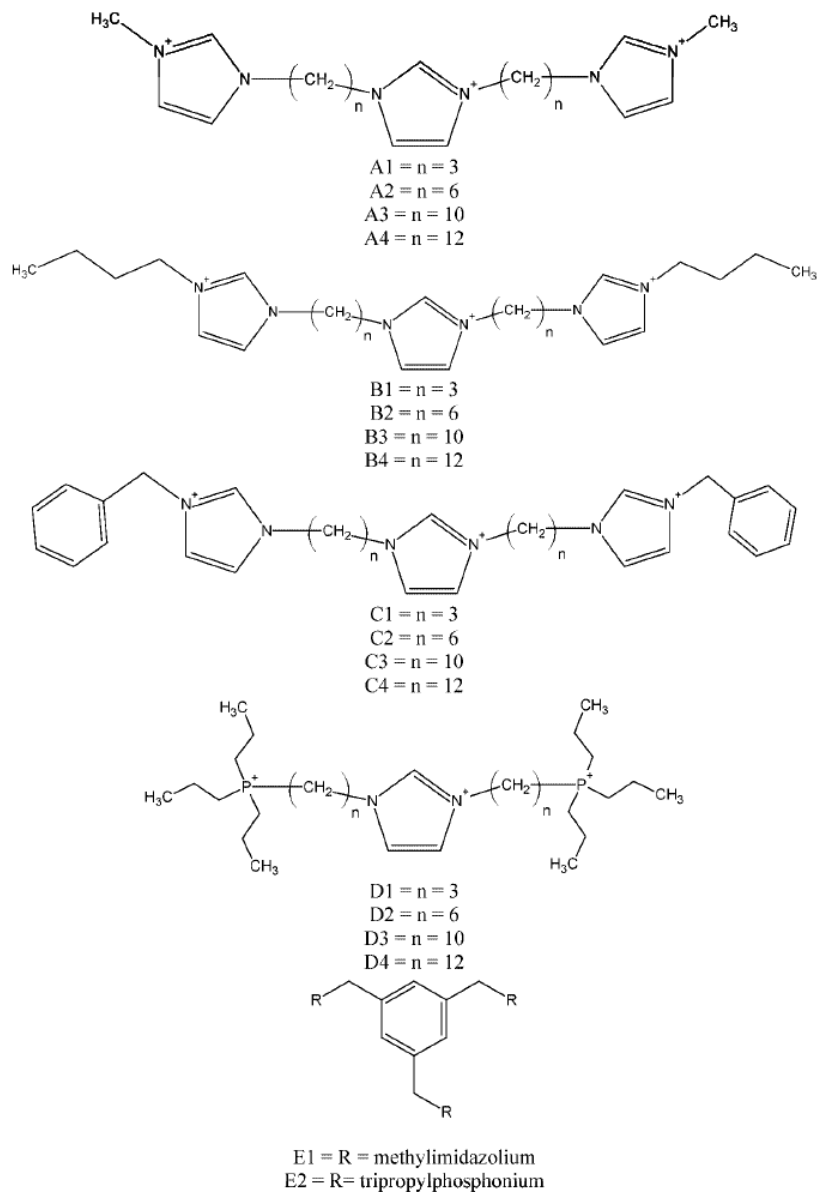


Figure 4.1 Structures of the tricationic ion pairing reagents used in this analysis

Recently, we devised a synthetic method to produce more flexible linear trications. In this work, we present the use of 16 newly synthesized linear tricationic ion-pairing reagents to determine the LOD for 11 divalent anions. Herein, we describe the differences and advantages of using the more flexible linear trications versus the more rigid trigonal trications. Also, we

show that MS/MS experiments can be performed on the linear trication-dianion complex and that by monitoring a fragment of the complex, the LOD often can be dramatically lowered. This is the first ever report of using this type of an MS/MS experiment to detect doubly charged anions in the positive ion mode with any tricationic ion-pairing agent.

4.3 Experiment Section

Materials and the synthetic procedure for the tricationic ionic liquids are described in literature.¹²⁹ Throughout this study, a Finnigan LXQ (Thermo Fisher Scientific, San Jose, CA) ESI-MS was used for all of the analyses. The MS was equipped with a six port injector (5 μ L loop) and was coupled with a Finnigan Surveyor MS pump. Between the injector and the ionization source, a Y-type mixing tee allowed for the addition of flow from a Shimadzu LC-6A pump. It was from this pump that the tricationic ion-pairing agent was introduced to the solvent flow. Overall, the total flow to the ESI was 400 μ L/min. The MS pump accounted for 300 μ L/min (67% MeOH/33% H₂O), while the LC pump applied the 40 μ M trication solution in water at a rate of 100 μ L/min. All the anions were dissolved HPLC grade water, such that their initial concentration was 1 mg/mL. Serial dilutions were made from the stock solutions, and the anions were directly injected using the six port injector. New stock solutions were prepared weekly, and the injector was expected to be the largest cause for possible experimental error (\pm 5%). The limits of detection were determined to be when an injection at a given concentration resulted in peaks giving a signal-to-noise ratio of 3. The ESI-MS conditions used here were the same as those previously used and optimized for the detection of perchlorate with a dicationic reagent, and were as follows: spray voltage, 3 kV; sheath gas flow, 37 arbitrary units (AU); auxiliary gas flow rate, 6 AU; capillary voltage, 11 V; capillary temperature, 350 $^{\circ}$ C; tube lens voltage, 105 V. When detecting the trication/dianion complex in the positive SIM mode, the SIM width was 5. When performing the SRM experiments, the isolation widths were between 1 and 5, the

normalized collision energy was 30, and the activation time was 30 ms. All data analysis was performed using the Xcalibur and Tune Plus software.

4.4 Results and Discussion

In previous reports, we have shown that dicationic ion-pairing reagents can be used to pair with singly charged anions, such that, the positively charged complex can be monitored in the positive mode, resulting in extremely low LODs.^{126, 127} More recently, we demonstrated that tricationic reagents could also be used to complex doubly charged anions, leading to much lower LODs for those divalent anions when detecting the complex in the positive mode.¹²⁸ Since the trications used previously had relatively rigid structures, a series of flexible ion-pairing agents were synthesized and tested to see if they offer greater sensitivity for the detection of anions in positive mode ESI. In addition, MS/MS of the paired ions was examined in hopes of further lowering the LOD in many cases.

Figure 4.1 shows the structures of the 16 linear trications used in this analysis (A1-4, B1-4, C1-4, and D1-4). All of the 16 linear trications have the same imidazolium core. They differ in the length of the alkyl chain (C_3 , C_6 , C_{10} , and C_{12}) that tethers the terminal charged moieties to the central imidazolium as well as in the nature of the terminal charged moieties (methylimidazolium, butylimidazolium, benzylimidazolium, and tripropylphosphonium). By examining this series of linear trications, we were able to observe possible advantages of varying the chain length (i.e., flexibility) as well as determine which cationic moieties produce the lowest LOD for the sample anions. Also shown in Figure 4.1 are the structures of two previously reported rigid trications.¹²⁸ Of these, the E1 trication was shown to be a moderately successful pairing agent, while trication E2 was found to be the best known trigonal tricationic ion-pairing agent.¹²⁸ The results of these two rigid trications allows for a definitive comparison to the new flexible trications developed for this study.

Table 4.1 lists the LODs for the 11 doubly charged anions, when paired with the 16 linear trications and monitored in the positive mode. Overall, the LODs for the divalent anions

ranged from the nanogram (ng) to the picogram (pg) level. In order to evaluate the effect of the chain length in the linear tricationic ion-pairing reagent, one can compare the trications of the same letter. For example, trications D1–4 differ only in the length of the hydrocarbon chain connecting the charged moieties (Figure 4.1). In general, it appears that the common trend is that linear trications with hexyl or decyl linkage chains gave the lowest LODs, whereas trications with propyl or dodecyl linkages resulted in higher LODs. This trend can be easily seen by comparing the LOD for thiosulfate when using the “D” series of linear trications. In this comparison, the order from best to worst ion-pairing agent was found to be D3, D2, D4, and D1. A likely explanation for this observation is that when the alkyl linkage chain is too short, the linear trication is less flexible and not as likely to “bend” around the anion. This finding supports our hypothesis that flexibility is a key feature in a good tricationic ion-pairing reagent. In contrast, when the alkyl chain gets too long, the cationic moieties are too far from each other and cannot work as a single unit when binding the anion. However, the effect of the linkage chain being too short is far more unfavorable than it being too long. An example of this can be seen in Table 4.1, where trication A1 with the shortest linkage chain was found to be one of the three worst ion-pairing agents for all anions. Clearly, the results (Table 4.1 and Figure 4.1) suggest that when using linear tricationic ion-pairing reagents, the alkyl linkage chain should be between 6 and 10 carbons in length.

Table 4.1 Limits of detection for divalent anions with linear tricationic reagents^a

sulfate		thiosulfate		oxalate		fluorophosphate	
trication	LOD (pg)	trication	LOD (pg)	trication	LOD (pg)	trication	LOD (pg)
D3	2.00×10^1	D3	6.25×10^1	C2	1.20×10^1	D4	2.50×10^1
D4	7.50×10^1	C2	6.25×10^1	D2	3.50×10^1	D3	2.63×10^1
D2	1.25×10^2	B3	6.25×10^1	A2	8.10×10^1	E2	3.75×10^1
B3	2.00×10^2	B2	6.25×10^1	D4	1.25×10^2	D2	4.25×10^1
B4	2.60×10^2	D2	7.50×10^1	B4	1.25×10^2	B3	9.00×10^1
C1	3.00×10^2	B4	7.50×10^1	D3	2.50×10^2	C3	1.50×10^2
B2	3.25×10^2	C1	8.75×10^1	E2	2.50×10^2	A3	2.00×10^2
C4	3.50×10^2	D4	9.00×10^1	A3	3.00×10^2	A2	2.00×10^2
C3	3.75×10^2	D1	1.00×10^2	B1	3.00×10^2	D1	2.00×10^2
C2	4.50×10^2	C4	1.00×10^2	B2	3.25×10^2	C4	2.10×10^2
B1	5.00×10^2	A3	1.00×10^2	C4	4.00×10^2	C2	2.25×10^2
E2	5.00×10^2	A4	1.00×10^2	C3	4.40×10^2	B2	2.75×10^2
A2	5.50×10^2	A2	1.25×10^2	C1	5.00×10^2	A4	4.50×10^2
A4	5.75×10^2	B1	1.25×10^2	E1	5.00×10^2	B4	5.00×10^2
A3	6.00×10^2	E2	1.25×10^2	A4	5.50×10^2	B1	8.75×10^2
D1	6.25×10^2	C3	1.75×10^2	A1	6.50×10^2	C1	1.50×10^3
E1	6.25×10^2	A1	5.00×10^2	D1	8.25×10^2	A1	4.50×10^3
A1	1.75×10^3	E1	7.50×10^2	B3	2.08×10^3	E1	5.00×10^4

Table 4.1 – *Continued*

dibromosuccinate		hexachloroplatinate		nitroprusside		dichromate	
trication	LOD (pg)	trication	LOD (pg)	trication	LOD (pg)	trication	LOD (pg)
D3	1.25×10^2	D2	3.50×10^1	C2	7.00	C4	3.50×10^3
E2	1.79×10^2	B2	3.50×10^1	D1	7.50	B4	3.75×10^3
D1	2.00×10^2	D1	3.75×10^1	E2	7.50	C3	3.88×10^3
C1	2.75×10^2	D3	4.00×10^1	C1	1.00×10^1	B3	4.25×10^3
B4	3.25×10^2	C2	5.00×10^1	D2	1.25×10^1	A3	5.00×10^3
B1	3.50×10^2	B1	7.00×10^1	B1	1.25×10^1	D4	5.50×10^3
B3	3.75×10^2	B3	7.50×10^1	D3	2.00×10^1	D3	6.25×10^3
A3	4.50×10^2	B4	7.50×10^1	B2	2.00×10^1	A4	6.25×10^3
C3	5.00×10^2	C1	7.50×10^1	C3	2.25×10^1	B1	6.25×10^3
D4	5.00×10^2	A2	7.50×10^1	B3	2.50×10^1	C2	6.38×10^3
A4	5.00×10^2	E2	7.50×10^1	A2	2.50×10^1	C1	6.50×10^3
D2	6.25×10^2	C4	8.50×10^1	A3	3.00×10^1	D2	7.50×10^3
C2	7.50×10^2	D4	1.00×10^2	B4	3.25×10^1	B2	7.50×10^3
B2	7.50×10^2	C3	1.25×10^2	D4	3.75×10^1	A2	7.50×10^3
A2	2.50×10^3	A3	1.25×10^2	C4	3.75×10^1	D1	8.75×10^3
A1	3.00×10^3	A4	1.75×10^2	A1	3.75×10^1	E2	1.00×10^4
E1	5.00×10^3	A1	5.00×10^2	E1	4.86×10^1	E1	1.25×10^4
C4	5.00×10^4	E1	1.58×10^3	A4	5.00×10^1	A1	1.50×10^4

Table 4.1 – *Continued*

selenate		o-benzenedisulfonate		bromosuccinate	
trication	LOD (pg)	trication	LOD (pg)	trication	LOD (pg)
E2	7.50×10^1	E2	1.50×10^1	E2	7.50×10^1
B3	2.50×10^2	D1	1.63×10^1	C4	6.25×10^2
C4	2.75×10^2	C1	1.75×10^1	D3	7.50×10^2
D3	3.75×10^2	B1	2.00×10^1	D1	7.50×10^2
B1	4.00×10^2	C2	3.20×10^1	A4	8.00×10^2
C2	4.25×10^2	B4	4.00×10^1	C2	1.00×10^3
C3	4.40×10^2	B2	4.00×10^1	B4	1.00×10^3
D4	5.00×10^2	D2	4.75×10^1	C3	1.50×10^3
D2	5.00×10^2	D3	6.50×10^1	D4	2.00×10^3
C1	5.00×10^2	A4	6.50×10^1	D2	2.25×10^3
B2	5.00×10^2	C3	7.50×10^1	A3	3.75×10^3
B4	5.25×10^2	E1	7.50×10^1	B3	4.00×10^3
A4	5.50×10^2	D4	1.00×10^2	E1	4.99×10^3
A3	7.00×10^2	B3	1.00×10^2	C1	5.00×10^3
D1	7.50×10^2	A3	1.00×10^2	A2	5.00×10^3
A2	7.50×10^2	A2	1.25×10^2	B2	5.50×10^3
E1	1.13×10^3	A1	3.75×10^2	B1	7.50×10^3
A1	3.38×10^3	C4	8.75×10^3	A1	1.25×10^4

a: The limit of detection was determined to be the amount of analyte that resulted in S/N = 3. Also, the data for E1 and E2 were extracted from ref¹²⁸. Note that the bold numbered ion-pairing agents are the two best linear trications, and the italicized ion-pairing agents are the two trigonal trications.

By evaluation of the data for a series of trications that all have the same linkage chain but different cationic moieties, the best terminal charged groups can be determined. Typically, the linear trications possessing the *N*-benzylimidazolium (the “C” moiety) and the

tripropylphosphonium (the “D” moiety) terminal charged groups resulted in lower LODs than the *N*-methylimidazolium (the “A” moiety) or butylimidazolium (the “B” moiety) cationic groups. This observation is shown by the LODs for oxalate when paired with the linear tricationic “2” series. The order from best to worst ion-pairing agents was found to be C2, D2, A2, and B2. Another example of this can be seen in the LODs for both nitroprusside and dichromate, where (from best to worst) the order was C2, D2, B2, and A2. These results, along with the previously noted optimum linkage chain lengths, allow for the determination that trications C2 and D3 were the overall best tricationic ion-pairing agents. Trication C2 has hexyl linkage chains and benzylimidazolium terminal charged groups, and trication D3 has decyl linkage chains and tripropylphosphonium cationic moieties. Interestingly, in the three comprehensive studies we have done on ion-pairing agent structures, the tripropylphosphonium cationic moiety is the only one that has always resulted in a recommended ion-pairing agent.^{127, 128}

The other important comparison to be made with the data in Table 4.1 is the LODs resulting from using the flexible linear trications versus the more rigid trigonal trications (E1 and E2). As can be seen, the best linear trications, C2 and D3, rank very near the top for most of the anions tested. However, the best trigonal trication, E2, also ranks very near the top for many of the tested anions. From this observation, it was determined that the best linear trications and the best trigonal trication both work well when monitoring the same divalent anions. Interestingly, the linear and trigonal ion-pairing reagents seem to be complimentary to one another. Overall, the best linear trication was not found to be a greatly superior ion-pairing agent when compared to the best trigonal trication. Yet, some very useful and somewhat complimentary tricationic ion-pairing reagents were added to our repertoire. However, if you compare trigonal trication E1 (the moderately successful trigonal trication) to the flexible linear trications, it can be seen that trication E1 ranks near the bottom for all the anions tested. It was determined that in general, the more flexible trications are better ion-pairing agents than the rigid trications. Obviously, there are other factors that play a part in finding the optimum ion-pairing agent, which allow

trication E2 to work as well as the linear trications. Perhaps the most important factor is that it contains the highly favorable tripropylphosphonium moiety.

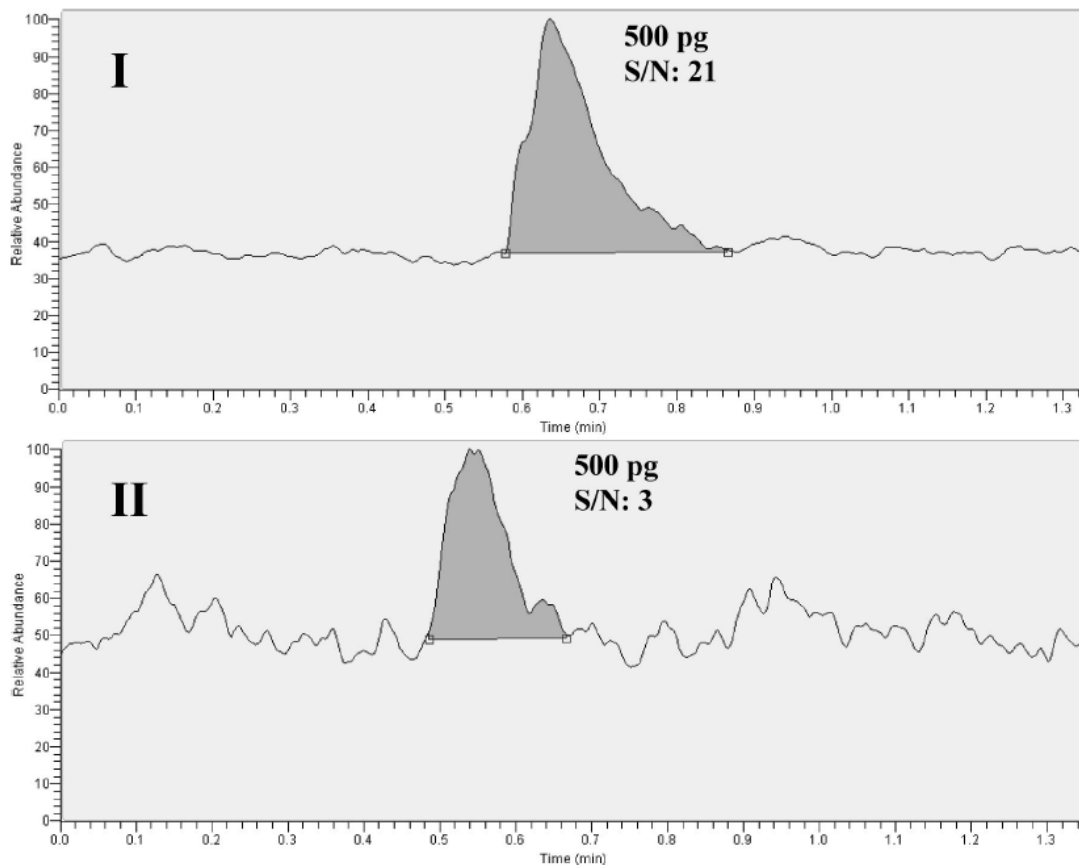


Figure 4.2 Comparison of the detection of sulfate in the positive mode using tricationic ion-pairing reagents D3 (I) and E2 (II)

Figure 4.2 illustrates the benefits of using a linear trication versus a trigonal trication for the detection of sulfate in the positive mode. In both detection scenarios, the same concentration of sulfate was injected (500 pg). In the upper panel (I), the ion-pairing agent was the best linear trication D3, and in the lower panel (II) the best trigonal trication E2 was used. It is apparent that the linear trication resulted in superior detection of sulfate, with a signal-to-noise 7 times greater than that for the trigonal trication. It should be noted that sulfate itself has a mass-to-charge ratio of -48 , thus falling below the low mass cutoff of our MS instrument and rendering itself undetectable in the negative mode.

Another facet of this study was to show that single reaction monitor (SRM) experiments could be performed on the trication–anion complex and that by monitoring a positively charged fragment of the complex, lower LODs for the divalent anions could be achieved. The key part of this type of experiment is to find the proper fragment to monitor. In many cases the fragmentation was the same but not always. Figure 4.3 shows a proposed fragmentation pattern for the more commonly observed disassociation of a trication D3–dianion complex. As is shown by Figure 4.3, collision induced disassociation (CID) typically resulted in a singly charged alkyl linked phosphonium imidazole, which had a mass-to-charge ratio of 367.4. Monitoring this fragment can lead to a decrease in the LOD for the anion that was part of the parent complex.

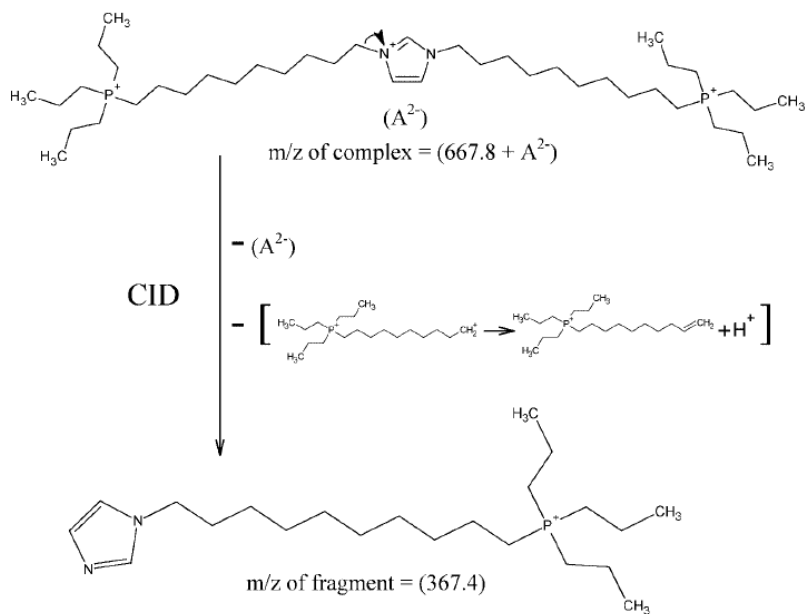


Figure 4.3 Proposed fragmentation pattern for a typical SRM experiment using trication D3

Table 4.2 lists the results for the SRM experiments that were performed in this analysis. Trications D3 and C2 were paired with 11 divalent anions and tested for their LOD using the SRM method. For comparison, the SIM results are listed next to the SRM results. As can be seen, the SRM mode often resulted in lower LODs than the SIM mode. There were two analytes (D3/bromosuccinate and C2/oxalate) that showed no improvement, but in general there was

nearly an order of magnitude improvement when using the SRM mode. In three cases, the SRM mode resulted in a 2 orders of magnitude decrease in the LOD. One of these cases was the detection of nitroprusside using tetrabutylammonium C2 as the ion-pairing agent and employing the SRM mode. For this system, the LOD for nitroprusside was determined to be 50 fg, which is the lowest LOD for any mono- or divalent anion that has been tested to date. Clearly this is a very facile and sensitive method.

Table 4.2 Comparison of LODs in the SIM positive and SRM positive modes

	trication D3			trication C2		
	SIM LOD (pg)	SRM LOD (pg)	SRM mass	SIM LOD (pg)	SRM LOD (pg)	SRM mass
sulfate	2.00×10^1	1.50×10^1	367.4	4.50×10^2	3.00×10^2	309.2
thiosulfate	6.25×10^1	5.00×10^{-1}	367.4	6.25×10^1	3.50×10^1	309.2
oxalate	2.50×10^2	1.00×10^2	367.4	1.20×10^1	7.50×10^1	549.2
fluorophosphate	2.63×10^1	2.05×10^1	367.4	2.25×10^2	1.00×10^2	309.2
dibromosuccinate	1.25×10^2	1.25×10^1	745/747	7.50×10^2	2.00×10^1	629/631
hexachloroplatinate	4.00×10^1	4.50	1003.5	5.00×10^1	2.00×10^1	889.4
nitroprusside	2.00×10^1	3.50	853.5	7.00	5.00×10^{-2}	737.4
dichromate	6.25×10^3	5.75×10^2	367.4	6.38×10^3	3.00×10^3	643.4
selenate	3.75×10^2	2.00	367.4	4.25×10^2	6.00×10^1	309.2
<i>o</i> -Benzenedisulfonate	6.50×10^1	1.00×10^1	367.4	3.20×10^1	3.75×10^1	309.2
bromosuccinate	7.50×10^2	1.00×10^3	745/747	1.00×10^3	1.00×10^3	629/631

Also, listed in Table 4.2 are the SRM fragment masses that were monitored. As noted previously, many complexes produce the same 367.4 fragment for trication D3 and the 309.2 fragment for trication C2. However, it was observed that there are some trication/dianions that

follow different disassociation pathways. For example, the trication D3–hexachloroplatinate complex produced a fragment with a mass-to-charge ratio of 1003.5. This fragment corresponds to the loss of one chlorine atom from the hexachloroplatinate, while the overall cation–anion complex remained intact. A similar effect was seen with the SRM detection for nitroprusside. Here, nitroprusside loses a nitro group and still stays complexed with the trication. For these cases, it is interesting to see that the noncovalent trication–dianion complex remains intact, while covalent bonds have been broken. One more example of this type of fragmentation was for bromine containing anions. Here the central imidazolium loses its acidic proton (in the 2 position of the imidazolium ring) and becomes a dication. This dication then complexes with a bromide anion that was lost from the dianion. This means that for any bromine containing dianions, the same fragment could be monitored (m/z 745/747 for D3 and m/z 629/631 for C2).

It should be noted that although the LODs for the 11 divalent anions in SIM and SRM are already quite low, they could be lowered further by completely optimizing the conditions for a particular complex. In this analysis, one general set of conditions were used for the entire study. Previously, we have shown that the LODs can be further decreased by a factor of 3–10 with individual optimization.¹²⁶⁻¹²⁸ Finally, the use of some other types of MS systems (triple quad, etc.) with this technique can further reduce detection limits.

4.5 Conclusion

A total of 16 newly synthesized linear tricationic ion-pairing agents were evaluated for their ability to detect doubly charged anions in positive mode ESI-MS. It was found that for linear trications, the optimum alkyl chain lengths coupling the cationic moieties should be between 6 and 10 carbons in length. It was determined that the best cationic moieties were tripropylphosphonium and benzylimidazolium. In comparison to previously reported rigid tricationic ion-pairing agents, the flexible linear trications presented here generally make better MS ion-pairing agents. It was shown that when the same amount of sulfate was injected, the

signal-to-noise ratio when using the best linear trication was 7 times greater than when using the best trigonal trication. However, it was found that trigonal trication E2 remained useful as it was often complementary to the linear trications. Lastly, 1–3 orders of magnitude decreases in the LODs were found when using SRM.

CHAPTER 5

LINEAR TRICATIONIC ROOM-TEMPERATURE IONIC LIQUIDS: SYNTHESIS, PHYSIOCHEMICAL PROPERTIES, AND ELECTROWETTING PROPERTIES

The synthesis of all the ILs and viscosity tests were shared by me and Eranda. Eranda took all the NMRs and elemental analysis. The electrowetting experiments were done by Yasith.

5.1 Abstract

Efficient and facile synthesis of novel linear tricationic room-temperature ionic liquids was performed, and their physiochemical properties were determined. Different physiochemical properties were observed according to the structural variations such as the cationic moiety and the counteranion of the ionic liquid. The electrowetting properties of these ionic liquids were also investigated, and linear tricationic ionic liquids were shown to be advantageous as effective electrowetting materials due to their high structural flexibility.

5.2 Introduction

Room-temperature ionic liquids (RTILs) are a class of salts that are liquids at or near room temperature.¹³⁰ Recently RTILs have attracted much attention in academic research and industry, since they have shown profound advantages in the context of green chemistry and have great technological potential.¹³¹⁻¹³³ Recently monocationic, dicationic, and tricationic ionic liquids have been used extensively in the field of analytical chemistry as ion-pairing reagents for the ultra trace detection of anions in the positive mode of electrospray ionization mass spectrometry (ESI-MS),^{134,135} high thermal stability gas chromatographic (GC) stationary

phases,¹³⁶⁻¹³⁹ capillary electrophoresis (CE),¹⁴⁰ and electrowetting applications.¹⁴¹⁻¹⁴³ We have recently reported the synthesis and physicochemical properties of a series of dicationic and tricationic ionic liquids.^{138, 144, 145} These reported ILs possessed good thermal stabilities and higher viscosities in comparison to monocationic ILs.^{146, 147} Moreover, it was shown by Payagala *et al.* that physicochemical properties such as viscosity, density, thermal stability, melting point, and solubility behaviors can be varied (tuned) to a greater extent in multicationic ILs than in the conventional ILs by changing the cation type, linkage chain length, etc.^{138, 144, 145} However, the tuning capability for trigonal tricationic ILs¹⁴⁵ was lower than that of linear dicationic ILs.¹⁴⁴ This was because, in most of the trigonal ILs synthesized, there were only two methylene moieties between the rigid trigonal core and the three pendant cationic moieties. The rigid trigonal geometry and the existence of three charge-carrying moieties in close proximity resulted in high apparent polarity and relatively high melting salts. On the basis of these observations, it was concluded that, for multicationic ILs, the linear geometry would give the best tunability in terms of physicochemical properties and the highest probability of forming RTILs.

The interesting physicochemical properties of the ILs have led to their use in applications involving electrowetting on dielectric-based microfluidic devices.¹⁴¹⁻¹⁴³ Electrowetting (EW) is the decrease in contact angle when an external voltage is applied across the solid/liquid interface. Simple EW which utilizes a metal base to hold the droplet is often associated with the drawback of droplet instability with change of the voltage, whereas electrowetting on a dielectric solid (e.g., Teflon) produces stable and reversible droplet shape with changes in the voltage.¹⁴⁸ Since reversibility of the droplet shape with a change in voltage is an important factor in microfluidic devices, electrowetting on dielectric (EWOD) has shown greater success in applications such as fluid lens systems, electrowetting displays, optical filters, paint drying, micromotors, electronic microreactors, and controlling fluids in multichannel structures.¹⁴⁸⁻¹⁵² Water or aqueous electrolytes are used in nearly all EWOD devices. Water-based systems are known to create complications due to their evaporation, low thermal stability,

and tendency to contribute to corrosion in integrated electronics.¹⁴⁸ The unique properties of RTILs, including negligible vapor pressure, ultra high stability over a wide temperature range, and large electrochemical windows,¹³⁰ make them ideal in EWOD applications over traditional aqueous or electrolyte solutions. Recently a detailed study was carried out to find the electrowetting properties of traditional and multifunctional ILs.¹⁴¹⁻¹⁴³ These EWOD-based micro reactors and micro extraction devices have been used in various scientific areas. Dubois et al. demonstrated the use of IL droplets as electronic microreactors on open digital microfluidic chips.¹⁵³ Also, Chatterjee et al. recently demonstrated that ILs can be used in digital microfluidic devices.¹⁵⁴ Moon et al. used ILs in an EWOD-based micro heat transfer device, and Kunchala et al. used an IL in a EWOD-based liquid–liquid extraction device.¹⁵⁵

The contact angle θ between a dielectric surface and an ionic liquid droplet under an external voltage of V is derived from a combination of Young's and Lippmann's equations (eq 5.1).^{141, 142} Here, c is the capacitance per unit area (specific capacitance), ϵ is the relative permittivity of the dielectric layer (dielectric constant), ϵ_0 is the permittivity of a vacuum, γ is the surface tension of the liquid, t is the thickness of the dielectric layer, θ is the contact angle at the designated voltage across a dielectric layer, and θ_0 is the contact angle at zero voltage. As the voltage increases, the contact angle also increases according to eq 5.1. After a certain point, the contact angle starts to deviate from regular behavior with increasing voltage. The voltage and corresponding contact angle where this occurs is referred to as the saturation voltage and saturation angle, respectively. According to eq 5.1, a plot of contact angle versus applied voltage should give a parabolic graph, as shown in Figure 5.1.

$$\cos \theta = \cos \theta_0 + \frac{c}{2\gamma} V^2 = \cos \theta_0 + \frac{\epsilon\epsilon_0}{2\gamma t} V^2$$

Equation 5.1

Our previous studies have shown the use of a series of RTILs in EW experiments and a correlation between contact angle variation and the structure of the ionic liquid (IL).

Monocationic, dicationic, and tricationic ILs were used in those experiments. The trigonal tricationic ILs in our previous study were of trigonal geometry and, hence, had a relatively rigid structure.¹⁴⁵

In this study, we report the synthesis and physiochemical properties and electrowetting properties of linear tricationic ionic liquids (LTILs) for the first time. Furthermore, we explore the electrowetting properties and their correlation with structural flexibility.

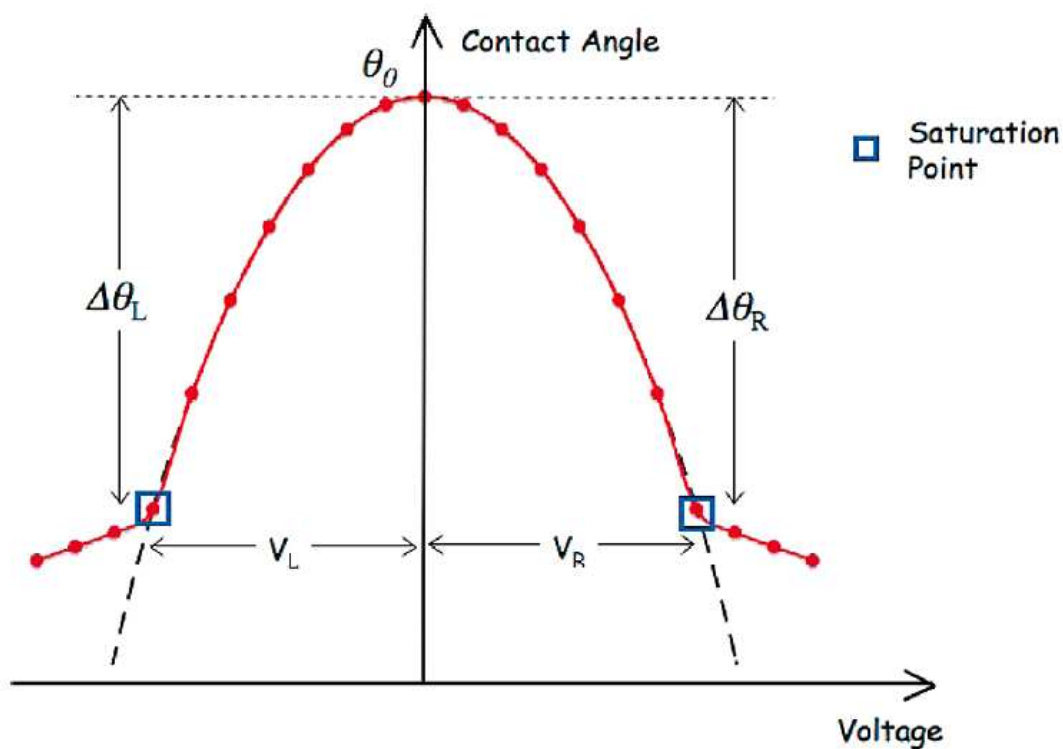


Figure 5.1 Plot of contact angle vs voltage according to Young's and Lippmann's equation.

5.3 Experimental Section

The structures of the LTILs synthesized are illustrated in Figure 5.2, and Scheme 5.1 illustrates the synthesis of the core structure. All ¹H NMR, ¹³C NMR (data reported are for

bromide salts), and ^{31}P NMR spectra were recorded at 295 ± 1 K on JEOL Eclipse 300 MHz spectrometer. All NMR spectra were recorded in deuterated dimethylsulfoxide and the chemical shifts were measured relative to residual nondeuterated solvent resonances. Electrowetting experiments were conducted by using a slightly modified contact angle goniometer (www.ksvltd.com, Monroe, CT). Elemental analysis was performed on a Perkin-Elmer 2400 CHN analyzer.

5.3.1 Materials

The reagents required for synthesis included anhydrous dimethylformamide, anhydrous acetonitrile, anhydrous tetrahydrofuran, sodium imidazole, 1,3-dibromopropane, 1,6-dibromohexane, 1,10-dibromodecane, 1-methylimidazole, 1-butylimidazole, 1-benzylimidazole, and tripropylphosphine, which were purchased from Sigma-Aldrich (Milwaukee, WI). All chemicals were of reagent grade and were used without further purification. For column chromatography, silica gel 60 Å (Sorbent Technologies, Inc.; 200–425 mesh) was used.

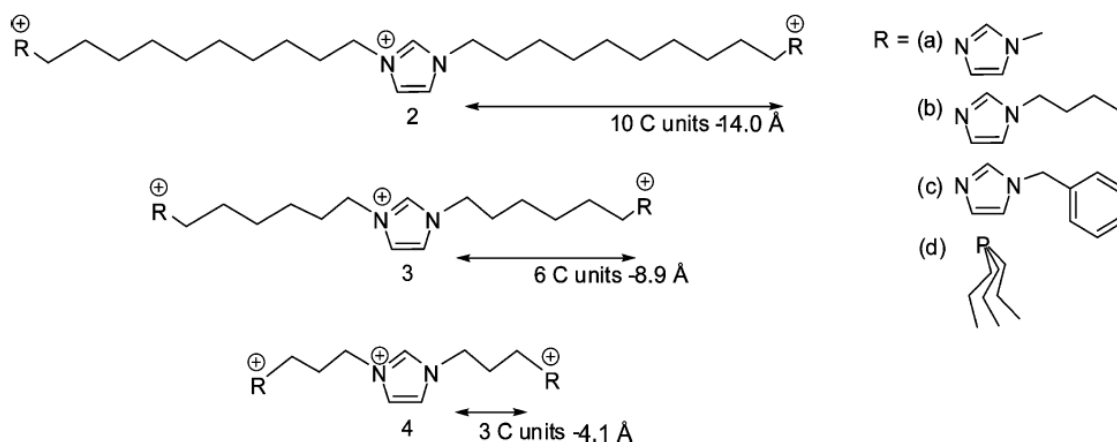
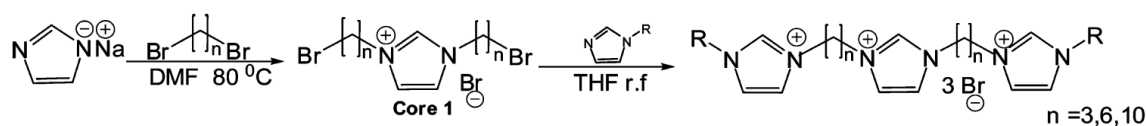


Figure 5.2 Structures of linear tricationic ionic liquids.



Scheme 5.1 Synthesis of LTIL with R-substituted imidazole as the charge-carrying moiety

5.3.2 Procedure for the synthesis of the core structure 1-(bromodecyl)-3-(bromodecyl)imidazolium bromide Salt (1a)

Sodium imidazole (1.0 g, 12.1 mmol) in 20 mL of anhydrous DMF was added slowly to a solution of dibromodecane (18.2 g, 60.5 mmol) in 100 mL of anhydrous DMF by using a syringe pump over a period of 3 h at room temperature. After completion of the addition, the reaction mixture was heated to 70 °C for 12 h. Then DMF was evaporated under vacuum and the resulting crude material was washed with hexane (5 × 100 mL) to remove excess dibromoalkane. At this point the resulting crude product was subjected to column chromatography using CH₃OH/CH₂Cl₂ (1:9) as the eluent system. The purified product was then dried under vacuum overnight to give the desired product in 65% yield. Brown liquid. ¹H NMR (300 MHz, DMSO-*d*₆): δ 9.21 (s, 1H), 7.80 (d, *J* = 1.7 Hz, 2H), 4.15 (t, *J* = 7.0 Hz, 4H), 3.51 (t, *J* = 7.0 Hz, 4H), 1.77 (m, 8H), 1.33 (m, 4H), 1.24 (br s, 20H). ¹³C NMR (75 MHz, DMSO-*d*₆): δ 136.4, 123.0, 49.4, 35.8, 32.7, 29.7, 29.2, 28.8, 28.6, 28.0, 25.9. Anal. Calcd for C₂₃H₄₃Br₃N₂: C, 47.04; H, 7.38; Br, 40.82; N, 4.77. Found: C, 47.08; H, 7.42; N, 4.81. ESI-MS (*m/z*): calcd 507.41 (M⁺), found 507.25.

5.3.3 Procedure for the synthesis of the core structure 1-(bromohexyl)-3-(bromohexyl)imidazolium bromide Salt (1b)

This compound was prepared by a procedure similar to that described above for 1a. Sodium imidazole (1.0 g, 12 mmol) in 20 mL of anhydrous DMF was added slowly to a solution of dibromodecane (14.8 g, 60.5 mmol) in 100 mL of anhydrous DMF by using a syringe pump over a period of 3 h at room temperature. After completion of the addition, the solution was

stirred for an additional 12 h. Then DMF was evaporated under vacuum and the resulting crude material was washed with hexane (5 × 100 mL) to remove excess dibromoalkane. At this point the resulting crude product was subjected to column chromatography using CH₃OH/CH₂Cl₂ (1:9) as the eluent system. The purified product was then dried under vacuum overnight to give the desired product in 72% yield. Brown liquid. ¹H NMR (300 MHz, DMSO-*d*₆): δ 9.38 (s, 1H), 7.84 (s, 2H), 4.18–4.13 (t, *J* = 7.2 Hz, 4H), 3.50–3.46 (t, *J* = 6.5 Hz, 4H), 1.81–1.70 (m, 8H), 1.41–1.31 (m, 4H), 1.25–1.15 (m, 4H). ¹³C NMR (75 MHz, DMSO-*d*₆): δ 136.48, 122.94, 60.93, 49.29, 32.69, 29.87, 25.86, 25.34. Anal. Calcd for C₁₅H₂₇Br₃N₂: C, 37.92; H, 5.73; N, 5.90. Found: C, 37.93; H, 5.80; N, 5.95. ESI-MS (*m/z*): calcd 475.10 (M⁺), found 475.10.

5.3.4 Procedure for the synthesis of the core structure 1-(bromopropyl)-3-(bromopropyl)imidazolium bromide salt (1c)

This compound was prepared by a procedure similar to that for 1b. ¹H NMR (300 MHz, DMSO-*d*₆): δ 9.27 (s, 1H), 7.83 (d, *J* = 1.4 Hz, 2H), 4.28 (t, *J* = 7 Hz, 4H), 3.54 (t, *J* = 7 Hz, 4H), 2.37 (m, 4H). ¹³C NMR (75 MHz, DMSO-*d*₆): δ 136.4, 122.9, 49.3, 29.9, 29.2, 28.9, 20.4, 19.8, 15.9, 15.2. Anal. Calcd for C₉H₁₅Br₃N₂: C, 27.65; H, 3.87; Br, 61.32; N, 7.17. Found: C, 27.68; H, 3.92; N, 7.20. ESI-MS (*m/z*): calcd 311.04 (M⁺), found 311.00.

5.3.5 Procedure for the synthesis of LTILs 2a–d, 3a–d, and 4a–d

All the reactions were carried out in tetrahydrofuran (THF), except for 4a–d, for which acetonitrile (ACN) was used as the reaction solvent. The linear core structures 1a–c (1 equiv in THF or ACN) were reacted with 2.5 equiv of methylimidazole, butylimidazole, benzylimidazole or tripropylphosphine under reflux over 36–48 h (phosphonium ILs need to be reacted for 48 h). Then the solvent was removed in vacuo and the resulting thick liquid or solid was dissolved in 5–10 mL of deionized water. The aqueous layer was then washed with ethyl acetate (6 × 100 mL), and water was removed in vacuo. The final product as the bromide salt was then dried under high vacuum (75–85% yield).

Final products were synthesized through a metathesis reaction of the bromide salts with lithium trifluoromethanesulfonimide (LiNTf₂), sodium tetrafluoroborate (NaBF₄), and lithium trifluoromethanesulfonate (LiTfO) according to the previously published procedure.¹⁴⁴ Elemental analysis were all measured by

5.3.5.1 1-(1'-Methyl-3'-decylimidazolium)-3-(1''-methyl-3''-decylimidazolium)imidazolium Tris[bis((trifluoromethyl)sulfonyl)imide] (2a)

¹H NMR (300 MHz, DMSO-*d*₆): δ 9.15 (s, 1H), 9.08 (s, 2H), 7.78 (d, *J* = 1.4 Hz, 2H), 7.75 (t, *J* = 1.4 Hz, 2H), 7.69 (t, *J* = 1.4 Hz, 2H), 4.14 (t, *J* = 7.2 Hz, 8H), 3.84 (s, 6 H), 1.65–1.80 (m, 8H), 1.24 (br s, 26H). ¹³C NMR (75 MHz, DMSO-*d*₆): δ 137.2, 136.4, 124.1, 122.9, 122.8, 49.3, 49.2, 36.3, 29.9, 29.3, 28.9, 26.06. ¹⁹F NMR (282 MHz): δ -78.6. Anal. Calcd for C₃₇H₅₅F₁₈N₉O₁₂S₆: C, 32.86; H, 4.10; N, 9.32. Found: C, 32.89; H, 4.15; N, 9.38. ESI-MS (*m/z*): calcd 170.48 (M³⁺), found 170.50.

5.3.5.2 1-(1'-Butyl-3'-decylimidazolium)-3-(1''-butyl-3''-decylimidazolium)imidazolium Tris[bis((trifluoromethyl)sulfonyl)imide] (2b)

¹H NMR (300 MHz, DMSO-*d*₆): δ 9.17 (s, 1H), 9.15 (s, 2H), 7.80–7.77 (m, 6H), 4.18–4.11 (q, *J* = 6.8 Hz, 12H), 1.81–1.74 (m, 12H), 1.30–1.18 (br s, 28H), 0.89 (t, *J* = 7.5 Hz, 6H). ¹³C NMR (75 MHz, DMSO-*d*₆): δ 136.5, 122.9, 122.8, 49.3, 49.0, 31.8, 29.8, 29.2, 28.8, 26.0, 19.3, 13.8. ¹⁹F NMR (282 MHz): δ -78.6. Anal. Calcd for C₄₃H₆₇F₁₈N₉O₁₂S₆: C, 35.95; H, 4.70; N, 8.78. Found: C, 35.50; H, 4.65; N, 8.80. ESI-MS (*m/z*): calcd 198.51 (M³⁺), found 198.58.

5.3.5.3 1-(1'-Benzyl-3'-decylimidazolium)-3-(1''-benzyl-3''-decylimidazolium)imidazolium Tris[bis((trifluoromethyl)sulfonyl)imide] (2c)

¹H NMR (300 MHz, DMSO-*d*₆): δ 9.25 (s, 2 H), 9.12 (s, 1H), 7.79–7.75 (m, 6H), 7.38 (d, *J* = 1.7 Hz, 10H), 5.38 (s, 2H), 4.14 (q, *J* = 7.0 Hz, 8H), 1.79–1.72 (m, 8H), 1.20 (br s, 24H). ¹³C NMR (75 MHz, DMSO-*d*₆): δ 136.6, 136.4, 135.4, 129.5, 129.3, 128.7, 123.3, 123.1, 122.9, 52.4,

49.5, 29.8, 29.3, 28.8, 26.1. ^{19}F NMR (282 MHz): δ -78.6. Anal. Calcd for $\text{C}_{49}\text{H}_{63}\text{F}_{18}\text{N}_9\text{O}_{12}\text{S}_6$: C, 39.12; H, 4.22; N, 8.38. Found: C, 39.18; H, 4.26; N, 8.42. ESI-MS (m/z): calcd 221.17 (M^{3+}), found 221.25.

5.3.5.4 1-(Decyltripropylphosphonium)-3-(decyltripropylphosphonium)imidazolium Tris[bis((trifluoromethyl)sulfonyl)imide] (2d)

^1H NMR (300 MHz, $\text{DMSO-}d_6$): δ 9.33 (s, 1H), 7.83 (d, $J = 1.4$ Hz, 2H), 4.18 (t, $J = 7.2$ Hz, 4H), 2.17–2.10 (m, 18H), 1.77–1.73 (m, 18H), 1.37–1.22 (m, 20H), 0.98 (t, $J = 7.0$ Hz, 18H). ^{13}C NMR (75 MHz, $\text{DMSO-}d_6$): δ 136.4, 122.9, 49.3, 29.9, 29.3, 28.8, 26.1, 21.24, 20.4, 19.8, 18.5, 17.9, 15.9, 15.2. ^{19}F NMR (282 MHz): δ -78.6. Anal. Calcd for $\text{C}_{47}\text{H}_{85}\text{F}_{18}\text{N}_9\text{O}_{12}\text{P}_2\text{S}_6$: C, 37.42; H, 5.68; N, 4.64. Found: C, 37.75; H, 5.70; N, 4.68. ESI-MS (m/z): calcd 222.54 (M^{3+}), found 222.56.

5.3.5.5 1-(1'-Methyl-3'-hexylimidazolium)-3-(1''-methyl-3''-hexylimidazolium)imidazolium Tris[bis((trifluoromethyl)sulfonyl)imide] (3a)

^1H NMR (300 MHz, $\text{DMSO-}d_6$): δ 9.50 (s, 1H), 9.35 (s, 2 H), 7.86 (s, 2H), 7.84 (s, 2H), 7.73 (s, 2H), 4.17 (m, 8H), 3.84 (s, 6H), 1.77 (m, 8H), 1.24 (m, 8H). ^{13}C NMR (75 MHz, $\text{DMSO-}d_6$): δ 137.07, 136.57, 124.09, 122.96, 122.82, 49.15, 49.08, 36.35, 29.63, 29.56, 25.32. ^{19}F NMR (282 MHz): δ -78.6. Anal. Calcd for $\text{C}_{29}\text{H}_{39}\text{F}_{18}\text{N}_9\text{O}_{12}\text{S}_6$: C, 28.09; H, 3.17; N, 10.17. Found: C, 28.11; H, 3.20; N, 10.20. ESI-MS (m/z): calcd 133.10 (M^{3+}), found 133.10.

5.3.5.6 1-(1'-Butyl-3'-hexylimidazolium)-3-(1''-butyl-3''-hexylimidazolium)imidazolium Tris[bis((trifluoromethyl)sulfonyl)imide] (3b)

^1H NMR (300 MHz, $\text{DMSO-}d_6$): δ 9.47 (s, 1H), 9.43 (s, 2H), 7.86 (s, 4H), 7.84 (s, 2H), 4.17 (t, $J = 7.2$ Hz, 12 H), 1.79–1.72 (m, 12 H), 1.24–1.17 (m, 12H), 0.85 (t, $J = 7.2$ Hz, 6H). ^{13}C NMR (75 MHz, $\text{DMSO-}d_6$): δ 136.56, 122.94, 49.17, 49.07, 31.84, 29.57, 25.32, 19.32, 13.84. ^{19}F NMR (282 MHz): δ -78.6. Anal. Calcd for $\text{C}_{35}\text{H}_{51}\text{F}_{18}\text{N}_9\text{O}_{12}\text{S}_6$: C, 31.75; H, 3.88; N, 9.52. Found: C, 31.78; H, 3.90; N, 9.55. ESI-MS (m/z): calcd 161.14 (M^{3+}), found 161.10.

5.3.5.6 1-(1'-Benzyl-3'-hexylimidazolium)-3-(1''-methyl-3''-hexylimidazolium)imidazolium Tris[bis((trifluoromethyl)sulfonyl)imide] (3c)

^1H NMR (300 MHz, DMSO- d_6): δ 9.52 (s, 1H), 9.44 (s, 2H), 7.85 (s, 6H), 7.44–7.34 (m, 10H), 5.45 (s, 4 H), 4.19–4.15 (m, 8H), 1.77 (s, 8H), 1.24 (m, 8H). ^{13}C NMR (75 MHz, DMSO- d_6): δ 136.68, 135.49, 129.53, 129.43, 128.86, 123.37, 123.05, 122.98, 52.34, 49.31, 49.17, 29.60, 29.53, 25.35. ^{19}F NMR (282 MHz): δ -78.6. Anal. Calcd for $\text{C}_{41}\text{H}_{47}\text{F}_{18}\text{N}_9\text{O}_{12}\text{S}_6$: C, 35.37; H, 3.40; N, 9.05. Found: C, 35.39; H, 3.45; N, 9.10. ESI-MS (m/z): calcd 183.79 (M^{3+}), found 183.85.

5.3.5.7 1-(Hexyltripropylphosphonium)-3-(hexyltripropylphosphonium)imidazolium Tris[bis((trifluoromethyl)sulfonyl)imide] (3d)

^1H NMR (300 MHz, DMSO- d_6): δ 9.55 (s, 1H), 7.87 (s, 2H), 4.21 (t, $J = 6.9$ Hz, 4H), 2.24–2.12 (m, 16H), 1.85–1.75 (m, 4H), 1.56–1.26 (m, 24H) 1.00–0.95 (t, $J = 6.8$ Hz, 18H). ^{13}C NMR (75 MHz, DMSO- d_6): δ 136.62, 122.98, 49.22, 29.55, 25.32, 21.09, 20.53, 19.91, 15.96, 15.74, 15.34. ^{19}F NMR (282 MHz): δ -78.6. Anal. Calcd for $\text{C}_{39}\text{H}_{69}\text{F}_{18}\text{N}_9\text{O}_{12}\text{P}_2\text{S}_6$: C, 33.55; H, 4.98; N, 5.02. Found: C, 33.60; H, 5.00; N, 5.05. ESI-MS (m/z): calcd 185.16 (M^{3+}), found 185.25.

5.3.5.8 (1'-Methyl-3'-propylimidazolium)-3-(1''-methyl-3''-propylimidazolium)imidazolium Tris[bis((trifluoromethyl)sulfonyl)imide] (4a)

^1H NMR (300 MHz, DMSO- d_6): δ 9.50 (s, 1H), 9.32 (s, 2H), 4.31–4.25 (m, 8H), 3.87 (s, 6H), 2.46–2.42 (m, 4H). ^{13}C NMR (75 MHz, DMSO- d_6): δ 137.1, 123.0, 49.6, 26.0, 22.1, 20.4, 19.8, 15.9, 15.7, 15.3. ^{19}F NMR (282 MHz): δ -78.6. Anal. Calcd for $\text{C}_{23}\text{H}_{27}\text{F}_{18}\text{N}_9\text{O}_{12}\text{S}_6$: C, 23.90; H, 2.35; N, 10.91. Found: C, 23.92; H, 2.40; N, 10.97. ESI-MS (m/z): calcd 105.07 (M^{3+}), found 105.17.

5.3.5.9 1-(1'-Butyl-3'-propylimidazolium)-3-(1''-butyl-3''-propylimidazolium)imidazolium Tris[bis((trifluoromethyl)sulfonyl)imide] (4b)

^1H NMR (300 MHz, DMSO- d_6): δ 9.50 (s, 1H), 9.43 (s, 2H), 7.90–7.84 (m, 6H), 4.32–4.29 (m, 8H), 4.19 (t, $J = 7.2$ Hz, 4H), 2.48–2.43 (m, 4H), 1.81–1.76 (m, 4H), 1.31–1.23 (m, 4H), 0.90 (t, $J = 7.2$, 6H). ^{13}C NMR (75 MHz, DMSO- d_6): δ 137.1, 136.8, 49.2, 46.4, 31.7, 29.9, 19.3, 13.8. ^{19}F NMR (282 MHz): δ -78.6. Anal. Calcd for $\text{C}_{29}\text{H}_{39}\text{F}_{18}\text{N}_5\text{O}_{12}\text{P}_2\text{S}_6$: C, 28.09; H, 3.17; F, 27.58; N, 10.17. Found: C, 28.09; H, 3.22; N, 10.20. ESI-MS (m/z): calcd 133.19 (M^{3+}), found 133.17.

5.3.5.10 1-(1'-Benzyl-3'-propylimidazolium)-3-(1''-benzyl-3''-propylimidazolium)imidazolium Tris[bis((trifluoromethyl)sulfonyl)imide] (4c)

^1H NMR (300 MHz, DMSO- d_6): δ 9.52 (s, 2H), 9.48 (s, 1H), 7.48–7.38 (m, 10H), 5.47 (s, 4H), 4.29 (q, $J = 5.8$ Hz, 8H), 2.45 (m, 4H). ^{13}C NMR (75 MHz, DMSO- d_6): δ 137.2, 123.0, 62.5, 49.4, 26.0, 22.1, 20.5, 19.9, 16.1, 15.9, 15.3. ^{19}F NMR (282 MHz): δ -78.6. Anal. Calcd for $\text{C}_{35}\text{H}_{35}\text{F}_{18}\text{N}_9\text{O}_{12}\text{S}_6$: C, 32.14; H, 2.70; N, 9.64. Found: C, 32.14; H, 2.78; N, 9.65. ESI-MS (m/z): calcd 155.76 (M^{3+}), found 155.75.

5.3.5.11 1-(Propyltripropylphosphonium)-3-(propyltripropylphosphonium)imidazolium Tris[bis((trifluoromethyl)sulfonyl)imide] (4d)

^1H NMR (300 MHz, DMSO- d_6): δ 9.12 (s, 1H), 7.84 (s, 2H), 4.24 (t, $J = 6.8$, 4H), 2.23–2.21 (m, 20H), 0.57–1.47 (m, 12H), 1.04–1.00 (m, 12H), 1.04 (t, $J = 7.2$ Hz, 18H). ^{13}C NMR (75 MHz, DMSO- d_6): δ 137.9, 123.0, 62.5, 49.6, 26.0, 22.1, 20.4, 19.8, 15.9, 15.3. ^{19}F NMR (282 MHz): δ -78.6. Anal. Calcd for $\text{C}_{33}\text{H}_{57}\text{F}_{18}\text{N}_5\text{O}_{12}\text{P}_2\text{S}_6$: C, 30.21; H, 4.38; N, 5.34. Found: C, 30.22; H, 4.44; N, 5.34. ESI-MS (m/z): calcd 157.13 (M^{3+}), found 155.17.

5.3.6 Glass transition temperature/melting point

The thermal measurements were performed with a differential scanning calorimeter (DSC, PerkinElmer Diamond DSC, 710 Bridgeport Ave., Shelton, CT). The Diamond DSC was

calibrated using an indium primary standard, with solid–solid transitions for cyclohexane and ethylbenzene as supplementary low-temperature standards. IL samples (5–10 mg) were sealed in aluminum pans, and an empty aluminum pan was used as reference. The measurements were carried out in the temperature range of $-120\text{ }^{\circ}\text{C}$ to a predetermined temperature. The samples were sealed in aluminum pans and then heated and cooled at a scan rate of $10\text{ }^{\circ}\text{C min}^{-1}$ under a flow of nitrogen. For solid compounds, the melting points were verified using a Mel-Temp capillary melting point apparatus (Cambridge, MA).

5.3.7 Density

The densities of the ionic liquids were determined at $23 \pm 1\text{ }^{\circ}\text{C}$ with a Kimble Glass specific gravity pycnometer (Vineland, NJ).

5.3.8 Refractive index

Refractive index measurements were conducted at $23 \pm 1\text{ }^{\circ}\text{C}$ using a Bausch & Lomb Abbe-3L refractometer.

5.3.9 Viscosity

Kinematic viscosities were determined at $30 \pm 1\text{ }^{\circ}\text{C}$ using a Cannon-Manning semi-micro capillary viscometer (State College, PA).

5.3.10 Thermal stability analysis

Thermogravimetric analysis (TGA) was done using a TGA 2050 instrument (TA Instruments Inc., Thermal Analysis & Rheology, New Castle, DE). Samples (ca. 20 mg) were placed on the platinum pans and heated at $10\text{ }^{\circ}\text{C min}^{-1}$ from room temperature to $600\text{ }^{\circ}\text{C}$ under a dynamic nitrogen atmosphere. The decomposition temperatures were reported as the temperatures of 1%, 5%, and 50% weight loss of the sample.

5.3.11 Electrowetting Experiments

Electrowetting experiments were conducted by using a slightly modified contact angle goniometer (www.ksvltd.com, Monroe, CT). Figure 5.3 shows the arrangement for the electrowetting experiment. Indium tin oxide (ITO, 30 nm thickness) precoated unpolished float glass slides (www.delta-technologies.com, Stillwater, MN) were used as purchased. They were dip-coated in a 4% (w/v) Teflon AF1600 (www2.dupont.com, Wilmington, DE) in Fluoroinert FC75 solvent (www.fishersci.com, Barrington, IL) solution. The dipping speed was approximately $0.78 \pm 0.03 \text{ mm s}^{-1}$ in a custom-made dipcoater. Only three-fourths of the slide was dipped in the solution; then the movement was stopped for 5 s, and after that the slide was raised at the same speed. The coated slides were kept in an oven at 112 °C for 6 min, at 165 °C for 5 min, and at 328 °C for 15 min. Once Teflon-coated glass slides were taken out from the oven, they were allowed to reach room temperature. Then they were washed thoroughly with acetone and deionized water followed by air drying. A capillary tube was used to place a drop of IL on top of the Teflon layer. CAM 200 software (www.ksvltd.com, Monroe, CT) was used to calculate the drop volume; it was between $5 \pm 2 \text{ }\mu\text{L}$ for all experiments. A Keithley 2400 SourceMeter (www.keithley.com, Cleveland, OH) was used to apply voltage in 5 V increments from 0 to +70 V. The positive probe was connected to the Pt wire, and the negative probe was connected to the ITO layer (see Figure5.3). Afterward, the above procedure was repeated for 0 to -70 V for a fresh drop of IL placed at a different position on the surface. At each voltage increment a picture was taken and then CAM 200 software was used to measure corresponding contact angles. Finally, the contact angle versus voltage curves were plotted.

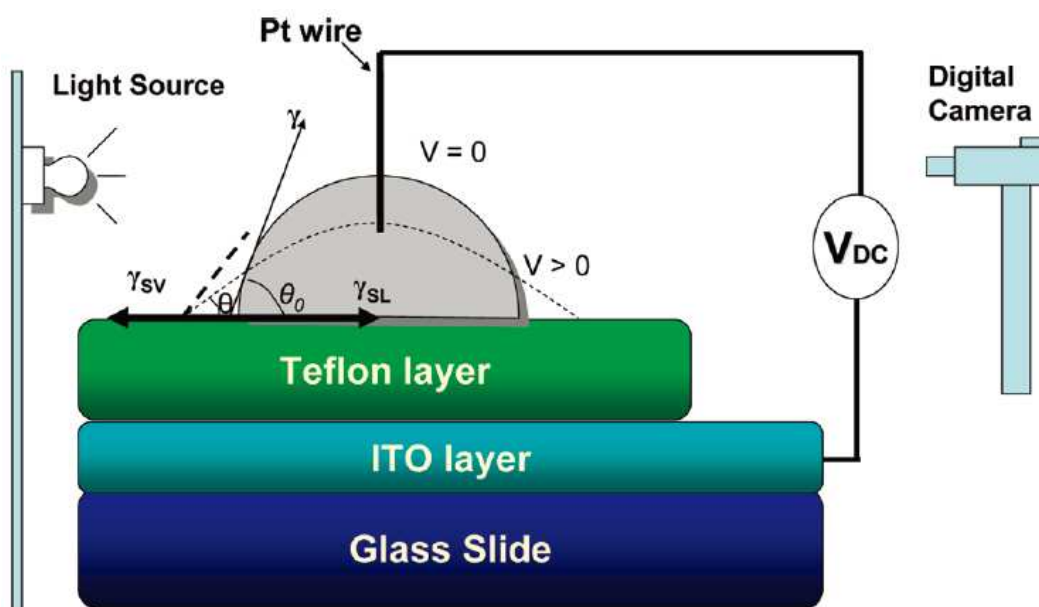


Figure 5.3 Electrowetting experimental setup. Here, γ , γ_{sv} , and γ_{sl} are the interfacial tensions associated with the liquid/vapor, solid/vapor, and solid/liquid interfaces.

All tested ILs were kept in a vacuum oven at room temperature overnight with phosphorus pentoxide (P_2O_5) to minimize the water content.

5.4 Results and discussion

The synthetic strategy involved in these linear tricationic ILs was different from previously reported ionic liquids for the following reasons. (1) Core 1 (Scheme 5.1) was designed and synthesized in-house. It was separated and isolated from the dicationic and polycationic impurities that were formed during the reaction, by running through a flash chromatography column (SiO_2 60 Å, CH_2Cl_2/CH_3OH 1:9). (2) In previous dicationic and trigonal tricationic IL syntheses, isopropyl alcohol was used as the reaction solvent in most cases.^{138, 144, 145} However, when alcohols were used, the basic imidazole tended to deprotonate the alcohol, enabling unwanted nucleophilic substitution reactions.¹⁵⁶ This complicated the separation of the pure LTILs from the reaction mixture. Therefore, the solvent used in the synthesis of Core 1 was dimethylformamide (DMF). This was because DMF dissolved sodium imidazole (NaIM) and it

minimized the side reactions that take place with protic solvents. Other reaction solvents for the synthesis of ILs involving imidazolium moieties were found to be acetonitrile (ACN) and tetrahydrofuran (THF). However, isopropyl alcohol can be used as the solvent in reactions involving tripropylphosphonium, which has a weakly nucleophilicity character compared to imidazole.

In this study, 14 linear tricationic ionic liquids were synthesized and their physicochemical properties were investigated. The results are given in Table 5.1. Phase transition temperatures, including glass transition temperatures (T_g), were determined using differential scanning calorimetry (DSC). LTILs show significantly lower glass transition temperatures (except for 4d) compared to many other types of ILs in the literature, such as symmetrical dicationic ILs.^{138, 144, 145} It has been shown for most dicationic ILs that when the chain length is smaller than three methylene units, the IL becomes solid regardless of other structural changes.¹³⁸ However, we found that LTILs with C3 linkage chains (4a-c) (Figure 5.1) do exist as RTILs when the counteranion is bis(trifluoromethylsulfonyl)imide (NTf_2^-). This can be explained by the relative flexibility of the LTILs. Unlike trigonal tricationic ILs, the LTILs have greater conformational degrees of freedom which help to minimize charge repulsion interactions.¹⁵⁷ The T_g values are mainly governed by the size and charge distribution of the anion and/or cation.¹⁵⁸ According to the literature, most ILs containing NTf_2^- are observed to be liquids at room temperature.^{138, 144, 145, 159, 158, 160, 161} When the negative charge carrying moiety is a halide, X^- ($\text{X}^- = \text{F}^-, \text{Cl}^-, \text{Br}^-, \text{I}^-$), BF_4^- , TfO^- (trifluoromethanesulfonate), or PF_6^- , the ILs tend to have higher melting points.^{138, 144, 145}

The LTILs with methylimidazolium charge carrying moieties 2a-4a showed the lowest melting temperatures of the series. According to the melting point data in Table 5.1, the butylimidazole cationic moiety produces ILs with higher melting points compared to the methylimidazole moiety. This is probably because of the butyl group's greater van der Waals interactions. Relatively higher melting temperatures were observed when the IL incorporated

the benzylimidazole moiety, mainly because of the additional π - π stacking introduced by the phenyl groups.^{138, 144, 145}

The kinematic viscosities of these LTILs range from 372 to 4200 cSt at 303 K. LTILs with the C6 linkage chain generally showed lower viscosities ranging from 600–840 cSt. Typically, monocationic ILs have lower kinematic viscosities.¹⁴⁷ The viscosities are markedly higher in ILs with benzyl groups (see Table 5.1). The same phenomenon was observed in dicationic and trigonal tricationic ILs.^{138, 144, 145} It is interesting to note that ILs with a C3 linkage chain have higher viscosities compared to ILs with C6 linkage chains and lower viscosities when compared to those with C10 linkage chains. According to these results, ILs having C3 linkage chains seem to possess greater ionic nature, owing to the closeness of the charged groups. When the distance between charged groups is increased to six methylene units (~ 8.9 Å), as in ILs with C6 linkage chains, the ionic nature is reduced, resulting in lower viscosity. However, when the linkage chain is further increased up to 10 methylene units (~ 14 Å), higher viscosities are observed, again due to the increase of intermolecular van der Waals interactions over ionic interactions.¹⁵⁸

The densities of LTILs with accompanying NTf_2^- anions range from 1.36 to 1.65 g cm^{-3} . The lowest density was observed for 2c, which has a benzylimidazolium cation and C10 linkage chains. Higher density values are obtained for LTILs with methylimidazolium groups. Moreover, when the chain length of the substituent at the 3-position of the imidazole increases from methylimidazolium to butylimidazolium, the density decreases (2a,b, 3a,b, and 4a,b). Similar observations have been reported for monocationic and dicationic ILs as well.^{138, 144, 145}

The refractive indices of the LTILs range from 1.44 to 1.49 and lie within the general range observed for monocationic ILs.^{160, 161} The solubility of these LTILs parallels that of monocationic ILs,^{162 160, 161} in which all Br^- , BF_4^- , and TfO^- (trifluoromethanesulfonate) salts synthesized were soluble in water, while all NTf_2^- salts were insoluble in water. All of the LTILs synthesized were insoluble in *n*-heptane.

For RTILs to be used in applications such as high-temperature organic reactions^{163, 164} and as GC stationary phases, they should possess a good thermal stability. Generally, phosphonium cation based ILs show higher thermal stabilities compared to nitrogen cation based ILs such as imidazolium and pyrolidinium ILs.^{138, 144, 145, 162} This trend was clearly seen in this study as well. LTIL 2d, with two tripropylphosphonium cations, has the highest thermal stability, displaying only 5% thermal degradation at 410 °C.

The electrowetting properties of ILs are given in Table 5.2. Figure 5.4 shows the electrowetting curves of linear tricationic ionic liquids with C6 linkage chains, and Figure 5.6 shows the electrowetting curves of benzylimidazolium-substituted tricationic ionic liquids with different linkage chain lengths and core structures.

Table 5.1 Physicochemical properties of linear tricationic ionic liquids

ionic liquid	mol wt	mp ^a (°C)	density ^b (g cm ⁻³)	refractive index	viscosity ^c (cSt)	thermal stability ^d			miscibility ^{e,f}	
						99% w	95% w	50% w	heptane	water
2a -NTf ₂	1352.25	-53.58	1.65	1.45	1800	334	400	444	I	I
2b -NTf ₂	1435.29	-53.17	1.54	1.44	2400	350	390	430	I	I
2c -NTf ₂	1504.44	-36.61	1.36	1.48	4200	320	390	450	I	I
2d -NTf ₂	1507.37	-41.58	1.46	1.45	2100	360	410	440	I	I
2b -BF ₄ ^f	856.55	-18.32	1.33			191	308	369	I	M
2b -TfO ^f	1043.18	-42.63	1.28			290	376	430	I	M
3a -NTf ₂	1240.03	-57.85	1.57	1.44	372	320	380	480	I	I
3b -NTf ₂	1324.19	-51.54	1.41	1.49	429	330	380	470	I	I
3c -NTf ₂	1391.14	-36.83	1.43	1.47	840	340	370	470	I	I
3d -NTf ₂	1396.30	-45.41	1.38	1.45	770	355	400	440	I	I
4a -NTf ₂	1155.88	-24.54	1.54	1.46	1200	290	360	410	I	I
4b -NTf ₂	1240.04	-44.13	1.48	1.49	600	310	370	470	I	I
4c -NTf ₂	1308.07	-27.26	1.41	1.48	4080	300	350	470	I	I
4d -NTf ₂	1312.14	71-72	1.59			320	390	480	I	I

^a Determined by using a differential scanning calorimeter upon heating cycle; melting points are reported as the onset temperature of the melting endotherm. ^b Determined by using a pycnometer. ^c Measured using a capillary viscometer at 30 °C. ^d The decomposition temperature was determined by using TGA: 99% w, temperature at 1% mass decrease of sample; 95% w, temperature at 5% mass decrease of the sample; 50% w, temperature at 50% mass decrease of sample. ^e Legend: I, immiscible; M, miscible. ^f Amorphous solid.

Table 5.2. Electrowetting properties of linear tricationic ionic liquids^a

ionic liquid	θ_0	$\Delta\theta_L$	$\Delta\theta_R$	V_L	V_R
2a	83	16	18	-40	50
2b	80	14	15	-35	30
2c	83	17	18	-50	40
2d	80	16	16	-60	40
3a	85	13	18	-40	40
3b	81	15	14	-30	35
3c	84	12	16	-35	40
3d	78	11	11	-30	35
4a	82	21	16	-35	40
4b	88	19	14	-40	50
4c	86	23	16	-60	55
4d					
IL13 ^b	77	>25	>20	<-70	>70
IL14 ^b	88	18	18	-65	60
IL15 ^b	77	20	25	-55	60
IL16 ^b	82	>15	>14	<-70	>70

a Legend: θ_0 , contact angle at zero voltage; $\Delta\theta_L$, apparent contact angle change at negative voltages; $\Delta\theta_R$, apparent contact angle change at positive voltages; V_L , saturation voltage in the negative voltage realm; V_R , analogous saturation voltage in the positive voltage realm. b Data taken from ref¹⁴¹.

Since there is no external voltage at θ_0 , only the three interfacial tensions (solid/liquid, liquid/air, and air/solid) govern the θ_0 value. However, solid (Teflon) is common in all experiments; therefore, only the surface tension of the IL governs the θ_0 value.¹⁴¹ The higher the surface tension value of the IL, the higher the θ_0 value obtained.¹⁴¹ Therefore, from the observed θ_0 values the relative surface tension of these ILs can be deduced. This is a good

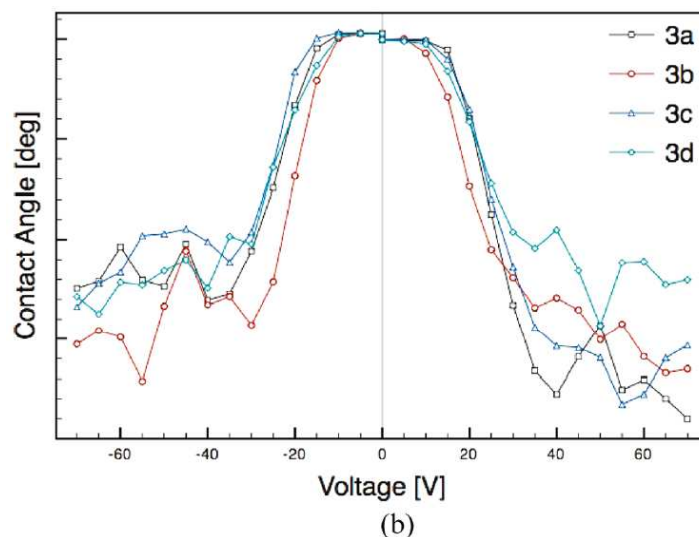
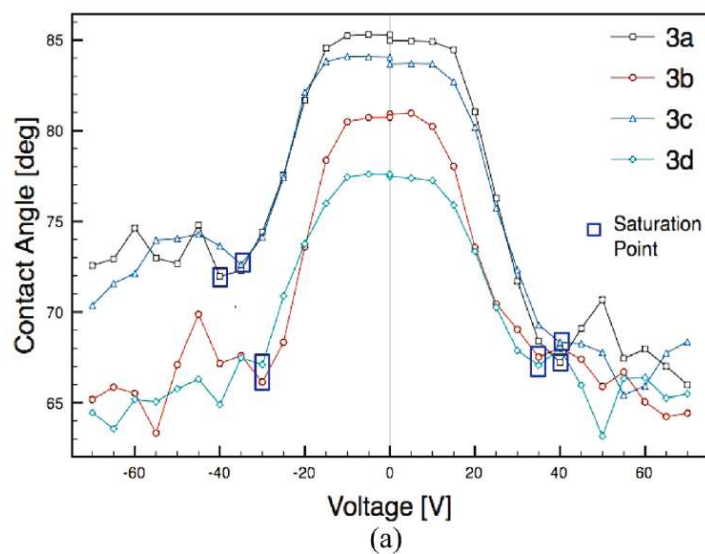


Figure 5.4 Electrowetting curves of (a) linear tricationic ionic liquids with C6 linkage chains and (b) linear tricationic ionic liquids with C6 linkage chains overlaid normal to the maximum θ_0 value.

indirect method to evaluate the relative surface tensions of this new class of ILs. According to Figure 5.4 and Table 5.2, for ionic liquids 3a–d, which have the same anion (NTf_2^-) and the same linkage chain length (C6), the θ_0 values decrease in the order $3a > 3c > 3b > 3d$. This decrease is solely due to the end cationic moieties. The θ_0 value directly correlates with the

surface tension. Therefore, the surface tension of these ILs decrease on the basis of the cation in the order methylimidazolium > benzylimidazolium > butylimidazolium > tripropylphosphonium.

According to Figure 5.6 and Table 5.2, by considering θ_0 , surface tension values of benzyl-substituted ILs decrease in the order IL 14 > 4c > 3c > 2c > IL 16. Surface tension values of liquids tend to increase with an increase in hydrophilicity.¹⁶⁶ IL 14, with a nitrogen core (see Figure 5.5), has more hydrophilic character compared to IL 16, with a mesitylene core. Therefore, IL 14 has higher surface tension than IL 16, which is reflected by the θ_0 value. Similarly, when the alkyl chain length of the LTILs increases from C3 to C10 as in 4c to 2c, the hydrophobic character increases and therefore surface tension decreases.

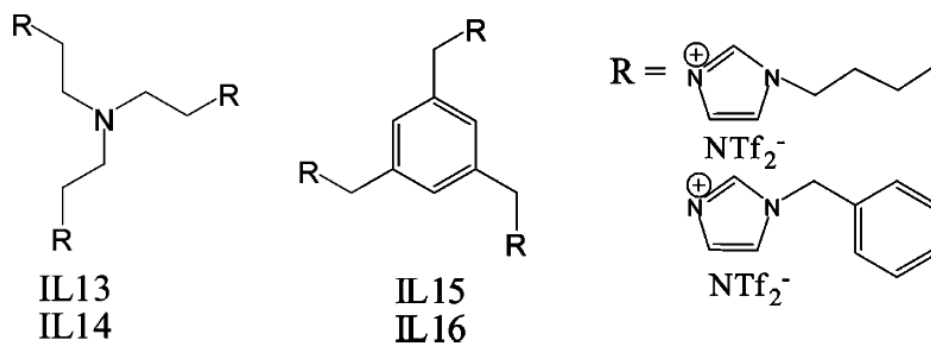
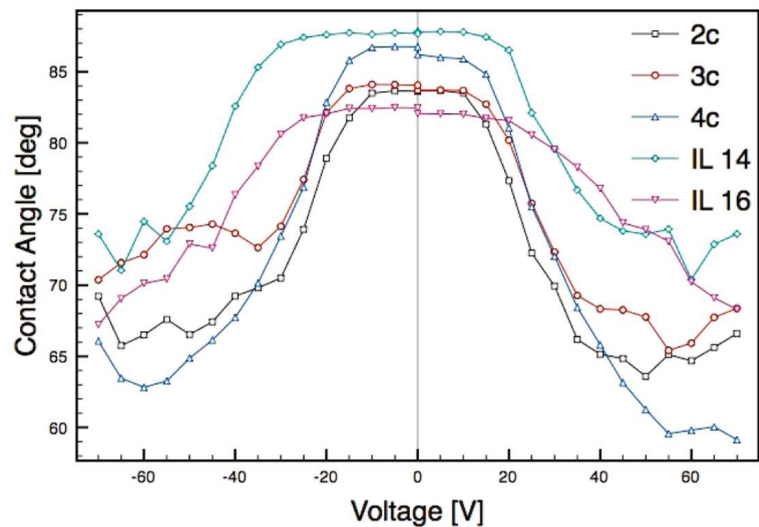


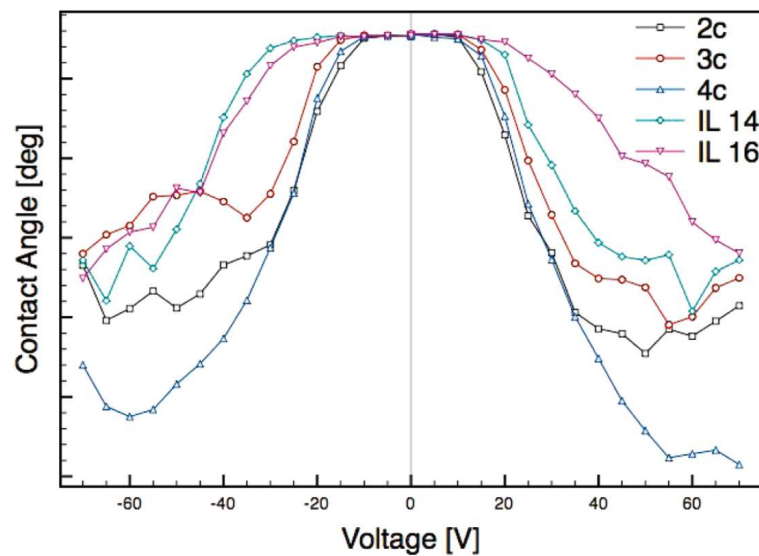
Figure 5.5 Structures of rigid core tricationic ionic liquids.

Figure 5.6a shows the electrowetting curves of benzylimidazole-substituted ILs, both rigid core (IL 14, IL 16) and flexible core (2c–4c) ILs. In Figure 5.6b curves are overlaid normal to the maximum θ_0 value. According to Figure 5.6b and Table 5.2, it can be clearly observed that rigid core ILs (IL 14 and IL 16) have V_L and V_R values wider than those of flexible core ILs (2c–4c). However, flexible core ILs produced much smoother curves than rigid core ILs. This means that their electrowetting properties are much closer to the ideal behavior expected according to Figure 5.6 Electrowetting curves of (a) benzylimidazole-substituted linear and rigid type tricationic ionic liquids and (b) benzylimidazole-substituted linear and rigid type tricationic ionic liquids overlaid normal to the maximum θ_0 value. Young's and Lippmann's equations.

Similar observations can be seen in butylimidazolium -substituted rigid ILs (IL 13, IL 15) and flexible ILs (2b-4b) as well.



(a)



(b)

Figure 5.6 Electrowetting curves of (a) benzylimidazole-substituted linear and rigid type tricationic ionic liquids and (b) benzylimidazole-substituted linear and rigid type tricationic ionic liquids overlaid normal to the maximum θ_0 value.

Electrowetting curves of linear tricationic ILs with C6 linkage chains, each with four different end groups, are plotted in Figure 5.4a. In Figure 5.4b these curves are overlaid normal to the maximum θ_0 value. There are no significant differences in electrowetting properties by changing the end groups, except for θ_0 values. θ_0 values are different from one IL to another, due to surface tension differences, which was explained previously. It is interesting to note that the electrowetting properties of these ILs are fairly similar, regardless of their different physicochemical properties. This unique situation enables one to choose an ionic liquid with the desired physical property from a large library of ionic liquids that have the same electrowetting properties. For example, if fast changes in contact angles are required in an electrowetting application, ILs with lower viscosities can be used. LTIL 3a has significantly lower viscosity than 3c, but their electrowetting properties are approximately the same (Table 5.2). These observations are valid for the other C3 linkage chain and C10 linkage chain ILs as well.

Examining electrowetting properties and physical properties of the relevant ILs listed here, one can find a suitable replacement for aqueous electrowetting in traditional EWOD-based devices.

5.5 Conclusion

The synthesis and physicochemical properties of 14 linear tricationic ionic liquids were reported, and these have been explored as potential electrowetting liquids. These LTILs have shown high thermal stabilities and considerably high viscosities compared to traditional monocationic and dicationic ionic liquids. Most of the LTILs synthesized were room-temperature ILs due to their higher structural flexibilities. This structural flexibility was advantageous in electrowetting applications, as LTILs were observed to be much closer to the ideal behavior described in Young's and Lippmann's equation than any other ionic liquids reported in the literature.

CHAPTER 6

IONIC CYCLODEXTRINS IN IONIC LIQUID MATRICES AS CHIRAL STATIONARY PHASES FOR GAS CHROMATOGRAPHY

In this work, I designed and synthesized all the chiral selectors. The column coating and evaluations were done by Ke Huang.

6.1 Abstract

Ionic liquids (ILs) are used to dissolve ionic cyclodextrin (CD) derivatives to produce a new type of gas chromatographic chiral stationary phase. Compared to a previous study with neutral cyclodextrin chiral selectors, the new ionic liquid-based stationary phase exhibits broader enantioselectivities, up to seven times higher efficiencies, and greater thermal stabilities. When compared to the analogous commercial column with polysiloxane matrix, it exhibits different enantioselectivities, more symmetric peak shapes and some complementary enantioseparations. The most profound separation enhancements are usually found for more polar analytes.

6.2 Introduction

Cyclodextrins (CDs) have been used successfully in different chromatographic techniques for enantiomeric separations.¹⁶⁷⁻¹⁷⁸ Modified cyclodextrins constitute the dominant type of chiral selectors for gas chromatography. They can be coated either as neat chiral stationary phases (CSPs) if they are viscous liquids at ambient temperatures or as cyclodextrin-

solvent mixtures if they possess higher melting points and exist as solids at room temperatures. Extensive studies have been performed on the successful use of different polysiloxanes as solvent matrices for derivatized cyclodextrins.^{179, 180} Although more scarce, research articles also suggest the potential of using modified cyclodextrins in polyethylene glycol matrices for enantioselective gas chromatographic applications.^{181, 182} However, no comparable applicability has been obtained with any solvent matrices other than polysiloxanes and polyethylene glycols.

Room temperature ionic liquids (RTILs) possess unique physicochemical properties including low melting points, negligible vapor pressures, wide temperature ranges for liquid state, non-flammability, high thermal stabilities, tunable viscosities and variable polarities. They have been developed as a very important and new class of GC stationary phase materials over the last a few years.¹⁸³⁻¹⁹¹

A single report has appeared on the use of achiral ionic liquids as stationary phase solvents for derivatized cyclodextrins in 2001.¹⁹² In this work, permethylated β -cyclodextrins (BPM) and dimethylated β -cyclodextrins (BDM) were dissolved in 1-butyl-3-methylimidazolium chloride (BMIM-Cl) and the column performances were evaluated against those of analogous polysiloxane-based commercial columns (ChiralDEX BPM and ChiralDEX BDM). It was found that the IL-based column efficiencies were up to 10 times higher than the commercial columns. However, they separated only about a fifth to a third of the racemic analytes that could be separated on the commercial columns.¹⁹² A reason for the narrower range of enantioselectivity was proposed by the authors and confirmed in later reports.^{193, 194} It was that the small BMIM-Cl ion pair can be included in the cyclodextrin cavity and consequently reduce the inclusion complexation interaction between the chiral selector and the analyte molecules, which can be crucial for chiral recognition of some molecules. Conversely, molecules that were separated by an external adsorption process were unaffected and showed excellent resolutions (because of the higher efficiencies).¹⁹⁵ Since this report, neat chiral ionic liquids have been used as GC

chiral stationary phases,¹⁹⁶ but there have been no further developments involving functionalized cyclodextrins dissolved in ionic liquids. The question arises, can a system be developed that combines the higher efficiency of the IL based chiral stationary phases as well as the superb enantioselectivity of the polysiloxane-based chiral stationary phases. Such a stationary phase could greatly enhance the GC separation of enantiomers.

In this work, two strategies are proposed to reduce the accessibility of IL matrices to the cyclodextrin cavity while maintaining the higher efficiencies observed in the 2001 study,¹⁹² they are: (1) use of bulkier ILs to make the IL molecule less able to fit inside the cyclodextrin cavity and (2) attachment of pendent cationic groups to the cyclodextrin structure, thereby providing an electrostatic barrier to other cations. In addition, we expect that by introducing ionic moieties to the cyclodextrin molecule, stronger solute–solvent interactions will occur, thereby enhancing the limited solubility of cyclodextrins in many ionic liquids.¹⁹² Also these bulky charged moieties could offer different selectivities.

Charged cyclodextrin derivatives have been widely employed as chiral selectors in capillary electrophoresis (CE) for years.^{173, 174, 197-199} However, the use of charged cyclodextrins as chiral selectors has not been reported in GC. In this study, permethylated mono-6-(butylimidazolium)-cyclodextrin (BIM-BPM) and permethylated mono-6-(tripropylphosphonium)-cyclodextrin (TPP-BPM) were synthesized and dissolved in various dicationic and tricationic ionic liquids and examined as GC chiral stationary phases. The performance of these columns was compared to that of their neutral cyclodextrin containing IL-based predecessors. The new IL column was also evaluated against the commercial polysiloxane-based CSPs with analogous chiral selectors.

6.3 Experimental

6.3.1. Materials

The reagents, imidazole, 1-methylimidazole, 1-butylimidazole, 1-(2-hydroxyethyl)imidazole, 1-tosylimidazole, tripropylphosphine, tris(2-aminoethyl)amine, pentaethylene glycol, 1,12-dibromododecane silver trifluoromethanesulfonate (TfO), lithium bis(trifluoromethanesulfonyl)imide (NTf₂), *p*-toluenesulfonyl chloride, β -cyclodextrin, methyl iodide, sodium hydroxide, sodium hydride, ammonium chloride (NH₄Cl), trifluoroacetic anhydride and silicone OV-101 were purchased from Sigma–Aldrich (Milwaukee, WI). The solvents, anhydrous dimethyl sulfoxide (DMSO), dimethylformamide (DMF), acetone, chloroform were also obtained from Sigma–Aldrich. Dichloromethane, ethyl acetate and toluene were obtained from EMD Chemicals (Gibbstown, NJ). The 70 test compounds were attained from different commercial sources (Sigma–Aldrich, etc.). They were either tested directly if they were obtained as racemates, or they were tested as mixtures of enantiomers if they were obtained as individual enantiomers. Chiraldex BPM column (2,3,6-tri-O-methyl- β -cyclodextrin in polysiloxane-based matrices, 30 m \times 250 μ m i.d. \times 0.12 μ m film thickness) was obtained from Supelco (Bellefonte, PA). A 10 m segment of this column was tailored and used for testing.

6.3.2. Methods

6-(Butylimidazolium)- β -cyclodextrin tosylate was prepared following the literature procedures.²⁰⁰ First, 6-tosyl- β -cyclodextrin was synthesized by reacting 35 g of β -cyclodextrin with 8 g of 1-tosylimidazole in 350 mL of deionized water. After the addition of 50 mL of aqueous NaOH (20%, w/v), the solids were filtered from the solution and the filtrate was collected and subsequently neutralized by NH₄Cl, washed by acetone and vacuum dried overnight. Subsequently, 13 g of the synthesized 6-tosyl- β -cyclodextrin was weighed out and reacted with 3 g of 1-butylimidazole in 25 mL DMF at 100 °C for two days. Acetone was then added to induce precipitation at ambient temperature. The reaction workup involved filtration of

the product followed by acetone washing and vacuum drying to afford the dry white powder of 6-(butylimidazolium)- β -cyclodextrin. The ^1H NMR spectrum indicates the 6-position substitutions on the cyclodextrin primary rim. Subsequently, this material was permethylated using the method described in a 1984 publication.²⁰¹ Resultantly, permethyl 6-(butylimidazolium)- β -cyclodextrin iodide (BIM-BPM-I) was obtained as the final product, which can be exchanged to trifluoromethanesulfonimide (NTf₂⁻) and trifluoromethanesulfonate (TfO) salt if needed. 6-(Tripropylphosphonium)- β -cyclodextrin tosylate was prepared and permethylated in the same fashion. The structure of the two charge bearing cyclodextrins is illustrated in Figure 6.1. Dicationic and tricationic ionic liquids were synthesized according to the literature guidelines^{183, 185, 186, 187} and their structures are depicted in Figure 6.2.

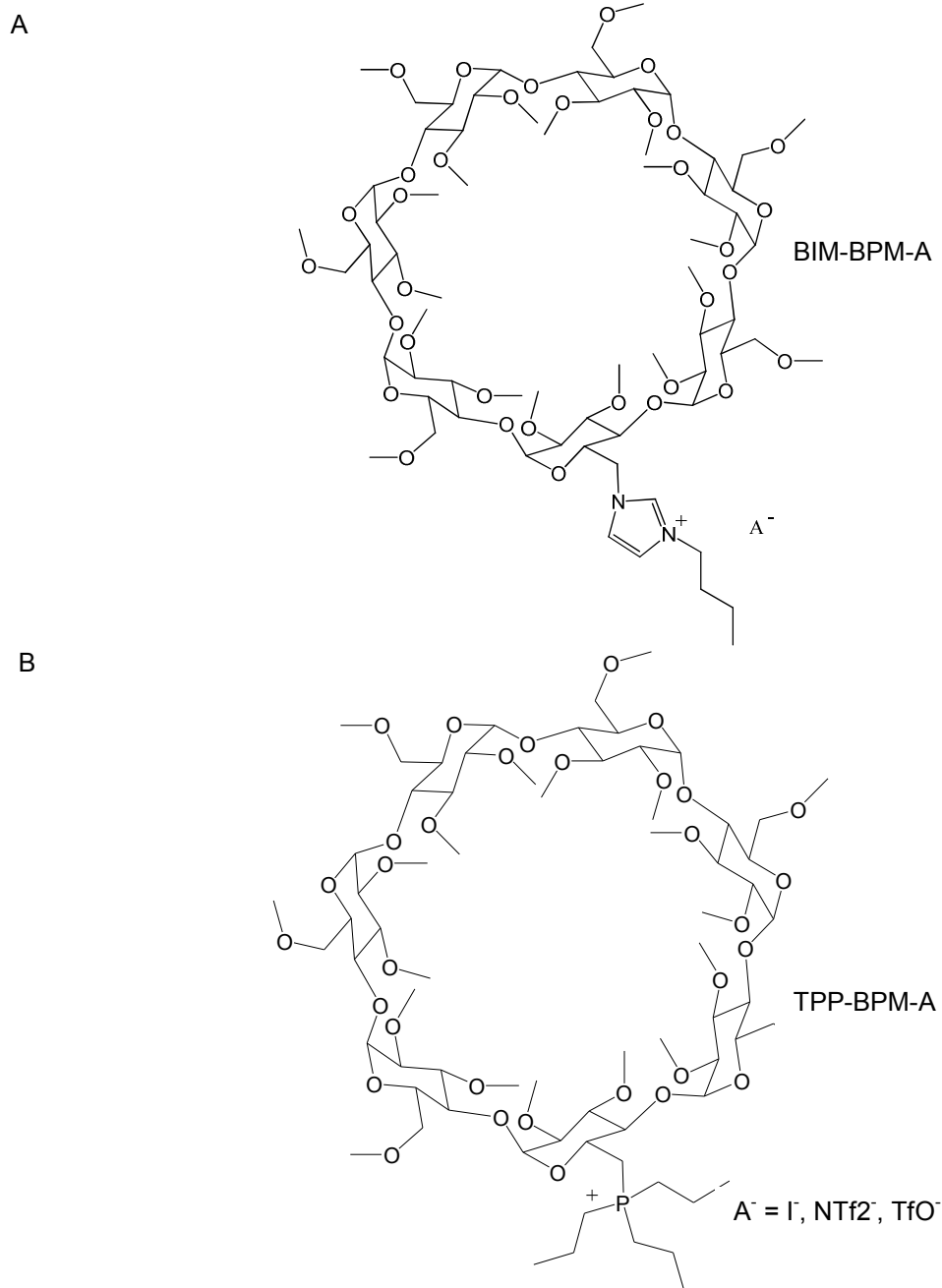


Figure 6.1 Structures of ionic permethyl β -cyclodextrins used in this study. A. BIM-BPM-A, B. TPP-BPM-A

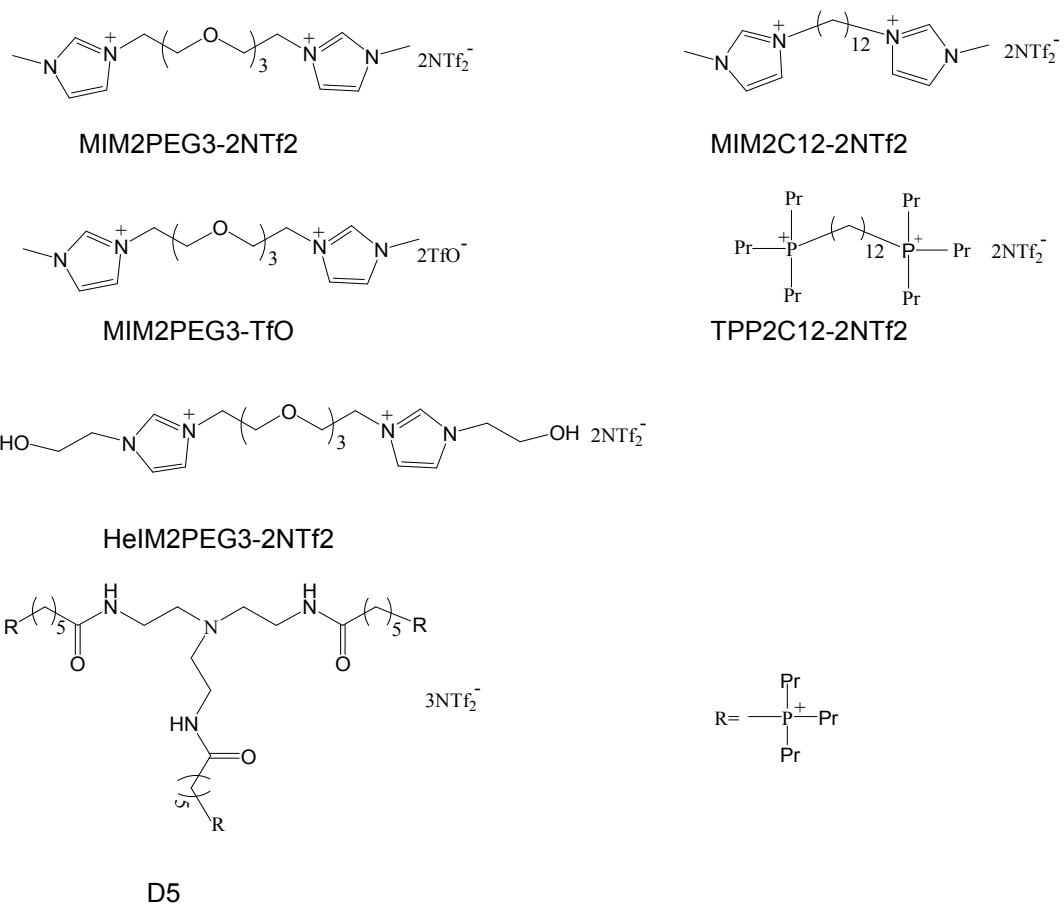


Figure 6.2 Structures of the ionic liquid matrices used for the dissolution of chiral selectors.

For comparison purposes, all GC columns were prepared following the literature recipe.
¹⁹² The derivatized cyclodextrins were dissolved in ionic liquids to make solution of 25% (w/w) concentration. The mixture was then dissolved in dichloromethane to give a coating solution of 0.45% (w/v) concentration. The static coating method was used in this work. In a water bath maintained at 40 °C, the coating solution was injected to completely fill a segment of the salt pretreated capillary. The capillary was then sealed at one end and the solvent was evaporated at a steady speed from the other end under vacuum. Coated columns were flushed with dry helium gas overnight and conditioned at 120 °C for 2 h prior to use. Column efficiency was

measured using naphthalene at 100 °C. Columns prepared in this study were made of a uniform length of 10 m. They were all determined to possess efficiencies of 4000–5000 plates/m and film thickness of 0.25 µm.

The samples assayed by thermogravimetric analysis (TGA) were made by dissolving target cyclodextrins in ionic liquids (25%, w/w). These solutions were analyzed in 20 mg aliquot and they were heated in a platinum pan from 100 °C to 500 °C at 10 °C/min in a dynamic nitrogen atmosphere. The decomposition profile for each sample was recorded and the 5% weight loss temperatures were marked to determine the stationary phase thermal stabilities.

6.3.3. *Equipment*

The GC equipment used was an Agilent (Columbia, MD) model 6892N (G 1540N) gas chromatograph equipped with a flame ionization detector and Agilent ChemStation data acquisition software. All analyses were performed isothermally with a helium carrier gas flow rate of 1 mL/min and a split ratio of 100/1. The injector and detector temperature was set at 250 °C and 300 °C, respectively. TGA measurements were performed using a TGA 2050 (TA Instruments Inc., New Castle, DE, USA).

6.4 Results and discussion

The structures of the modified cyclodextrins used in this study are shown in Figure 6.1. They are permethyl-6-(butylimidazolium)-β-cyclodextrin (BIM-BPM) and permethyl-6-(tripropylphosphonium)-β-cyclodextrin (TPP-BPM) paired with iodide, NTf₂, and triflate anions. Different cyclodextrin and ionic liquid combinations were evaluated for optimization of the stationary phase composition.

6.4.1. Optimization of the stationary phase composition

6.4.1.1. Optimization of the chiral selector

The two cyclodextrin derivatives investigated as chiral selectors were permethyl-6-(butylimidazolium)- β -cyclodextrin iodide (BIM-BPM-I) and permethyl-6-(tripropylphosphonium)- β -cyclodextrin iodide (TPP-BPM-I). They were dissolved in MIM2PEG3-2NTf2 (1,11-di(3-methylimidazolium)-3,6,9-trioxaundecane bis(trifluoromethane)sulfonimide) and TPP2C12-2NTf2 (1,12-di(triethylphosphonium)dodecane bis(trifluoromethane)sulfonimide) (see Figure 6.2) and coated as GC stationary phases using the same procedures (see Section 2). The enantioseparation of α -ionone on the four stationary phases is shown in Figure 6.3.

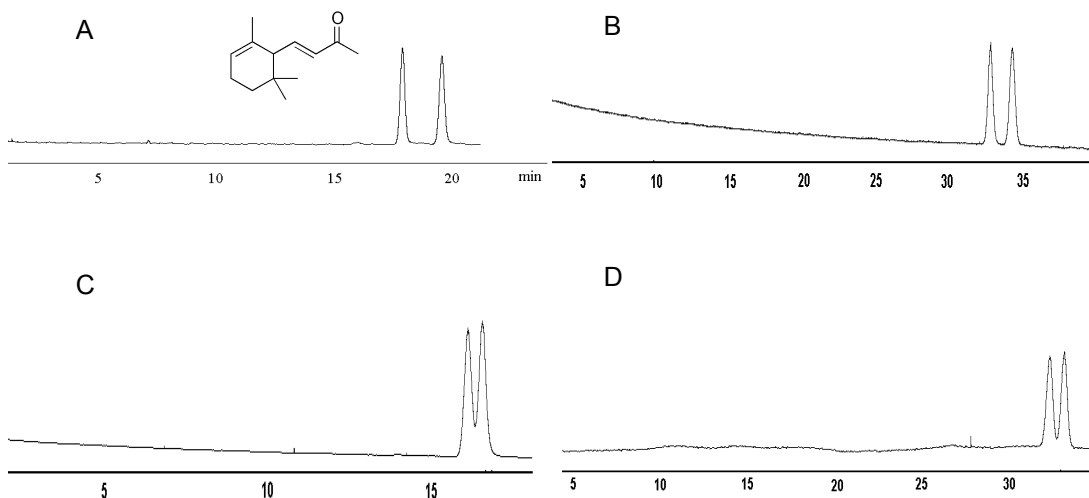


Figure 6.3 Separation of α -ionone on: A. BIM-BPM-I plus MIM2PEG3-2NTf2 B. BIM-BPM-I plus TPP2C12-2NTf2 C. TPP-BPM-I plus MIM2PEG3-2NTf2 D. TPP-BPM-I plus TPP2C12-2NTf2. Helium at 1 mL/min, 100°C

All four ionic cyclodextrin containing CSPs showed good efficiencies in the range of 4000–5000 plates/m. However the enantioselectivity of the TPP-BPM-I stationary phase was relatively low. As indicated by Figure 6.3, the enantioselectivity of α -ionone ($\alpha_{\alpha\text{-ionone}}$) was only 1.03 when MIM2PEG3-2NTf2 was used as the solvent matrix. Even when TPP2C12-2NTf2 was used as the solvent, the enantioselectivity remained low for the TPP-BPM-I chiral selector. On

the contrary, the BIM-BPM-I containing IL stationary phases provided not only high efficiencies but also high enantioselectivities. Therefore, the BIM-BPM-I chiral selector appears to be quite advantageous compared to its tripropylphosphonium derivatized counterpart. It appears that while high efficiency columns can be achieved with both these ionic chiral selectors, the nature of the ionic functionality has a significant impact on the enantioselectivity of the stationary phases.

After BIM-BPM was determined to be the best cationic moiety for the chiral selector, attention was focused on the counter ion that provides the best efficiency, enantioselectivity and thermal stability. For this purpose, BIM-BPM-I, permethyl-6-(butylimidazolium)- β -cyclodextrin bis(trifluoromethane)sulfonimide (BIM-BPM-NTf₂), and permethyl-6-(butylimidazolium)- β -cyclodextrin trifluoromethanesulfonate (BIM-BPM-TfO) were prepared for evaluation. To obtain their thermal stabilities, they were individually dissolved in MIM2PEG3-2NTf₂ (25%, w/w) and subjected to thermogravimetric analysis (TGA). As was indicated by the TGA readings, when mixed with MIM2PEG3-2NTf₂, the three compounds yielded very similar decomposition/volatilization profiles in the temperature range of 100–250 °C. They all showed a weight loss of approximately 5% at 250 °C. Thus, at normal chiral GC operating temperatures, anion identity has little effect on the thermal stability of the chiral selector molecules.

Subsequently, analytes with a range of different functionalities were assayed on the three columns to evaluate the impact of the anion on the stationary phase enantioselectivities. A few examples are given in Figure 6.4. Symmetrical peaks were observed for these analytes on both the BIM-BPM-I and BIM-BPM-TfO columns. However, BIM-BPM-NTf₂ induced severe tailings for these analytes. Since BIM-BPM-I and BIM-BPM-TfO exhibited similar chromatographic behaviors, the iodide salt form of the chiral selector was used for the rest of the study due to its ease of preparation.

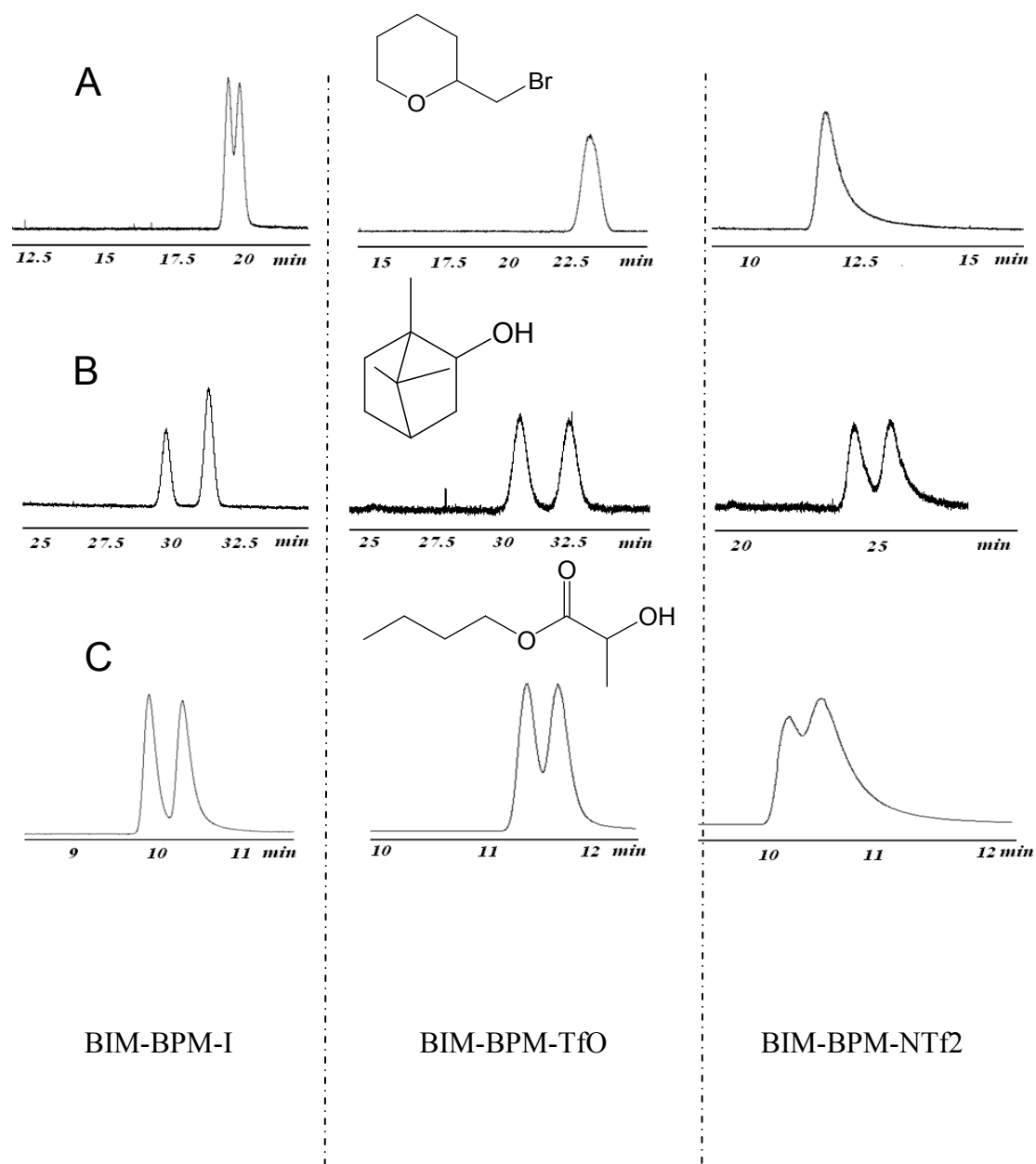


Figure 6.4 Examples of separations achieved on BIM-BPM-I, BIM-BPM-TfO, and BIM-BPM-NTf2 containing columns. Helium at 1 mL/min.

A. Separation of 2-(bromomethyl) tetrahydro-2H-pyran, 60°C.

B. Separation of borneol, 80°C.

C. Separation of butyl lactate, 80°C.

*Borneol samples were manual mixtures of the (+) and (-) enantiomers. The peak area ratios of the two enantiomer peaks were therefore not always identical

6.4.1.2. Optimization of the matrix

Based on their merits established in previous studies,^{183, 185-187} six different ionic liquids were investigated to determine the most appropriate ionic liquid matrix for this work. The ionic liquids tested are shown in Figure 6.3 (referred to as: MIM2PEG3-2NTf2, MIM2C12-2NTf2, MIM2PEG3-2TfO, HeIM2PEG3-2NTf2, D5, and TPP2C12-2NTf2). Silicone OV-101 was also investigated as a solvent for comparison with the selected ionic liquids. The column containing MIM2PEG3-2NTf2 matrix produced the highest efficiency (ca. 5000 plates/m) and the best enantioselectivity (e.g. $\alpha_{\alpha\text{-ionone}} = 1.1$). Meanwhile the polysiloxane-based stationary phase displayed decent enantioselectivity ($\alpha_{\alpha\text{-ionone}} = 1.07$) but extremely low efficiency in the 500–1000 plates/m range. This is probably due to the low polarity of the polysiloxane used which is unfavorable for the dissolution of the ionic substances. Therefore MIM2PEG3-2NTf2 was employed in the following studies.

6.4.2. Improvement over the first ionic liquid containing cyclodextrin-based CSPs

According to the 2001 report,¹⁹² of the 68 pairs of enantiomers separated on a commercial ChiralDex BPM column, only 21 were separated on the neutral permethyl- β -cyclodextrin-based stationary phase (BPM), albeit with much higher efficiency. Conversely in this study by using an imidazolium salt cyclodextrin derivative, very different results were obtained. A total number of 70 compounds were selected and tested based on their previously proved separation on ChiralDex BPM and/or ChiralDex BDM column.²⁰² Fifty-one compounds showed enantiomeric separation on the BIM-BPM-I stationary phase. In addition, 6 compounds that were not separated on the commercial ChiralDex BPM column were separated on the BIM-BPM-I column.

A performance comparison between the BIM-BPM-I stationary phase and the neutral BPM containing IL-based stationary phase was carried out by examination of the enantioseparations achieved on the two stationary phases (Table 6.1). When testing Table 6.1

compounds under the same conditions, the BIM-BPM-I column produced up to seven times more efficient enantioseparations than the neutral BPM stationary phase. Generally, the BIM-BPM-I stationary phase produced greater analyte retention than the BPM stationary phase, with two exceptions, i.e. α -pinene and β -pinene. Moreover, the majority of analytes showed better enantioselectivities on the BIM-BPM-I stationary phase. The biggest improvement of enantioselectivity from 1.04 to 1.10 was achieved for 2-ethoxytetrahydrofuran. With higher enantioselectivities, efficiencies and retentions, the BIM-BPM-I stationary phase afforded up to six times greater resolutions than the neutral BPM stationary phase (see tetrahydro-2-(2-propynyloxy)-2H-pyran).

In the previous 2001 work it was also observed that a ring structure was important for enantiomeric separations on the neutral BPM-based IL CSP. However, compounds without ring structures, e.g. acetoin, 3-butyn-2-ol, linalool, *t*-butyloxy-2-propanol, methyl-2-chloropropionate, methyl-2-bromopropionate, methyl lactate and butyl lactate (see Table 6.3), were easily separated on the new ionic cyclodextrin-based IL CSP. For example, methyl-2-chloropropionate enantiomers were baseline separated with a retention factor of 4.00 at 55 °C. Clearly, structural rigidity of analytes becomes less of a requirement for enantiomeric separation on the charged CD-based stationary phase.

When the column stability was studied, it was noted that no compounds were tested over 110 °C in the previous work.¹⁹² That was because the BMIM-Cl ionic liquid used in this early work was stable only up to around 140 °C.¹⁸³ Since MIM2PEG3-2NTf₂ has a decomposition/volatilization temperature of over 300 °C,¹⁸⁵ it clearly is a more robust matrix material for GC stationary phases. The compounds in this study were separated at temperatures up to 175 °C (see 2,3-dihydro-7a-methyl-3-phenylpyrrolo[2,1-b]oxazol-5(7aH)-one). Now that the IL column operation temperature has been extended, a broader pool of less volatile compounds can be analyzed.

Table 6.1 Performance improvement of the new IL phase gained over its 2001 predecessor¹⁹².

Compound	T (°C)	BPM in BMIM-Cl, 10 m				BIM-BPM-I in MIM2PEG3-2NTf2, 10 m			
		k'_1 ^a	α ^b	Rs ^c	N (plates)	k'_1	α	Rs	N (plates)
camphene	25	10.2	1.11	0.9	1400	11.9	1.05	0.7	1850
α -pinene	25	15.8	1.07	1.2	5000	9.3	1.10	1.0	2100
β -pinene	30	25.8	1.03	1.0	15300	12.1	1.05	1.2	3640
2-ethoxy tetrahydrofuran	30	3.24	1.04	0.8	11200	4.6	1.10	1.5	6820
2-acetyl-5-norbornene	40	55.7	1.05	0.9	6000	105.8	1.04	2.0	43560
Fenchone	40	27.7	1.04	1.0	13600	61.0	1.02	1.0	14570
tetrahydro-2-(2-propynyloxy)-2H-pyran	50	19.1	1.02	0.5	19400	35.8	1.08	2.9	26530
3-chloro-2-norbornanone	60	70.4	1.05	1.1	7500	164.8	1.08	4.0	36560
α -ionone	100	21.2	1.06	1.5	12300	26.8	1.10	4.4	39100
4-methyl-tetralone	100	35.1	1.03	1.2	21500	82.3	1.06	2.7	51650

^a k'_1 is the retention factor of the first eluted enantiomer. It is calculated as $k'_1 = (t_1 - t_0)/t_0$, whereas t_1 is the retention time of the first eluted peak and t_0 is the column dead time.

^b α is the enantioselectivity exhibited by a pair of enantiomers. It can be obtained from equation $\alpha = k'_2/k'_1$, whereas k'_1 and k'_2 are the retention factors of the first and second eluted peak, respectively.

^c Rs is the resolution obtained for a pair of enantiomers. It can be retrieved as follows, $Rs = 2*(t_2 - t_1)/(W_1 + W_2)$. Note that t_1 and t_2 are the retention times of the first and second eluted enantiomers, while W_1 and W_2 are the baseline peak width of the first and second peaks.

Table 6.2 Performance comparison of neutral BPM stationary phases based on the monocationic IL (BMIM-Cl) and a dicationic IL (MIM2PEG3-2NTf2).¹⁹²

Compound	T (°C)	BPM in BMIM-Cl, 10 m				BIM-BPM-I in MIM2PEG3-2NTf2, 10 m			
		k'_1	α	R_s	N (plates)	k'_1	α	R_s	N (plates)
2-acetyl-5-norbornene	40	55.7	1.05	0.9	6000	48.6	1.0	0	2760
tetrahydro-2-(2-propynyloxy)-2H-pyran	50	19.1	1.02	0.5	19400	4.8	1.0	0.8	7300
3-chloro-2-norbornanone	60	70.4	1.05	1.1	7500	86.9	1.03	0.8	9240
α -ionone	100	21.2	1.06	1.5	12300	18.2	1.04	1.3	15680
4-methyl-tetralone	100	35.1	1.03	1.2	21500	50.0	1.02	0.6	8950

Table 6.3 Enantioseparation of 56 compounds on BIM-BPM-I column and Chiraldex BPM column.

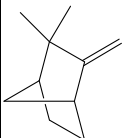
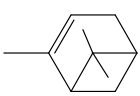
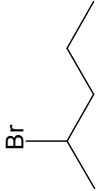
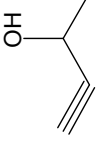
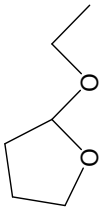
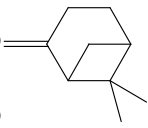
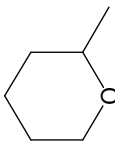
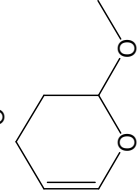
Compound ^a	Structure	T (°C)	BIM-BPM-I in MIM2PEG3-2NTf2, 10 m				Chiraldex BPM, 10 m			
			k'_1	α	Rs	N (plates)	k'_1	α	Rs	N (plates)
camphene		25	11.9	1.05	0.7	1890	33.0	1.09	2.1	8000
α -pinene		25	9.26	1.10	1.0	2100	25.5	1.15	3.4	8310
2-bromopentane		25	2.08	1.06	0.8	3000	4.96	1.05	1.3	13680
3-butyne-2-ol		25	16.0	1.05	1.2	9120	3.27	1.14	2.7	10050
2-ethoxytetrahydrofuran		30	4.62	1.10	1.5	6820	5.75	1.09	2.1	11980
β -pinene		30	12.1	1.05	0.7	3640	30.5	1.06	1.2	6360
2-methyltetrahydro-2H-pyran		30	2.06	1.0	0	2070	3.07	1.05	1.0	9110
3,4-dihydro-2-methoxy-2H-pyran		30	7.69	1.0	0	3238	8.80	1.06	1.6	13485

Table 6.3 Continued

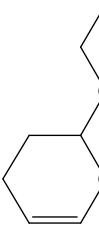
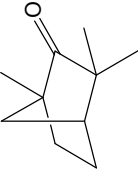
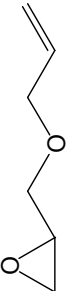
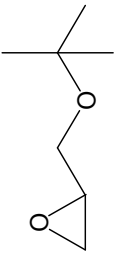
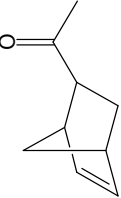
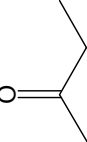
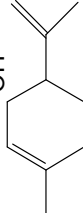
Compound ^a	Structure	T (°C)	BIM-BPM-I in MIM2PEG3-2NTf2, 10 m			Chiraldex BPM, 10 m				
			k'_1	α	R_s	N (plates)	k'_1	α	R_s	N (plates)
2-ethoxy-3,4-dihydro-2H-pyran		40	6.54	1.0	0	5500	9.18	1.06	1.7	17790
fenchone		40	61.0	1.02	1.5	14570	62.2	1.07	1.8	9640
allyl glycidyl ether		40	26.6	1.01	0.5	14500	10.0	1.05	1.9	32160
t-butyl glycidyl ether		40	22.0	1.04	1.3	14430	14.6	1.07	2.4	23411
2-acetyl-5-norbornene, endo and exo*		40	105.8	1.04	2.0	43560	91.3	1.02	0.7	25000
acetoin		50	10.3	1.08	1.6	8150	2.24	1.13	3.7	24230
limonene		50	6.87	1.05	1.3	12770	11.8	1.04	1.5	30660

Table 6.3 Continued

Compound ^a	Structure	T (°C)	BIM-BPM-I in MIM2PEG3-2NTF2, 10 m				Chiraldex BPM, 10 m			
			k'_1	α	R_s	N (plates)	k'_1	α	R_s	N (plates)
5-norbornene-2-ol, endo and exo*		50	57.1	1.0	0	18360	37.6	1.03	1.0	25920
<i>t</i> -butyloxy-2-propanol		50	70.6	1.03	1.5	39900	55.5	1.0	0	15380
5-norbornene-2-ol, endo and exo*		50	7.88	1.06	1.4	10700	6.54	1.23	5.2	13020
tetrahydro-2-(2-propynyloxy)-2H-pyran*		50	35.8	1.08	2.9	26520	27.2	1.07	2.4	24180
methyl-2-chloropropionate		55	4.00	1.05	1.6	20630	1.82	1.08	2.4	27540
2,5-dimethoxytetrahydrofuran		60	3.38	1.11	3.7	25730	2.60	1.14	4.0	25170
3-chloro-2-norbornanone*		60	164.8	1.08	4.0	36560	69.0	1.11	1.8	3240
3-methyl-1-cyclohexanone*		60	16.4	1.02	0.7	28800	8.42	1.0	0	7370

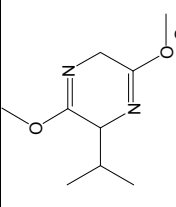
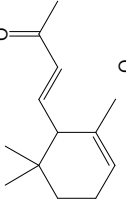
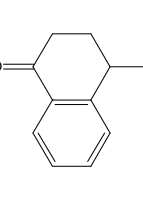
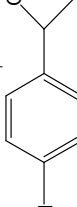
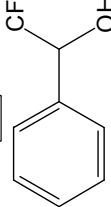
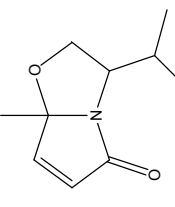
Table 6.3 Continued

Compound ^a	Structure	m			10			10 m				
		T (°C)	BIM-BPM-I	MIM2PEG3-2NTf2	T (°C)	BIM-BPM-I	MIM2PEG3-2NTf2	T (°C)	BIM-BPM-I	MIM2PEG3-2NTf2		
		α	Rs	N (plates)	k' ₁	α	Rs	N (plates)	k' ₁	α	Rs	N (plates)
2-(bromomethyl)tetrahydr o-2H-pyran*		60	21.5	1.02	0.9	25030	22.9	1.0	0	16070		
2-(chloromethyl)tetrahydr o-2H-pyran*		60	11.3	1.01	0.6	30480	11.3	1.0	0	18680		
methyl-2-bromopropionate		60	15.3	1.02	0.8	25090	8.96	1.3	1.0	33030		
linalool*		60	30.1	1.03	1.5	31990	32.1	1.6	1.1	28100		
3-methylcyclohexanol, cis and trans*		60	19.2	1.07	2.4	19750	16.9	1.04	0.9	28100		
4-(chloromethyl)-2,2-dimethyl-1,3-dioxane		60	24.6	1.04	1.5	21640	17.6	1.0	0	27730		
2-methylpiperidine dr*		70	4.57	1.05	1.7	28760	3.97	1.10	3.0	23200		
3-methylpiperidine dr*		70	20.7	1.04	1.6	31320	11.2	1.04	1.5	30050		
3-methylpiperidine dr*		70	19.4	1.02	0.8	25600	10.6	1.02	0.7	25380		

Table 6.3 Continued

Compound ^a	Structure	T (°C)	BIM-BPM-I in MIM2PEG3-2NTf2, 10 m				Chiraldex BPM, 10 m			
			k'_1	α	Rs	N (plates)	k'_1	α	Rs	N (plates)
2-(2-butynyloxy)tetrahydro-2H-pyran		70	19.93	1.0	0	21130	17.48	1.07	2.4	22360
4-methoxymethyl-1,3-dioxane-2-one		80	68.22	1.0	0	37200	37.75	1.07	3.0	39220
styrene oxide		80	17.6	1.01	0.7	38400	6.22	1.05	2.3	38800
borneol		80	29.4	1.06	2.6	39150	32.3	1.09	3.4	27940
1-phenylethanol		80	48.8	1.04	2.1	40830	15.4	1.14	3.9	16930
N-trifluoroacetyl alanine ethyl ester		80	21.1	1.01	0.7	36700	3.20	1.06	2.9	37240
methyl lactate*		80	3.69	1.07	2.0	20370	0.69	1.08	1.0	1770
butyl lactate*		80	13.0	1.04	1.5	23750	4.93	1.02	0.6	2260
2-(3-chloropropoxy)-tetrahydro-2H-pyran		80	21.9	1.01	0.7	35710	24.8	1.02	0.7	11290

Table 6.3 Continued

Compound ^a	Structure	T (°C)	BIM-BPM-I in MIM2PEG3-2NTf2, 10 m				Chiraldex BPM, 10 m			
			k' ₁	α	Rs	N (plates)	k' ₁	α	Rs	N (plates)
2,5-dihydro-3,6-dimethoxy-2-isopropyl-pyrazine*		90	5.66	1.15	4.9	25210	6.85	1.07	3.1	41300
α -ionone*		100	26.8	1.10	4.4	39100	20.6	1.07	3.4	44330
4-methyl-1-tetralone*		100	82.3	1.06	2.7	51640	34.3	1.06	2.4	28370
4-chloro- α -methylbenzyl alcohol		100	58.8	1.03	1.2	34300	23.5	1.16	3.5	10840
1-phenyl-2,2,2-trifluoroethanol*		100	39.0	1.03	1.5	38770	11.0	1.10	1.4	5030
2,3-dihydro-7a-methyl-3-isopropylpyrrolo-[2,1-b]-oxazol-5(7aH)-one		100	41.1	1.04	1.9	34460	13.5	1.08	3.4	40570

^a Compounds that are better separated on BIM-BPM-I stationary phase are indicated with the sign *, and compounds that were derivatized with trifluoroacetic anhydride prior to assay are noted with dr.

6.4.3. Comparison of the BIM-BPM-I CSP to the corresponding commercial CSP

Given the improved enantioseparation power of the charged cyclodextrin containing CSP, it is valid to assume the BIM-BPM-I column may accomplish comparable or possibly better enantiomeric separations than its commercialized analog. The Chiraldex BPM column was selected for comparison as the commercial stationary phase. The stationary phase of this column is composed of permethylated β -cyclodextrin (BPM) dissolved in a polysiloxane-based matrix.

In total, 56 compounds achieved enantiomeric resolution on BIM-BPM-I and Chiraldex BPM combined. The structures, retention factors, selectivities, resolutions and theoretical plate numbers of the 56 compounds are shown in Table 6.3. Due to the doubled film thickness of stationary phase on the BIM-BPM-I column (film thickness: 0.25 μm), compound retentions were usually longer on this column than on the Chiraldex BPM column (film thickness: 0.12 μm). Respectively, 28 and 33 compounds showed baseline separation on the BIM-BPM-I column and the Chiraldex BPM column. In the meantime, 23 compounds showed improved enantioseparations on the ionic liquid-based column, while 33 showed comparable or better enantioseparation on the commercial column.

The compounds showing better enantioseparations on the ionic liquid column were mostly ketones, esters, secondary and tertiary alcohols. Despite the fact there were 6 racemates separated solely on the commercial column, 6 other racemates that displayed no enantioselectivity on Chiraldex BPM were separated on BIM-BPM-I. Figure 6.5 provides examples of the enantioseparation of these compounds on both stationary phases. As is indicated by the structure, 5-norbornene-2-ol is composed of two pairs of enantiomers, one for the endo-configuration and one for the exo-configuration. One pair of enantiomers was separated on the BIM-BPM-I column while the other pair was separated on the Chiraldex BPM column. This demonstrates the complementary enantioselectivity of the two stationary phases. When the endo- and exo-isomers of 2-benzoyl-5-norbornene were injected on the commercial

column, only one pair of enantiomers was partially separated while the other pair eluted in one single tailing peak. However, both pairs of enantiomers were separated on the IL-based column, with excellent peak shape and one baseline separation. Also on the IL phase, the endo- and exo-isomers were better separated from each other. Indeed, it has been reported that IL phases show better separations of structural and geometric isomers than conventional GC stationary phases.²⁰³

Interestingly, for compounds with higher polarities, BIM-BPM-I offered improved peak shapes over the commercial column. The chromatograms of some of these compounds on both stationary phases are shown in Figure 6.6. These analytes were also injected on the neat MIM2PEG3-2NTf2 stationary phase and a neat polysiloxane stationary phase (Rtx-5). Their peak shapes on the two neat stationary phases are shown in Figure 6.7. Slight to moderate peak tailing was observed for these compounds on the polysiloxane stationary phase, however, little tailing was found for the eluted peaks on the MIM2PEG3-2NTf2 stationary phase. Therefore, it is highly possible the distorted peak shapes on Chiraldex BPM were caused by the polysiloxane matrix used for the commercial column.

In this study, it was observed that the efficiencies on the two CSPs were also largely dependent on the analytes' polarities. Hydrocarbons, tetrahydro-2*H*-pyrans and ethers are compounds of low to moderate polarities. They exhibited worse efficiency on the IL-based column than on the Chiraldex BPM column (see pinenes, 2-methyltetrahydro-2*H*-pyran and 2-ethoxytetrahydrofuran). However, more polar compounds, such as ketones and alcohols, produced plate numbers up to 10 times higher on the BIM-BPM-I CSP than on the Chiraldex BPM CSP (see 3-chloro-2-norbornanone).

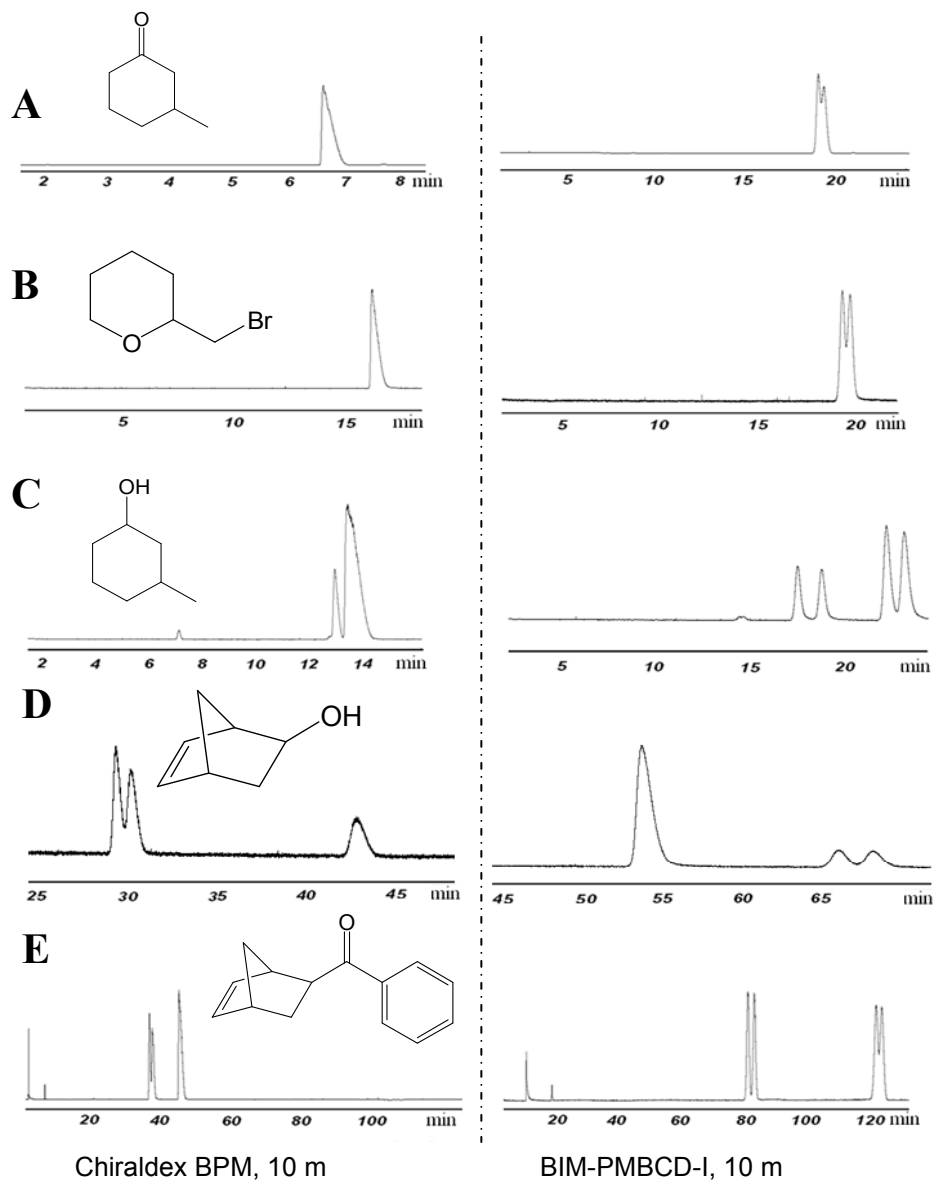


Figure 6.5 Examples of compounds showing improved separation on the BIM-BPM-I column

compared to on the Chiraldex BPM column. Helium at 1 mL/min

- A. Separation of 3-methyl-1-cyclohexanone, 60°C
- B. Separation of 2-(bromomethyl) tetrahydro-2*H*-pyran, 60°C
- C. Separation of 3-methylcyclohexanol (cis+trans), 60°C
- D. Separation of 5-norbornene-2-ol (endo+exo), 50°C
- E. Separation of 2-benzoyl-5-norbornene (endo+exo), 110°C

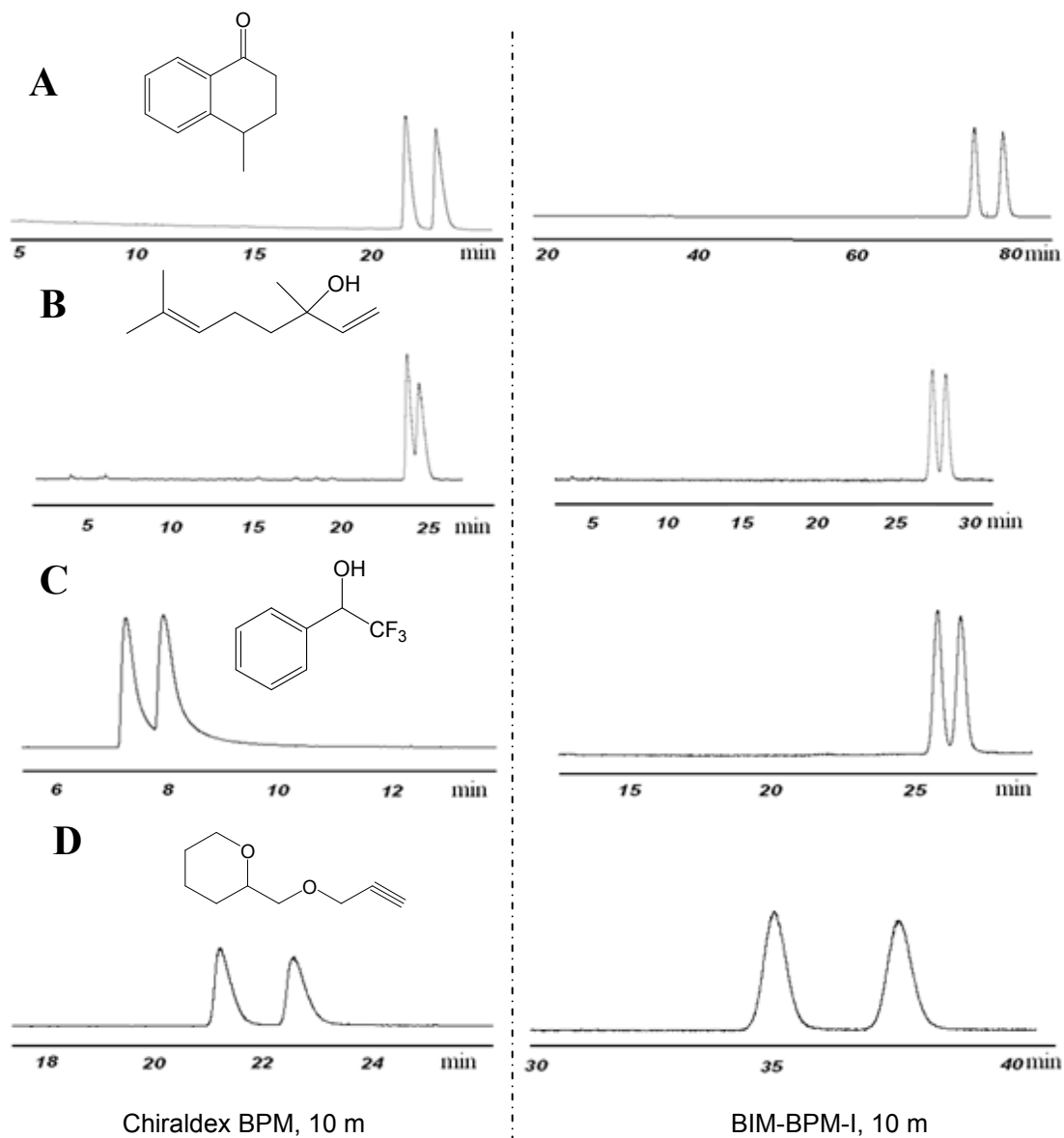


Figure 6.6 Comparison of compound peak shapes obtained on the Chiraldex BPM column and the BIM-BPM-I column. Helium at 1 mL/min

A. Separation of 4-methyl-1-tetralone, 100°C,
 B. Separation of linalool, 60°C
 C. Separation of 1-phenyl-2,2,2-trifluoroethanol, 100°C
 D. Separation of tetrahydro-2-(2-propynyloxy)-2H-pyran, 50°C

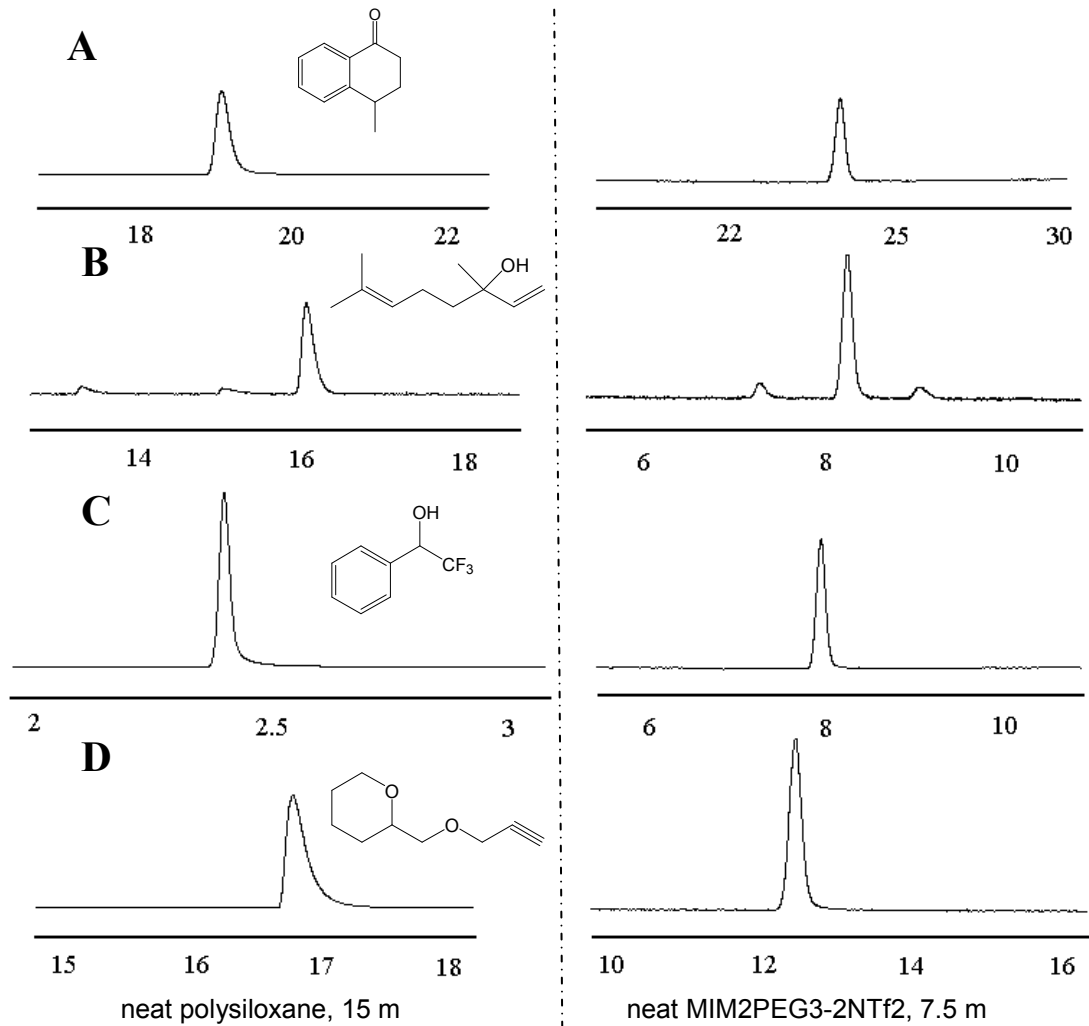


Figure 6.7 Comparison of compound peak shapes obtained on neat polysiloxane column (Rtx-5) and neat MIM2PEG3-2NTf2 column. Helium at 1 mL/min
 A. 4-methyl-1-tetralone, 100°C,
 B. linalool, 60°C
 C. 1-phenyl-2,2,2-trifluoroethanol, 100°C
 D. tetrahydro-2-(2-propynyloxy)-2H-pyran, 50°C

6.5 Conclusions

A charged cyclodextrin GC chiral selector was introduced in combination with ionic liquid matrices and successfully applied to the enantioseparation of a variety of chiral molecules. While the nature of cationic cyclodextrin chiral selectors makes a crucial contribution to the significantly enhanced column efficiency, the type of ionic functional group on the cyclodextrin has a major impact on the chiral recognition capabilities of the stationary phase. When compared to a comparable commercial stationary phase, the new IL-based stationary phase not only improved enantioseparations for more than one-third of the test solutes, but also managed to separate some compounds that were not separated on the commercial column. Furthermore, the IL-based column provided better peak shapes and improved peak efficiencies for racemic analytes with higher polarities.

This work demonstrated comparable and complementary performance of IL-based columns to the potent commercial chiral stationary phase. It not only introduced a new concept of using charged cyclodextrins as chiral selectors in GC, but also demonstrated the feasibility of using ionic liquids for high enantioselectivity GC-CSPs. With the large pool of ionic liquids and variety of ionic cyclodextrin structures available nowadays, these types of GC-CSPs offer a new avenue of potentially useful and interesting research and development.

CHAPTER 7

GENERAL SUMMARY

7.1 Part one (Chapter 1-2)

The first chapter provided a background to chirality and explained what chirality is and why chiral separation is critical to industries and especially for pharmaceutical companies. The history, mechanism and properties of each of the major types of chiral GC and chiral HPLC stationary phases have been discussed briefly. In the second chapter, the macrocyclic antibiotic dalbavancin was linked to silica gel by two different binding chemistries. The enantiomeric separation capabilities of the two columns D1 and D2 were evaluated and compared with Chirobiotic T and T2 commercial columns. The dalbavancin based columns can separate some racemic solutes that cannot be separated on commercial teicoplanin based columns. Moreover, dalbavancin based CSPs exhibits enhanced enantioselectivities to carboxylic acids, where the additional cationic site of the chiral selector may play an important role during the chiral recognition process.

7.2 Part two (Chapter 3-6)

Chapter three gives a general introduction to the history and properties of ionic liquids and their applications in analytical chemistry. The next chapter focused on the evaluation of linear tricationic ion pairing reagents for divalent anion detection in positive mode ESI-MS. It has been revealed that these linear ion pairing reagents provided improved LOD for anions than trigonal ion pairing reagents in general. The optimum chain length was found to be either 10 or 6 carbons. The best ionic moieties are tripropylphosphonium and benzyimidazolium. The synthesis of these linear tricationic ionic liquids was described in Chapter five. The physicochemical properties of these linear ionic liquids and their ability to be used in

electrowetting applications have been studied. The linear tricationic ionic liquids have lower melting points compared to more rigid trigonal tricationic ionic liquids.

Chapter 6 reported a new type of chiral GC stationary phases using a methylated cationic cyclodextrin derivative as chiral selector and ionic liquids as matrices. High efficiencies and broad enantioselectivities were obtained on these columns. When evaluated against the commercial stationary phase using polysiloxanes as matrix and neutral cyclodextrin as chiral selector, the IL-based stationary phase showed comparable and complementary selectivity for the 70 compounds tested. Furthermore, the IL-based column provides improved peak shapes and peak efficiencies for compounds with higher polarities. However, the commercial column still provides in broader applicability in general.

APPENDIX 1

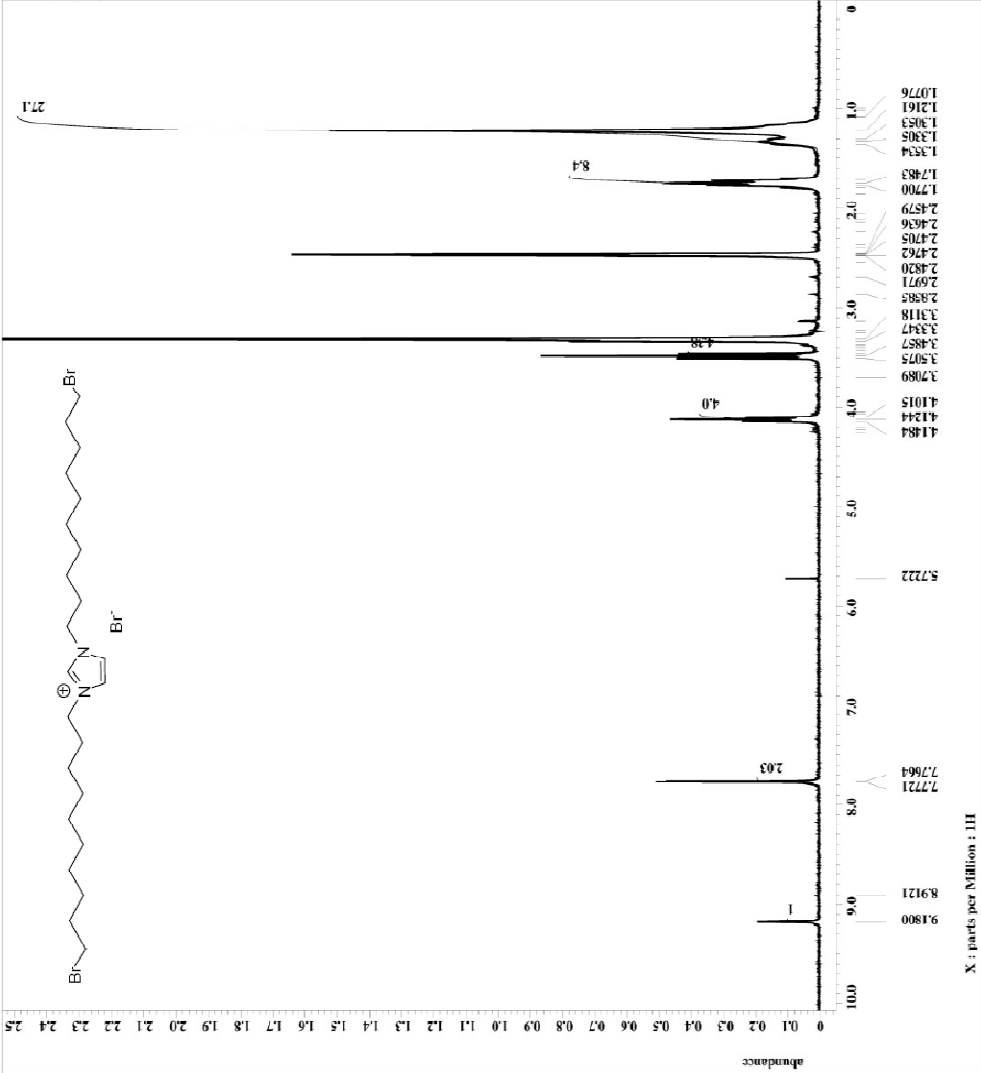
¹H AND ¹³C NMR SPECTRA OF
1-BROMODECYL-3-BROMODECYL IMIDAZOLIUM BROMIDE SALT (1a)



```

= EM060308 (C10L7Core1) -
File Name = data
Author =
Sample Name = sample_pulse_cx2
Sample ID = SM44954
Solvent = DMSO-D6
Creation Time = 3-JUN-2008 18:14:40
Revision Time = 3-JUN-2008 18:02:39
Current Time = 12-SEP-2010 00:22:39
Comment = single pulse
Date Format = DD-MMM-YY
Dim Title =
Dim Units = [ppm]
Dimensions =
X_CK_200 =
Spectrometer = DEPTAQ2_NMR
X_read_strength = 7.0585031 [1] (300) [MHz]
X_resolution = 10.9717696 [s]
X_domain =
X_freq = 300.52965592 [MHz]
X_offset = 5 [ppm]
X_precans = 0
X_resolution = 0.34397631 [Hz]
X_sweep = 5.63570784 [MHz]
X_resolution = 300.52965592 [MHz]
Irr_Offset = 5 [ppm]
Tri_Domain =
Tri_Offset = 10
Tri_Offset = 5 [ppm]
Clipped =
Mod_Return = 1
Scans = 22
Total_Scans = 22
X_90_width = 13.01 [us]
X_acq_time = 4.9717696 [s]
X_gate = 4 [dB]
X_atn = 6.505 [us]
X_pulse =
P1_mode =
P2_mode =
Dante_Preset = FNAME
Initia_wait = 1 [s]
Recvr_gain = 48
P1_delay = 4 [s]
Repetition_time = 7.9717696 [s]
Temp_get = 24.6 [dC]

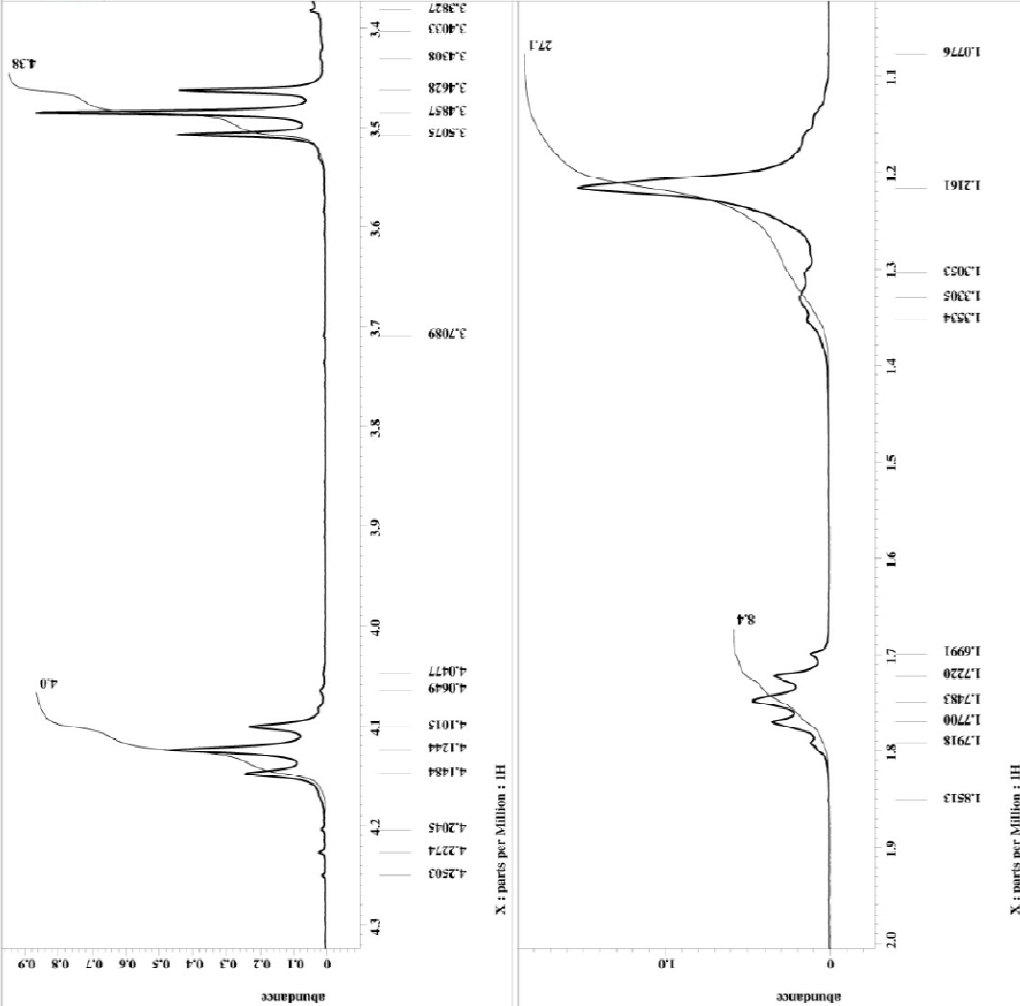
```





```

File Name = RW060308 (ClO4Core1) -
Author = delta
Experiment = single pulse.ex2
Pulse program = zgpg30
Solvent =
Creation Time = 3-JUN-2008 18:14:40
Revision Time = 3-JUN-2008 18:04:29
Current Time = 12-SEP-2010 00:24:19
Comment = single pulse
Data Format = 1D COMPLEX
Data Size = 32768
Sweep Rate = 10.000000
Dimensions = X
Spectrometer = ECK_300
Site = REFLX_NMR
Field strength = 7.0586013 T (300 MHz)
X_acq_duration = 2.90717696 [s]
X_domain = 1H
X_freq = 300.52965592 [MHz]
X_gain = 16384
X_points = 6
X_prescans = 1
X_resolution = 0.34397631 [Hz]
X_sweep = 1H 63970784 [kHz]
X_start = 300.52965592 [MHz]
X_stop = 300.52965592 [MHz]
IRF_freq = 1H
IRF_offset = 1 [ppm]
IRF_start = 300.52965592 [MHz]
IRF_stop = 300.52965592 [MHz]
Modulated = FALSE
Mod_return = 1
Scans = 22
Total_scans = 22
X_90_width = 13.01 [us]
X_acq_time = 2.90717696 [s]
X_angle = 45 [deg]
X_delay = 1.000000 [s]
X_pulse = 4.905 [us]
X_rec_mode = Cff
Xri_mode = Cff
Date_presat = FALSE
Date_acq_start = 20080603
Date_acq_end = 20080603
Relaxation_delay = 2 [s]
Repetition_time = 7.90717696 [s]
Temp_get = 24.6 [dC]
  
```





```

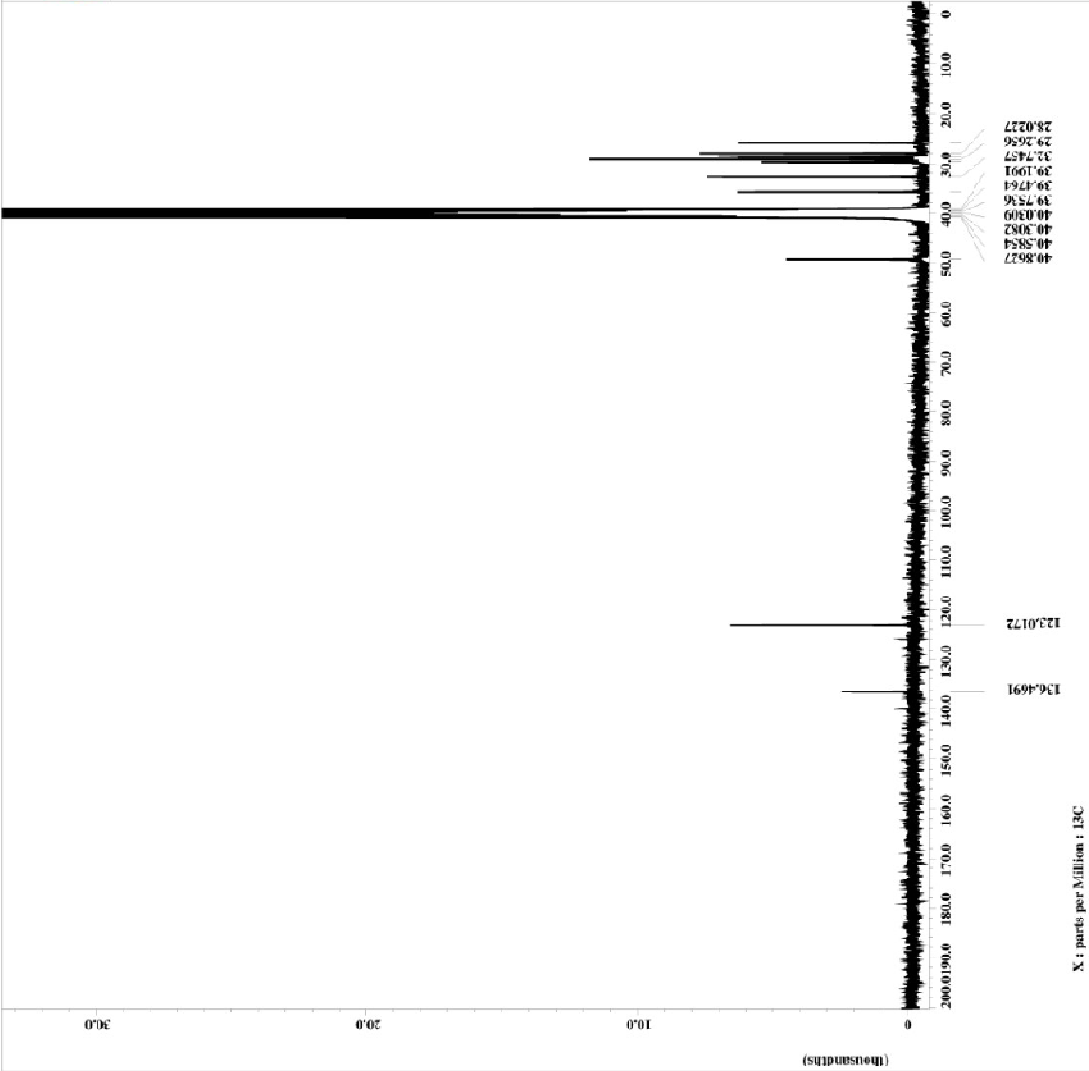
=====
Name      = 89060508 (LPCClOcrzr)-
Date_Exp  =
Time      =
Date      =
Author    =
Experiment = single_pulse_dec
Sample_id = 8776291
Solvent   = DMSO-D6
Creation_time = 6-JUN-2008 09:38:19
Revision_time = 06-JUN-2008 13:02:11
Current_time = 12-SEP-2010 12:28:50

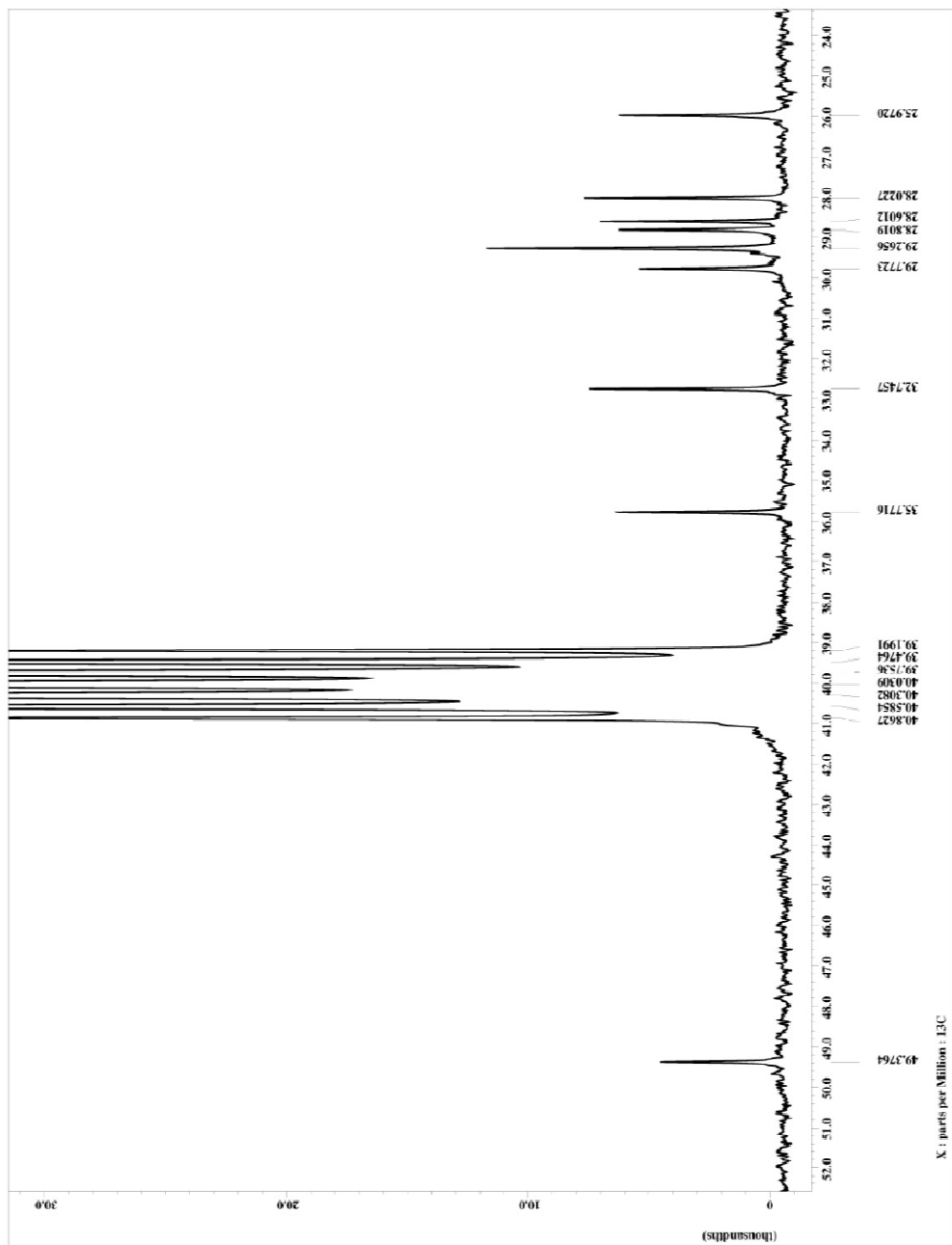
=====
Comment   = single pulse decouple
Data_format = ID COMPLEX
Data_size  = 5248
Data_title =
Data_units = [ppm]
Dimensions =
Sfile     = ECX 330
Spectrometer = DELTA2.NMR

=====
Field_strength = 7.05650131E+08 [MHz]
Acq_duration   = 4.76624064 [s]
X_freq         = 75.5623426 [MHz]
X_offset       = 100 [ppm]
X_points       = 55536
X_prescans     = 4
X_resolution   = 0.36124027 [Hz]
X_resolution_ppm = 0.5166666666666667 [ppm]
X_sweep_rate   = 18.6746442 [MHz]
Ycq_domain    =
Ycq_freq       = 300.62965592 [MHz]
Ycq_offset     = 5 [ppm]
Clipped       = FALSE
Mod_return    = 8200
Sweep         = 8200
Total_scans   = 8200

=====
X_p0_width    = 9.75 [us]
X_acq_time    = 2.76624064 [s]
X_angle       = 30 [deg]
X_p1          = 9 [us]
X_p2          = 9 [us]
X_p3          = 25 [us]
X_p4          = 25 [us]
X_p5          = 25 [us]
X_p6          = 25 [us]
X_p7          = 25 [us]
X_p8          = 25 [us]
X_p9          = 25 [us]
X_p10         = 25 [us]
X_p11         = 25 [us]
X_p12         = 25 [us]
X_p13         = 25 [us]
X_p14         = 25 [us]
X_p15         = 25 [us]
X_p16         = 25 [us]
X_p17         = 25 [us]
X_p18         = 25 [us]
X_p19         = 25 [us]
X_p20         = 25 [us]
X_p21         = 25 [us]
X_p22         = 25 [us]
X_p23         = 25 [us]
X_p24         = 25 [us]
X_p25         = 25 [us]
X_p26         = 25 [us]
X_p27         = 25 [us]
X_p28         = 25 [us]
X_p29         = 25 [us]
X_p30         = 25 [us]
X_p31         = 25 [us]
X_p32         = 25 [us]
X_p33         = 25 [us]
X_p34         = 25 [us]
X_p35         = 25 [us]
X_p36         = 25 [us]
X_p37         = 25 [us]
X_p38         = 25 [us]
X_p39         = 25 [us]
X_p40         = 25 [us]
X_p41         = 25 [us]
X_p42         = 25 [us]
X_p43         = 25 [us]
X_p44         = 25 [us]
X_p45         = 25 [us]
X_p46         = 25 [us]
X_p47         = 25 [us]
X_p48         = 25 [us]
X_p49         = 25 [us]
X_p50         = 25 [us]
X_p51         = 25 [us]
X_p52         = 25 [us]
X_p53         = 25 [us]
X_p54         = 25 [us]
X_p55         = 25 [us]
X_p56         = 25 [us]
X_p57         = 25 [us]
X_p58         = 25 [us]
X_p59         = 25 [us]
X_p60         = 25 [us]
X_p61         = 25 [us]
X_p62         = 25 [us]
X_p63         = 25 [us]
X_p64         = 25 [us]
X_p65         = 25 [us]
X_p66         = 25 [us]
X_p67         = 25 [us]
X_p68         = 25 [us]
X_p69         = 25 [us]
X_p70         = 25 [us]
X_p71         = 25 [us]
X_p72         = 25 [us]
X_p73         = 25 [us]
X_p74         = 25 [us]
X_p75         = 25 [us]
X_p76         = 25 [us]
X_p77         = 25 [us]
X_p78         = 25 [us]
X_p79         = 25 [us]
X_p80         = 25 [us]
X_p81         = 25 [us]
X_p82         = 25 [us]
X_p83         = 25 [us]
X_p84         = 25 [us]
X_p85         = 25 [us]
X_p86         = 25 [us]
X_p87         = 25 [us]
X_p88         = 25 [us]
X_p89         = 25 [us]
X_p90         = 25 [us]
X_p91         = 25 [us]
X_p92         = 25 [us]
X_p93         = 25 [us]
X_p94         = 25 [us]
X_p95         = 25 [us]
X_p96         = 25 [us]
X_p97         = 25 [us]
X_p98         = 25 [us]
X_p99         = 25 [us]
X_p100        = 25 [us]
=====

```



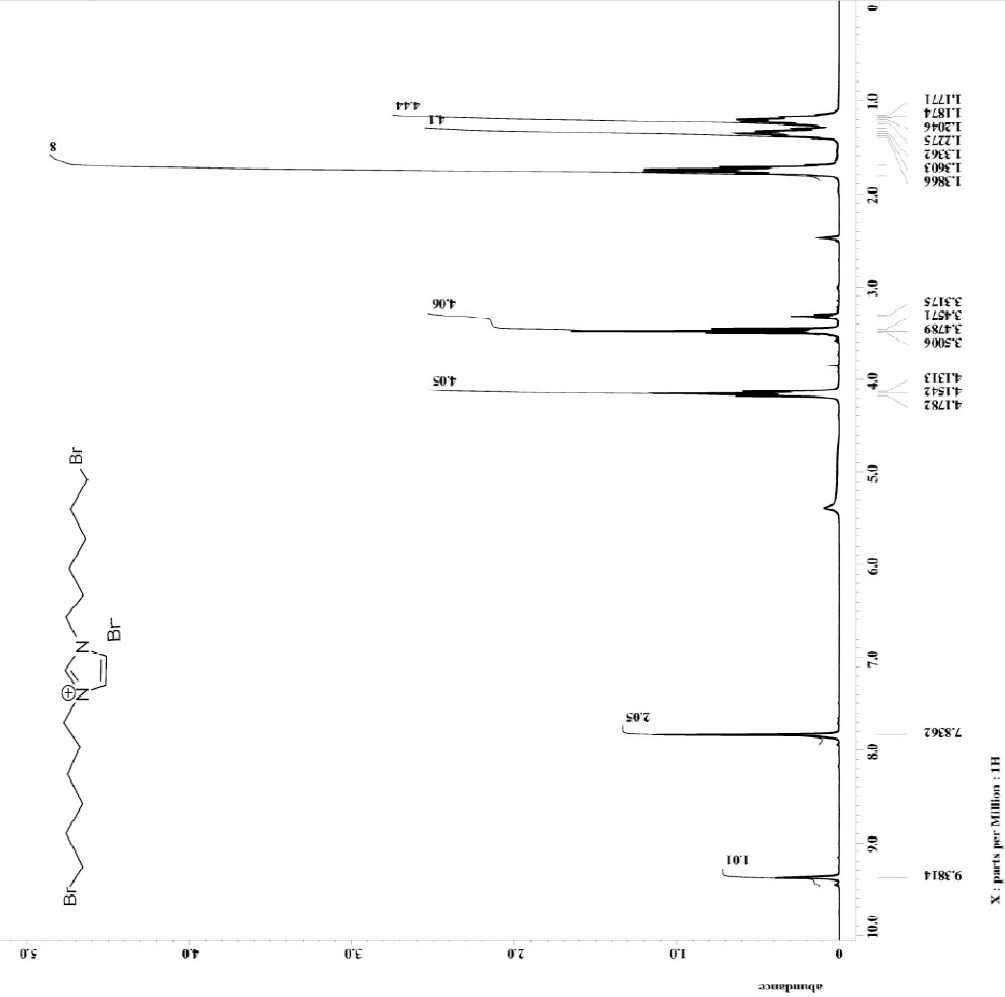
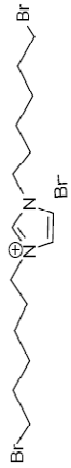


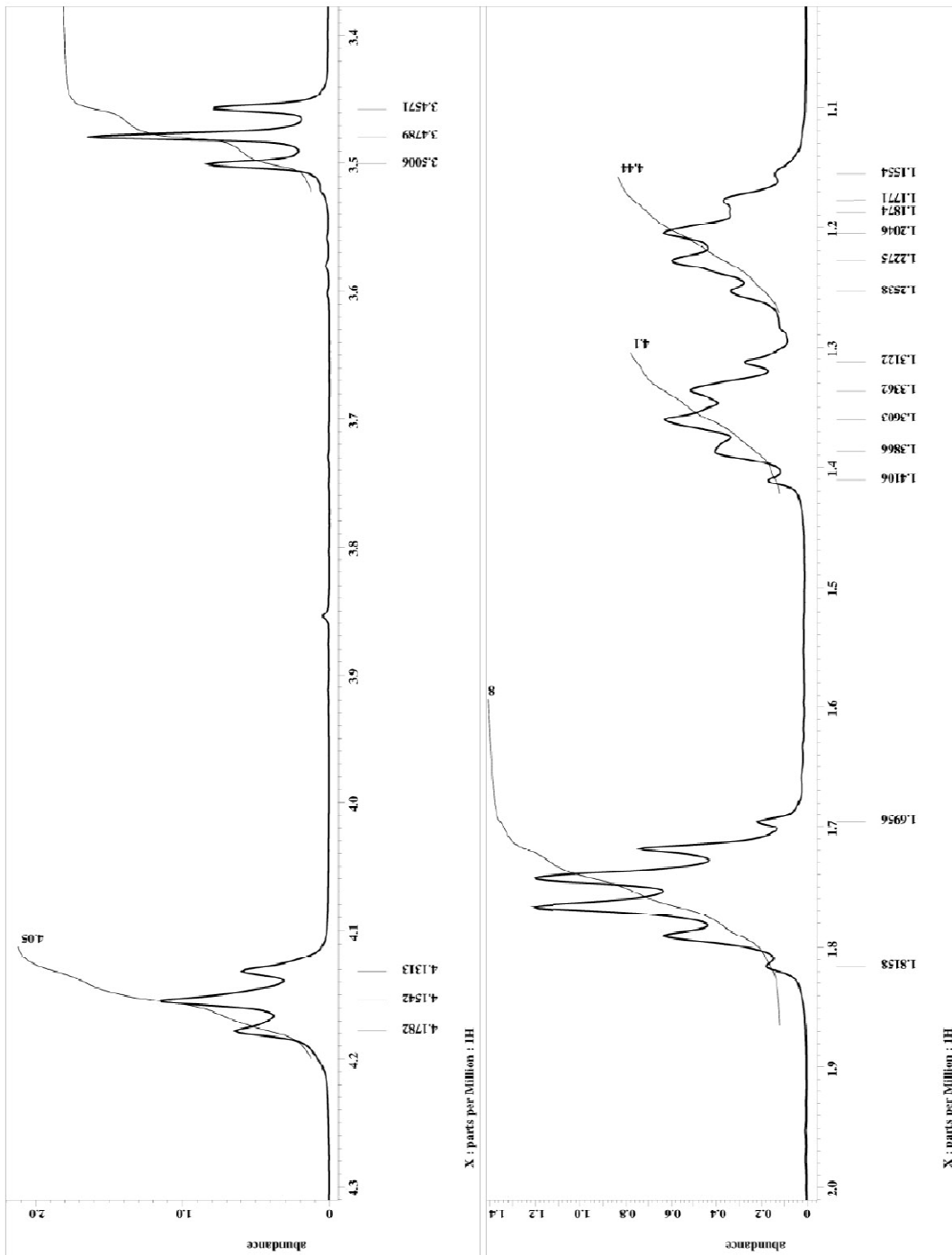
APPENDIX 2

¹H AND ¹³C NMR SPECTRA OF
1-BROMOHEXYL-3-BROMOHEXYL IMIDAZOLIUM BROMIDE SALT (1b)



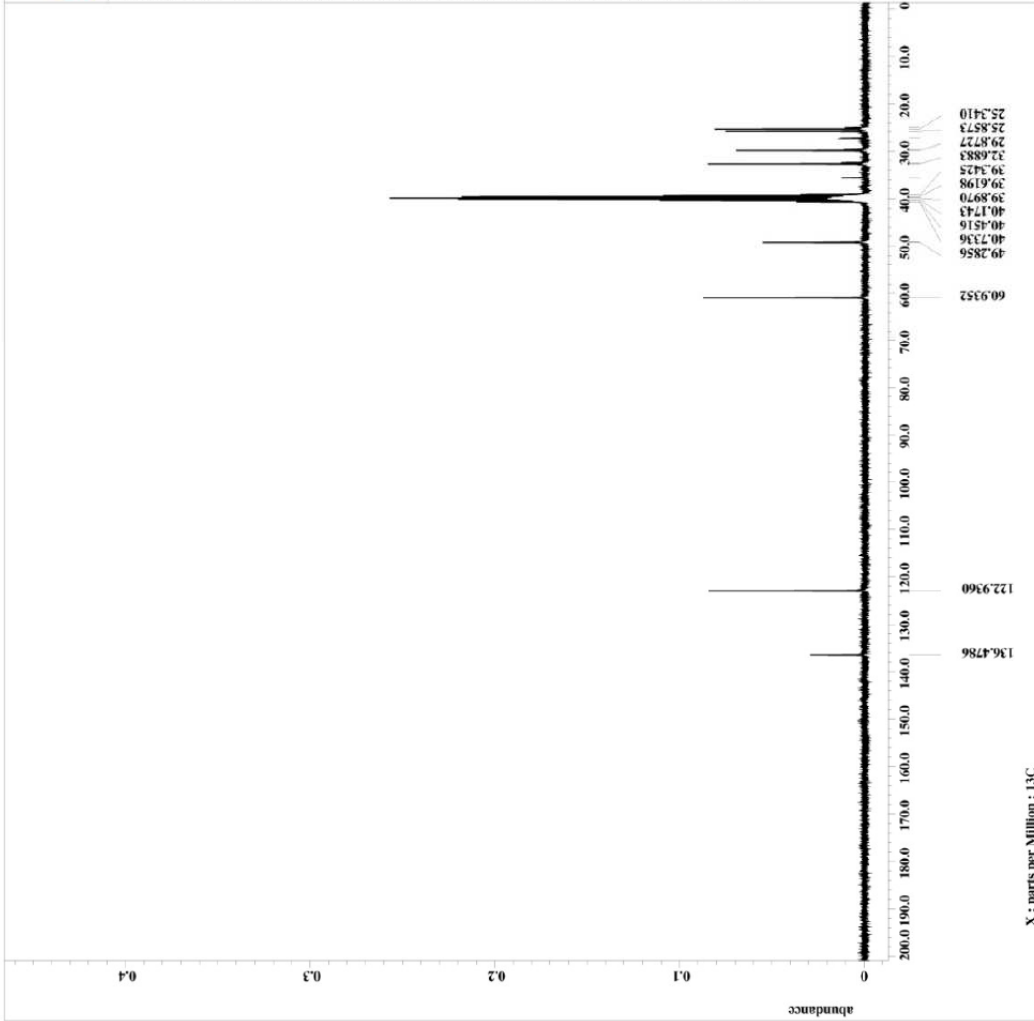
Filename = dichloroMG6H-2_2df
AUtHer = delta
Experiment = single_pulse_esp2
Sample_id = 8M5543f
Creation_time = 12-SEP-2010 16:41:13
Revision_time = 12-SEP-2010 00:02:55
Current_time = 12-SEP-2010 00:03:20
Comment = single_pulse
Data_format = 1D COMEJHX
Dim_size = 13107
Dim_title = 1H
Dim_units = (ppm)
Dimensions = 1
Site = ECX 300
Spectrometer = DELTA2_RMR
Field_strength = 7.05860131(T) (300(MHz)
X_acq_duration = 2.90717696(s)
X_domain = 1H
X_freq = 300.32965592(MHz)
X_offset = 1.0384
X_procsas = 0
X_resolution = 0.34397631(Hz)
X_sweep = 5.63570784(kHz)
Xf1_domain = 1H
Xf1_freq = 300.32965592(MHz)
Xf1_offset = 5(ppm)
Xf1_domain = 1H
Xf1_freq = 300.32965592(MHz)
Xf1_offset = 5(ppm)
Mod_return = FALSE
Scans = 1
Total_scans = 12
X_90_width = 13.01(us)
X_acq_time = 2.90717696(s)
X_angle = 45(deg)
X_pulse = 6.00(us)
Xf1_pulse = 6.00(us)
Xf1_mode = OFF
Data_preset = FALSE
Pulse_program = zgpg30
Recv_gain = 30
Relaxation_delay = 5(s)
Repetition_time = 7.90717696(s)
Temp_get = 22.9(dc)







Filename = 20081125-2_1.jdf
Author = delta
Experiment = pulse_dec
Sample_id = S473486
Solvent = DMSO-D6
Creation_time = 25-NOV-2008 22:20:02
Revision_time = 21-SEP-2010 22:06:45
Current_time = 21-SEP-2010 22:09:56
Comment = single pulse decouple
Data_format = 1D COMPLEX
Dim_1 = 128
Dim_2 = 128
Dim_units = [ppm]
Dimensions = X
Site = ECK 300
Spectrometer = DELTA2_NMR
Field_strength = 7.0486013[T] (300[MHz]
X_acq_duration = 2.76824064[s]
X_domain = 13C
X_freq = 15.56823426[MHz]
X_offset = 65536
X_points = 4
X_prescans = 4
X_resolution = 0.36124027[Hz]
X_sweep = 23.57424242[kHz]
X_time = 8.000
X_width = 8[db]
Irr_freq = 300.52965592[MHz]
Irr_offset = 5[ppm]
Mod_return = FALSE
Scan_delay = 10
Total_scans = 800
X_90_width = 9.75[us]
X_acq_time = 2.76824064[s]
X_delay = 8.000
X_gain = 8[db]
X_pulse = 3.25[us]
Irr_atn_dec = 25[db]
Irr_atn_noe = 25[db]
Irr_delay = 10.000
Decoupling = TRUE
Initial_wait = 1[s]
Noe_time = TRUE
Noe_time_delay = 2[s]
Relaxation_delay = 2[s]
Repetition_time = 4.76824064[s]
Temp_get = 23.2[degC]





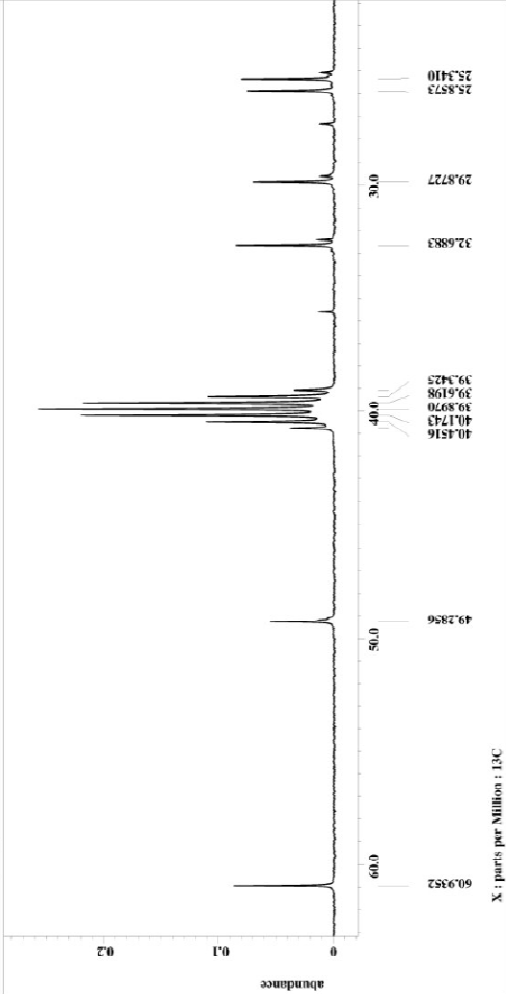
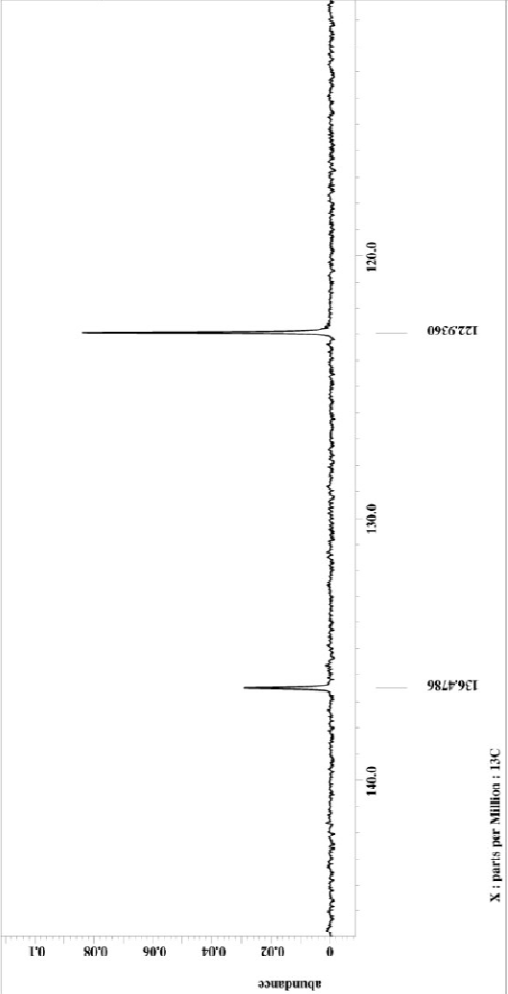
```

Filename = 20081225-3_-dfe
Author = delta
Experiment = single_pulse_dec
Sample_ID = DMSO-d6
Date_Exp = DMSO-d6
Creation_time = 23-NOV-2008 23:20:02
Revision_time = 21-SEP-2010 22:10:07
Current_time = 21-SEP-2010 22:10:29

Comment = single pulse decouple
Data_format = 1D COMPLEX
Dia_size = 22428
Dir_title = 13C
Dimensions = X[F1]
Site = ECK 300
Spectrometer = DELTA 300

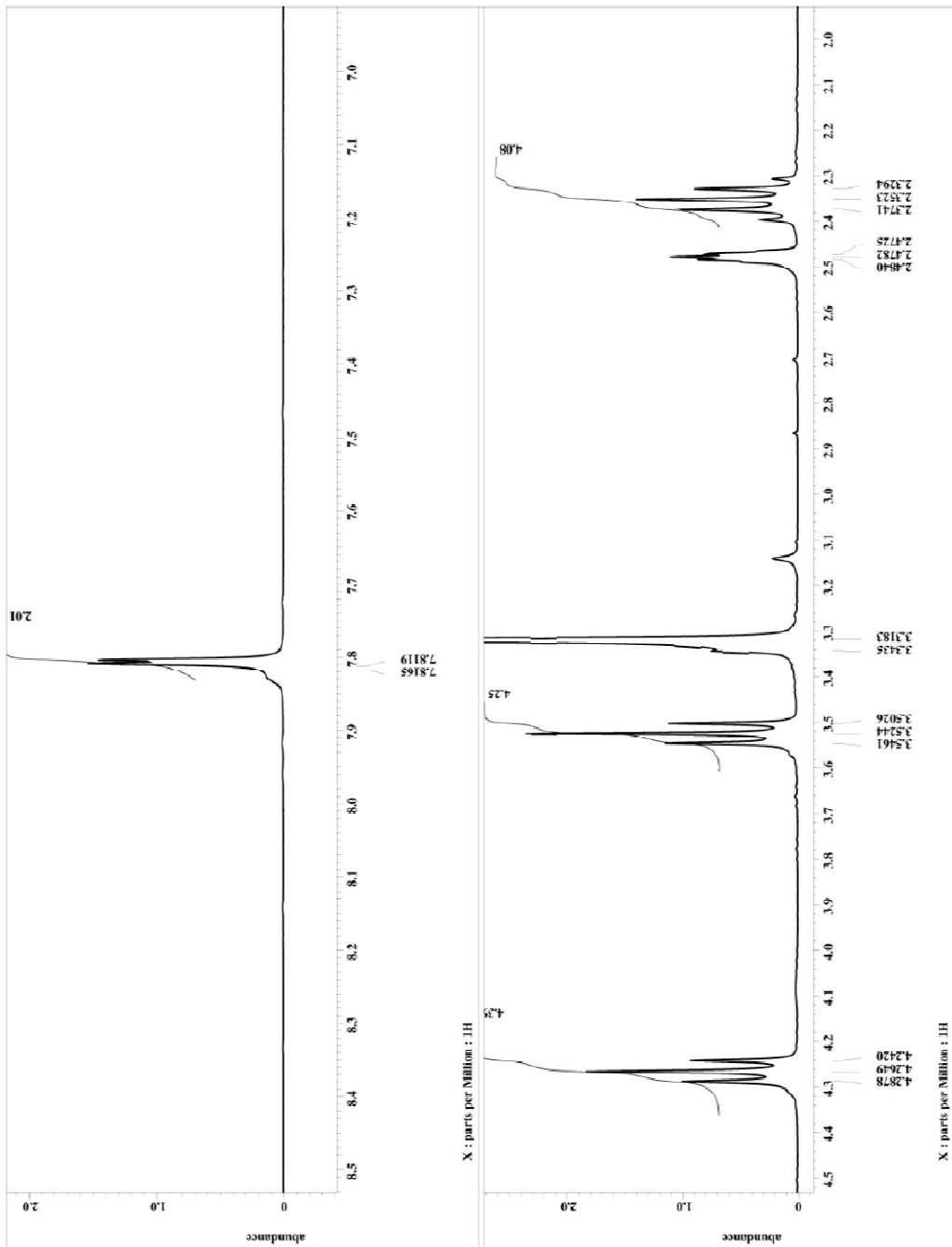
Field strength = 7.6586013 [T] (300 [MHz])
Acq duration = 2.76824064 [s]
X_domain = 13C
X_freq = 75.56623428 [MHz]
X_low = 85533
X_points = 4
X_prescans = 4
X_resolution = 0.36124027 [Hz]
X_sweep_gain = 23.6742442 [MHz]
X_sweep = 300.52965592 [MHz]
Irr_freq = 5 [ppm]
Irr_offset = FNU5B
Clipped = 0
Acq return = 800
TOTAL_scans = 800

X_90_width = 9.75 [us]
X_acq_time = 2.76824064 [s]
X_angle = 30 [deg]
X_atn = 8 [dB]
X_pulse = 2.25 [us]
Irr_atn_cop = 22 [dB]
Irr_noise = WALTZ
Decoupling = TPRZ
Initial_wait = 1 [s]
X_100_time = 31 [s]
X_100_time = 50 [s]
Recur_gain = 2 [s]
Relaxation_delay = 2 [s]
Repetition_time = 2.76824064 [s]
Temp_set = 23.2 [dC]
  
```



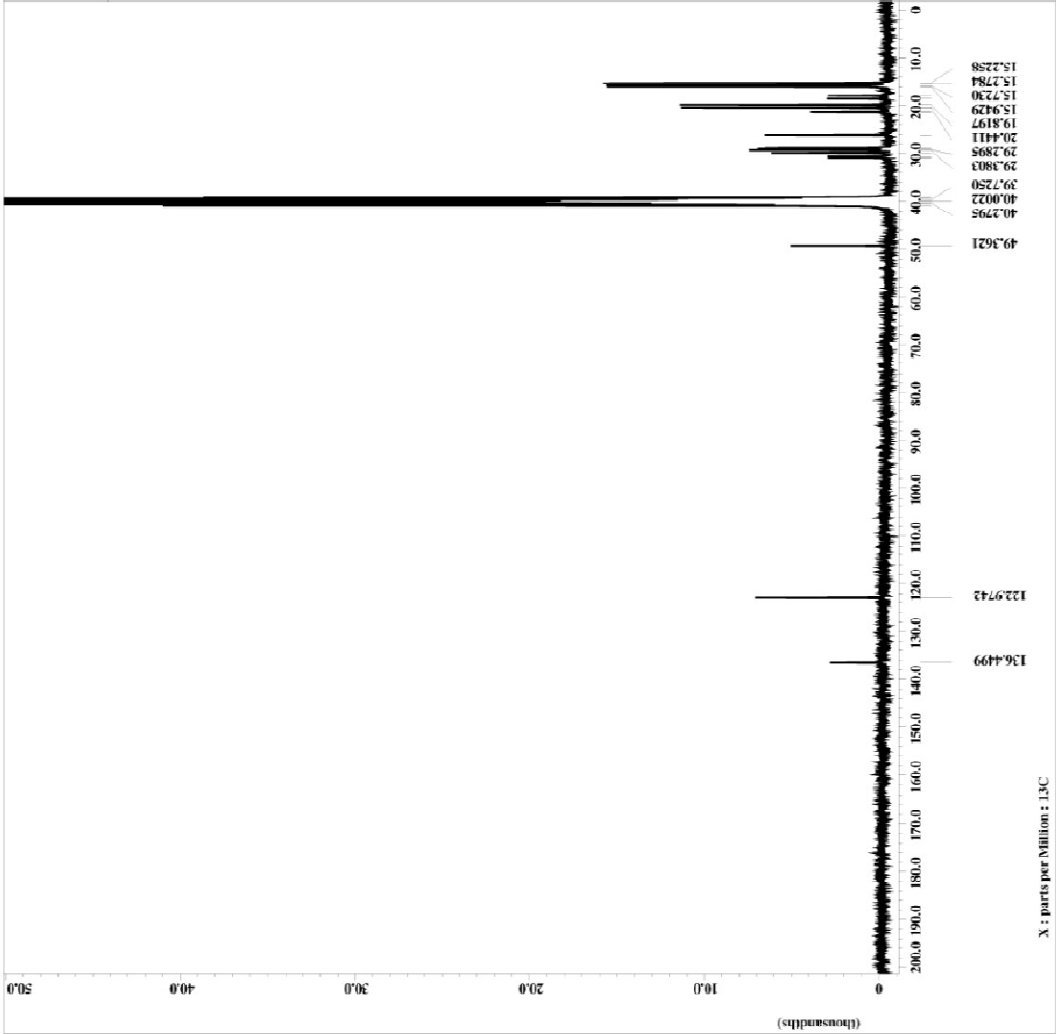
APPENDIX 3

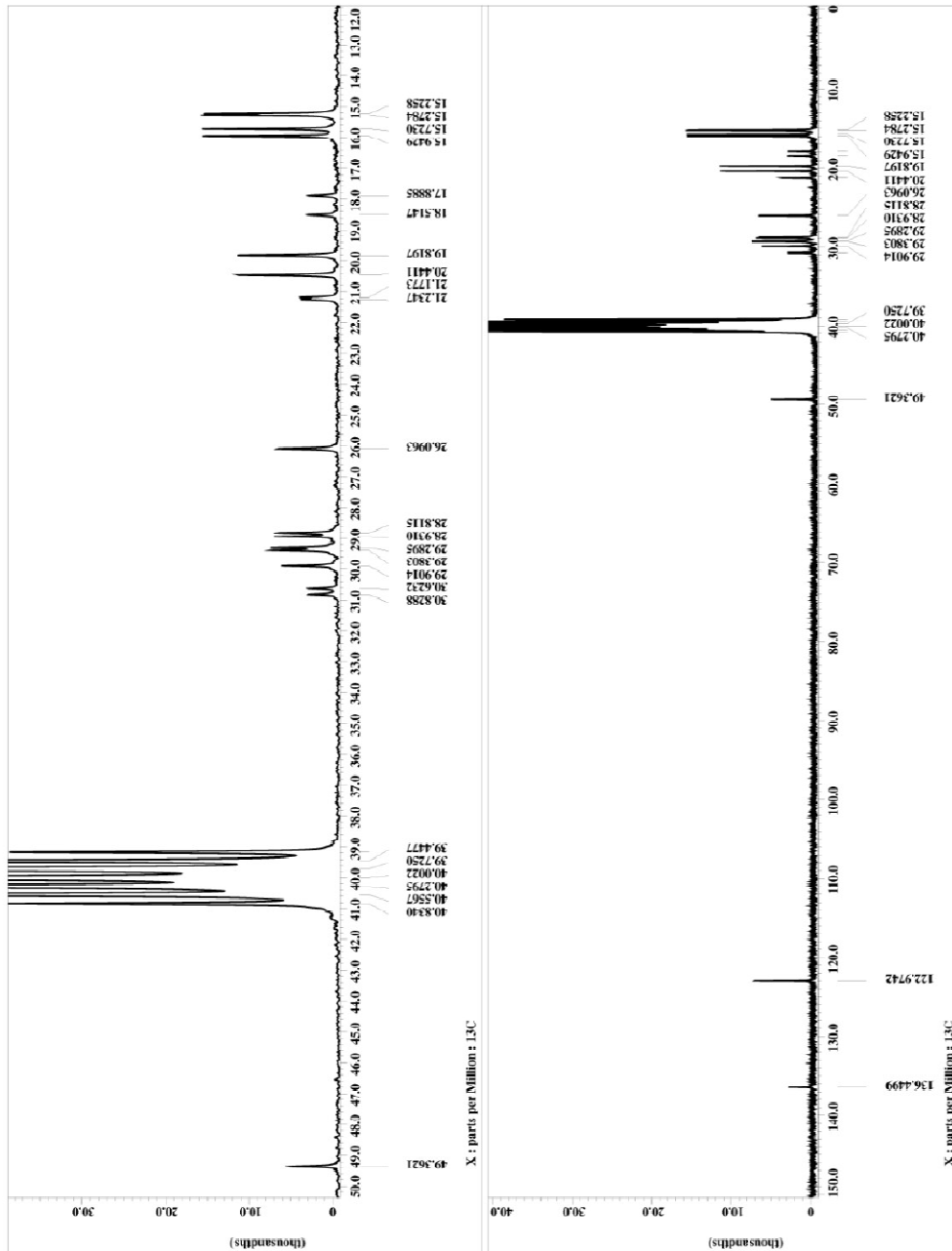
¹H AND ¹³C NMR SPECTRA OF
1- BROMOPROPYL-3-BROMOPROPYL IMIDAZOLIUM BROMIDE SALT (1c)





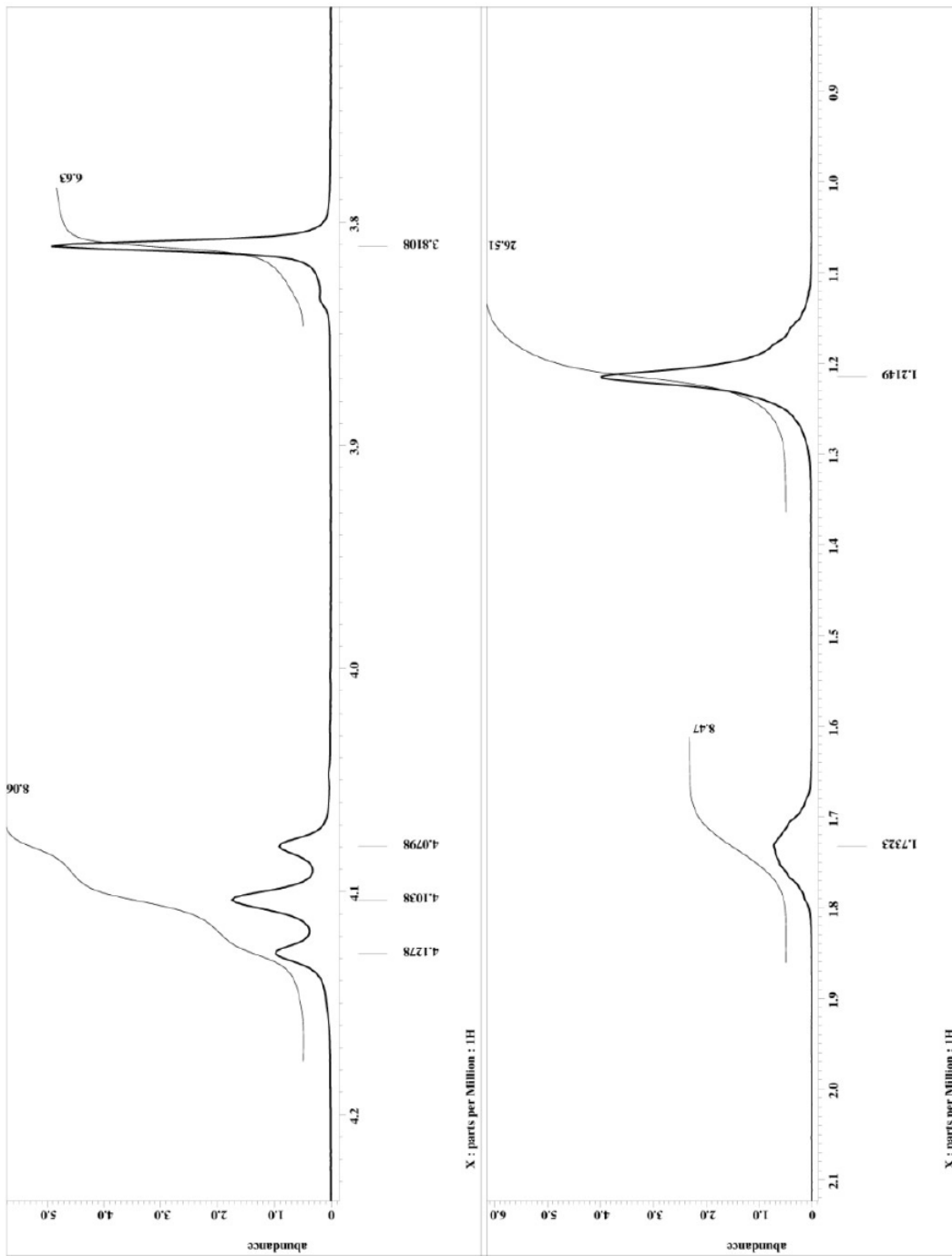
File Name = EW091109 (MCC3Core)-4
Author = delta
Experiment = single_pulse_dec
Sample_id = SF757692
Solvent = DMSO-D6
Acquisition_time = 12-SEP-2010 10:04:01
Resolution_time = 12-SEP-2010 11:49:42
Current_time = 12-SEP-2010 11:50:13
Comment = single pulse decouple
Data format = D3
D1 name = D3COREX
D1 title = 13C
D1A units = [ppm]
Dimensions = X
Site = ECK 300
Spectrometer = DMRF2_NMR
Field strength = 7.0586013 [T] (300 MHz)
X_acq_duration = 2.76924064 [s]
X_domain = 13C
X_freq = 100.623426 [MHz]
X_points = 65536
X_prescans = 4
X_resolution = 0.96124027 [Hz]
X_sweep = 23.67428242 [kHz]
Irr_freq = 300.5296592 [MHz]
Irr_offset = 5 [ppm]
Clipped = FALSE
Mod return = 3
Sens = 5800
Total_scans = 9800
X_90_width = 9.75 [us]
X_acq_time = 2.76924064 [s]
X_angle = 8 [deg]
X_pulse = 3.25 [us]
Irr_atn_dec = 25 [dB]
Irr_atn_noe = 25 [dB]
Irr_noise = WNUZ
Irr_program = WNUZ
Instal_wait = 1 [s]
Noe_time = 2 [s]
Recvr_gain = 50
Repetition_delay = 1.1 [s]
Repetition_time = 4.76924064 [s]
Temp_get = 23.9 [C]

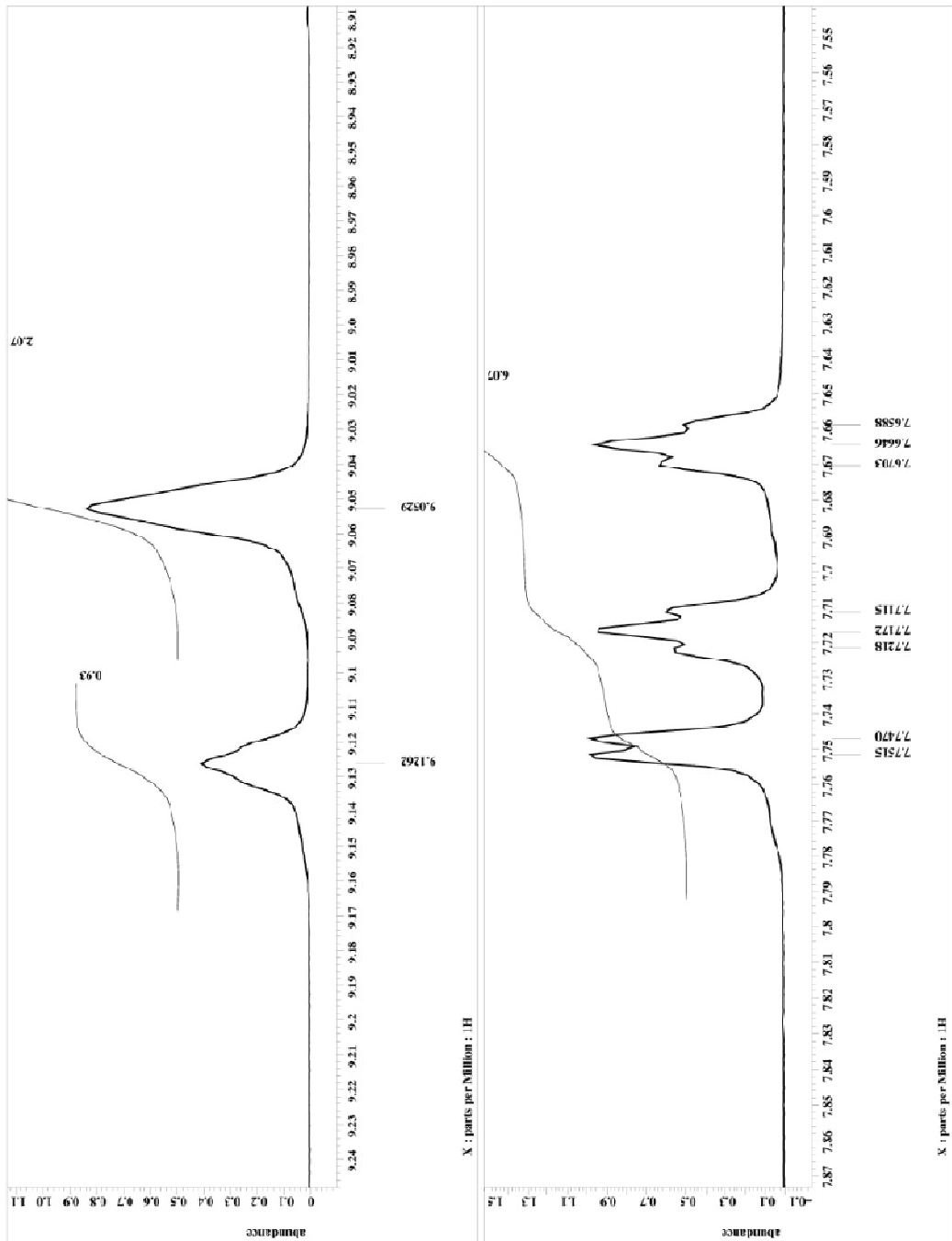


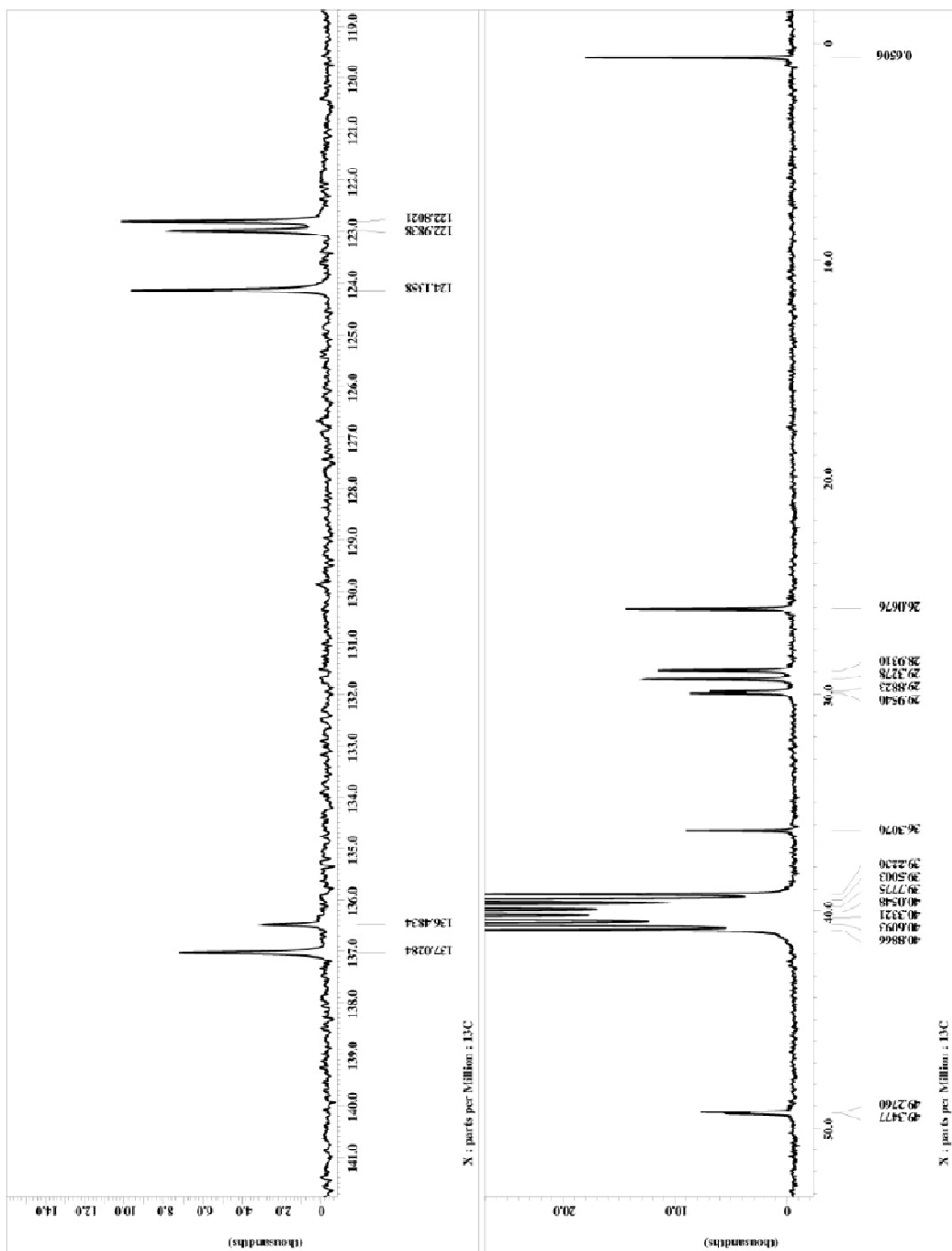


APPENDIX 4

¹H AND ¹³C NMR SPECTRA OF
1-(1'-METHYL-3'-DECYLIMIDAZOLIUM)-3-(1"-METHYL-3"-DECYLIMIDAZOLIUM)
IMIDAZOLIUM TRI [BIS(TRIFLUOROMETHANESULFONYL)IMIDE] (2a)







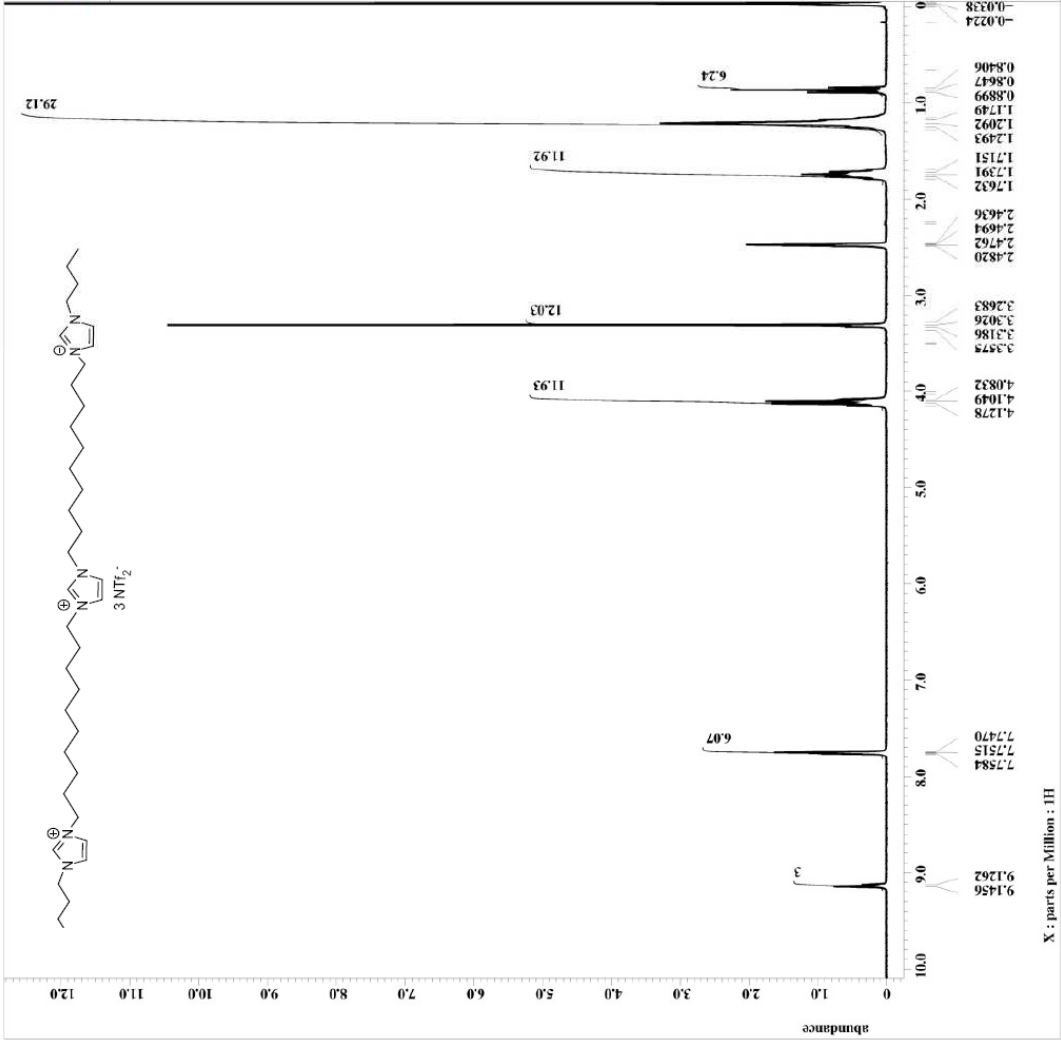
APPENDIX 5

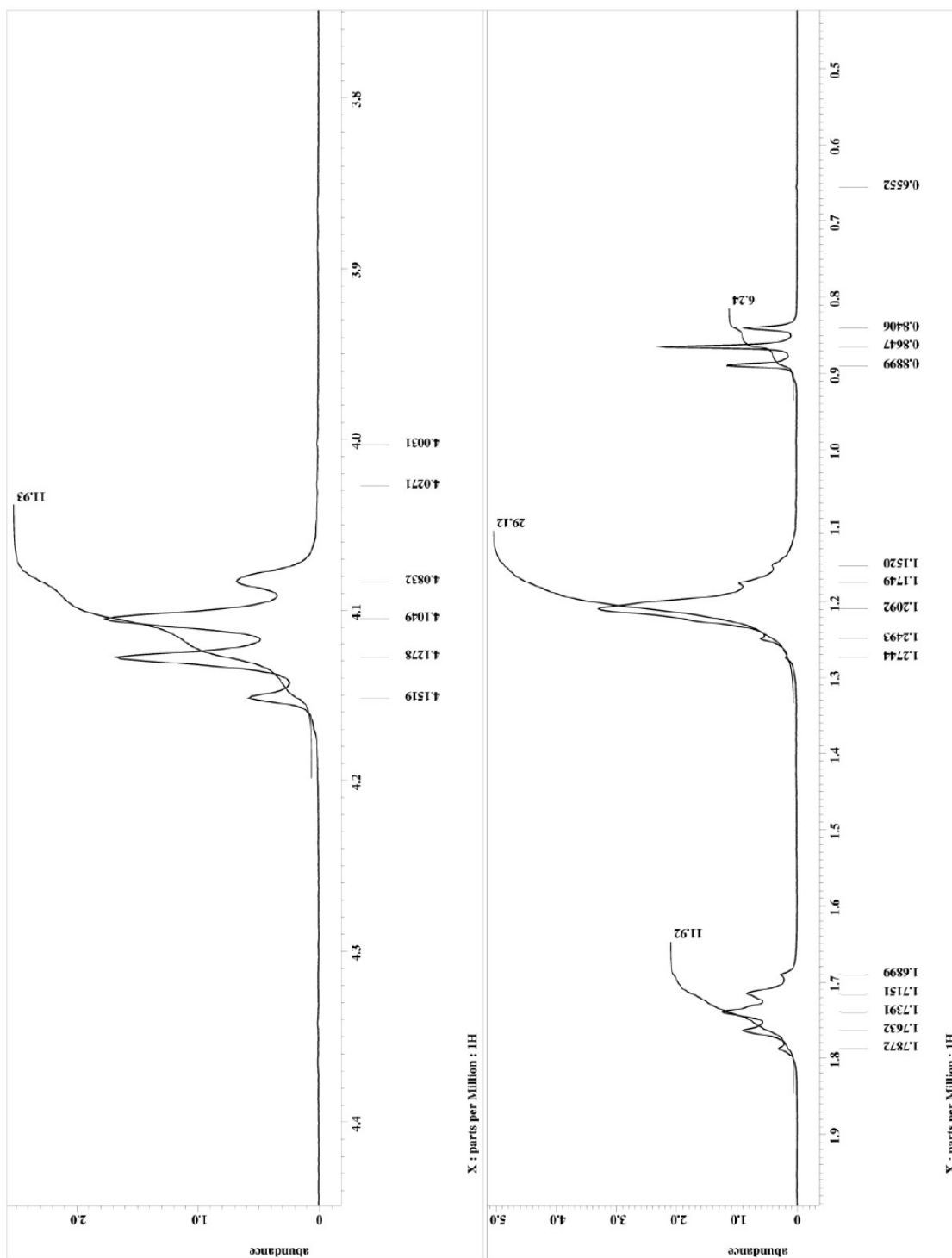
1H AND 13C NMR SPECTRA OF
1-(1'-BUTYL-3'-DECYLIMIDAZOLIUM)-3-(1"-BUTYL-3"-DECYLIMIDAZOLIUM)IMIDAZOLIUM
TRI [BIS(TRIFLUOROMETHANESULFONYL)IMIDE] (2b)

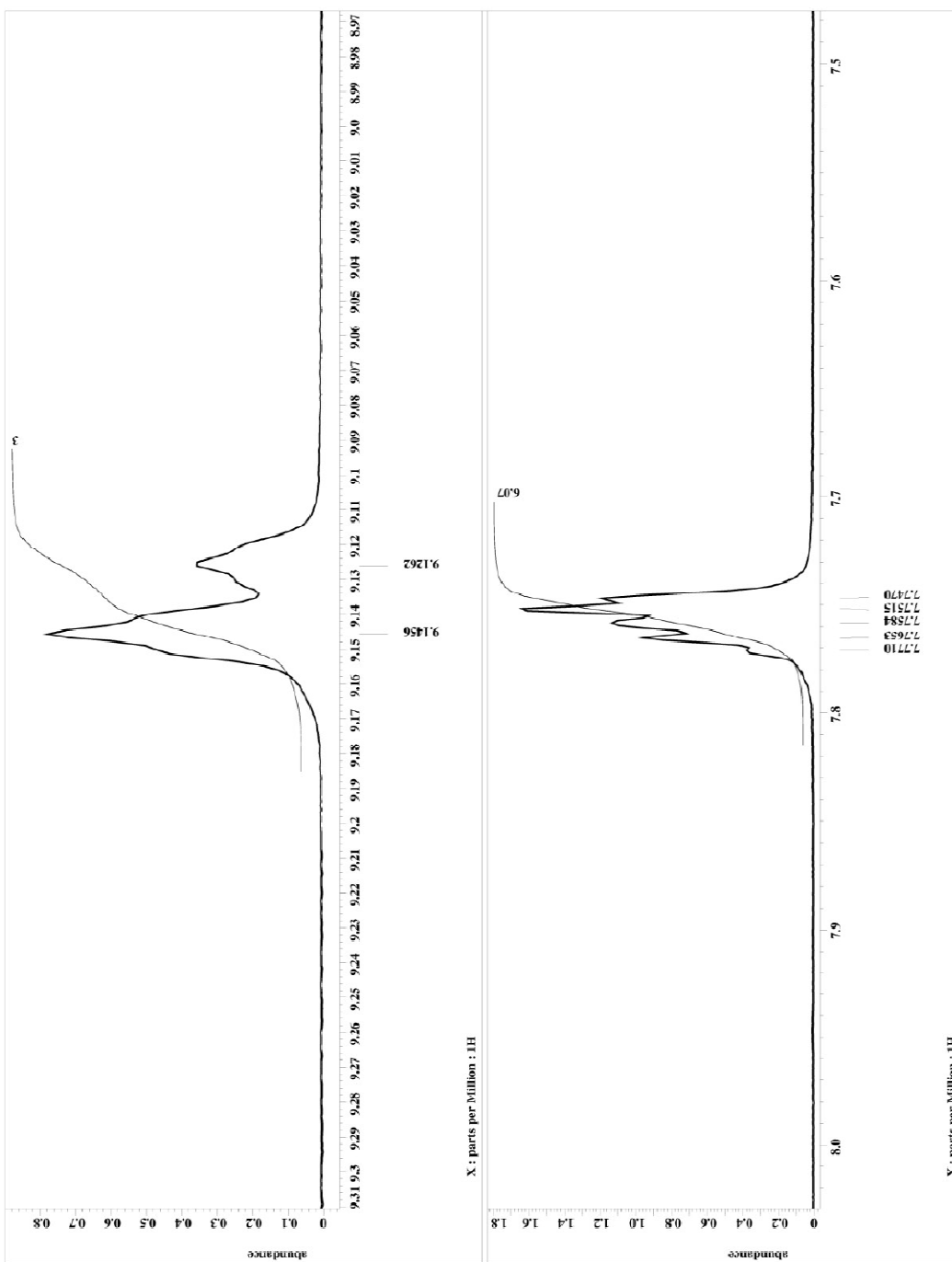


```

Filename = EM071808 (LTCC10BuIm) -
Author = delta
Experiment = single_pulse.ex2
Sample_id = SF36623
Date_ime = 18-SEP-2010 09:43:31
Creation_time = 18-SEP-2010 13:34:39
Revision_time = 12-SEP-2010 13:35:03
Current_time = 12-SEP-2010 13:35:03
Comment = single_pulse
Date_acq = 18-SEP-2010
Date_instr = 13107
Dim_size = 1H
Dim_title = [ppm]
Dim_units = [ppm]
Dimensions = X CW 300
Spectrometer = DELTA2_NMR
Field_strength = 7.0586013[T] (300[MHz]
X_acq_duration = 2.90717696[s]
X_domain = 1H
X_offset = 300.52965592[MHz]
X_points = 16384
X_prescans = 0
X_resolution = 0.34397651[Hz]
X_sweep_rate = 1H 63570784[KHz]
Irr_domain = 1H
Irr_freq = 300.52965592[MHz]
Irr_offset = 5[ppm]
Tri_domain = 1H
Tri_freq = 300.52965592[MHz]
Clipped = FALSE
Mod_return = 1
Total_scans = 22
X_50_width = 13.01[us]
X_acq_time = 2.90717696[s]
X_angle = 45[deg]
X_atn = 4[db]
X_pulse = 6[us]
X_offset = 6[us]
Tri_mode = Off
Dante_presat = FALSE
Initial_wait = 1[s]
Recvr_gain = 50
Relaxation_delay = 5[s]
Repetition_time = 7.90717696[s]
Temp_get = 22.3[degC]
  
```









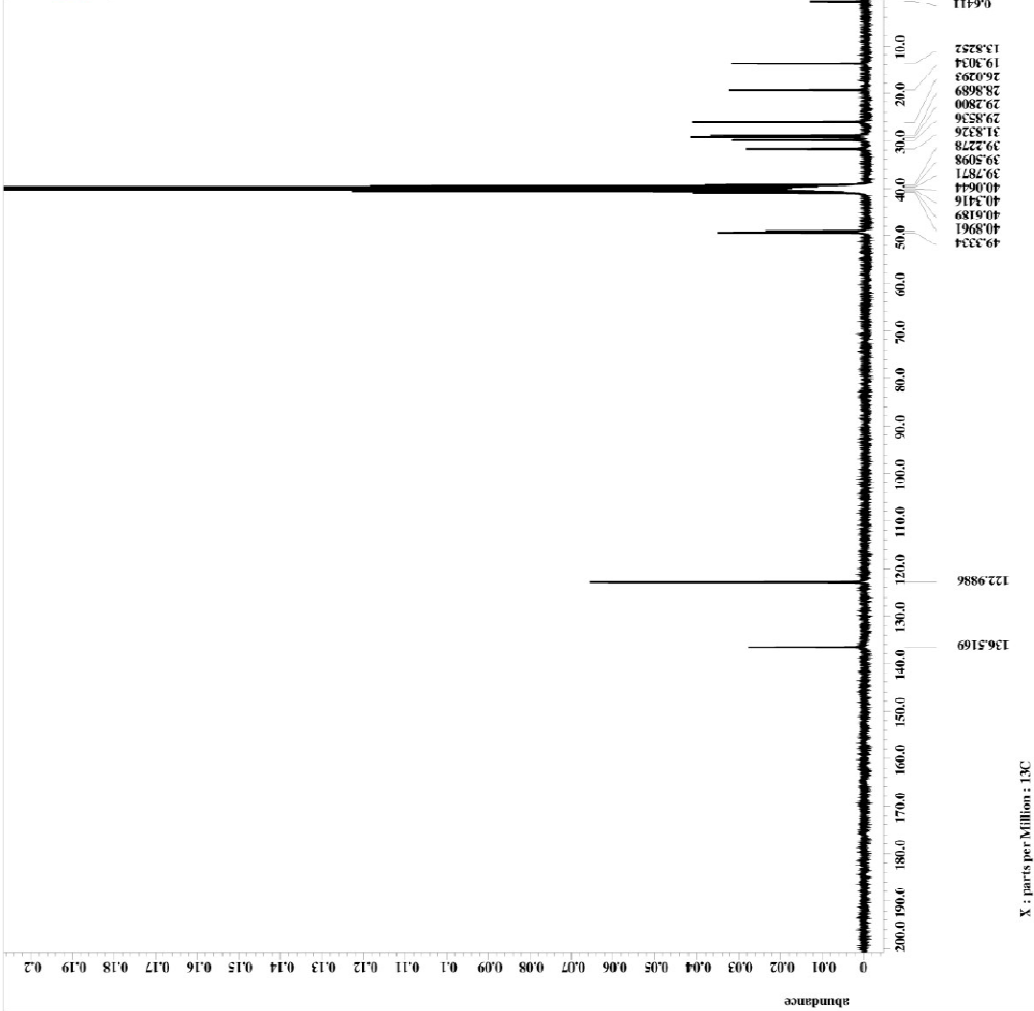
```

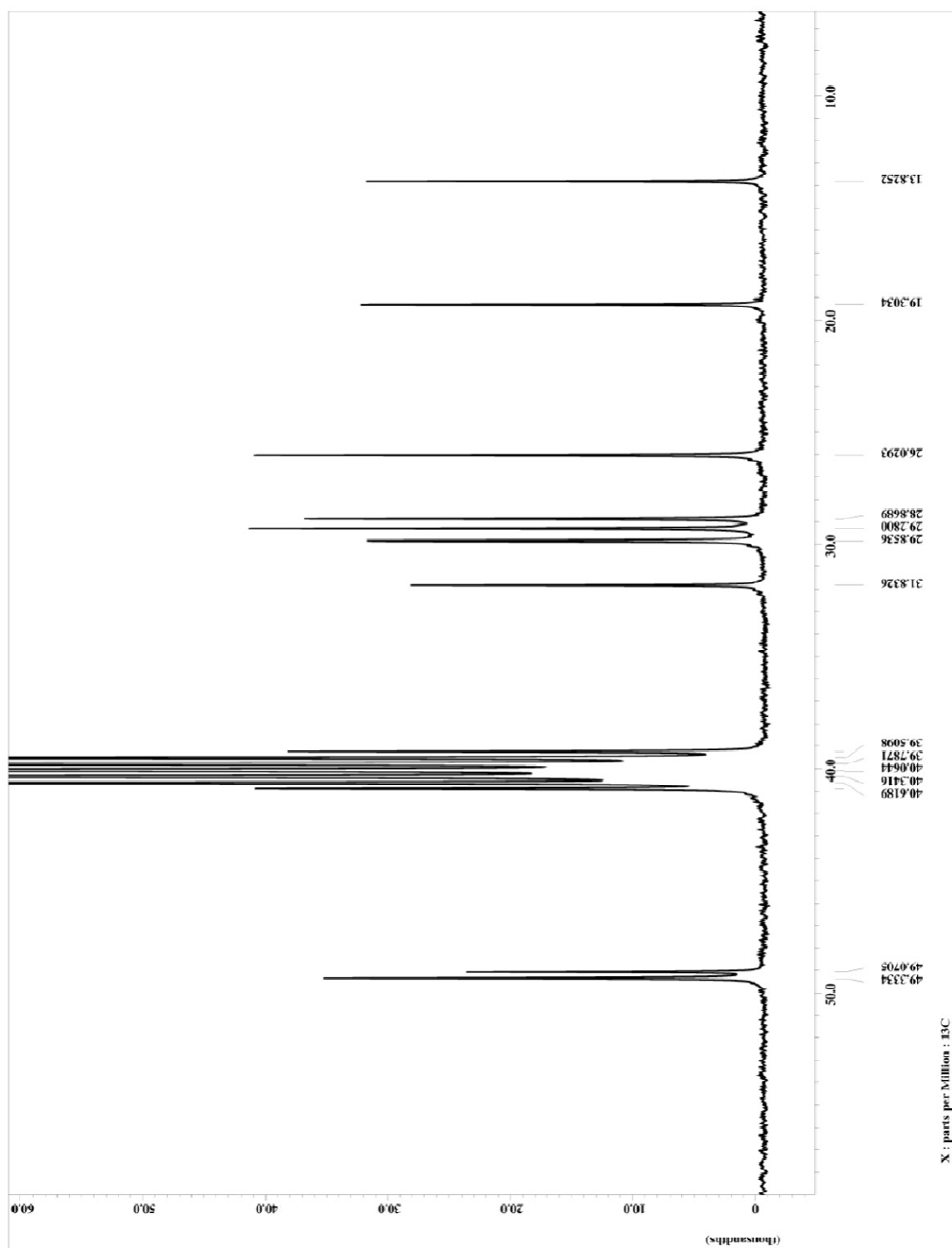
Filename = SWHFC10Bain-3_1.je
Date_ = 
Experiment = single_pulse_dec
Sample_id = S817241
Solvent = DMSO-d6
Creation_time = 20-08-2008 10:12:39
Revision_time = 20-08-2008 11:45:10
Current_time = 12-SEP-2010 11:45:10

Comment = single pulse decouple
Date_format = D COMPLEX
Data_size = 1228
Dim_title = 
Dim_units = [ppm]
Dimensions = X
Site = ECX 300
Spectrometer = DELTA2_NMR

Field_strength = 7.0586013 [T] (300 [MHz]
X_acq_duration = 2.76924364 [s]
X_domain = 13
X_offset = 56823426 [MHz]
X_points = 65536
X_prescans = 4
X_resolution = 0.36124027 [Hz]
X_resolution_hz = 18.674242 [kHz]
Irr_domain = 
Irr_freq = 300.5296592 [MHz]
Irr_offset = 5 [ppm]
Clipped = FALSE
No_return = 
Scans = 8467
Total_scans = 8467

X_90_width = 9.75 [us]
X_couple_time = 2.76924364 [s]
X_pulse = 50 [dB]
X_atn = 8 [dB]
X_pulse = 3.25 [us]
Irr_atn_dec = 25 [dB]
Irr_atn = 25 [dB]
Irr_pulse = WALTZ
Decoupling = TRUE
Initial_wait = 1 [s]
Noe_time = TRUE
Noe_delay = 5 [s]
Recr_delay = 50
Relaxation_delay = 2 [s]
Repetition_time = 4.76924364 [s]
Temp_set = 22.1 [dC]
  
```





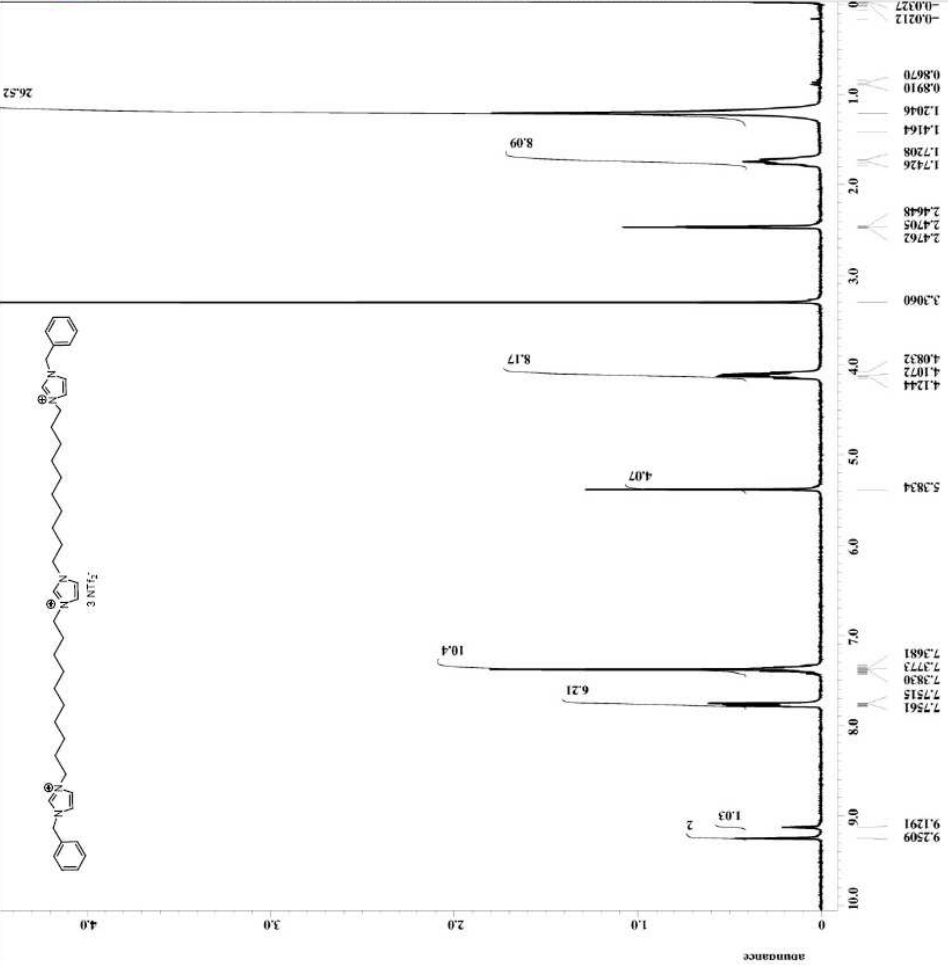
APPENDIX 6

¹H AND ¹³C NMR SPECTRA OF
1-(1'-BENZYL-3'-DECYLIMIDAZOLIUM)-3-(1"-BENZYL-3"-

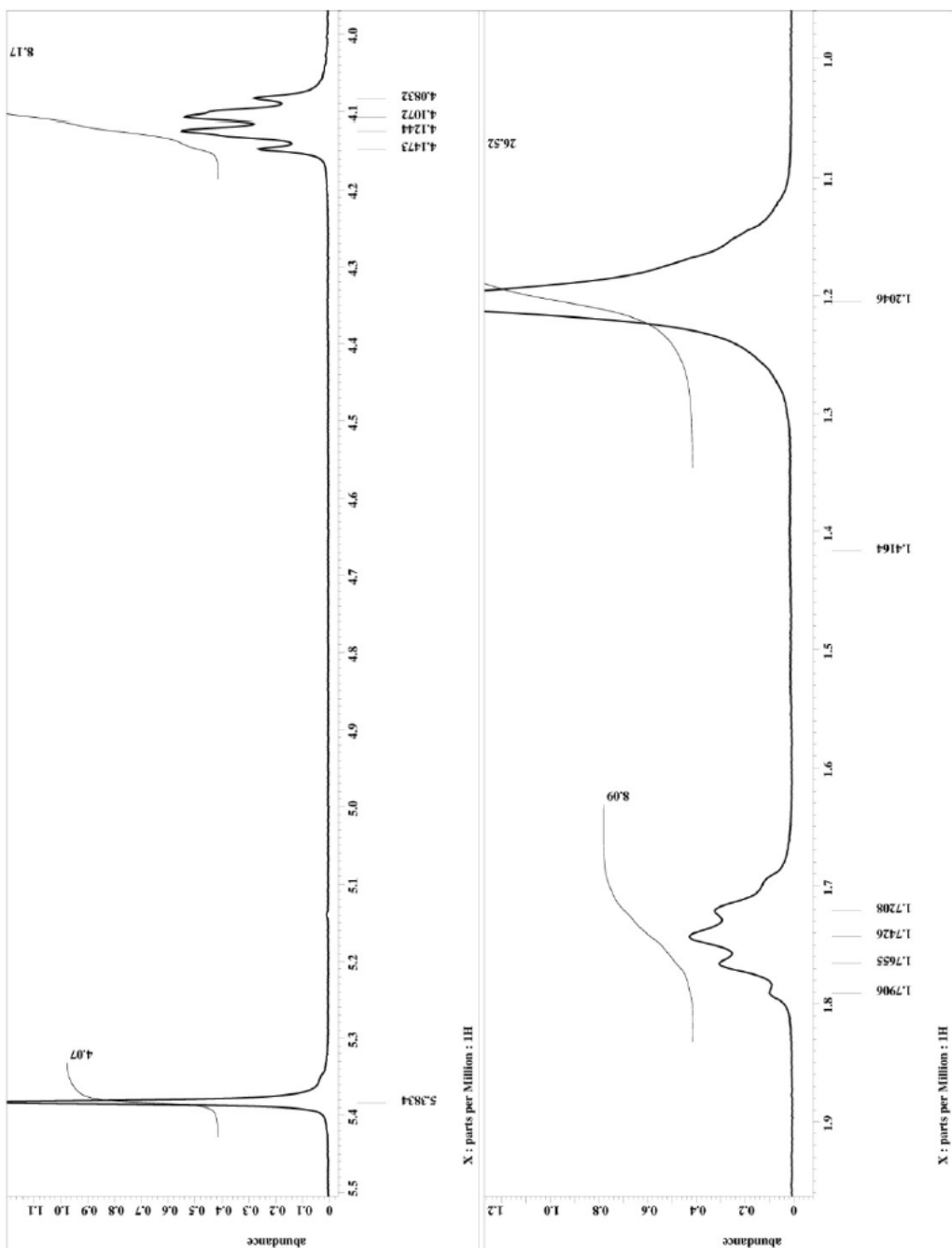
DECYLIMIDAZOLIUM)IMIDAZOLIUM TRI [BIS(TRIFLUOROMETHANESULFONYL)IMIDE] (2c)

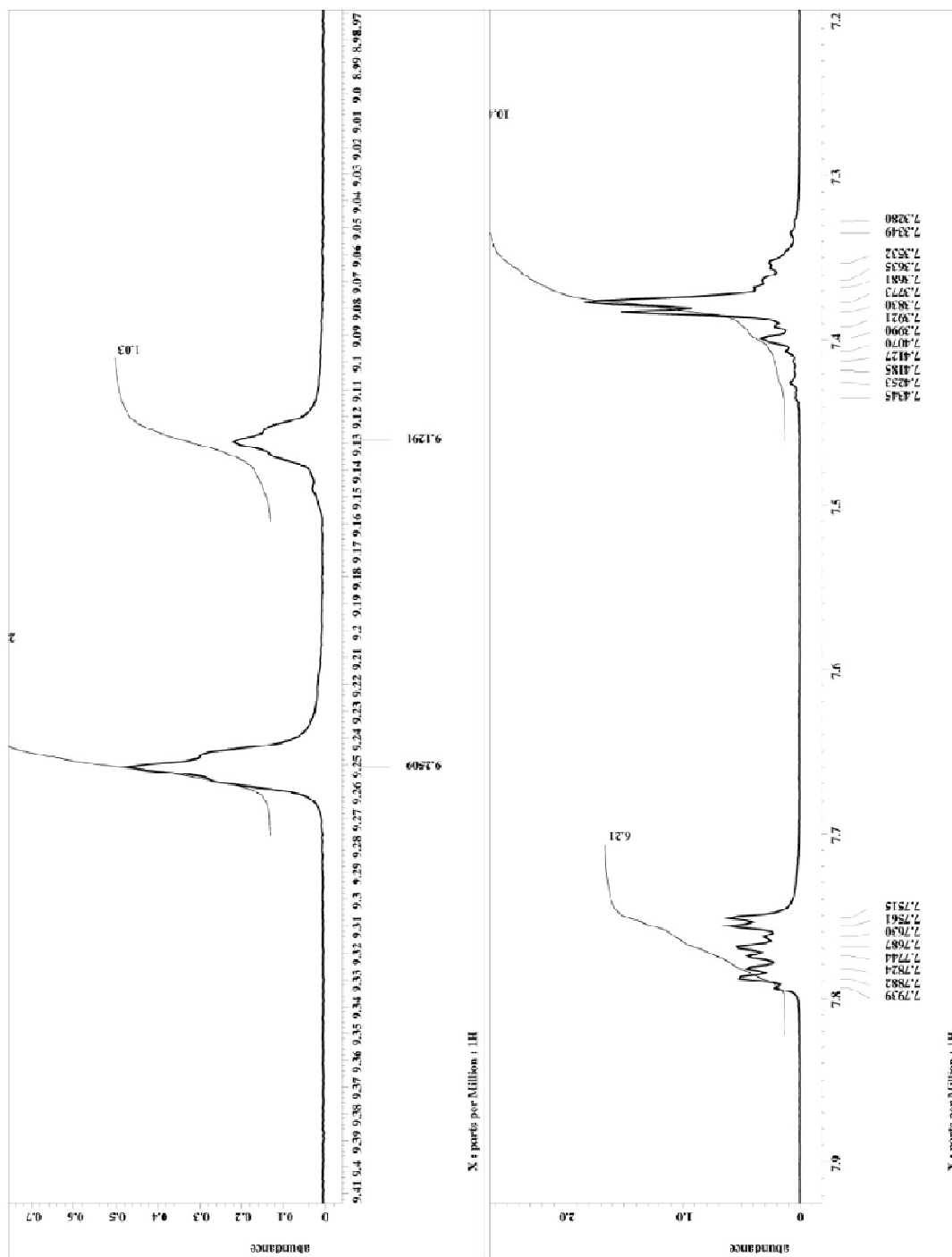


Filename = EW072608 (LTCCL0P4Im) -
Author = delta
Experiment = delta_pulse.exe2
Sample_id = S468126
Solvent = DMSO-d6
Creation time = 28-JUL-2008 19:29:24
Operator = delta
Current_time = 12-SEP-2010 13:38:44
Comment = single_pulse
Date_acq = 12-SEP-2010
Dir_name = 13107
Dir_title = 13107
Diam_units = [ppm]
Dimensions = [ppm]
Spectrometer = ECK 300
Spectrometer = DELTA2_MMR
F1rd_strength = 7.0366031[M] (300[MHz]
X_resolution = 2.90717696[s]
X_domain = 1H
X_freq = 300.52965592[MHz]
X_offset = 5[ppm]
X_precans = 0
X_resolution = 0.34397631[Hz]
X_sweep = 5.62570784[kHz]
X_gain = 1H
Irr_freq = 300.52965592[MHz]
Irr_offset = 5[ppm]
Tri_domain = 1H
Tri_freq = 300.52965592[MHz]
Tri_offset = 5[ppm]
Clipped = FALSE
Mod_return = 1
Name = 13107
Total_scans = 8
X_90_width = 13.01[um]
X_acq_time = 4.9727696[s]
X_delay = 4.00[s]
X_atn = 4[db]
X_pulse = 6.505[um]
Irr_mode = Off
Irr_phase = 0
Dance_preset = FALSE
Initial_wait = 1[s]
Reovr_gain = 44
Acq_delay = 44
Repetition_time = 7.90717696[s]
Temp_get = 21.7[c]



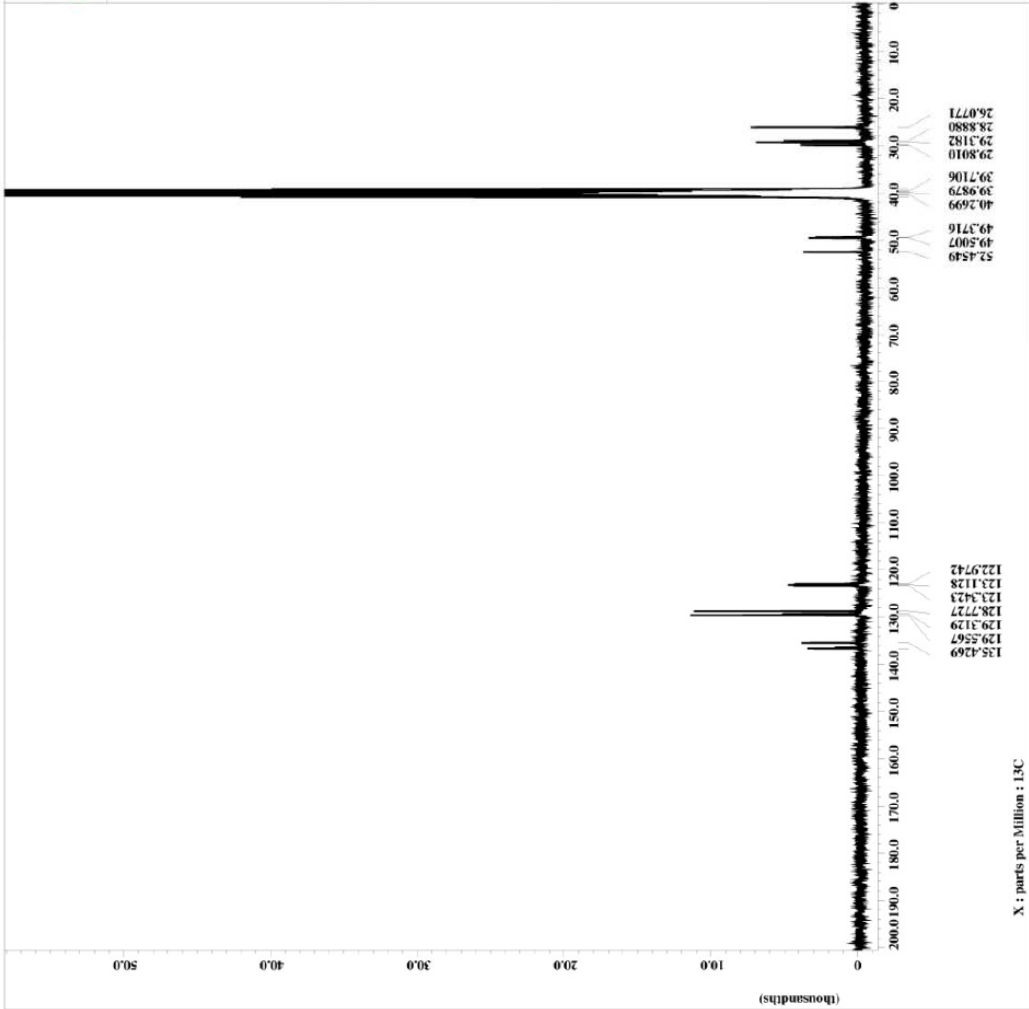
X : parts per Million : 1H

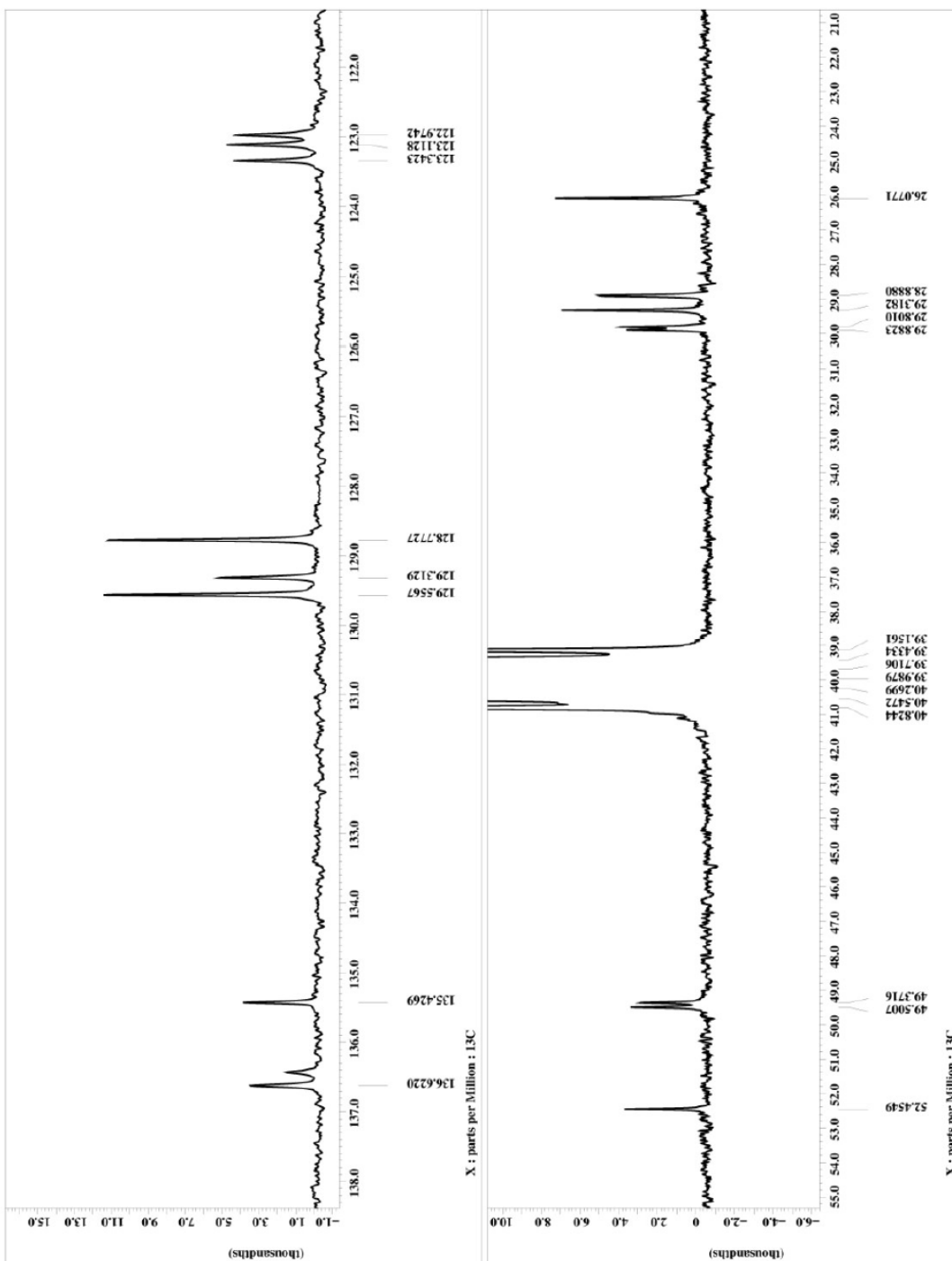






Filename = EW072908 (LACPhim)-3.f
Author = delta
Experiment = single pulse dec
Spectrometer = DELTA2_NMR
Solvent = DMSO-D6
Creation_time = 30-JUL-2008 10:09:49
Revision_time = 12-SEP-2010 13:46:39
Current_time = 12-SEP-2010 13:47:10
Comment = single pulse decouple
Data_format = 1D COMPLEX
Data_size = 52428
Dim_size = 1024
Dim_units = [ppm]
Dimensions = X
Site = ECK 300
Spectrometer = DELTA2_NMR
Field_strength = 7.0586013 [T] (300 [MHz])
X_acq_duration = 2.76624064 [s]
X_domain = 13C
X_freq = 75.56823426 [MHz]
X_offset = 65536
X_points = 4
X_prescans = 4
X_resolution = 0.36124027 [Hz]
X_sweeps = 23.67424242 [kHz]
Irr_freq = 300.52965592 [MHz]
Irr_offset = 5 [ppm]
Clipped = FALSE
Soc_return = 500
Soc_cycles = 500
Total_scans = 500
X_90_width = 9.75 [us]
X_acq_time = 2.76624064 [s]
X_acquire = 20.500 [s]
X_gain = 81 [dB]
X_pulse = 3.25 [us]
Irr_atn_dec = 25 [dB]
Irr_atn_roc = 10 [dB]
Irr_atn_ramp = WALTZ
Decoupling = TRIG
Initial_wait = 1 [s]
Noe_time = TRUE
Noe_delay = 5 [s]
Recvr_gain = 50
Relaxation_delay = 2 [s]
Repetition_time = 4.76624064 [s]
Temp_get = 23.9 [dC]





APPENDIX 7

^1H , ^{13}C AND ^{31}P NMR SPECTRA OF 1-DECYLTRIPROPYLPHOSPHONIUM-3-
DECYLTRIPROPYLPHOSPHONIUM IMIDAZOLIUM TRI
[BIS(TRIFLUOROMETHANESULFONYL)IMIDE] (2d).



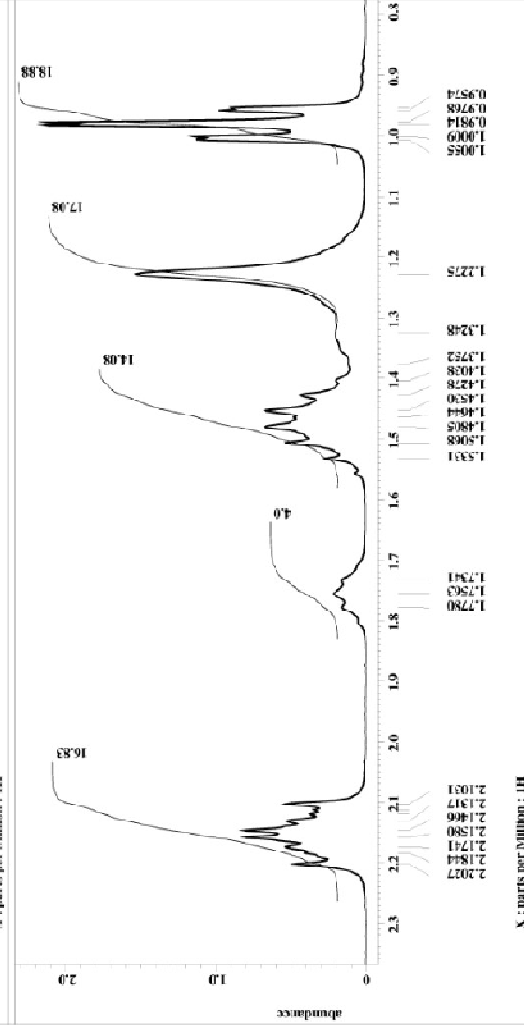
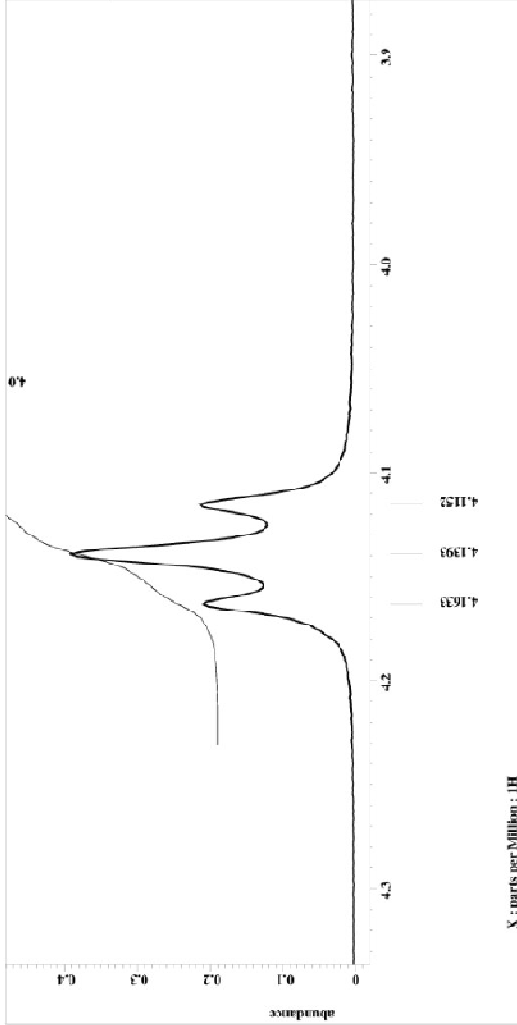
```

File Name      = R0905408 (R0CC1.0P)-7-3
Author        = delia
Experiment    = single_pulse.ex2
Sample_id     = S8766153
Solvent       = DMSO-D6
Acquisition_time = 12-SEP-2010 11:43:03
Pulse_prog    = zgpg30
Current_time  = 12-SEP-2010 11:43:59

Comment       = single_pulse
Dir_format    = 13
Dir_path      = 13
Dir_title     = 18
Dir_units     = [ppm]
Dimensions    = X 512 Y 320
Site          = BBE132_002
Spectrometer =

Field strength = 7.0566013 [T] (300 [MHz])
X_acq_duration = 2.9017696 [s]
X_domain       = 300.52965592 [MHz]
X_offset       = 5 [ppm]
X_points       = 16384
X_prescans     = 0
X_resolution   = 0.3437621 [Hz]
X_sfs          = 18
X_start        = 18.3570768 [kHz]
X_stop         = 300.52965592 [MHz]
Irr_freq       = 5 [ppm]
Irr_offset     = 18
Irr_domain     = 300.52965592 [MHz]
Irr_offset     = 5 [ppm]
Mod_return     = 1
Sease         = 23
Total_scans   = 23

X_90_width    = 13.01 [us]
X_acq_time    = 2.9017696 [s]
X_angle       = 45 [deg]
X_atn         = 6 [dB]
X_delay       = 6 [us]
X_offset       = 0 [ppm]
X_resolution   = 0.3437621 [Hz]
Irr_mode      = Off
Dante_preset  = FALSE
Initial_wait  = 4 [s]
Relaxation_delay = 5 [s]
Repetition_time = 7.9017696 [s]
Temp_get      = 21.8 [dC]
  
```





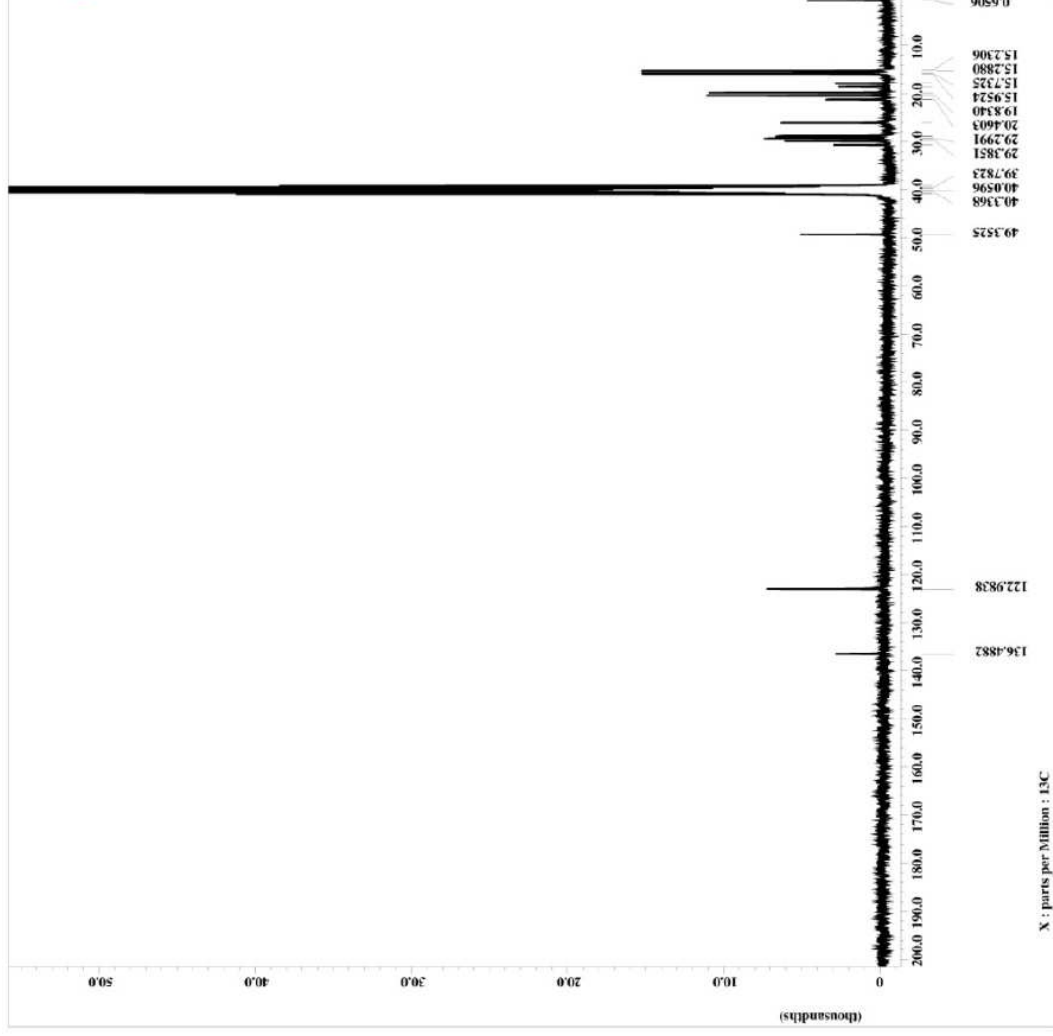
```

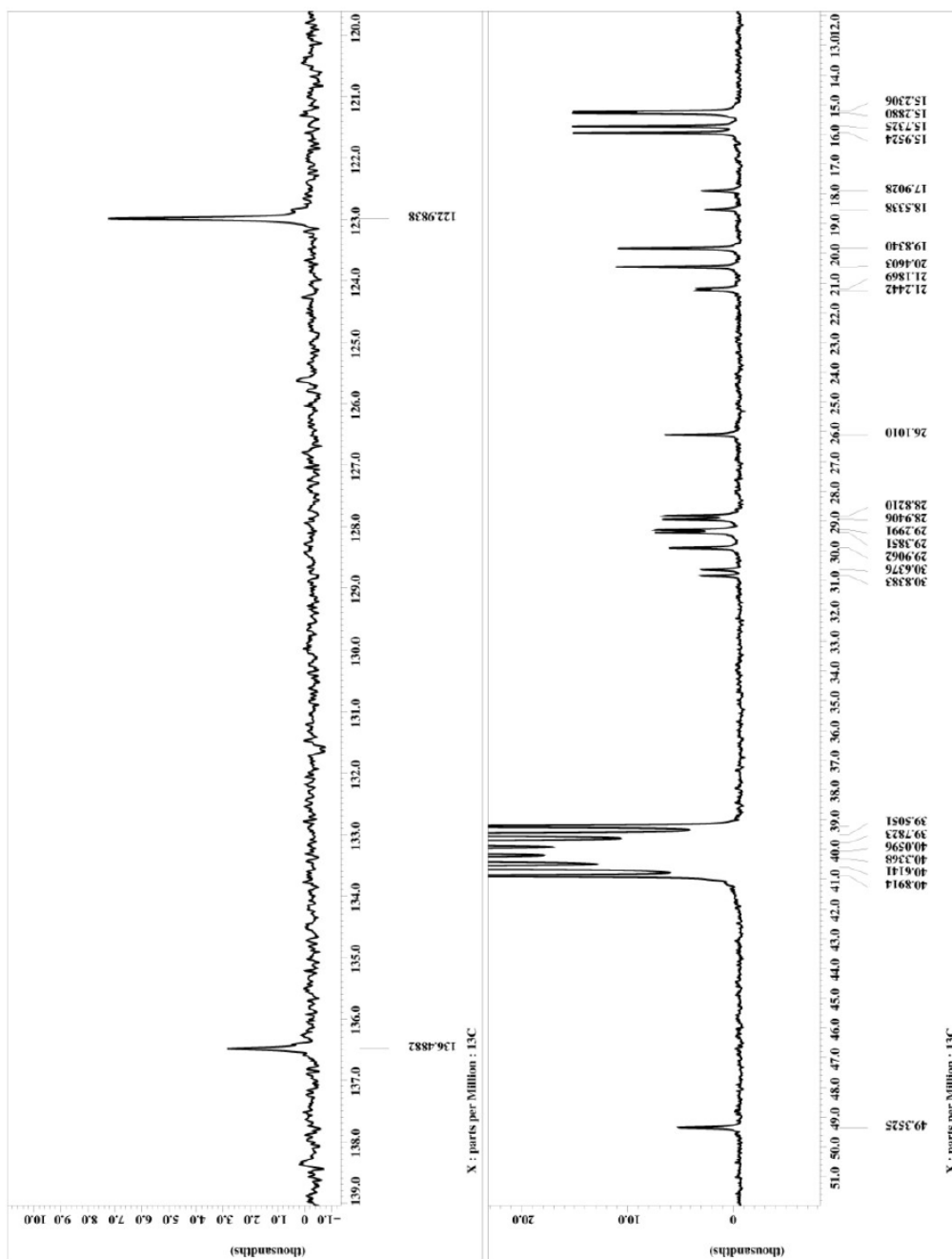
Filename = E9062408 (d7cc10p)-5-j
Author = delta
Experiment = single_pulse_dec
Sample_id = S8769082
Solvent = DMSO-d6
Acquisition_time = 25-JUN-2008 09:41:15
Revision_time = 25-JUN-2008 09:27:52
Current_time = 12-SEP-2010 13:48:47

Comment = single_pulse_decouple
Data_format = 52
Pulse_program = zgpg30
Din_size = 132
Din_title =
Din_units = [ppm]
Dimensions =
Site = X
Pulse_program_2 = X
Spectrometer = DELTA2_NMR

Field_strength = 7.0586013[T] (300[MHz]
X_acq_duration = 2.76624064[s]
X_domain = 12
X_resolution = 7.058623426[MHz]
X_rf_offset = 100[ppm]
X_points = 65536
X_prescans = 4
X_resolution_2 = 0.36124027[Hz]
X_sweep_rate = 18.67424242[MHz]
Irr_dblevel = 18
Irr_freq = 300.52965592[MHz]
Irr_offset = 5[ppm]
Clipped = FALSE
Scan_return = 9035
Total_scans = 9035

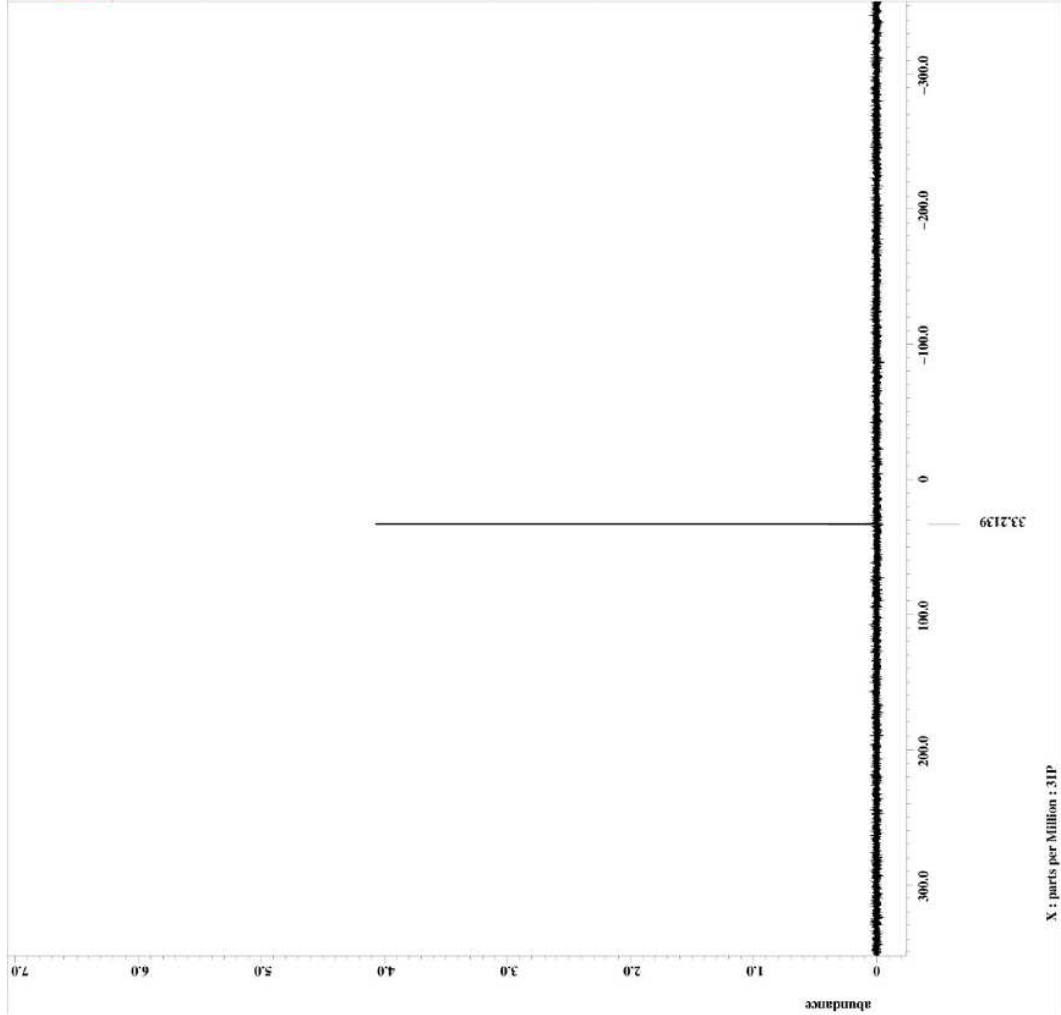
X_90_width = 9.75[us]
X_acq_time = 2.76624064[s]
X_delay = 50[us]
X_eta = 6[db]
X_pulse = 3.25[us]
Irr_atn_dec = 25[db]
Irr_atn_noe = 25[db]
Relaxation_delay = 2[s]
Decoupling = TRUE
Initial_wait = 1[s]
Noe_time = TRUE
Noe_time_2 = 2[s]
Relaxation_delay_2 = 2[s]
Repetition_delay = 4.76624064[s]
Repetition_time = 24.5[dc]
Temp_get =
  
```

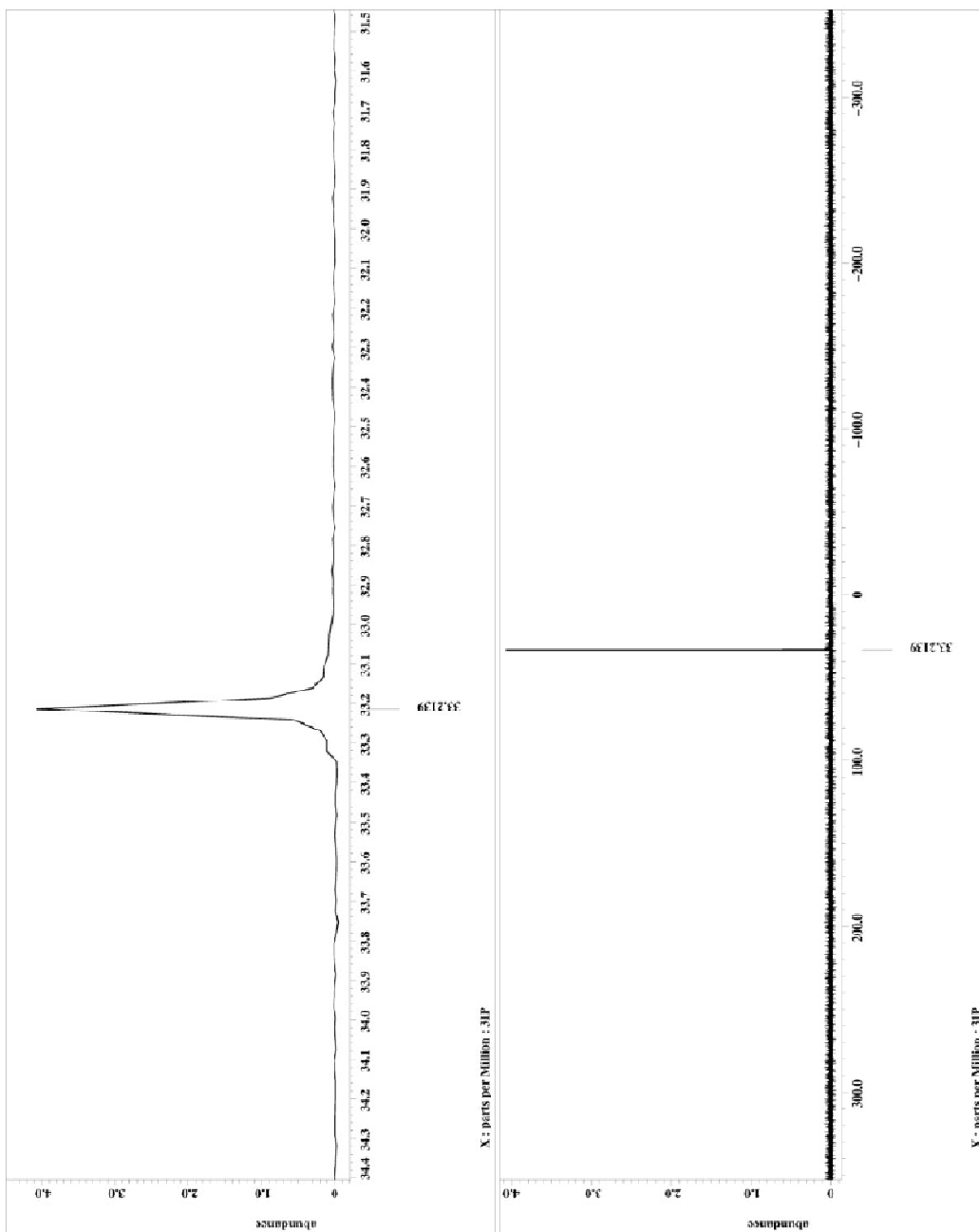






Filename = F31_IVCC107r1P-2_jd
Author = delta
Experiment = single_pulse_dec
Sample_id = S#432265
Solvent = DMSO-d6
Date_1 = 10-OCT-2010 01:58:42
Date_2 = 10-OCT-2010 13:03:39
Revision_time = 10-OCT-2010 13:07:20
Current_time = 10-OCT-2010 13:07:20
Comment = single pulse decouple
Data_format = 1D
Data_processing = COMPLEX
Date_acq = 20101013
Dim_title = 31P
Dim_units = [ppm]
Dimensions = X
Site = X
Spectrometer = JNM-SKA500
ECA = ECA 500
Field_strength = 11.7473579[T] (500[MH]
X_acq_duration = 0.1835008[s]
X_domain = 31P
X_freq = 125.76146831075[MHz]
X_offset = 0.0000000000000000
X_points = 32768
X_prescans = 4
X_resolution = 5.44956752[Hz]
X_sweep = 178.57142857[KHz]
X_swept_freq = 500.15991521[MHz]
Irr_freq = 500.15991521[MHz]
Irr_offset = 5.0[ppm]
Clipped = FALSE
Mod_return = 10
Gans = 10
Total_scans = 93
X_90_width = 11.9[us]
X_acq_time = 0.1835008[s]
X_angle = 30[deg]
X_pulse = 3.96666667[us]
Irr_atn_dec = 20[dB]
Irr_atn_noe = 20[dB]
Irr_noise = WALTZ
Decoupling = TRUE
Initial_wait = 1[s]
Noe_time = 2[s]
Revr_gain = 50
Relaxation_delay = 2[s]
Relaxation_time = 2.1835008[s]
Temp_get = 21.9[dc]





APPENDIX 8

¹H AND ¹³C NMR SPECTRUM OF 1-(1-METHYL-3-HEXYLIMIDAZOLIUM)-3-(1"-METHYL-3"-HEXYLIMIDAZOLIUM)IMIDAZOLIUM TRI [BIS(TRIFLUOROMETHANESULFONYL)IMIDE]
(3a).

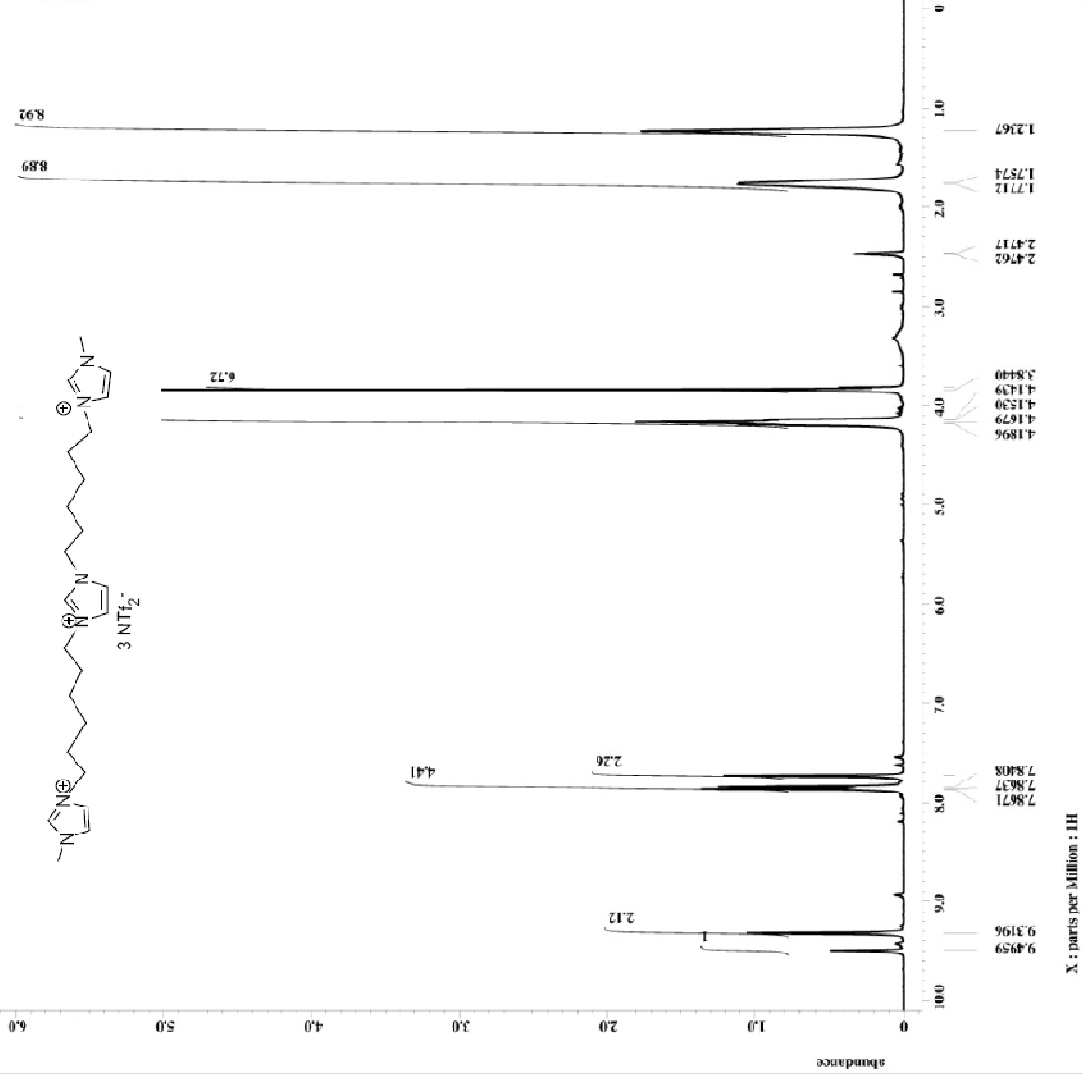
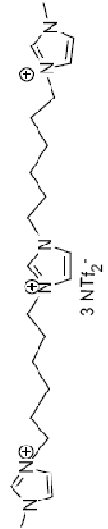


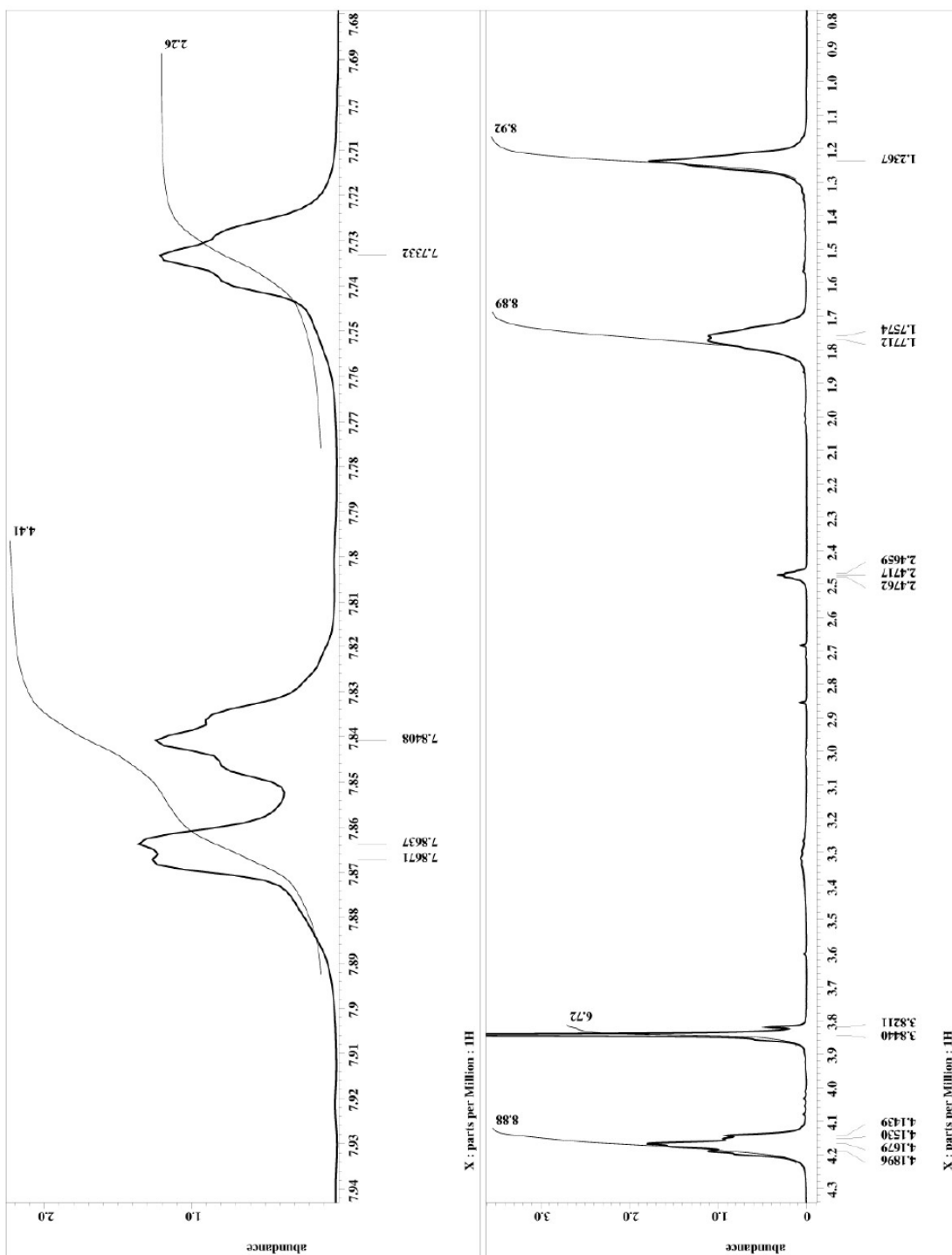
```

File Name      = methylmagnesiumchloride-2
Author         = delta
Experiment     = single_pulse_ex2
Sample Id      = 84394121
Solvent        = DMSO-d6
Pulse Program = 12-SEP-2010
Rotation Time  = 12-SEP-2010 13:13:23
Current Time   = 12-SEP-2010 13:13:41

Comment       = single pulse
Data Format    = ID COMPLEX
Dm size       = 32.07
Dm units      = ppm
Dimensions    = X
Site          = ECX 300
Spectrometer  = DELTA2_300

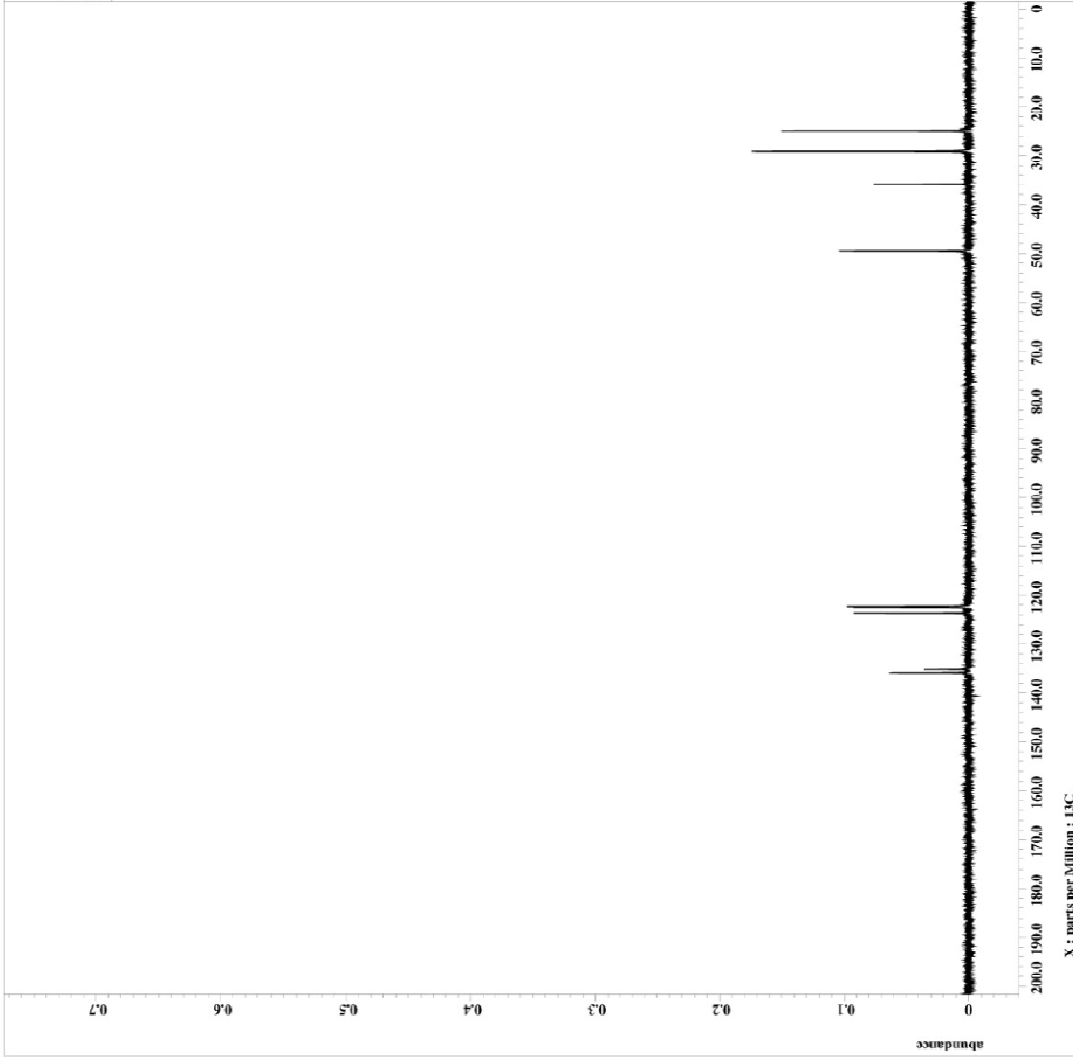
Field strength = 7.050601101 (300 MHz)
K_osc_frequency = 7.09717696 [s]
K_channel      = 1
K_freq         = 300.52965592 [MHz]
K_offset       = 5 [ppm]
K_points       = 16394
K_pressure     = 0
K_resolution   = 0.44397611 [Hz]
K_sweep        = 5.43270748 [MHz]
IRF_channel    = 1M_GOMAIN
IRF_freq       = 300.52965592 [MHz]
IRF_offset     = 5 [ppm]
IRF_gain       = 10
IRF_gain_min  = 10.52965592 [MHz]
IRF_gain_max  = 10.52965592 [MHz]
IRF_offset     = FALSE
Mod_return     = 1
Scans          = 12
Total scans   = 12
X_90_width     = 13.01 [us]
X_acq_time     = 2.90717696 [s]
X_angle        = 45 [deg]
X_atr          = 4 [dB]
X_pulse        = 6.505 [us]
X2_mode        = 04E
X2_offset      = FALSE
X2_gain        = 1 [s]
X2_wait        = 1 [s]
X2_gain_min    = 1 [s]
X2_gain_max    = 20 [s]
Relaxation_delay = 5 [s]
Repeat_scan_time = 7.90717696 [s]
Temp_gut       = 23.2 [degC]
  
```

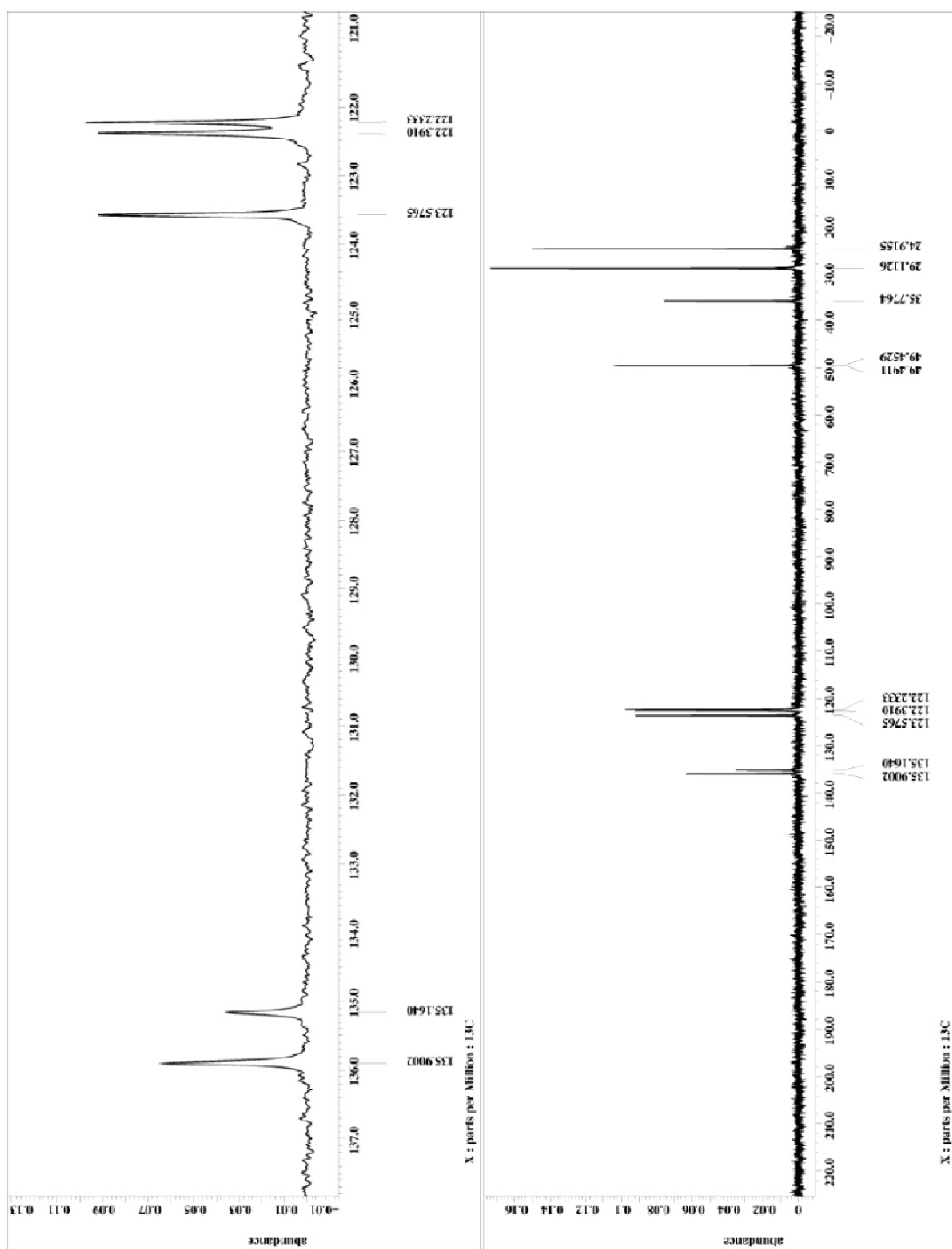






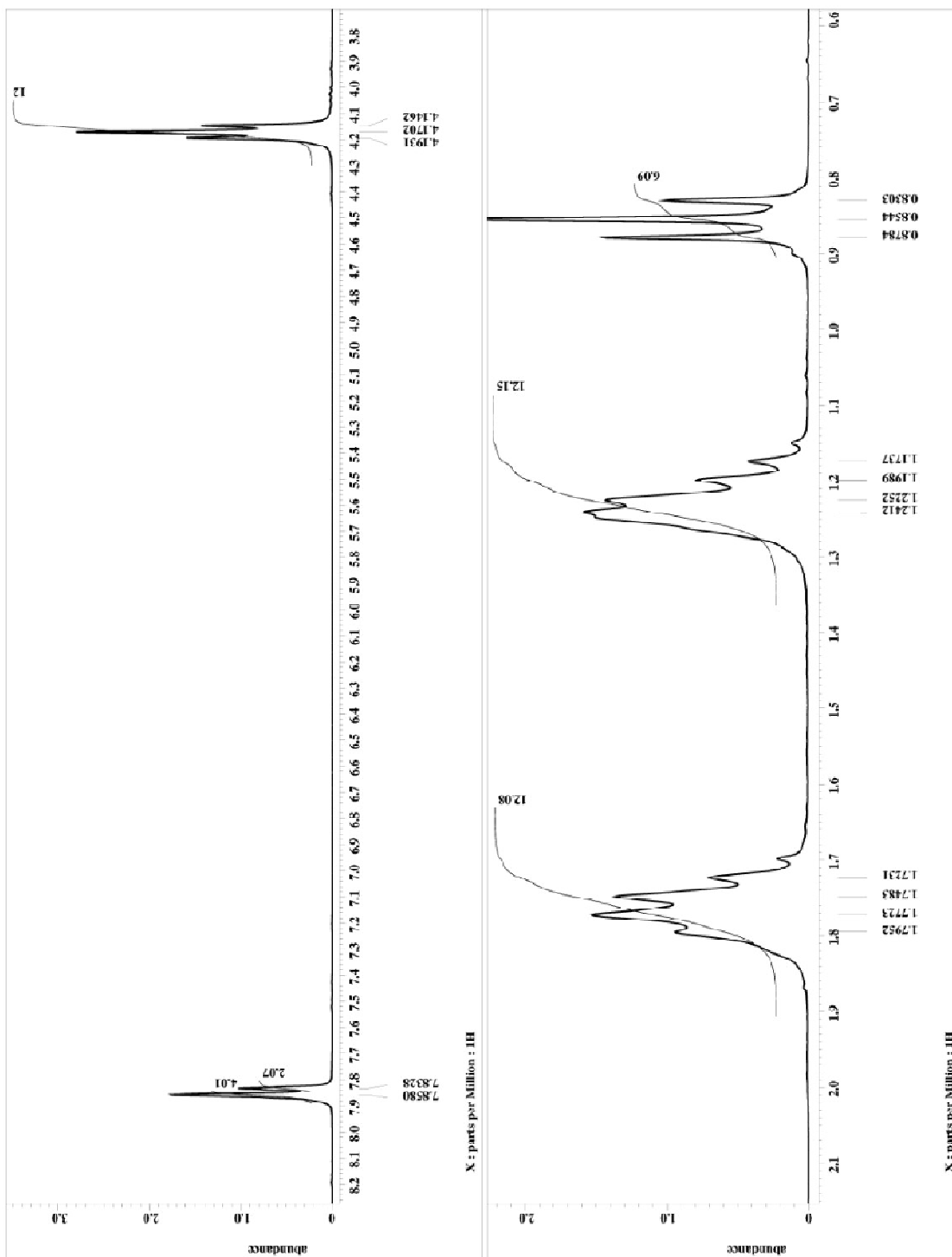
Filename = 90510m1mt-3.jef
Acq_date = 2010-06-23 21:08:10
Experiment = single pulse dec
Sample_id = S#793918
Solvent = D2O
Creation_time = 10-JUN-2008 23:23:00
Revision_time = 21-SEP-2010 20:49:27
Current_time = 21-SEP-2010 21:08:10
Comment = single pulse decouple
Data_format = 1D COSY2D
Dim_size = 32424
Dim_title = 13C
Dim_units = X [ppm]
Dimensions = 2
Size = 65536
Spectrometer = ECA 500
Field_strength = 7.0566033 [T], 300 [MHz]
Acq_duration = 13.2824064 [s]
X_gain = 13C
X_freq = 75.5682324 [MHz]
X_offset = 100 [ppm]
X_points = 65536
X_prescans = 4
X_resolution = 36724027 [Hz]
X_sweep = 23.6742424 [kHz]
Irr_domain = 1H
Irr_freq = 300.5296552 [MHz]
Irr_offset = 5 [ppm]
Clipped = TRUE
Spool_return = 0
Total_scans = 800
X_90_width = 9.75 [us]
X_acq_time = 2.76824064 [s]
X_angle = 80 [deg]
X_atn = 3.25 [us]
X_pulse = 23 [dB]
Irr_atn_dec = 23 [dB]
Irr_atn_poe = 23 [dB]
Irr_noise = WALTZ
Spectrum = 13C
Init_wait = 1 [s]
Noise = TRUE
Noe_time = 2 [s]
Recv_gain = 56
Relaxation_delay = 2 [s]
Relaxation_time = 23.2 [dC]
Temp_9st =





APPENDIX 9

^1H AND ^{13}C NMR SPECTRUM OF 1-(1-BUTYL-3-HEXYLIMIDAZOLIUM)-3-(1"-BUTYL-3"-HEXYLIMIDAZOLIUM)IMIDAZOLIUM TRI [BIS(TRIFLUOROMETHANESULFONYL)IMIDE] (3b).





```

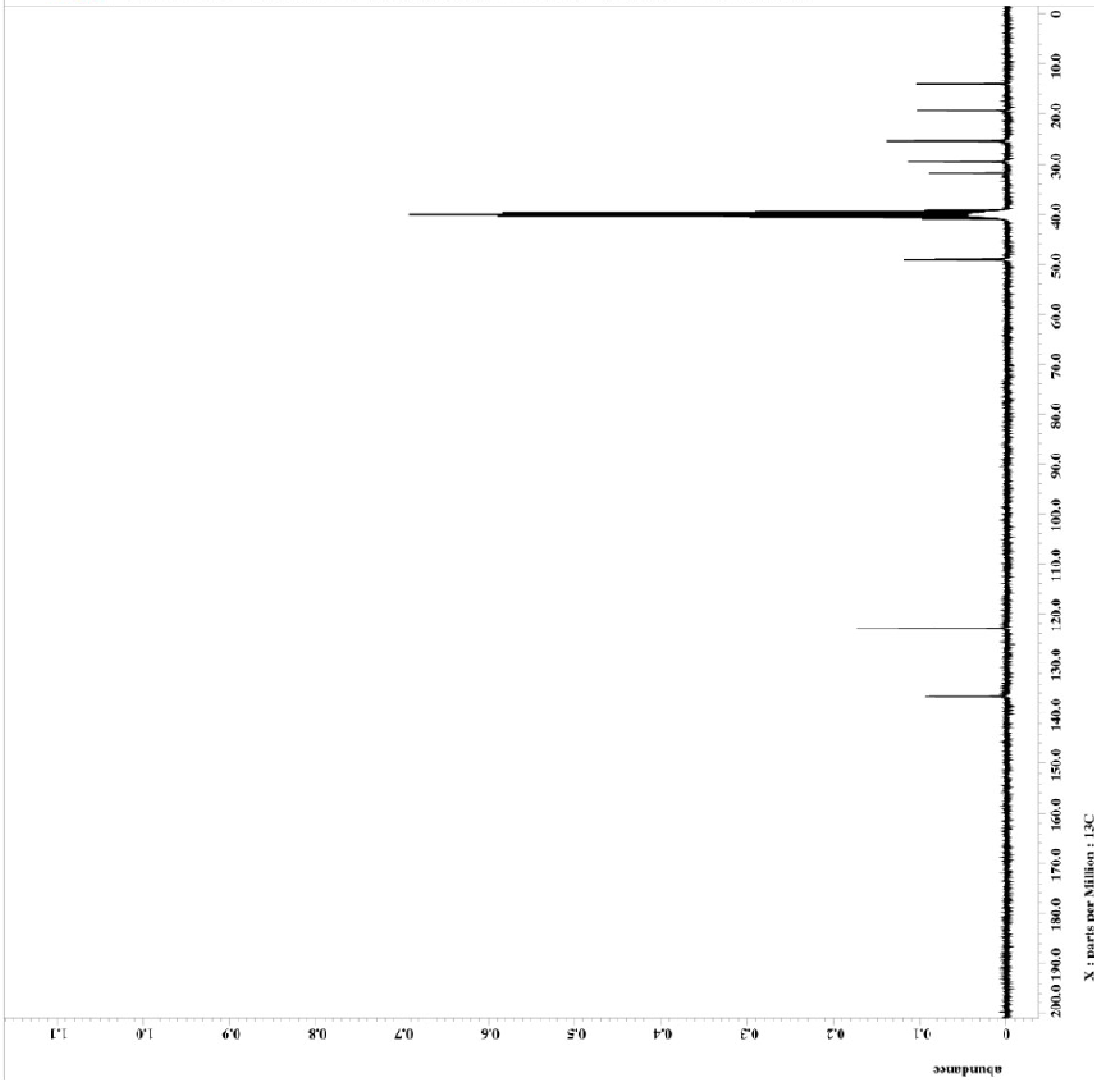
File Name      = 20091010butyl-2.fid
Author        = delta
Experiment    = single pulse dec
Sample_ID     = 8860494
Solvent       = DMSO-d6
Acquisition  = 2009-10-10 10:20
Relaxation_time = 31.588-2010 21:57:22
Constat_time  = 21-08E-2010 21:50:02

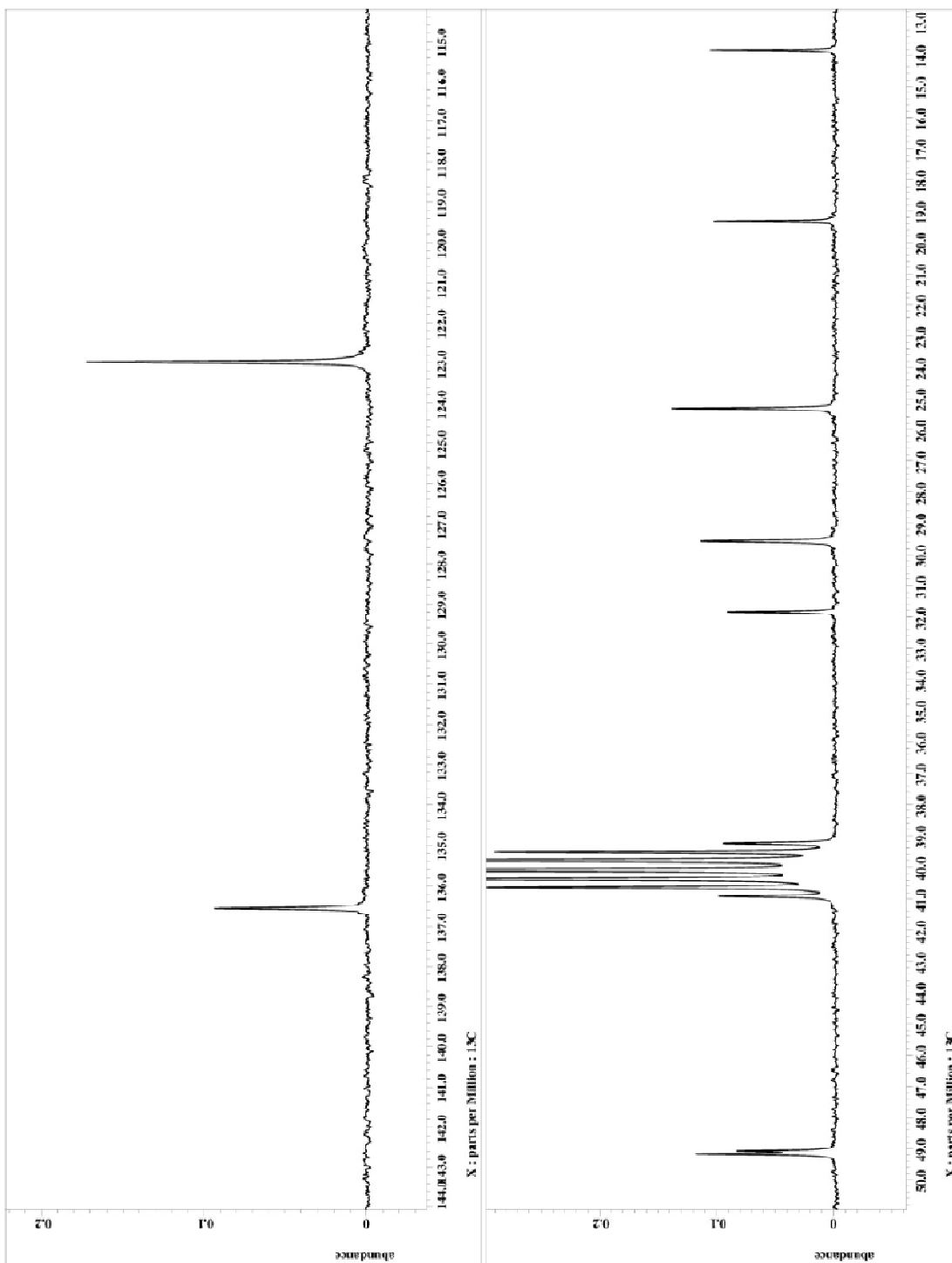
Comment       = single pulse decouple
Date_Forma    = 1D COMPLEX
Dir_Size     = 8228
Dir_Path     = 20091010
Dir_Units    = [ppm]
Dimensions   = X
Site         = ECX 300
Spectrometer = DELTA2_NMR

Field strength = 7.5524064 [T] (300 [MHz]
X_domain      = 2.75524064 [s]
X_freq        = 75.56823426 [MHz]
X_offset      = 100 [ppm]
X_points      = 65536
X_fscars      = 1
X_resolution  = 35124027 [Hz]
X_resolution  = 33.574242 [kHz]
Iz_domain     = 16.574242 [kHz]
Iz_freq       = 300.52965592 [MHz]
Iz_offset     = 5 [ppm]
Clipped       = 0
Mod_return    = 1000
Total_scans   = 1000

X_50_width    = 9.75 [us]
X_acq_time    = 2.75524064 [s]
X_angle       = 30 [deg]
X_p1          = 1 [us]
X_p2          = 3 [us]
X_p3          = 25 [us]
Iz_atn_pos    = 25 [dB]
Iz_atn_neg    = VALVE
Decoupling    = waltz
Initia_wait   = 1 [s]
Noe_time      = 2 [s]
Repr_time     = 58
Relaxation_delay = 2 [s]
Repetition_time = 4.75524064 [s]
Temp_set      = 33 [dC]

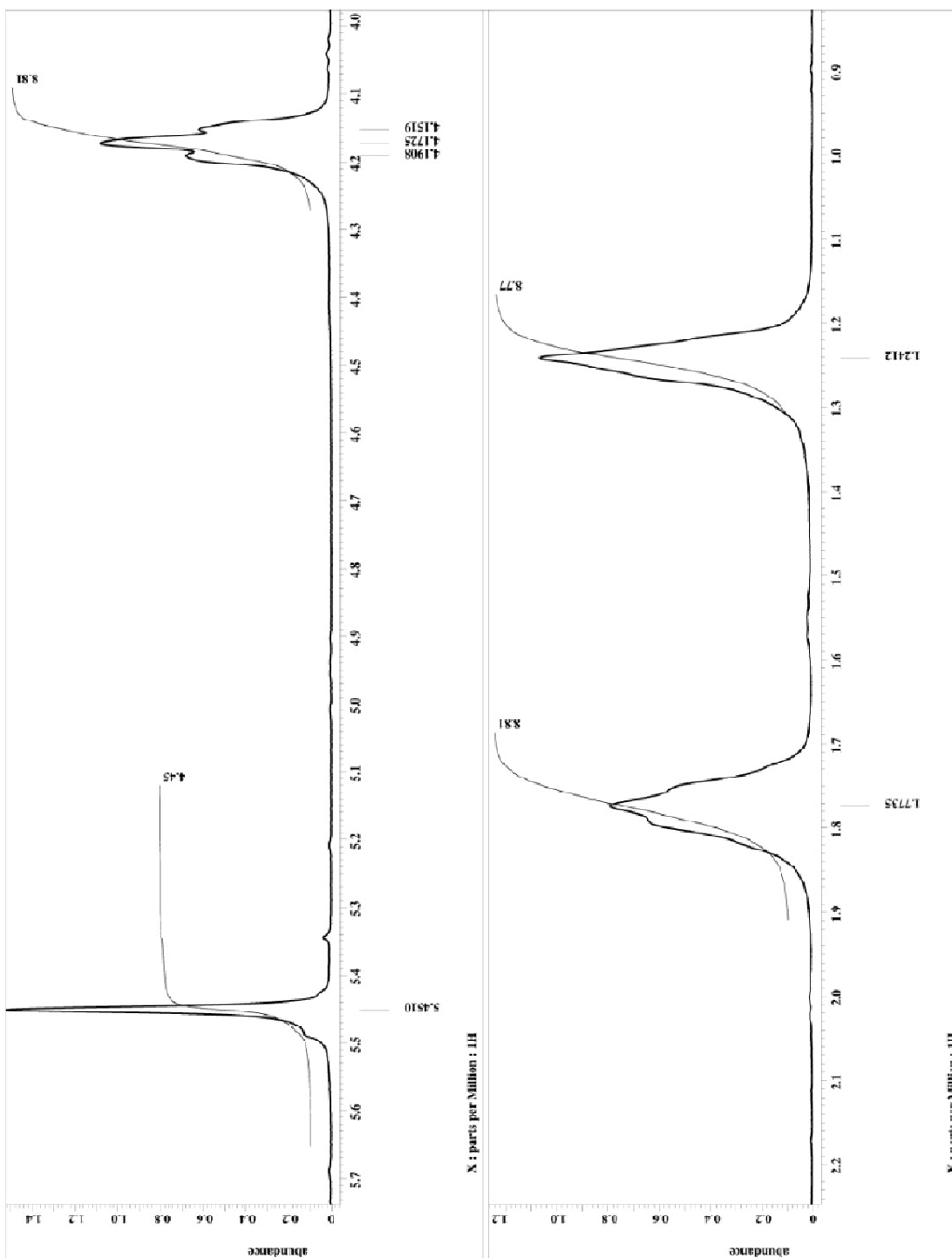
```

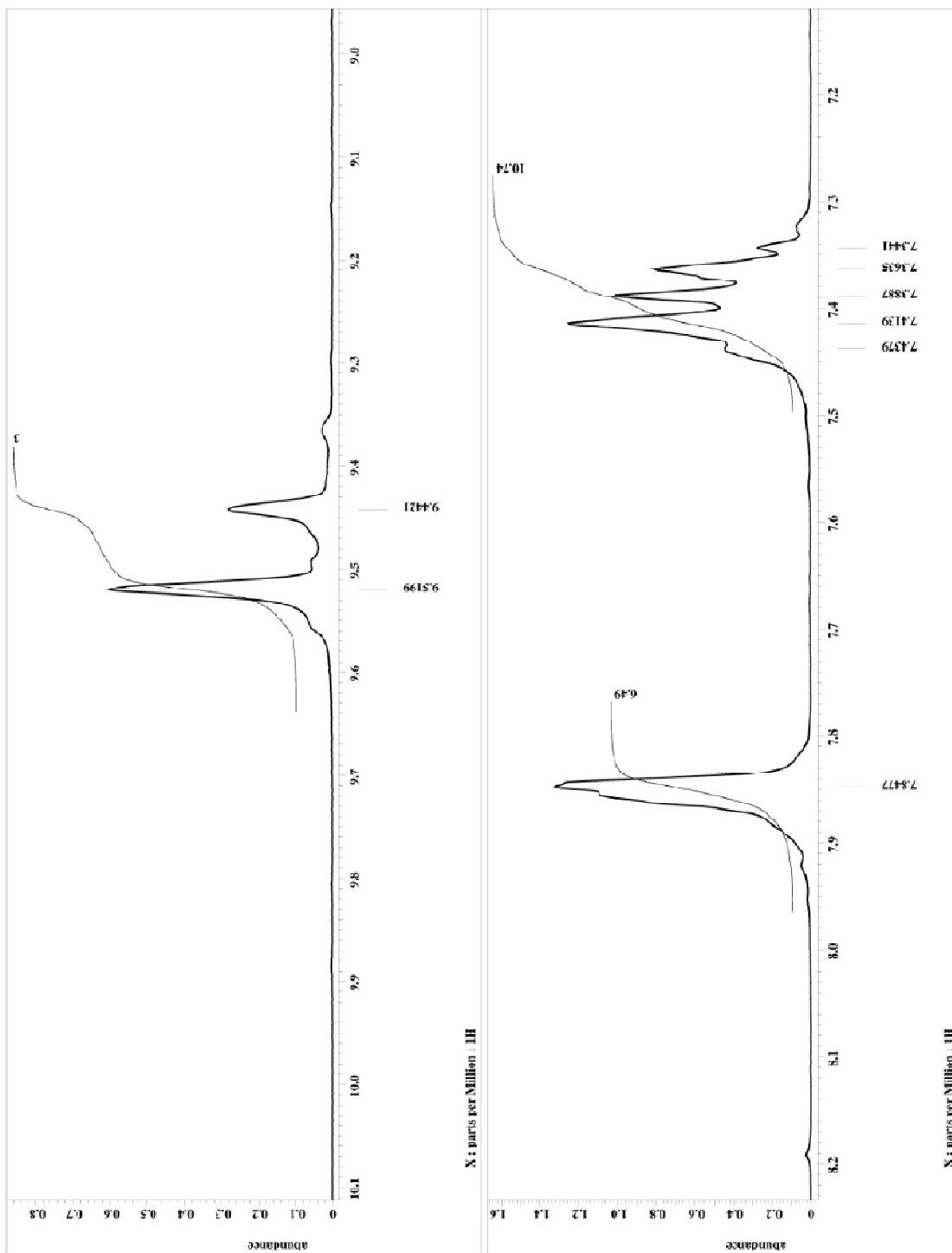




APPENDIX 10

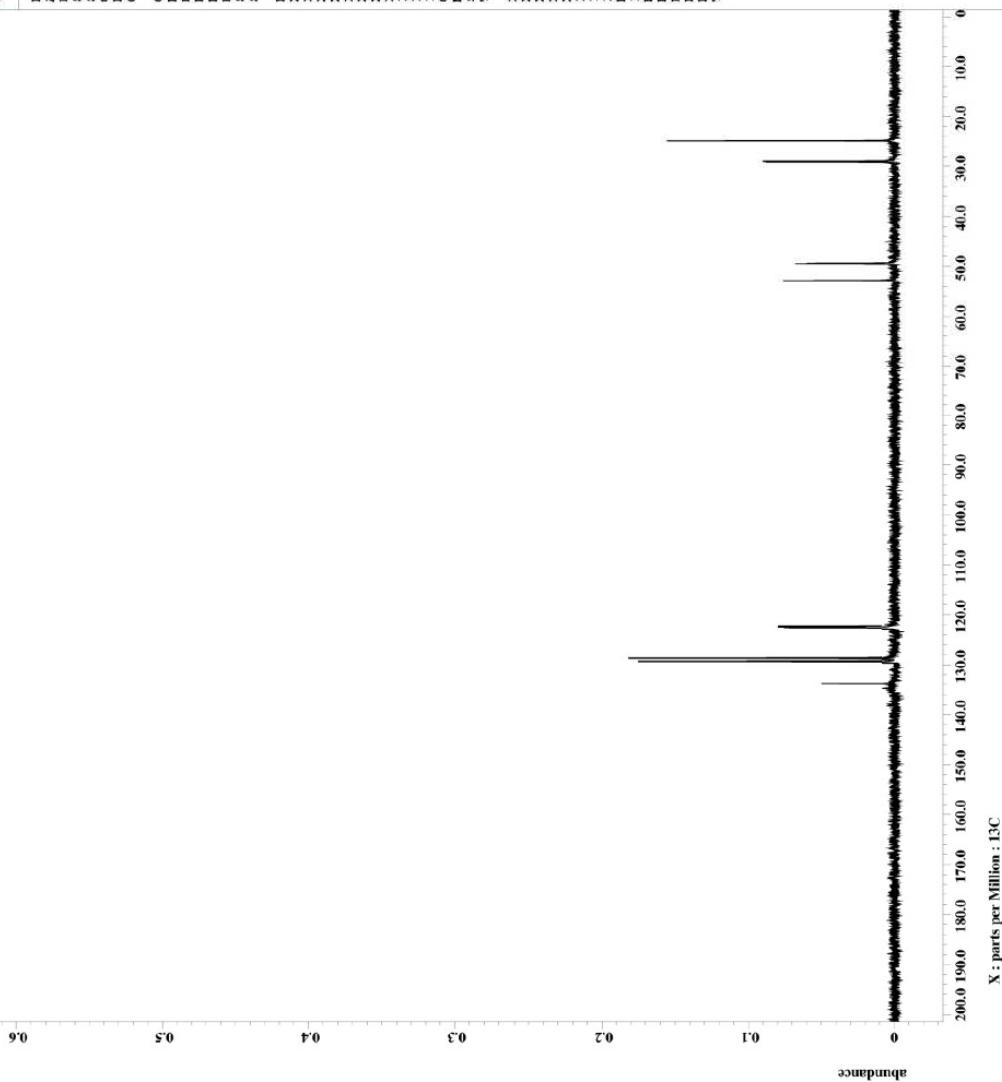
¹H AND ¹³C NMR SPECTRUM OF 1-(1-BENZYL-3-HEXYLIMIDAZOLIUM)-3-(1-BENZYL-3-HEXYLIMIDAZOLIUM)IMIDAZOLIUM TRI [BIS(TRIFLUOROMETHANESULFONYL)IMIDE]
(3b).

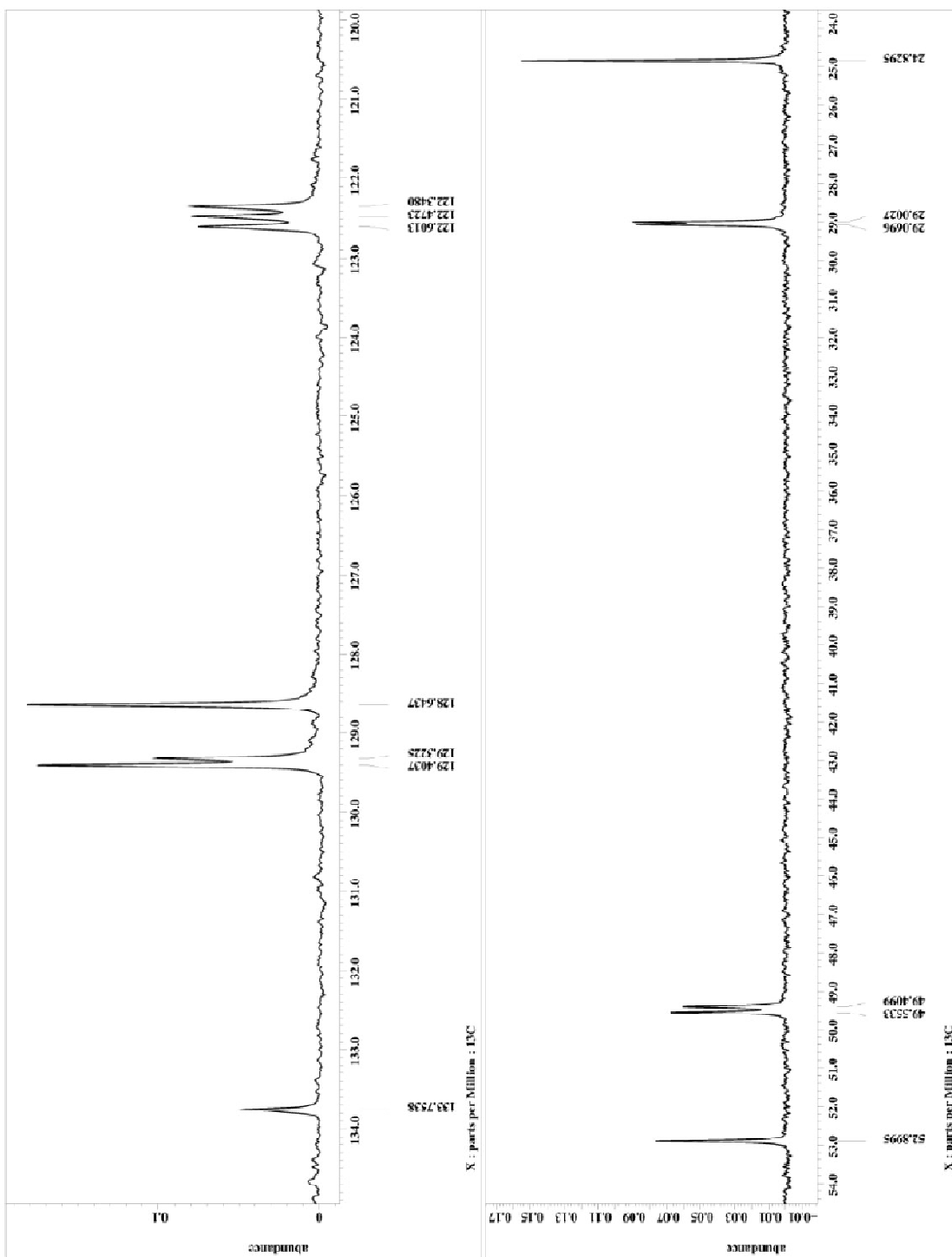






Filename = 080610bzimit-2.jdf
Author = delta
Experiment = single_pulse_dec
Sample_id = 8F852822
Solvent = D2O JUN-2008 01-01-08
Revision_time = 21-SEP-2010 21:09:10
Current_time = 21-SEP-2010 21:10:27
Comment = single pulse decouple
Date_format = ID COMPLEX
Dim = 8
Dim_units = [ppm]
Dimensions = X
Site = ECX 300
Spectrometer = DELTA2_NMR
Field_strength = 7.0586013 [T] (300 [MHz]
X_acq_duration = 2.76824064 [s]
X_domain = 13C
X_freq = 75.56823426 [MHz]
X_offset = 100 [ppm]
X_points = 65336
X_resolution = 0.36124027 [Hz]
X_sweep = 23.67424242 [kHz]
Irr_domain = 1H
Irr_freq = 300.52965592 [MHz]
Irr_offset = 5 [ppm]
Clipped = TRUE
Scan_return = 0
Spans = 800
Total_scans = 800
X_90_width = 9.75 [us]
X_acq_time = 2.76824064 [s]
X_angle = 30 [deg]
X_delay = 3 [us]
X_pulse = 3 [us]
X_pulse_width = 25 [us]
Irr_atn_dec = 25 [dB]
Irr_atn_noe = 25 [dB]
Irr_noise = WALTZ
Decoupling = TRUE
Initial_wait = 1 [s]
Noe_time = 2 [s]
Recvr_gain = 58
Relaxation_delay = 2 [s]
Repetition_time = 4.76824064 [s]
Temp_get = 24.9 [dC]





APPENDIX 11

^1H , ^{13}C AND ^{31}P NMR SPECTRA OF 1-(HEXYLTRIPROPYLPHOSPHONIUM)-3-(HEXYLTRIPROPYLPHOSPHONIUM)IMIDAZOLIUM TRI[BIS(TRIFLUOROMETHANESULFONYL)IMIDE] (3d).

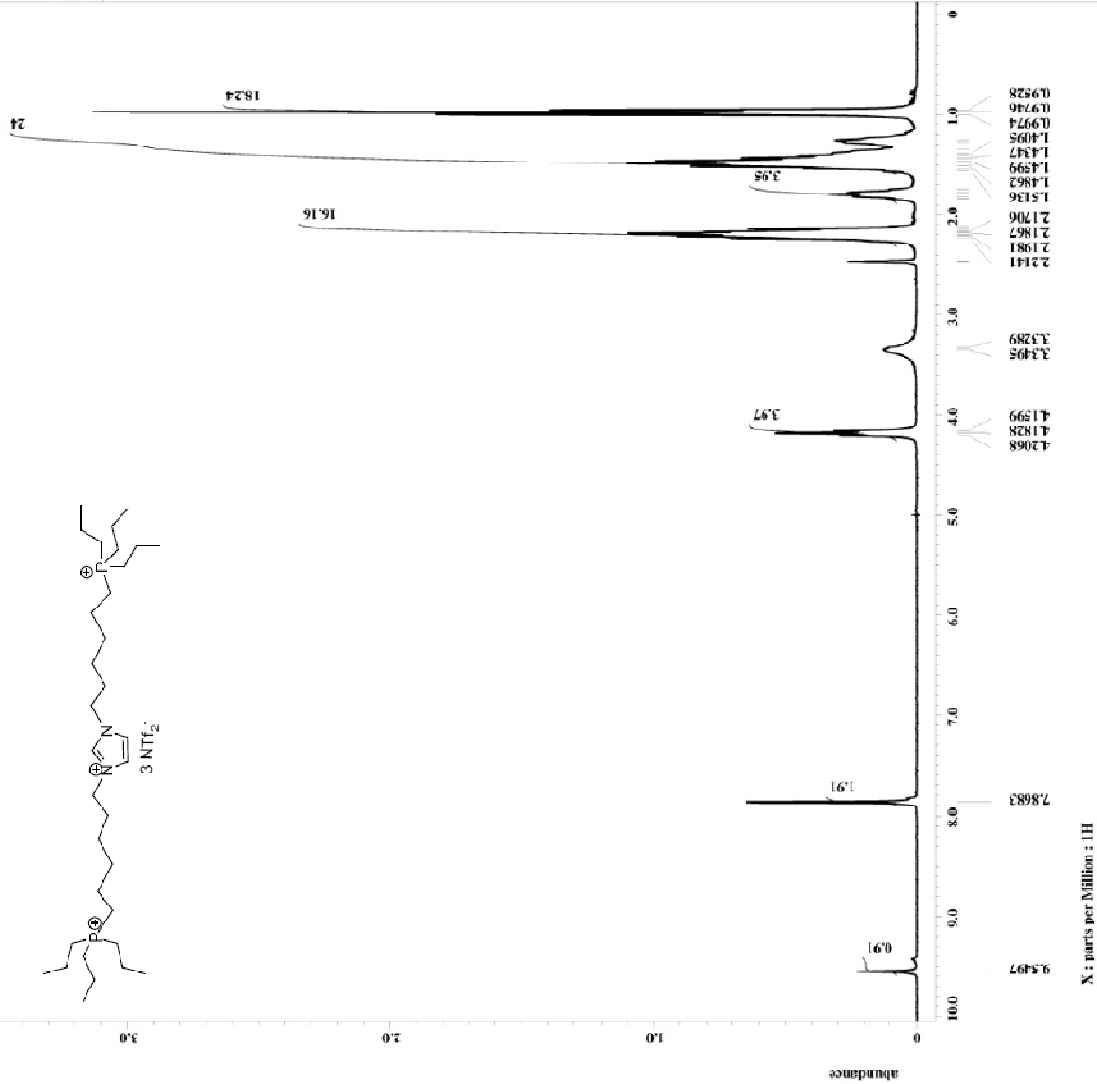
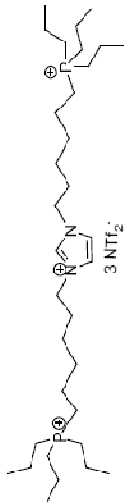


```

Filename = TripPhosphazeneCGH-2.1
Author = delta
Experiment = 419746
Sample_CD = 0
Solvent = DMSO-D6
Creation_time = 10-Oct-2008 00:46:42
Revision_time = 20-Nov-2008 21:48:49
Current_time = 12-SEP-2010 13:25:45

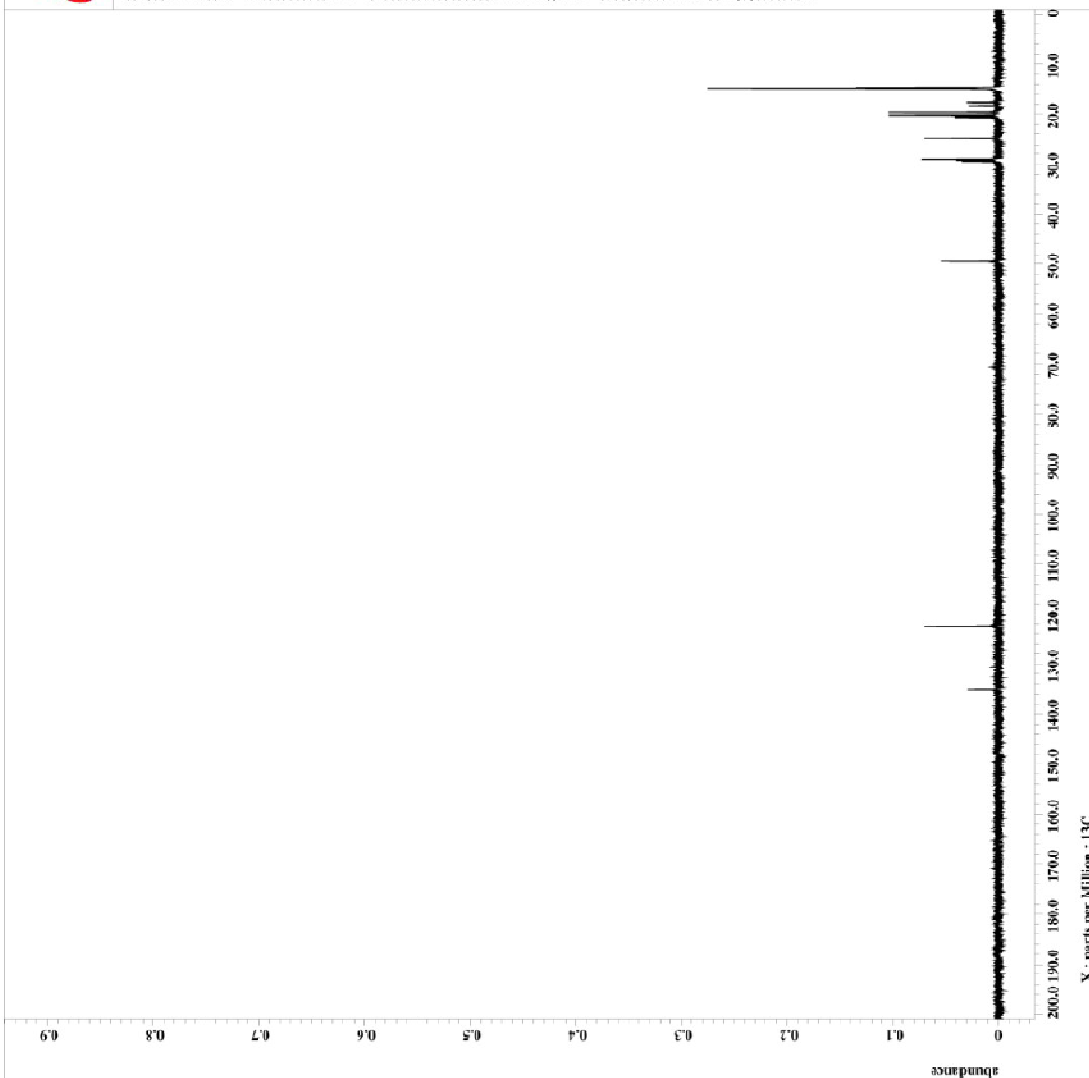
Comment = sing_pulse
          100MHz
          131.07
          :H
          :ppm
          :X
          ECY 300
          DELTA_NMR

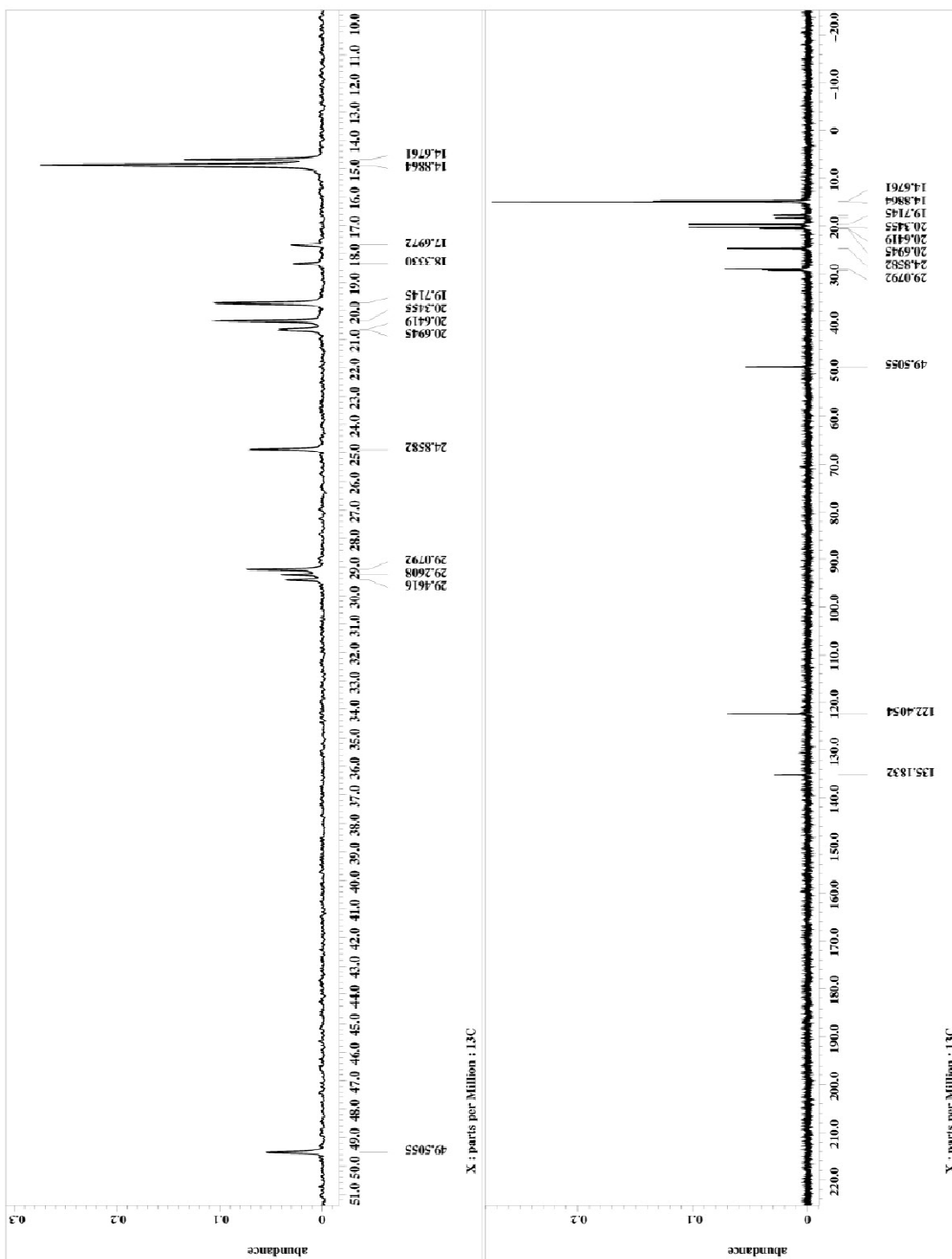
Spectrometer
Field strength = 7.0586013[T] (300 MHz)
X_acq_duration = 2.80717696[s]
X_domain = 300.52865592[MHz]
X_freq = 5[ppm]
X_offset = 26364
X_points = 65536
X_resolution = 6.34397631[Hz]
X_sweep = 5.63370784[kHz]
Irr_domain = 300.52865592[MHz]
Irr_freq = 5[ppm]
Irr_offset = 26364
Irr_points = 65536
Irr_resolution = 6.34397631[Hz]
Irr_sweep = 5.63370784[kHz]
Clipped = FALSE
Mag_return = 1
Scans = 12
Total_scans = 12
X_90_width = 19.0[us]
X_acq_time = 2.80717696[s]
X_angle = 45[deg]
X_atn = 4[dB]
X_pulse = 8.803[us]
Irr_mode = off
Irr_mode2 = off
Pulse_program = zgpg30
Receiver_gain = 26
Balance_delay = 4[s]
Repetition_time = 7.80717696[s]
Temp_get = 23.1[dc]
  
```





Filename = 09010pit-2.jdf
Author = delts
Experiment = single_pulse_dec
Sample_ID = SF6232
Solvent = D2O
Acquisition_time = 21-SEP-2010 01:03:38
Relaxation_time = 21-SEP-2010 21:02:26
Current_time = 21-SEP-2010 21:11:57
Comment = single pulse decouple
Data_format = 1D CAMELX
Bin_size = 32.8
Bin_units = [ppm]
Dimensions = X
Site = ECK 300
Spectrometer = DELTA2_NMR
Field_strength = 7.056011[T] (300 MHz)
X_acq_duration = 2.75824064[s]
X_consist = 13C
X_freq = 75.5682426[MHz]
X_offset = 100[ppm]
X_points = 65536
X_resolution = 0.3612027[Hz]
X_resolution_ppm = 23.674442[MHz]
X_sweep = 14.5296592[MHz]
Xz_domain = 14.5296592[MHz]
Xz_freq = 300.5296592[MHz]
Xz_offset = 5[ppm]
Clipped = TRUE
Scan_rate = 800
Total_scans = 800
X_50_width = 9.75[us]
X_acq_time = 2.75824064[s]
X_angle = 30[deg]
X_delay = 3.00[us]
X_pulse = 3.25[us]
Xz_atn_dec = 25[db]
Xz_atn_poe = 25[db]
Xz_noise = WALTZ
Decoupling = TRUE
Initial_wait = 10[s]
Max_time = 21[s]
Recvr_GAIN = 56
Relaxation_delay = 21[s]
Repetition_time = 4.75824064[s]
Temp_get = 22.2[deg]



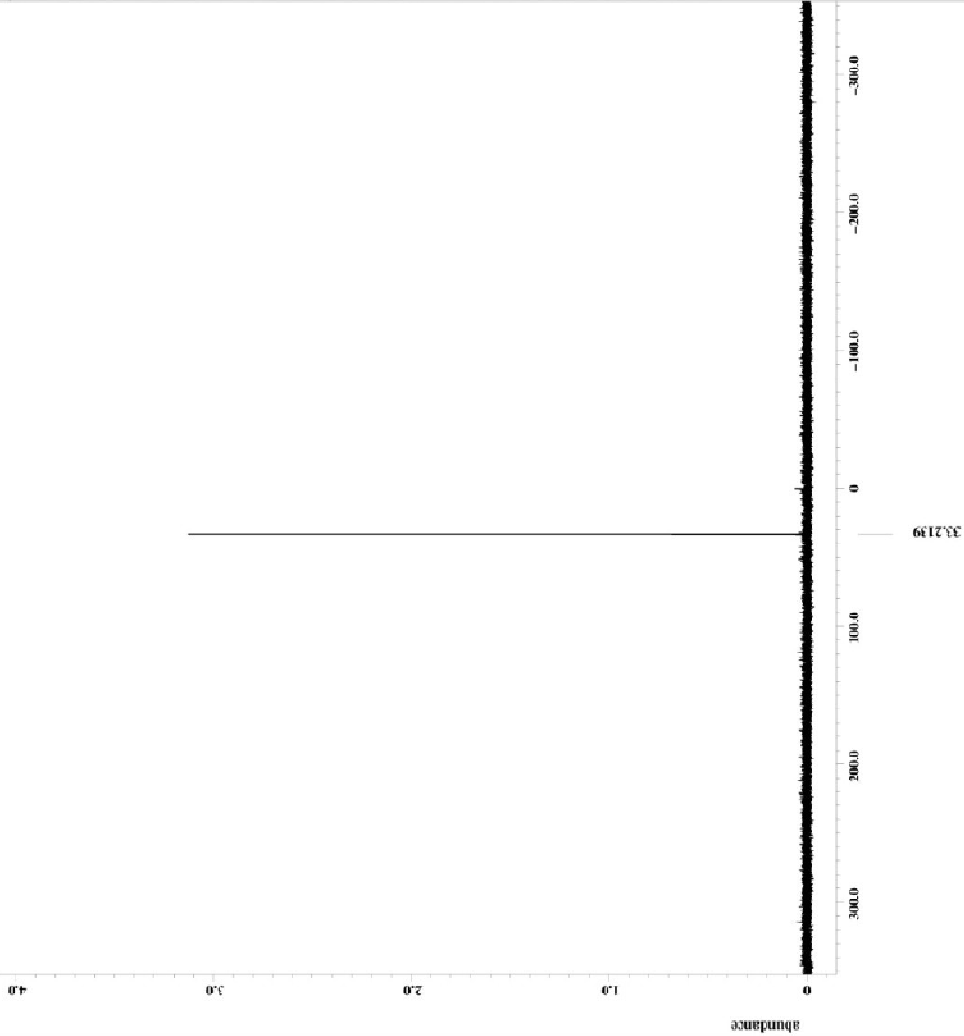




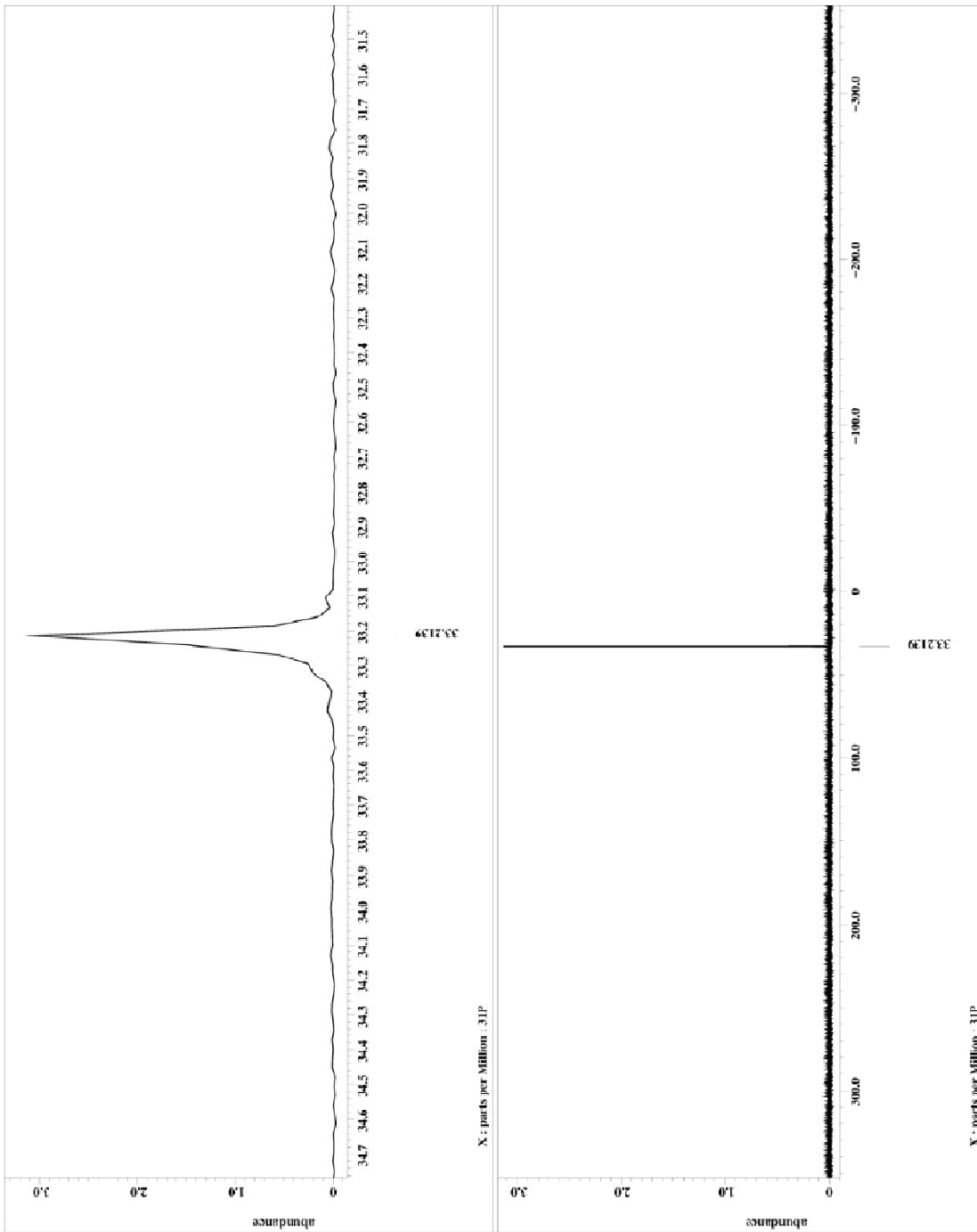
```

Filename = P31_F0C6Fr1P3-3.j4f
Author = delta
Experiment = single_pulse_dec
Sample_id = 843591
Spectrometer = spect
Creation_time = 11-OCT-2010 02:04:08
Revision_time = 10-OCT-2010 12:10:27
Current_time = 10-OCT-2010 13:02:25
Comment = single pulse decouple
Data_format = 1D COMPLEX
Dir = /data/100
Dim = 31P
Dim_units = [ppm]
Dimensions = X
Site = ECA 500
Spectrometer = OMR-SCA500
Field_strength = 11.743378[GT] (500[MH]
X_acq_duration = 0.1835008[s]
X_domain = 31P
X_freq = 202.4691073[MHz]
X_offset = 0[ppm]
X_points = 32768
X_resolution = 5.44956752[Hz]
X_sweep = 1H
Irr_domain = 1H
Irr_freq = 500.15991521[MHz]
Irr_offset = 5.0[ppm]
Clipped = FALSE
Scans_return = 135
Total_scans = 135
X_90_width = 11.9[us]
X_acq_time = 0.1835008[s]
X_angle = 90[deg]
X_pulse = 3.95656667[us]
Irr_atn_dec = 20[db]
Irr_atn_noise = 20[db]
Irr_noise = WALTZ
Decoupling = TRUE
Initial_wait = 2[s]
Noe_time = 2[s]
Recvr_gain = 50
Relaxation_delay = 2[s]
Repetition_time = 2.1835008[s]
Temp_get = 21.9[degC]

```



X : parts per Million : 31P



APPENDIX 12

¹H AND ¹³C NMR SPECTRA OF (1'-METHYL-3'-PROPYLMIDAZOLIUM)-3-(1''-METHYL-3''-PROPYLMIDAZOLIUM)IMIDAZOLIUM TRI [BIS(TRIFLUOROMETHANESULFONYL)IMIDE]

(4a).

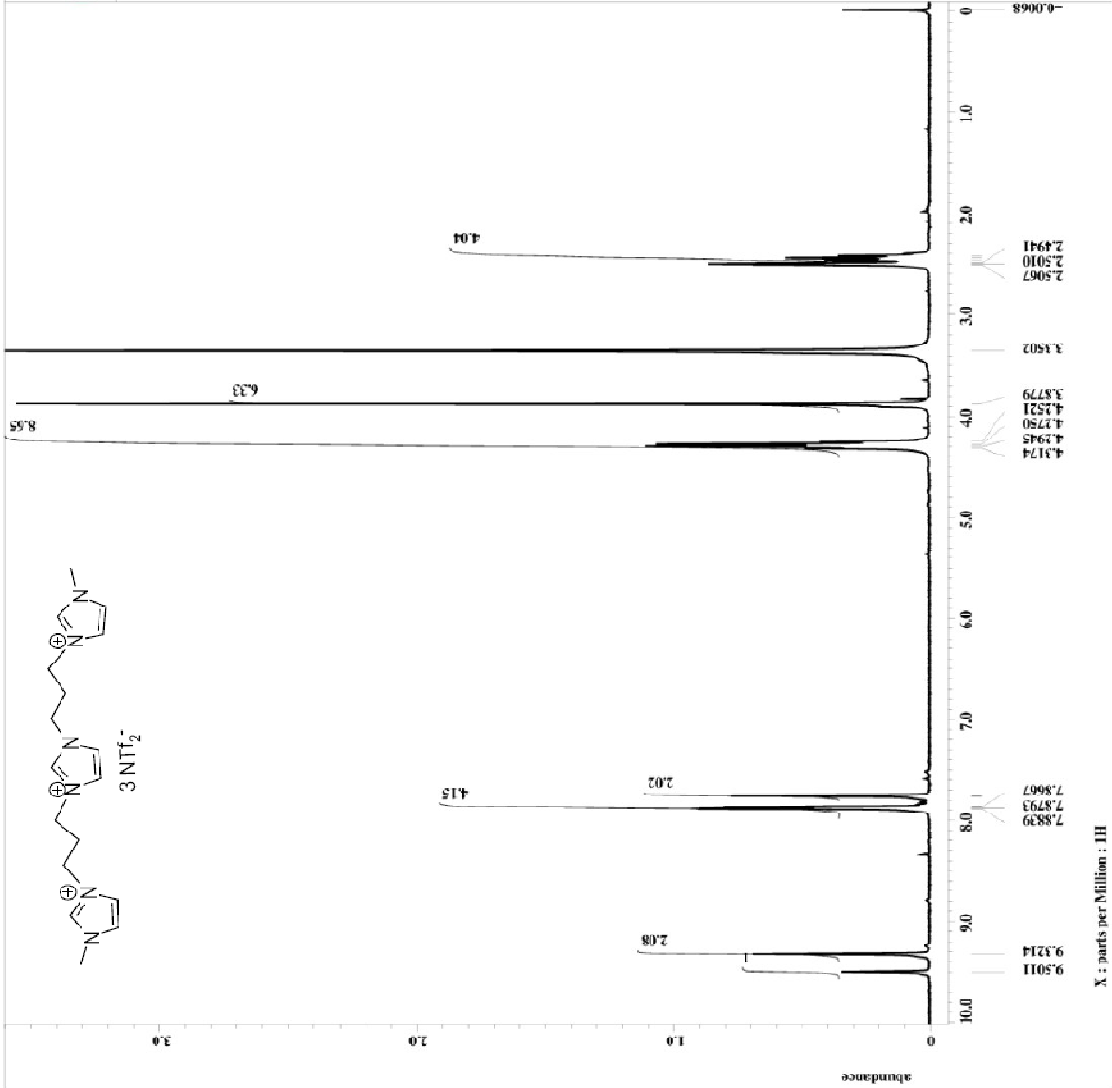


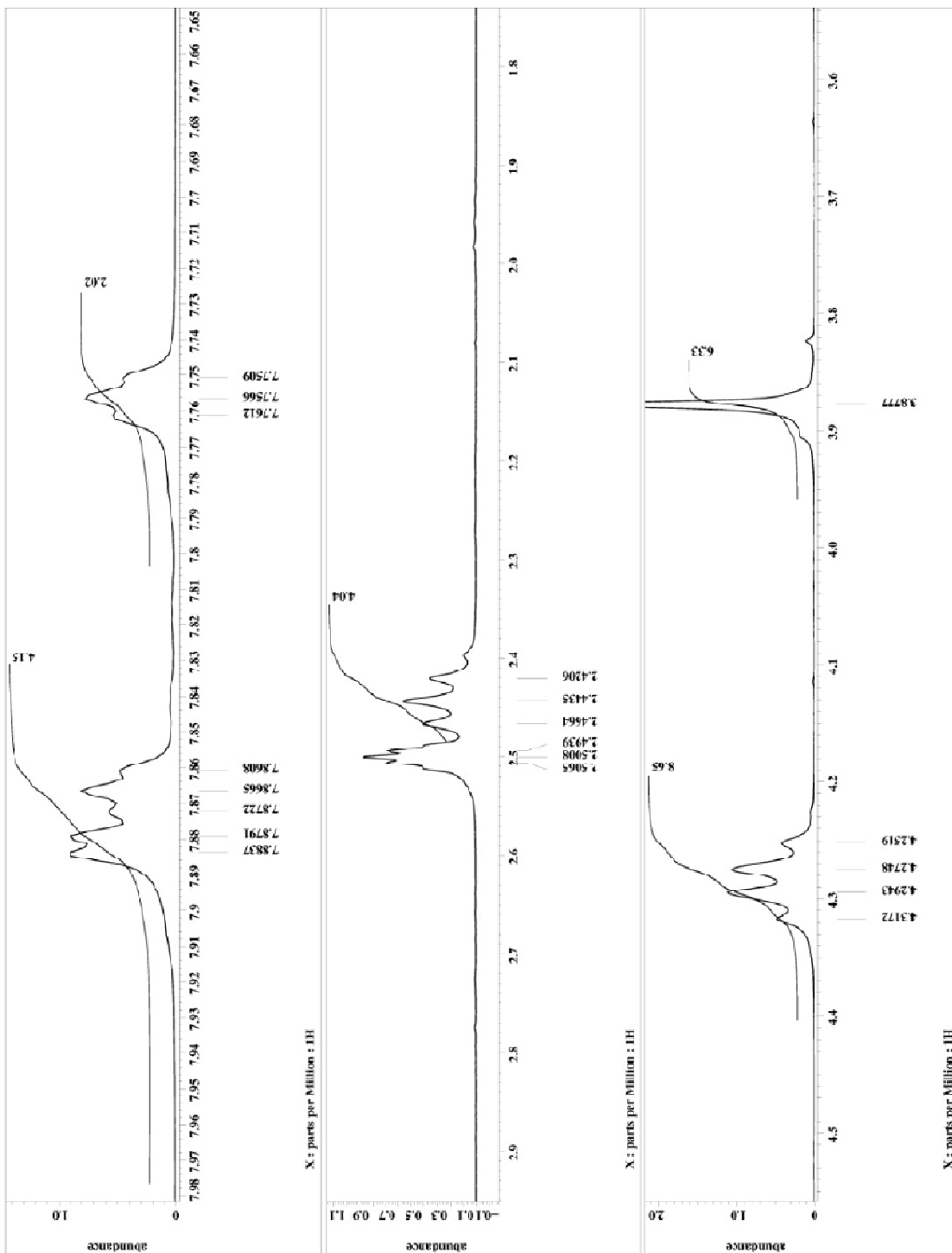
```

Filename = EWO90308 (TTC(Me)Im)-6
Author = delta
Experiment = single_pulse_ex2
Sample_id = 882/0181
Date_1 = 12-SEP-2008 10:57:35
Date_2 = 12-SEP-2010 12:59:15
Revision_time = 12-SEP-2010 12:59:15
Current_time = 12-SEP-2010 12:59:42

Comment = single_pulse
Data_format = 1D_CDFLEX
Dir_path = 1R107
Dir_title = [ppm]
Dir_units = [ppm]
Dimensions = X
Site = ECX 300
Spectrometer = DELTA2_NMR

Field_strength = 7.0586013 [T] (300 [MHz]
X_sca_duration = 2.90717696 [s]
X_domain = 1H
X_freq = 300.52966592 [MHz]
X_offset = 51 [ppm]
X_points = 16384
X_prescans = 0
X_acq_dir_com = 0
X_sweep = 5.63570784 [kHz]
Irr_domain = 1H
Irr_freq = 300.52966592 [MHz]
Irr_offset = 51 [ppm]
Irr_domain = 1H
Irr_freq = 300.52966592 [MHz]
Irr_offset = 51 [ppm]
Irr_domain = 1H
Irr_freq = 300.52966592 [MHz]
Irr_offset = 51 [ppm]
Mod_return = 1
PULSE =
Scaans = 38
Total_scaas = 38
X_50_width = 13.01 [use]
X_50_time = 2.6071696 [s]
X_angle = 45 [deg]
X_etm = 4 [dB]
X_pulse = 6.505 [use]
Irr_mods = off
Hertz_preset = off
Phase = PULSE
Recovery = 44
Recovery_delay = 4 [s]
Relaxation_delay = 5 [s]
Repetition_time = 7.50717696 [s]
Temp_get = 22.6 [degC]
  
```







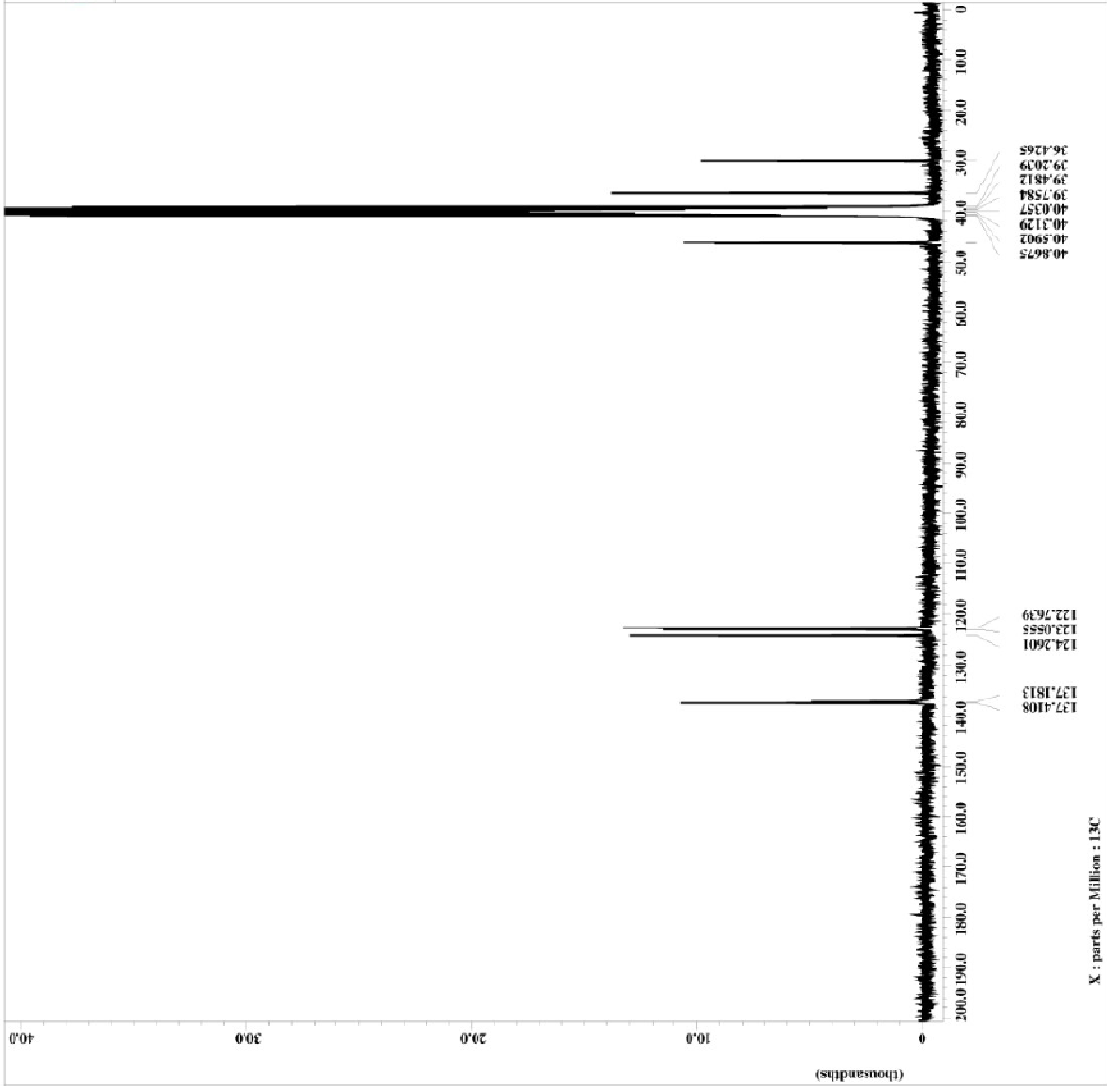
```

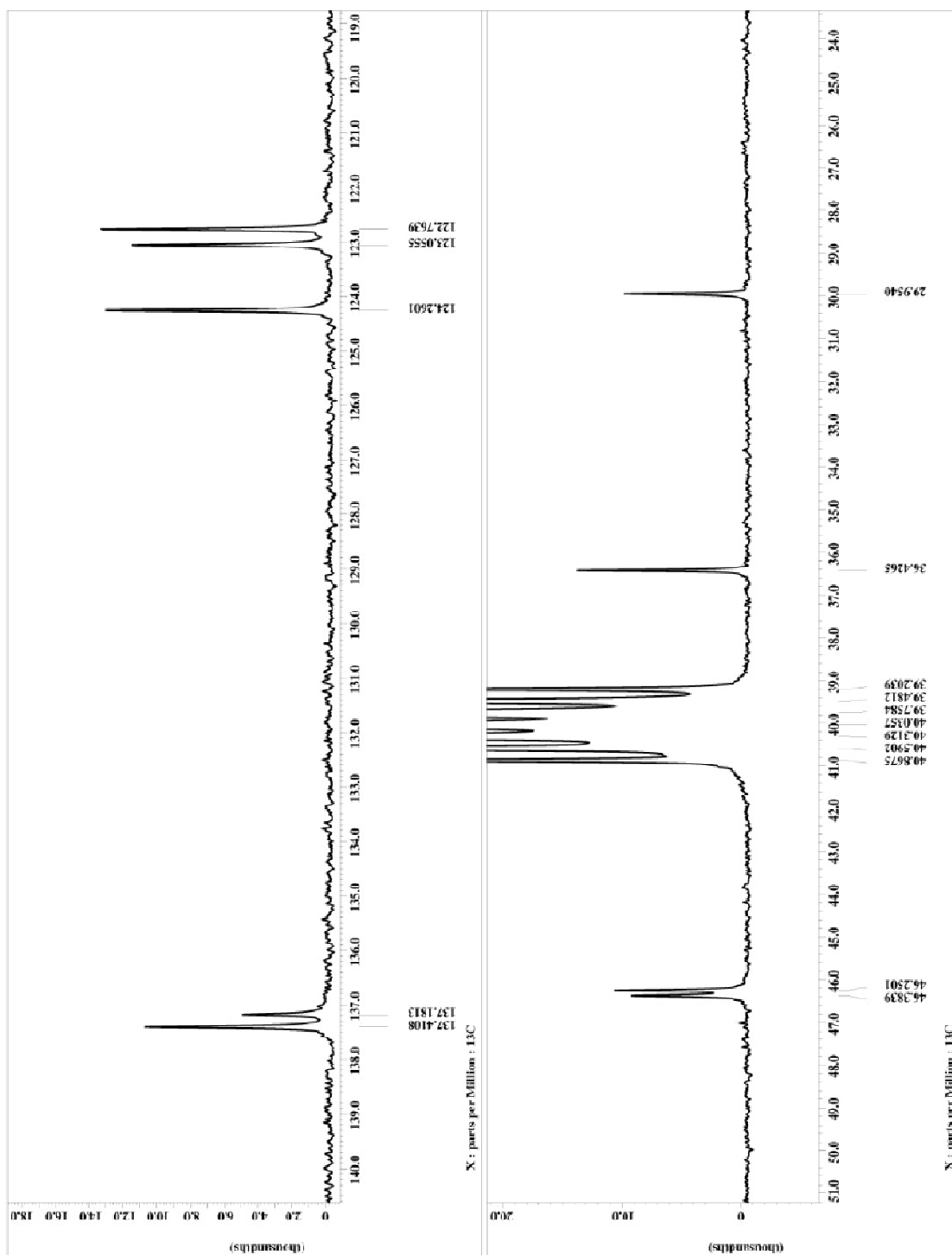
File Name = EW090808 (17CC3MeIm) -2
Author = delta
Experiment = single pulse dec
Sample ID = SP0902
Spectrometer = JEOL
Creation Time = 9-SEP-2008 10:11:04
Revision Time = 11-SEP-2008 21:00:46
Current Line = 12-SEP-2010 12:44:34

Comment = single pulse decouple
          = DELTA
          = 13C
          = [ppm]
          = X
          = EXX 300
          = DELTA2_30M

Spectrometer = DELTA2_30M
Field strength = 7.05860131(T) (300 [MHz]
X_acq_duration = 2.76824064 [s]
X_domain = 13C
X_freq = 75.56823426 [MHz]
X_offset = 100 [ppm]
X_points = 65536
X_resolution = 0.78124027 [Hz]
X_sweep = 23.6742424 [MHz]
Irr_domain = 1H
Irr_freq = 300.52365532 [MHz]
Irr_offset = 5 [ppm]
Clipped = FALSE
Noisefloor = 8317
Total_scans = 9317

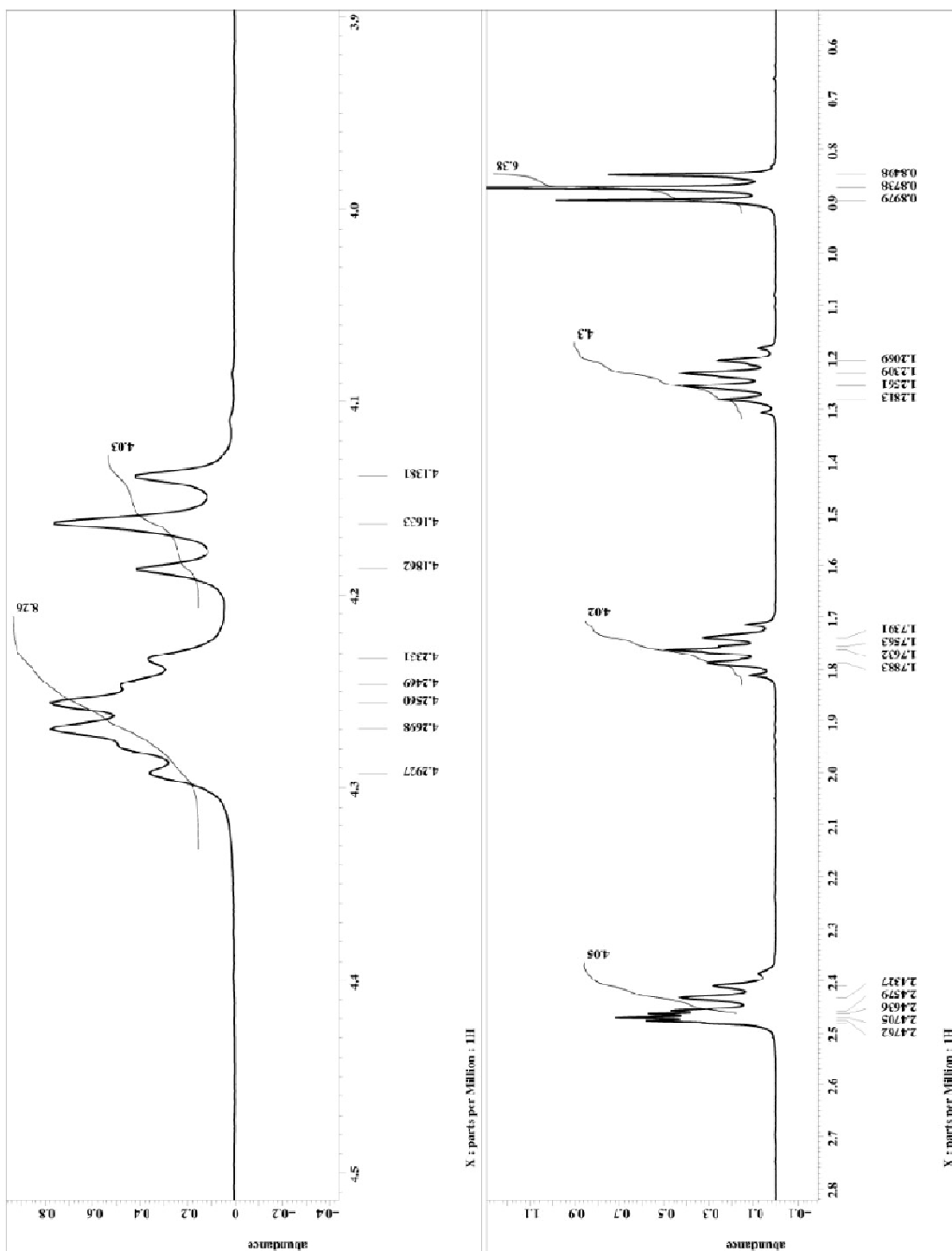
X_30_width = 9.75 [us]
X_acq_time = 2.76824064 [s]
X_angle = 30 [deg]
X_delay = 30 [us]
X_pulse = 3.25 [us]
Irr_atn_dec = 25 [dB]
Irr_atn_noe = 25 [dB]
Irr_noise = waltz
Decoupling = TRUE
Initial_wait = 7 [s]
Nox_time = 2 [s]
Recvr_gain = 50
Relaxation_delay = 2 [s]
Repetition_time = 4.76824064 [s]
Temp_yec = 22.5 [OC]
  
```

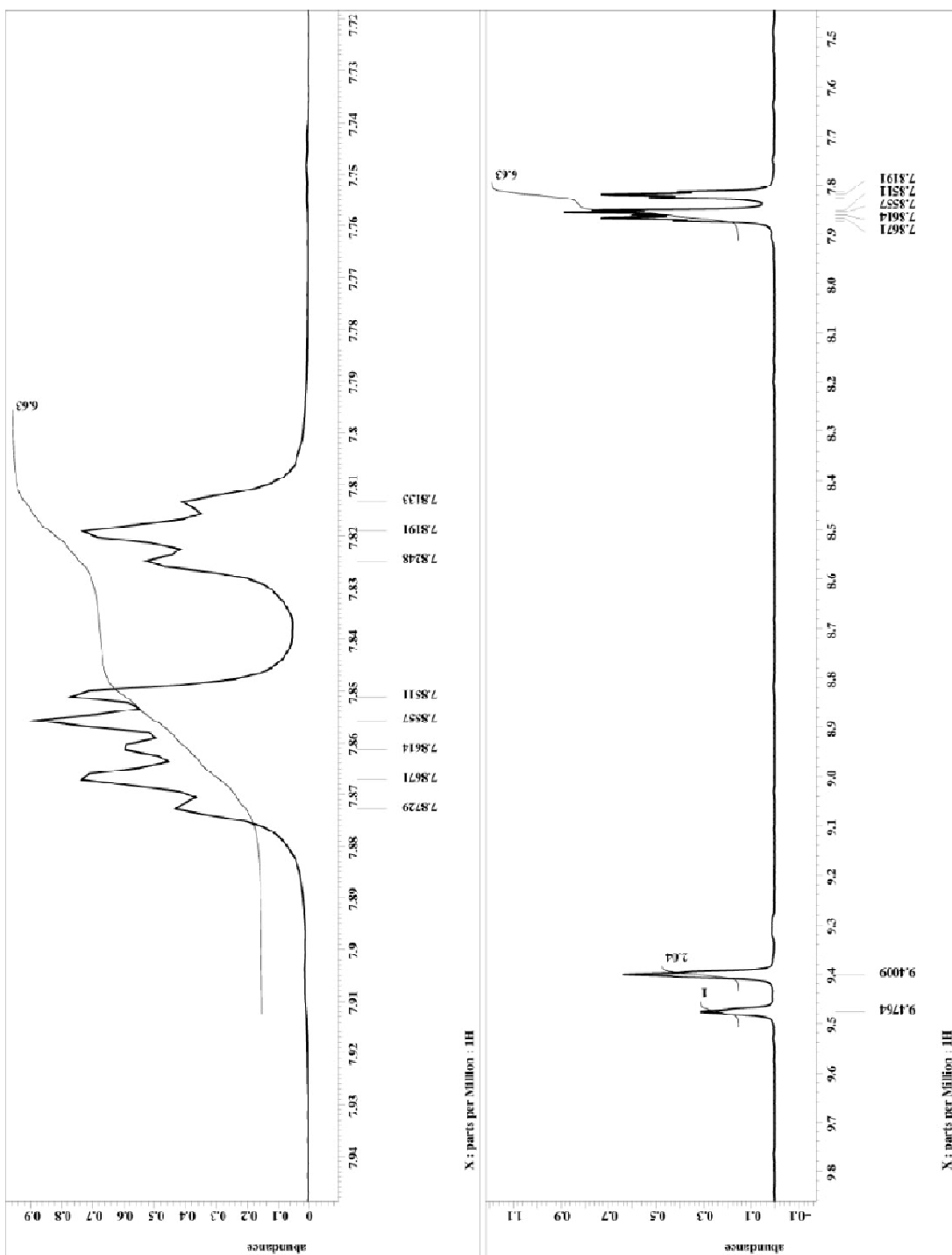




APPENDIX 13

¹H AND ¹³C NMR SPECTRA OF (1'-BUTYL-3'-PROPYLMIDAZOLIUM)-3-(1''-BUTYL-3''-PROPYLMIDAZOLIUM)IMIDAZOLIUM TRI [BIS(TRIFLUOROMETHANESULFONYL)IMIDE] (4b).







```

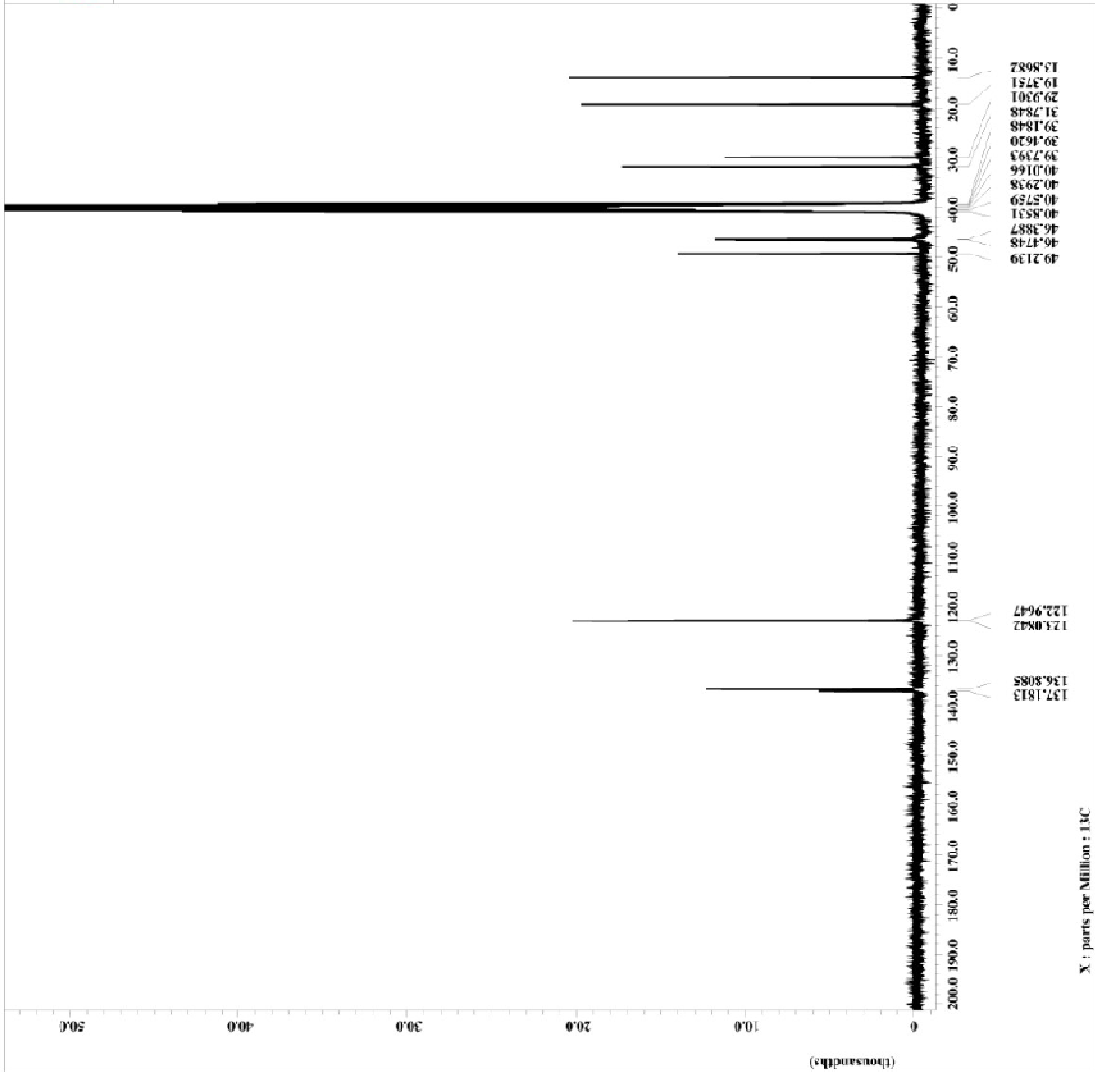
=====
File Name      = BK022808 (LTC038A10)-6
Aqker         = delta
Experiment    = single_pulse_dec
SAMP16_13    = SF75JZ1Z
Solvent       = DMSO-D6
Creation_time = 20-ACC-2008 10:12:47
Revision_time = 20-APR-2010 12:51:42
Current_date  = 12-SEP-2010 12:51:44

Comment       = single pulse decouple
Data_format   = ID COMPLEX
Dir_size      = 21428
Dir_path      = /ac
Dimensions    = X (ppm)
Site          = ECK 300
Spectrometer  = DELTA2_NMR

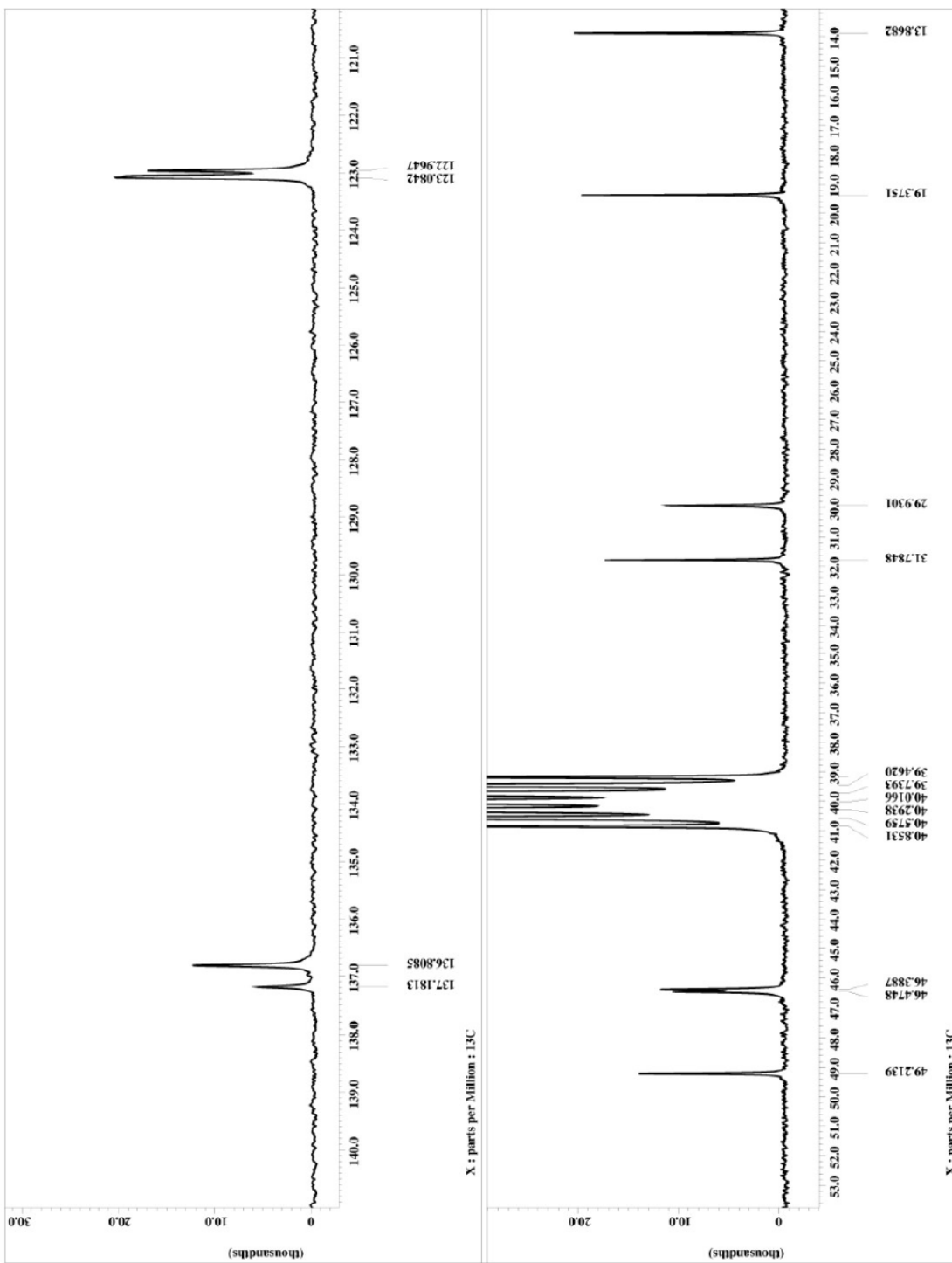
Field_strength = 7.556502317 (300 MHz)
X_acquisition = 15.362406418
X_freq         = 75.36823426 (MHz)
X_offset       = 100 [ppm]
X_points       = 65536
X_prescans    = 4
X_resolution   = 23.3742621 (Hz)
X_sweep        = 19.27426212 (kHz)
F1c_domain    = 1H
F1c_freq       = 300.52965592 (MHz)
F1c_offset     = 5 [ppm]
Clipped        = FALSE
Mod_retu      = 1
Scan          = 1
Total_scans   = 9500

X_90_width    = 9.75 (use)
X_acq_time    = 2.73024064 (s)
X_angle       = 30 (deg)
X_sts         = 9 [bits]
X_pulse       = 25 (use)
F1c_sfn_dec   = 25 (dB)
F1c_sfn_rec   = 25 (dB)
F1c_noise     = NALVZ
Decoupling    = PRDZ
Initial_wait  = 2 [s]
Pulse_prog    = 2 [s]
Nox_time      = 2 [s]
Repr_gain     = 56
Relaxation_delay = 2 [s]
Repetition_time = 4.73624064 (s)
Temp_get      = 23.7 (deg)
=====

```

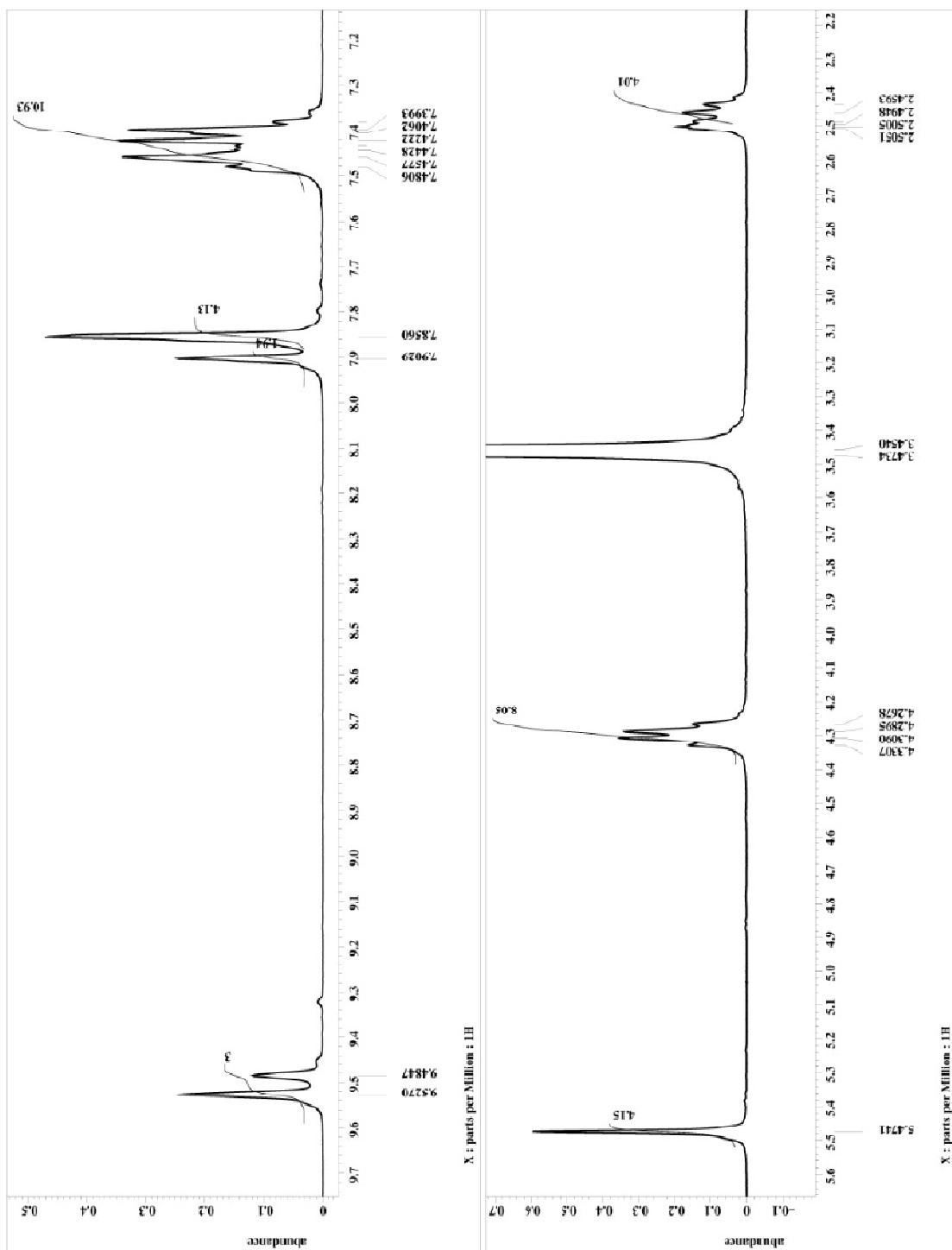


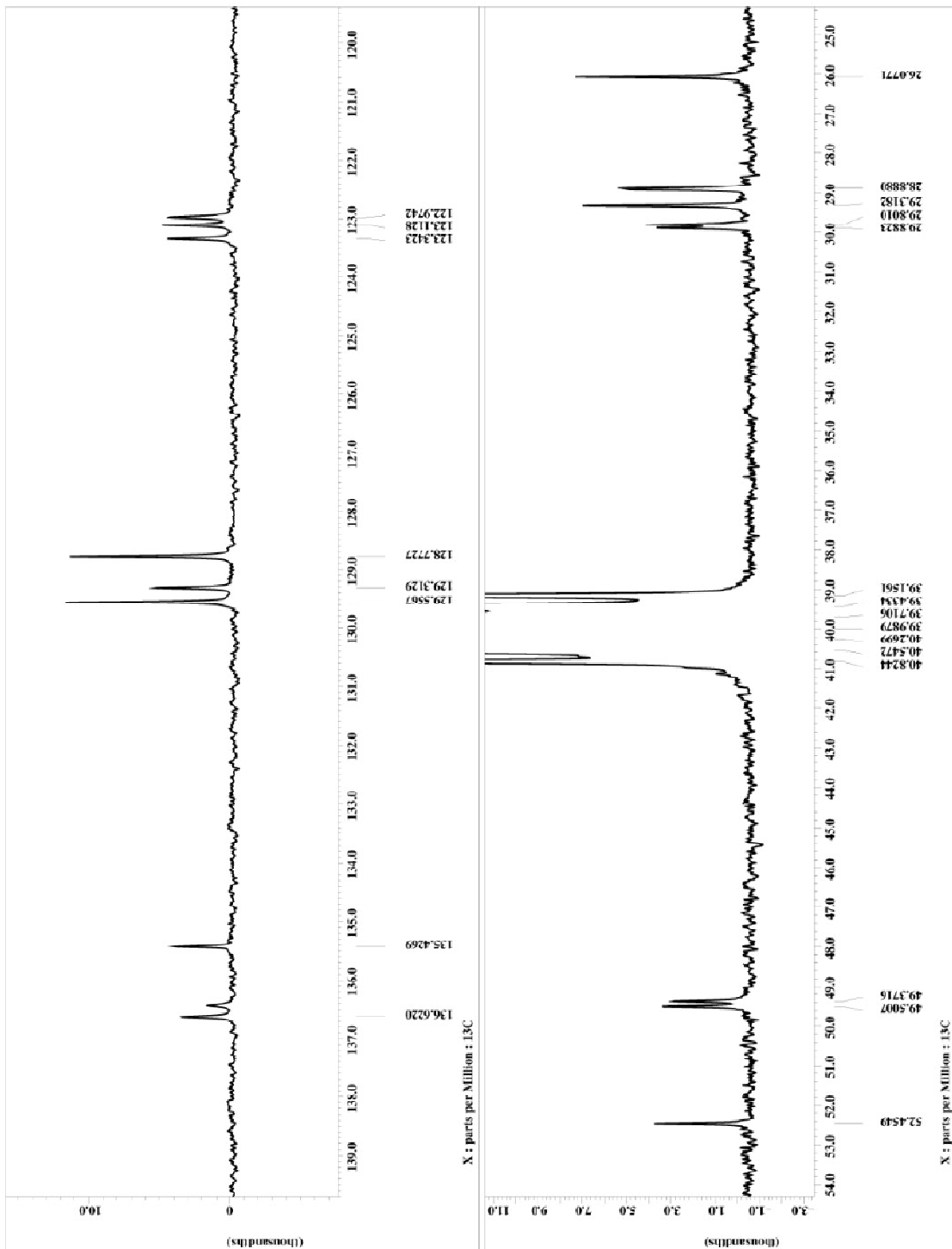
X : parts per Million : 1H



APPENDIX 14

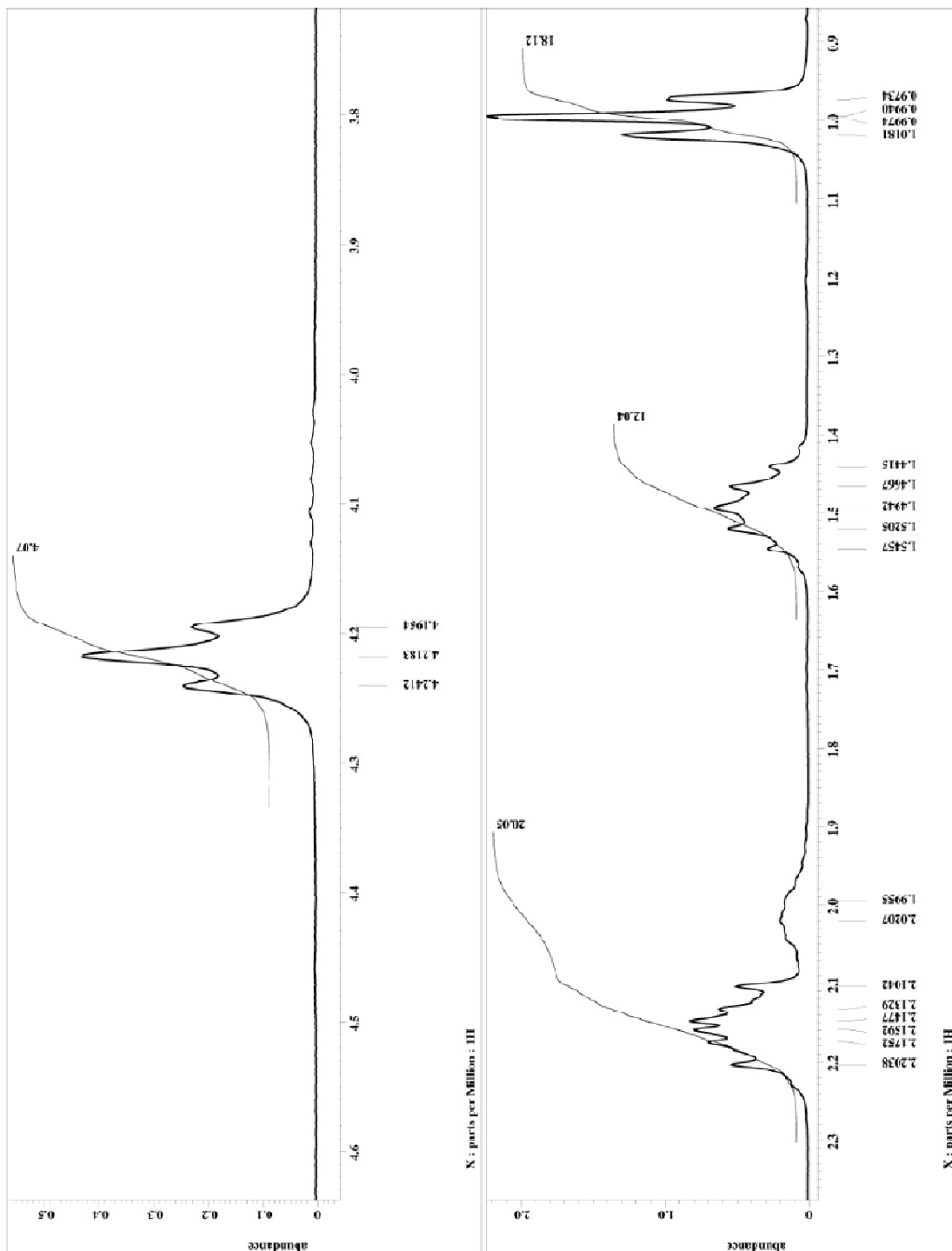
¹H AND ¹³C NMR SPECTRA OF (1'-BENZYL-3'-PROPYLMIDAZOLIUM)-3-(1''-BENZYL-3''-PROPYLMIDAZOLIUM)IMIDAZOLIUM TRI [BIS(TRIFLUOROMETHANESULFONYL)IMIDE]
(4c).





APPENDIX 15

^1H , ^{13}C AND ^{31}P NMR SPECTRA OF 1-PROPYLTRIPROPYLPHOSPHONIUM-3-
PROPYLTRIPROPYLPHOSPHONIUM IMIDAZOLIUM
TRI[BIS(TRIFLUOROMETHANESULFONYL)IMIDE] (4d)





```

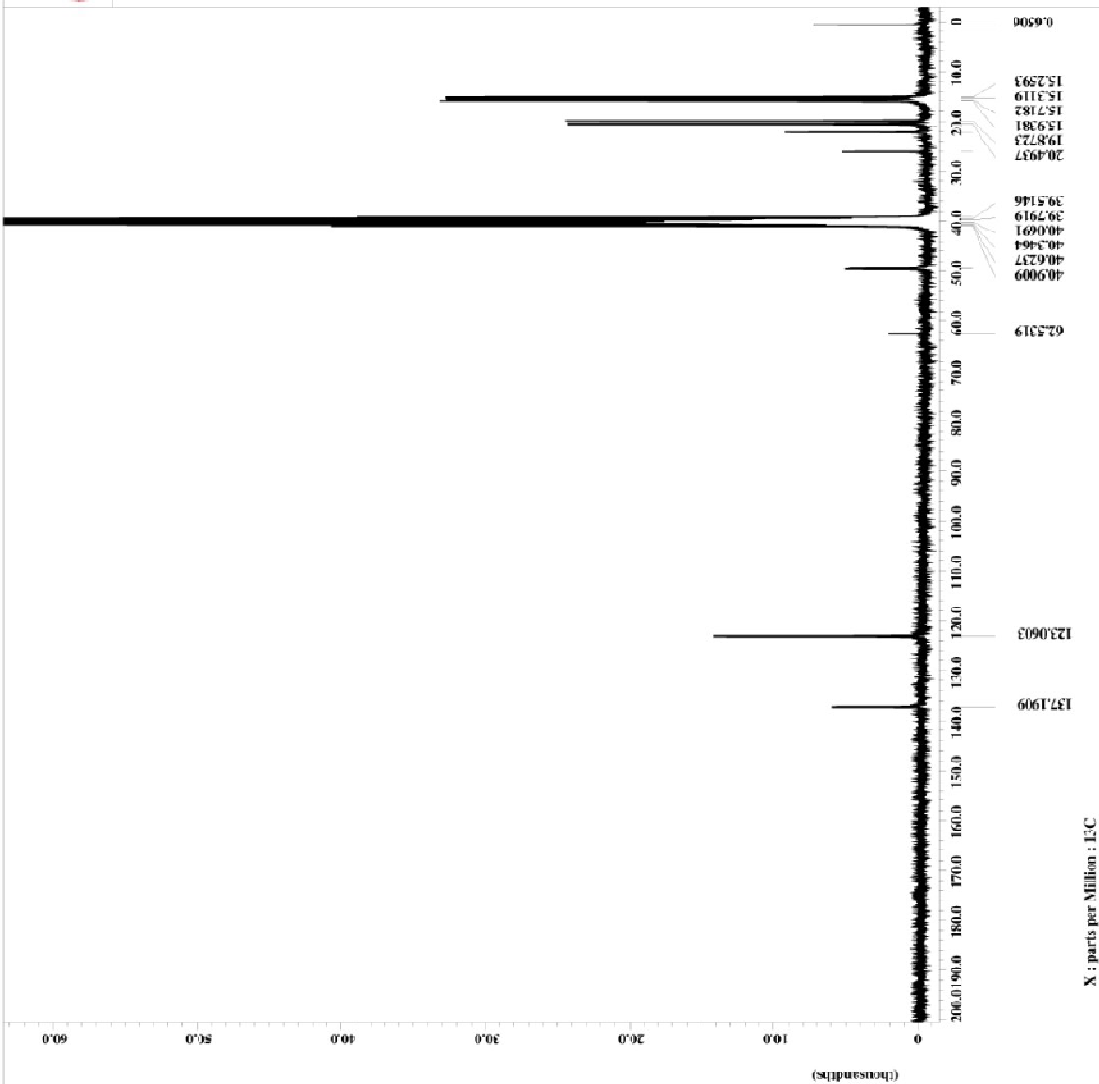
=====
Filmname      = EN033068 (LTCCTrIP) - 4
Author       = delta
Experiment   = single_pulse_dec
Sample_id    = SF771076
Solvent      = DMSO-d6
Acq_date     = 21-NOV-2008 10:10:55
Revision_time = 21-NOV-2008 12:38:37
Current_time = 12-SEP-2010 13:09:20

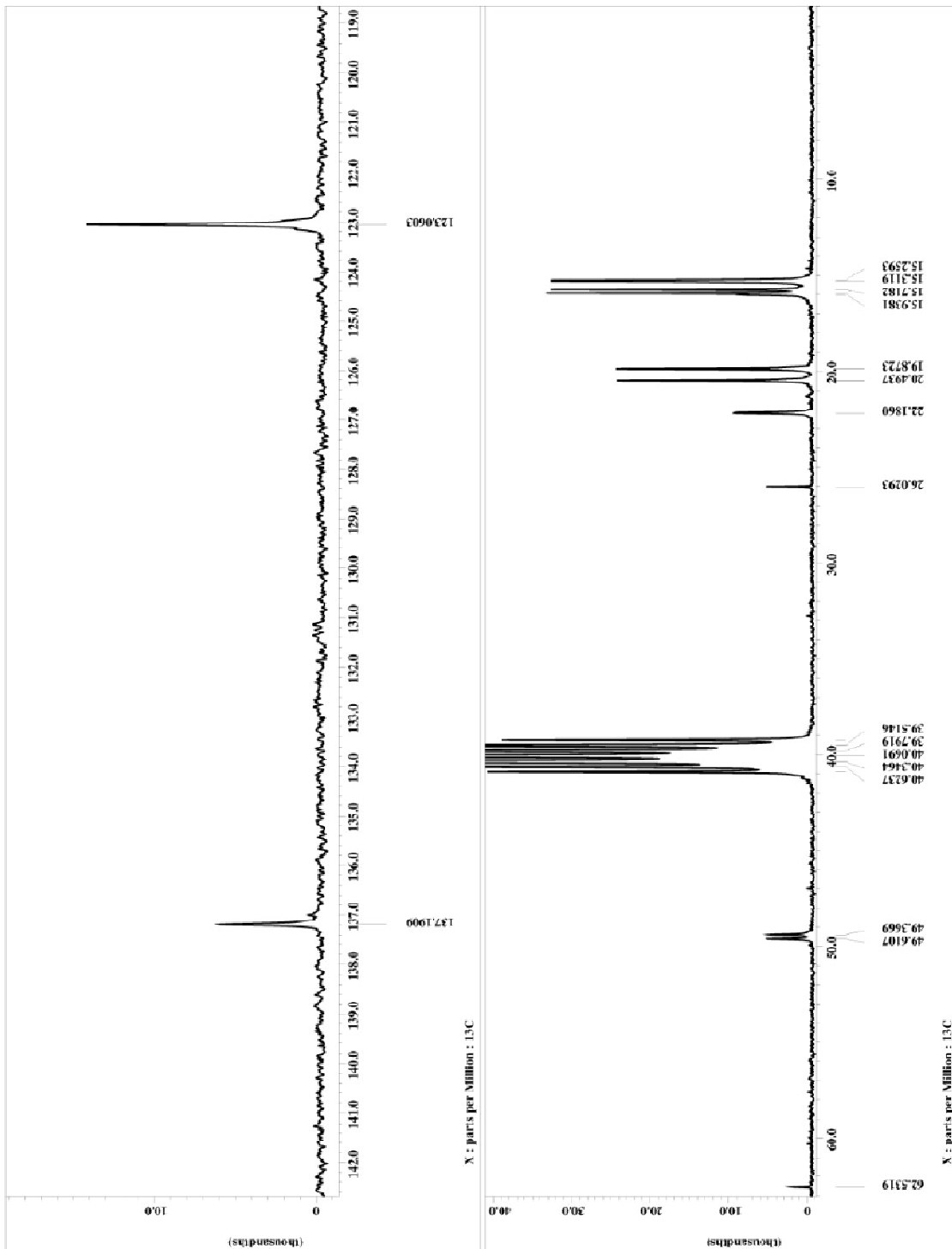
=====
Comment      = single pulse decouple
Data_format  = CD COMPLEX
Dim 1 size   = 628
Dim 2 size   = 130
Dim 1 units  = [ppm]
Dim 2 units  = [ppm]
Dimensions   = X
Site         = ECX 300
Spectrometer = DELTAZ_NMR

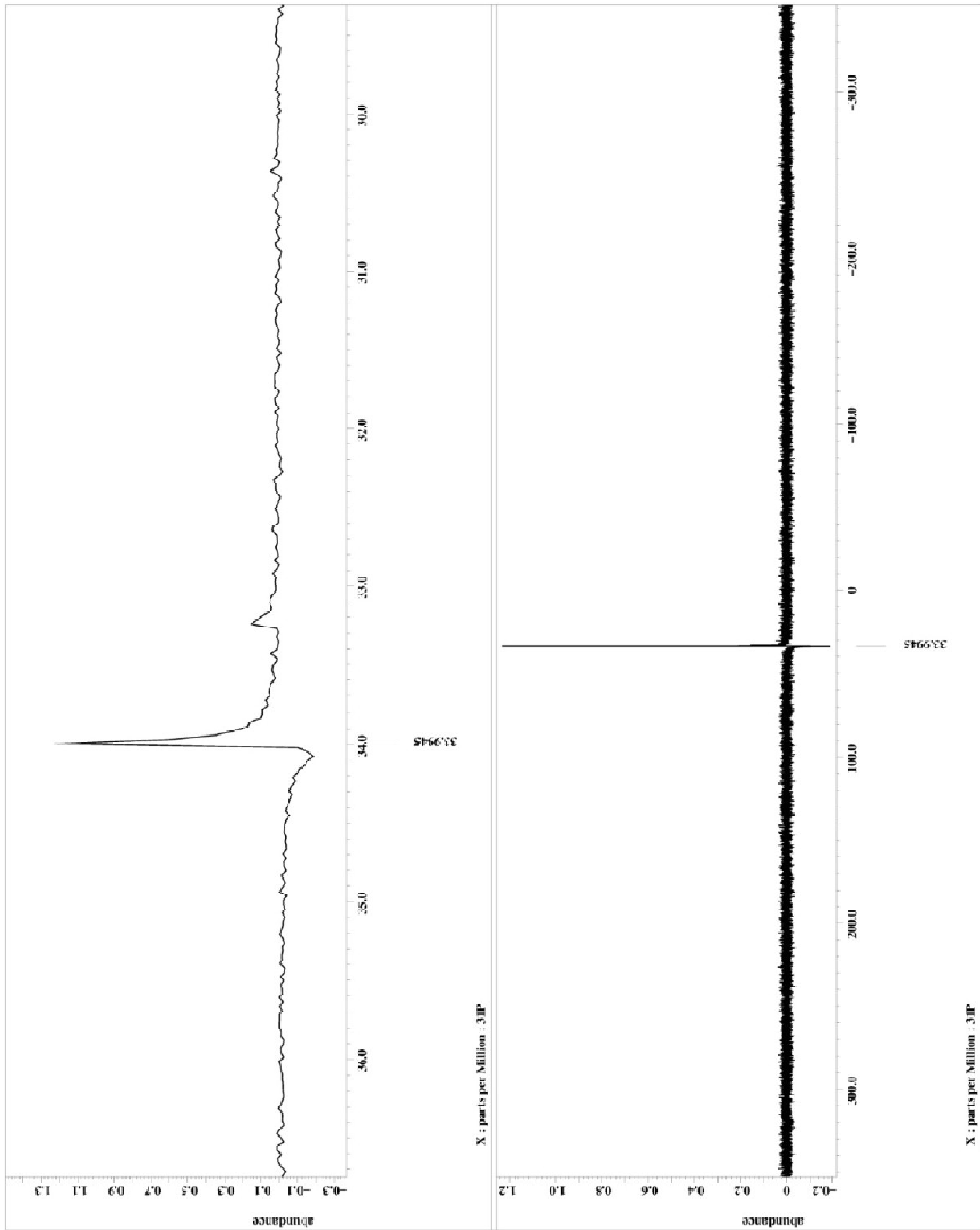
=====
Field strength = 7.059601371 (300) MHz
X axis offset   = -2.76824064 [s]
X domain        = 130
X freq          = 75.56823426 [MHz]
X offset        = 100 [ppm]
X points        = 65236
X prescan      = 0
X prescan time = 0.26124027 [Sec]
X resolution    = 23.67424242 [MHz]
X speed         = 1H
IRF domain     = 1H
IRF file       =
IRF offset     = 5 [ppm]
Clipped        = FALSE
Scan return    = 9500
Total scans    = 9500

=====
X 30 width     = 9.75 [us]
X acq time     = 2.76824064 [s]
X angle        = 30 [deg]
X delay        = 3.00 [us]
X pulse        = 3.25 [us]
IRF attn_dec   = 25 [dB]
IRF attn_pos   = 25 [dB]
IRF noise      = WAIT
Decoupling     = TRUC
Initial wait   = 15 [Sec]
NSG time       = 2 [s]
NSG gain       = 50
Relaxation_delay = 2 [s]
Repetition_time = 4.76824064 [s]
Temp_yec      = 23.2 [degC]
=====

```







REFERENCES

- (1) Drayer, D. E. Pharmacodynamic and pharmacokinetic differences between drug enantiomers in humans: an overview. *Clin. Pharmacol. Ther. (St. Louis)* **1986**, *40*, 125-133.
- (2) Ariens, E. J. Stereochemistry in the analysis of drug-action. Part II. *Med Res Rev* **1987**, *7*, 367-387.
- (3) Ariens, E. J. Implications of the neglect of stereochemistry in pharmacokinetics and clinical pharmacology. *Drug Intell Clin Pharm* **1987**, *21*, 827-829.
- (4) Anonymous FDA's policy statement for the development of new stereoisomeric drugs. *Chirality* **1992**, *4*, 338-340.
- (5) Schurig, V. Separation of enantiomers by gas chromatography. *J Chromatogr A* **2001**, *906*, 275-299.
- (6) Juvancz, Z.; Petersson, P. Enantioselective gas chromatography. *J. Microcolumn Sep.* **1996**, *8*, 99-114.
- (7) Koenig, W. A.; Hochmuth, D. H. Enantioselective gas chromatography in flavor and fragrance analysis: Strategies for the identification of known and unknown plant volatiles. *J. Chromatogr. Sci.* **2004**, *42*, 423-439.
- (8) Konig, W. A.; Fricke, C.; Saritas, Y.; Momeni, B.; Hohenfeld, G. Adulteration of natural variability? Enantioselective gas chromatography in purity control of essential oils. *J. High Resolut. Chromatogr.* **1997**, *20*, 55-61.
- (9) Welch, C. J.; Leonard, W. R., Jr.; DaSilva, J. O.; Biba, M.; Albaneze-Walker, J.; Henderson, D. W.; Laing, B.; Mathre, D. J. Preparative chiral SFC as a green technology for rapid access to enantiopurity in pharmaceutical process research. *LCGC North Am.* **2004**, *23*, 16,18,22,24,26-29.
- (10) Araujo, J. M. M.; Rodrigues, R. C. R.; Eusebio, M. F. J.; Mota, J. P. B. Chiral separation by two-column, semi-continuous, open-loop simulated moving-bed chromatography. *J. Chromatogr. , A* **2010**, *1217*, 5407-5419.
- (11) Gil-Av, E.; Feibush, B.; Charles-Sigler, R. Separation of enantiomers by gas liquid chromatography with an optically active stationary phase. *Tetrahedron Lett.* **1966**, 1009-1015.

- (12) Feibush, B. Interaction between asymmetric solutes and solvents. N-Lauroyl-L-valyl-tert-butylamide as stationary phase in gas-liquid partition chromatography. *J. Chem. Soc. D* **1971**, 544-545.
- (13) Frank, H.; Nicholson, G. J.; Bayer, E. Rapid gas chromatographic separation of amino acid enantiomers with a novel chiral stationary phase. *J Chromatogr Sci* **1977**, 15, 174-176.
- (14) Frank, H.; Nicholson, G. J.; Bayer, E. Gas chromatographic--mass spectrometric analysis of optically active metabolites and drugs on a novel chiral stationary phase. *J Chromatogr* **1978**, 146, 197-206.
- (15) Schurig, V. Enantiomer separation of a chiral olefin by complexation chromatography on an optically active rhodium(I) complex. *Angew. Chem.* **1977**, 89, 113-114.
- (16) Schurig, V.; Buerkle, W. Quantitative separation of enantiomers of trans-2,3-epoxybutane by complexation chromatography on an optically active nickel(II) complex. *Angew. Chem.* **1978**, 90, 132-133.
- (17) Schurig, V.; Koppenhoefer, B.; Buerkle, W. Correlation of the absolute configuration of chiral epoxides by complexation chromatography; synthesis and enantiomeric purity of (+)- and (-)-1,2-epoxypropane. *Angew. Chem.* **1978**, 90, 993-995.
- (18) Schurig, V. Chirodichroism of various enantiomeric compounds of a planar d8-metal complex. *Angew. Chem.* **1981**, 93, 806, 811.
- (19) Schurig, V.; Buerkle, W. Extending the scope of enantiomer resolution by complexation gas chromatography. *J. Am. Chem. Soc.* **1982**, 104, 7573-7580.
- (20) Schurig, V.; Schmalzing, D.; Schleimer, M. Enantiomer separation on immobilized Chirasil-Metal and Chirasil-Dex by gas chromatography and chromatography with above-critical gases. *Angew. Chem.* **1991**, 103, 994-6 (See also *Angew. Chem., Int. Ed. Engl.*, 1991, 30(8), 987-9).
- (21) Schleimer, M.; Schurig, V. Enantiomer separation by complexation gas and supercritical fluid chromatography on immobilized polysiloxane-bonded nickel(II) bis[(3-heptafluorobutanoyl)-10-methylene-(1R)camphorate] (Chirasil-nickel). *J. Chromatogr.* **1993**, 638, 85-96.
- (22) Schleimer, M.; Fluck, M.; Schurig, V. Enantiomer Separation by Capillary SFC and GC on Chirasil-Nickel: Observation of Unusual Peak Broadening Phenomena. *Anal. Chem.* **1994**, 66, 2893-2897.
- (23) He, L.; Beesley, T. E. Applications of enantiomeric gas chromatography: A review. *J. Liq. Chromatogr. Relat. Technol.* **2005**, 28, 1075-1114.
- (24) Koscielski, T.; Sybilska, D.; Jurczak, J. New chromatographic method for the determination of the enantiomeric purity of terpenic hydrocarbons. *J. Chromatogr.* **1986**, 364, 299-303.

- (25) Koenig, W. A.; Lutz, S.; Wenz, G. Modified cyclodextrin - a new highly enantioselective stationary phase for gas chromatography. *Angew. Chem.* **1988**, *100*, 989-990.
- (26) Schurig, V.; Nowotny, H. P. Separation of enantiomers on diluted permethylated β -cyclodextrin by high-resolution gas chromatography. *J. Chromatogr.* **1988**, *441*, 155-163.
- (27) Armstrong, D. W.; Li, W.; Chang, C. D.; Pitha, J. Polar-liquid, derivatized cyclodextrin stationary phases for the capillary gas chromatography separation of enantiomers. *Anal. Chem.* **1990**, *62*, 914-923.
- (28) Schurig, V.; Schmalzing, D.; Schleimer, M. Enantiomer separation on immobilized Chirasil-Metal and Chirasil-Dex by gas chromatography and chromatography with above-critical gases. *Angew. Chem.* **1991**, *103*, 994-6 (See also *Angew. Chem., Int. Ed. Engl.*, 1991, *30*(8), 987-9).
- (29) Armstrong, D. W.; Tang, Y.; Ward, T.; Nichols, M. Derivatized cyclodextrins immobilized on fused-silica capillaries for enantiomeric separations via capillary electrophoresis, gas chromatography, or supercritical fluid chromatography. *Anal. Chem.* **1993**, *65*, 1114-1117.
- (30) Tang, Y.; Zhou, Y.; Armstrong, D. W. Examination of the enantioselectivity of wall-immobilized cyclodextrin copolymers in capillary gas chromatography. *J. Chromatogr. , A* **1994**, *666*, 147-159.
- (31) Schurig, V.; Zhu, J.; Muschalek, V. Enantiomer separation on amylose tris(n-butylcarbamate) by gas chromatography. *Chromatographia* **1993**, *35*, 237-240.
- (32) Ding, J.; Welton, T.; Armstrong, D. W. Chiral ionic liquids as stationary phases in gas chromatography. *Anal. Chem.* **2004**, *76*, 6819-6822.
- (33) Zhang, Y.; Breitbach, Z. S.; Wang, C.; Armstrong, D. W. The use of cyclofructans as novel chiral selectors for gas chromatography. *Analyst* **2010**, *135*, 1076-1083.
- (34) Kasat, R. B.; Wang, N. L.; Franses, E. I. Effects of Backbone and Side Chain on the Molecular Environments of Chiral Cavities in Polysaccharide-Based Biopolymers. *Biomacromolecules* **2007**, *8*, 1676-1685.
- (35) Hesse, G.; Hagel, R. Complete separation of a racemic mixture by elution chromatography on cellulose triacetate. *Chromatographia* **1973**, *6*, 277-280.
- (36) Okamoto, Y.; Kawashima, M.; Hatada, K. Chromatographic resolution. 7. Useful chiral packing materials for high-performance liquid chromatographic resolution of enantiomers: phenylcarbamates of polysaccharides coated on silica gel. *J. Am. Chem. Soc.* **1984**, *106*, 5357-5359.
- (37) Ikai, T.; Yamamoto, C.; Kamigaito, M.; Okamoto, Y. Immobilized-type chiral packing materials for HPLC based on polysaccharide derivatives. *J. Chromatogr. , B: Anal. Technol. Biomed. Life Sci.* **2008**, *875*, 2-11.

- (38) Zhang, T.; Nguyen, D.; Franco, P.; Isobe, Y.; Michishita, T.; Murakami, T. Cellulose tris(3,5-dichlorophenylcarbamate) immobilised on silica: A novel chiral stationary phase for resolution of enantiomers. *J. Pharm. Biomed. Anal.* **2008**, *46*, 882-891.
- (39) Armstrong, D. W.; Tang, Y.; Chen, S.; Zhou, Y.; Bagwill, C.; Chen, J. Macrocyclic Antibiotics as a New Class of Chiral Selectors for Liquid Chromatography. *Anal. Chem.* **1994**, *66*, 1473-1484.
- (40) Armstrong, D. W.; Liu, Y.; Ekborgott, K. H. A covalently bonded teicoplanin chiral stationary phase for HPLC enantioseparations. *Chirality* **1995**, *7*, 474-497.
- (41) Ekborg-Ott, K.; Liu, Y.; Armstrong, D. W. Highly enantioselective HPLC separations using the covalently bonded macrocyclic antibiotic, ristocetin A, chiral stationary phase. *Chirality* **1998**, *10*, 434-483.
- (42) Ekborg-Ott, K. H.; Kullman, J. P.; Wang, X.; Gahm, K.; He, L.; Armstrong, D. W. Evaluation of the macrocyclic antibiotic avoparcin as a new chiral selector for HPLC. *Chirality* **1998**, *10*, 627-660.
- (43) Peter, A.; Torok, G.; Armstrong, D. W.; Toth, G.; Tourwe, D. Effect of temperature on retention of enantiomers of β -methyl amino acids on a teicoplanin chiral stationary phase. *J. Chromatogr. , A* **1998**, *828*, 177-190.
- (44) Berthod, A.; Chen, X.; Kullman, J. P.; Armstrong, D. W.; Gasparrini, F.; D'Acquarica, I.; Villani, C.; Carotti, A. Role of the Carbohydrate Moieties in Chiral Recognition on Teicoplanin-Based LC Stationary Phases. *Anal. Chem.* **2000**, *72*, 1767-1780.
- (45) Anonymous In *Chirobiotic handbook*; Advanced Separation Technology Inc: Whippany, NJ, 2004; .
- (46) Berthod, A.; Liu, Y.; Bagwill, C.; Armstrong, D. W. Facile liquid chromatographic enantioresolution of native amino acids and peptides using a teicoplanin chiral stationary phase. *J Chromatogr A* **1996**, *731*, 123-137.
- (47) Armstrong, D. W.; DeMond, W. Cyclodextrin bonded phases for the liquid chromatographic separation of optical, geometrical, and structural isomers. *J. Chromatogr. Sci.* **1984**, *22*, 411-415.
- (48) Hermansson, J. Direct liquid chromatographic resolution of racemic drugs using α 1-acid glycoprotein as the chiral stationary phase. *J. Chromatogr.* **1983**, *269*, 71-80.
- (49) Yamaguchi, T. Liquid membrane, sensor, and column chromatography based on chiral crown ethers. *Kagaku to Kogyo (Tokyo)* **1989**, *42*, 255-259. (Abstract)
- (50) Pirkle, W. H.; Brice, L. J.; Terfloth, G. J. Liquid and subcritical CO₂ separations of enantiomers on a broadly applicable polysiloxane chiral stationary phase. *J. Chromatogr. , A* **1996**, *753*, 109-119.

- (51) Sun, P.; Wang, C.; Breitbach, Z. S.; Zhang, Y.; Armstrong, D. W. Development of new HPLC chiral stationary phases based on native and derivatized cyclofructans. *Anal. Chem.* **2009**, *81*, 10215-10226.
- (52) Sun, P.; Wang, C.; Padivitage, N. L. T.; Nanayakkara, Y. S.; Perera, S.; Qiu, H.; Zhang, Y.; Armstrong, D. W. Evaluation of aromatic-derivatized cyclofructans 6 and 7 as HPLC chiral selectors. *Analyst* **2011**, *136*, 787-800.
- (53) Armstrong, D. W.; Tang, Y.; Chen, S.; Zhou, Y.; Bagwill, C.; Chen, J. Macrocyclic Antibiotics as a New Class of Chiral Selectors for Liquid Chromatography. *Anal. Chem.* **1994**, *66*, 1473-1484.
- (54) Armstrong, D. W.; Rundlett, K.; Reid, G. L., III Use of a Macrocyclic Antibiotic, Rifamycin B, and Indirect Detection for the Resolution of Racemic Amino Alcohols by CE. *Anal. Chem.* **1994**, *66*, 1690-1695.
- (55) Rundlett, K. L.; Armstrong, D. W. Effect of Micelles and Mixed Micelles on Efficiency and Selectivity of Antibiotic-Based Capillary Electrophoretic Enantioseparations. *Anal. Chem.* **1995**, *67*, 2088-2095.
- (56) Armstrong, D. W.; Liu, Y.; Ekborgott, K. H. A covalently bonded teicoplanin chiral stationary phase for HPLC enantioseparations. *Chirality* **1995**, *7*, 474-497.
- (57) Berthod, A.; Liu, Y.; Bagwill, C.; Armstrong, D. W. Facile LC enantioresolution of native amino acids and peptides using a teicoplanin chiral stationary phase. *J. Chromatogr. , A* **1996**, *731*, 123-137.
- (58) D'Acquarica, I.; Gasparrini, F.; Misiti, D.; Villani, C.; Carotti, A.; Cellamare, S.; Muck, S. Direct chromatographic resolution of carnitine and O-acylcarnitine enantiomers on a teicoplanin-bonded chiral stationary phase. *J. Chromatogr. , A* **1999**, *857*, 145-155.
- (59) Armstrong, D. W.; Gasper, M. P.; Rundlett, K. L. Highly enantioselective capillary electrophoretic separations with dilute solutions of the macrocyclic antibiotic ristocetin A. *J. Chromatogr. , A* **1995**, *689*, 285-304.
- (60) Cancelliere, G.; D'Acquarica, I.; Gasparrini, F.; Misiti, D.; Villani, C. Synthesis and applications of novel, highly efficient HPLC chiral stationary phases: a chiral dimension in drug research analysis. *Pharm. Sci. Technol. Today* **1999**, *2*, 484-492.
- (61) Reilly, J.; Risley, D. S. The separation of enantiomers by counter current capillary electrophoresis using the macrocyclic antibiotic A82846B. *Lc-Gc* **1998**, *16*, 170, 172, 174, 176, 178.
- (62) Sharp, V. S.; Risley, D. S.; McCarthy, S.; Huff, B. E.; Strege, M. A. Evaluation of a new macrocyclic antibiotic as a chiral selector for use in capillary electrophoresis. *J. Liq. Chromatogr. Relat. Technol.* **1997**, *20*, 887-898.

- (63) Ekborg-Ott, K. H.; Kullman, J. P.; Wang, X.; Gahm, K.; He, L.; Armstrong, D. W. Evaluation of the macrocyclic antibiotic avoparcin as a new chiral selector for HPLC. *Chirality* **1998**, *10*, 627-660.
- (64) Berthod, A.; Yu, T.; Kullman, J. P.; Armstrong, D. W.; Gasparrini, F.; D'Acquarica, I.; Misiti, D.; Carotti, A. Evaluation of the macrocyclic glycopeptide A-40,926 as a high-performance liquid chromatographic chiral selector and comparison with teicoplanin chiral stationary phase. *J. Chromatogr. , A* **2000**, *897*, 113-129.
- (65) Berthod, A. Chiral recognition mechanisms with macrocyclic glycopeptide selectors. *Chirality* **2008**, *21*, 167-175.
- (66) Berthod, A.; Chen, X.; Kullman, J. P.; Armstrong, D. W.; Gasparrini, F.; D'Acquarica, I.; Villani, C.; Carotti, A. Role of the Carbohydrate Moieties in Chiral Recognition on Teicoplanin-Based LC Stationary Phases. *Anal. Chem.* **2000**, *72*, 1767-1780.
- (67) Guay, D. R. Dalbavancin: an investigational glycopeptide. *Expert Rev. Anti-Infect. Ther.* **2004**, *2*, 845-852.
- (68) Anderson, V. R.; Keating, G. M. Dalbavancin. *Drugs* **2008**, *68*, 639-648.
- (69) Berthod, A.; Chen, X.; Kullman, J. P.; Armstrong, D. W.; Gasparrini, F.; D'Acquarica, I.; Villani, C.; Carotti, A. Role of the carbohydrate moieties in chiral recognition on teicoplanin-based LC stationary phases. *Anal Chem* **2000**, *72*, 1767-1780.
- (70) Berthod, A.; Chang, C. D.; Armstrong, D. W. β -Cyclodextrin chiral stationary phases for liquid chromatography. Effect of the spacer arm on chiral recognition. *Talanta* **1993**, *40*, 1367-1373.
- (71) Franco, P.; Lammerhofer, M.; Klaus, P. M.; Lindner, W. Novel cinchona alkaloid carbamate C9-dimers as chiral anion-exchange type selectors for high-performance liquid chromatography. *J. Chromatogr. , A* **2000**, *869*, 111-127.
- (72) Hyun, M. H.; Kim, D. H. Spacer length effect of a chiral stationary phase based on (+)-(18-crown-6)-2,3,11,12-tetracarboxylic acid. *Chirality* **2004**, *16*, 294-301.
- (73) Thunberg, L.; Allenmark, S.; Friberg, A.; Ek, F.; Frejd, T. Evaluation of two pairs of chiral stationary phases: Effects from the length of the achiral spacers. *Chirality* **2004**, *16*, 614-624.
- (74) Zhong, Q.; He, L.; Beesley, T. E.; Trahanovsky, W. S.; Sun, P.; Wang, C.; Armstrong, D. W. Optimization of the synthesis of 2,6-dinitro-4-trifluoromethylphenyl ether substituted cyclodextrin bonded chiral stationary phases. *Chromatographia* **2006**, *64*, 147-155.
- (75) Krossing, I.; Slattery, J. M.; Daguinet, C.; Dyson, P. J.; Oleinikova, A.; Weingartner, H. Why are ionic liquids liquid? A simple explanation based on lattice and solvation energies. *J. Am. Chem. Soc.* **2006**, *128*, 13427-13434.

- (76) Walden, P. Molecular weights and electrical conductivity of several fused salts. *Bull. Acad. Imp. Sci. St. -Petersbourg* **1914**, 405-422. (abstract)
- (77) Wilkes, J. S.; Zaworotko, M. J. Air and water stable 1-ethyl-3-methylimidazolium based ionic liquids. *J. Chem. Soc., Chem. Commun.* **1992**, 965-967.
- (78) Suarez, P. A. Z.; Dullius, J. E. L.; Einloft, S.; De Souza, R. F.; Dupont, J. The use of new ionic liquids in two-phase catalytic hydrogenation reaction by rhodium complexes. *Polyhedron* **1996**, *15*, 1217-1219.
- (79) Dyson, P. J. Synthesis of organometallics and catalytic hydrogenations in ionic liquids. *Appl. Organomet. Chem.* **2002**, *16*, 495-500.
- (80) Ding, J.; Armstrong, D. W. Chiral ionic liquids. Synthesis and applications. *Chirality* **2005**, *17*, 281-292.
- (81) Huddleston, J. G.; Rogers, R. D. Room temperature ionic liquids as novel media for 'clean' liquid-liquid extraction. *Chem. Commun. (Cambridge)* **1998**, 1765-1766.
- (82) Liu, R.; Liu, J.; Yin, Y.; Hu, X.; Jiang, G. Ionic liquids in sample preparation. *Anal. Bioanal. Chem.* **2009**, *393*, 871-883.
- (83) Aguilera-Herrador, E.; Lucena, R.; Cardenas, S.; Valcarcel, M. The roles of ionic liquids in sorptive microextraction techniques. *TrAC, Trends Anal. Chem.* **2010**, *29*, 602-616.
- (84) Anderson, J. L.; Armstrong, D. W. Immobilized ionic liquids as high-selectivity/high-temperature/high-stability gas chromatography stationary phases. *Anal. Chem.* **2005**, *77*, 6453-6462.
- (85) Huang, K.; Han, X.; Zhang, X.; Armstrong, D. W. PEG-linked geminal dicationic ionic liquids as selective, high-stability gas chromatographic stationary phases. *Anal. Bioanal. Chem.* **2007**, *389*, 2265-2275.
- (86) Breitbach, Z. S.; Armstrong, D. W. Characterization of phosphonium ionic liquids through a linear solvation energy relationship and their use as GLC stationary phases. *Anal. Bioanal. Chem.* **2008**, *390*, 1605-1617.
- (87) Shetty, P. H.; Youngberg, P. J.; Kersten, B. R.; Poole, C. F. Solvent properties of liquid organic salts used as mobile phases in microcolumn reversed-phase liquid chromatography. *J. Chromatogr.* **1987**, *411*, 61-79.
- (88) Waichigo, M. M.; Hunter, B. M.; Riechel, T. L.; Danielson, N. D. Alkylammonium formate ionic liquids as organic mobile phase replacements for reversed-phase liquid chromatography. *J. Liq. Chromatogr. Relat. Technol.* **2007**, *30*, 165-184.
- (89) Qiu, H.; Jiang, S.; Liu, X. N-Methylimidazolium anion-exchange stationary phase for high-performance liquid chromatography. *J. Chromatogr., A* **2006**, *1103*, 265-270.

- (90) Soukup-Hein, R. J.; Remsburg, J. W.; Dasgupta, P. K.; Armstrong, D. W. A General, Positive Ion Mode ESI-MS Approach for the Analysis of Singly Charged Inorganic and Organic Anions Using a Dicationic Reagent. *Anal. Chem.* **2007**, *79*, 7346-7352.
- (91) Berthod, A.; Crank, J. A.; Rundlett, K. L.; Armstrong, D. W. A second-generation ionic liquid matrix-assisted laser desorption/ionization matrix for effective mass spectrometric analysis of biodegradable polymers. *Rapid Commun. Mass Spectrom.* **2009**, *23*, 3409-3422.
- (92) Mank, M.; Stahl, B.; Boehm, G. 2,5-Dihydroxybenzoic acid butylamine and other ionic liquid matrixes for enhanced MALDI-MS analysis of biomolecules. *Anal. Chem.* **2004**, *76*, 2938-2950.
- (93) Hebert, G. N.; Odom, M. A.; Craig, P. S.; Dick, D. L.; Strauss, S. H. Method for the determination of sub-ppm concentrations of perfluoroalkylsulfonate anions in water. *J. Environ. Monit.* **2002**, *4*, 90-95.
- (94) Magnuson, M. L.; Urbansky, E. T.; Kelty, C. A. Microscale extraction of perchlorate in drinking water with low level detection by electrospray-mass spectrometry. *Talanta* **2000**, *52*, 285-291.
- (95) Hansen, K. J.; Johnson, H. O.; Eldridge, J. S.; Butenhoff, J. L.; Dick, L. A. Quantitative characterization of trace levels of PFOS and PFOA in the Tennessee River. *Environ Sci Technol* **2002**, *36*, 1681-1685.
- (96) Cahill, T. M.; Benesch, J. A.; Gustin, M. S.; Zimmerman, E. J.; Seiber, J. N. Simplified method for trace analysis of trifluoroacetic acid in plant, soil, and water samples using headspace gas chromatography. *Anal. Chem.* **1999**, *71*, 4465-4471.
- (97) Ghanem, A.; Bados, P.; Kerhoas, L.; Dubroca, J.; Einhorn, J. Glyphosate and AMPA Analysis in Sewage Sludge by LC-ESI-MS/MS after FMOC Derivatization on Strong Anion-Exchange Resin as Solid Support. *Anal. Chem.* **2007**, *79*, 3794-3801.
- (98) Wujcik, C. E.; Cahill, T. M.; Seiber, J. N. Extraction and Analysis of Trifluoroacetic Acid in Environmental Waters. *Anal. Chem.* **1998**, *70*, 4074-4080.
- (99) Martinelango, P. K.; Anderson, J. L.; Dasgupta, P. K.; Armstrong, D. W.; Al-Horr, R. S.; Slingsby, R. W. Gas-Phase Ion Association Provides Increased Selectivity and Sensitivity for Measuring Perchlorate by Mass Spectrometry. *Anal. Chem.* **2005**, *77*, 4829-4835.
- (100) Martinelango, P. K.; Guemues, G.; Dasgupta, P. K. Matrix interference free determination of perchlorate in urine by ion association-ion chromatography-mass spectrometry. *Anal. Chim. Acta* **2006**, *567*, 79-86.
- (101) Martinelango, P. K.; Tian, K.; Dasgupta, P. K. Perchlorate in seawater. *Anal. Chim. Acta* **2006**, *567*, 100-107.

- (102) Barron, L.; Paull, B. Simultaneous determination of trace oxyhalides and haloacetic acids using suppressed ion chromatography-electrospray mass spectrometry. *Talanta* **2006**, *69*, 621-630.
- (103) Wuilloud, R. G.; Altamirano, J. C.; Smichowski, P. N.; Heitkemper, D. T. Investigation of arsenic speciation in algae of the Antarctic region by HPLC-ICP-MS and HPLC-ESI-Ion Trap MS. *J. Anal. At. Spectrom.* **2006**, *21*, 1214-1223.
- (104) Tsikas, D. Mass spectrometry-validated HPLC method for urinary nitrate. *Clin. Chem.* **2004**, *50*, 1259-1261.
- (105) Blount, B. C.; Valentin-Blasini, L. Analysis of perchlorate, thiocyanate, nitrate and iodide in human amniotic fluid using ion chromatography and electrospray tandem mass spectrometry. *Anal. Chim. Acta* **2006**, *567*, 87-93.
- (106) Olsen, G. W.; Hansen, K. J.; Stevenson, L. A.; Burris, J. M.; Mandel, J. H. Human Donor Liver and Serum Concentrations of Perfluorooctanesulfonate and Other Perfluorochemicals. *Environ. Sci. Technol.* **2003**, *37*, 888-891.
- (107) Dyke, J. V.; Kirk, A. B.; Kalyani Martinelango, P.; Dasgupta, P. K. Sample processing method for the determination of perchlorate in milk. *Anal. Chim. Acta* **2006**, *567*, 73-78.
- (108) Elkins, E. R.; Heuser, J. R. Detection of adulteration in apple juice by L-malic/total malic acid ratio: collaborative study. *J. AOAC Int.* **1994**, *77*, 411-415.
- (109) El Aribi, H.; Le Blanc, Y. J. C.; Antonsen, S.; Sakuma, T. Analysis of perchlorate in foods and beverages by ion chromatography coupled with tandem mass spectrometry (IC-ESI-MS/MS). *Anal. Chim. Acta* **2006**, *567*, 39-47.
- (110) Guo, Z.; Cai, Q.; Yu, C.; Yang, Z. Determination of bromate and bromoacetic acids in water by ion chromatography-inductively coupled plasma mass spectrometry. *J. Anal. At. Spectrom.* **2003**, *18*, 1396-1399.
- (111) Dudoit, A.; Pergantis, S. A. Ion chromatography in series with conductivity detection and inductively coupled plasma-mass spectrometry for the determination of nine halogen, metalloid and non-metal species in drinking water. *J. Anal. At. Spectrom.* **2001**, *16*, 575-580.
- (112) van Staden, J. F.; Tlowana, S. I. Spectrophotometric determination of chloride in mineral and drinking waters using sequential injection analysis. *Fresenius' J. Anal. Chem.* **2001**, *371*, 396-399.
- (113) Yamashita, N.; Kannan, K.; Taniyasu, S.; Horii, Y.; Okazawa, T.; Petrick, G.; Gamo, T. Analysis of Perfluorinated Acids at Parts-Per-Quadrillion Levels in Seawater Using Liquid Chromatography-Tandem Mass Spectrometry. *Environ. Sci. Technol.* **2004**, *38*, 5522-5528.

- (114) Salov, V. V.; Yoshinaga, J.; Shibata, Y.; Morita, M. Determination of inorganic halogen species by liquid chromatography with inductively coupled argon plasma mass spectrometry. *Anal Chem* **1992**, *64*, 2425-2428.
- (115) Ahrer, W.; Buchberger, W. Analysis of low-molecular-mass inorganic and organic anions by ion chromatography-atmospheric pressure ionization mass spectrometry. *J. Chromatogr. , A* **1999**, *854*, 275-287.
- (116) Nischwitz, V.; Pergantis, S. A. Optimization of an HPLC selected reaction monitoring electrospray tandem mass spectrometry method for the detection of 50 arsenic species. *J. Anal. At. Spectrom.* **2006**, *21*, 1277-1286.
- (117) Kappes, T.; Schnierle, P.; C. Hauser, P. Potentiometric detection of inorganic anions and cations in capillary electrophoresis with coated-wire ion-selective electrodes. *Anal. Chim. Acta* **1997**, *350*, 141-147.
- (118) Isildak, I.; Asan, A. Simultaneous detection of monovalent anions and cations using all solid-state contact PVC membrane anion and cation-selective electrodes as detectors in single column ion chromatography. *Talanta* **1999**, *48*, 967-978.
- (119) Isildak, I. Potentiometric detection of monovalent anions separated by ion chromatography using all solid-state contact PVC matrix membrane electrode. *Chromatographia* **1999**, *49*, 338-342.
- (120) Chakraborty, D.; Das, A. K. Indirect determination of iodate by atomic-absorption spectrophotometry. *Talanta* **1989**, *36*, 669-671.
- (121) Buchberger, W. W. Detection techniques in ion analysis: what are our choices?. *J. Chromatogr. , A* **2000**, *884*, 3-22.
- (122) Cech, N. B.; Enke, C. G. Practical implications of some recent studies in electrospray ionization fundamentals. *Mass Spectrom Rev* **2001**, *20*, 362-387.
- (123) Henriksen, T.; Juhler, R. K.; Svensmark, B.; Cech, N. B. The relative influences of acidity and polarity on responsiveness of small organic molecules to analysis with negative ion electrospray ionization mass spectrometry (ESI-MS). *J. Am. Soc. Mass Spectrom.* **2005**, *16*, 446-455.
- (124) Straub, R. F.; Voyksner, R. D. Negative ion formation in electrospray mass spectrometry. *J. Am. Soc. Mass Spectrom.* **1993**, *4*, 578-587.
- (125) Cole, R. B.; Zhu, J. Chloride anion attachment in negative ion electrospray ionization mass spectrometry. *Rapid Commun. Mass Spectrom.* **1999**, *13*, 607-611.
- (126) Soukup-Hein, R. J.; Remsburg, J. W.; Dasgupta, P. K.; Armstrong, D. W. A General, Positive Ion Mode ESI-MS Approach for the Analysis of Singly Charged Inorganic and Organic Anions Using a Dicationic Reagent. *Anal. Chem.* **2007**, *79*, 7346-7352.

- (127) Remsburg, J. W.; Soukup-Hein, R. J.; Crank, J. A.; Breitbach, Z. S.; Payagala, T.; Armstrong, D. W. Evaluation of dicationic reagents for their use in detection of anions using positive ion mode ESI-MS via gas phase ion association. *J. Am. Soc. Mass Spectrom.* **2008**, *19*, 261-269.
- (128) Soukup-Hein, R. J.; Remsburg, J. W.; Breitbach, Z. S.; Sharma, P. S.; Payagala, T.; Wanigasekara, E.; Huang, J.; Armstrong, D. W. Evaluating the Use of Tricationic Reagents for the Detection of Doubly Charged Anions in the Positive Mode by ESI-MS. *Anal. Chem.* **2008**, *80*, 2612-2616.
- (129) Wanigasekara, E.; Zhang, X.; Nanayakkara, Y.; Payagala, T.; Moon, H.; Armstrong, D. W. Linear Tricationic Room-Temperature Ionic Liquids: Synthesis, Physiochemical Properties, and Electrowetting Properties. *ACS Appl. Mater. Interfaces* **2009**, *1*, 2126-2133.
- (130) Welton, T. Room-Temperature Ionic Liquids. Solvents for Synthesis and Catalysis. *Chem. Rev.* **1999**, *99*, 2071-2083.
- (131) Rogers, R. D.; Seddon, K. R.; Editors Ionic Liquids as Green Solvents: Progress and Prospects. (Proceedings of the 224th American Chemical Society Natl. Meeting held 18-22 August 2002 in Boston Massachusetts.) [In: ACS Symp. Ser., 2003; 856]. **2003**, 599.
- (132) Plechkova, N. V.; Seddon, K. R. Applications of ionic liquids in the chemical industry. *Chem. Soc. Rev.* **2008**, *37*, 123-150.
- (133) Rogers, R. D.; Seddon, K. R. Chemistry. Ionic liquids--solvents of the future? *Science* **2003**, *302*, 792-793.
- (134) Soukup-Hein, R. J.; Remsburg, J. W.; Dasgupta, P. K.; Armstrong, D. W. A General, Positive Ion Mode ESI-MS Approach for the Analysis of Singly Charged Inorganic and Organic Anions Using a Dicationic Reagent. *Anal. Chem.* **2007**, *79*, 7346-7352.
- (135) Soukup-Hein, R. J.; Remsburg, J. W.; Breitbach, Z. S.; Sharma, P. S.; Payagala, T.; Wanigasekara, E.; Huang, J.; Armstrong, D. W. Evaluating the Use of Tricationic Reagents for the Detection of Doubly Charged Anions in the Positive Mode by ESI-MS. *Anal. Chem.* **2008**, *80*, 2612-2616.
- (136) Anderson, J. L.; Armstrong, D. W.; Wei, G. Ionic Liquids in Analytical Chemistry. *Anal. Chem.* **2006**, *78*, 2893-2902.
- (137) Ding, J.; Armstrong, D. W. Chiral ionic liquids. Synthesis and applications. *Chirality* **2005**, *17*, 281-292.
- (138) Anderson, J. L.; Ding, R.; Ellern, A.; Armstrong, D. W. Structure and Properties of High Stability Geminal Dicationic Ionic Liquids. *J. Am. Chem. Soc.* **2005**, *127*, 593-604.
- (139) Payagala, T.; Zhang, Y.; Wanigasekara, E.; Huang, K.; Breitbach, Z. S.; Sharma, P. S.; Sidisky, L. M.; Armstrong, D. W. Trigonal tricationic ionic liquids: a generation of gas chromatographic stationary phases. *Anal Chem* **2009**, *81*, 160-173.

- (140) Vaher, M.; Koel, M.; Kaljurand, M. Application of 1-alkyl-3-methylimidazolium-based ionic liquids in non-aqueous capillary electrophoresis. *J. Chromatogr. , A* **2002**, *979*, 27-32.
- (141) Nanayakkara, Y. S.; Moon, H.; Payagala, T.; Wijeratne, A. B.; Crank, J. A.; Sharma, P. S.; Armstrong, D. W. A Fundamental Study on Electrowetting by Traditional and Multifunctional Ionic Liquids: Possible Use in Electrowetting on Dielectric-Based Microfluidic Applications. *Anal. Chem.* **2008**, *80*, 7690-7698.
- (142) Millefiorini, S.; Tkaczyk, A. H.; Sedev, R.; Efthimiadis, J.; Ralston, J. Electrowetting of Ionic Liquids. *J. Am. Chem. Soc.* **2006**, *128*, 3098-3101.
- (143) Law, G.; Watson, P. R. Surface Tension Measurements of N-Alkylimidazolium Ionic Liquids. *Langmuir* **2001**, *17*, 6138-6141.
- (144) Payagala, T.; Huang, J.; Breitbach, Z. S.; Sharma, P. S.; Armstrong, D. W. Unsymmetrical Dicationic Ionic Liquids: Manipulation of Physicochemical Properties Using Specific Structural Architectures. *Chem. Mater.* **2007**, *19*, 5848-5850.
- (145) Sharma, P. S.; Payagala, T.; Wanigasekara, E.; Wijeratne, A. B.; Huang, J.; Armstrong, D. W. Trigonal Tricationic Ionic Liquids: Molecular Engineering of Trications to Control Physicochemical Properties. *Chem. Mater.* **2008**, *20*, 4182-4184.
- (146) Wasserscheid, p.; Welton, T. Ionic liquids in synthesis. **2003**.
- (147) Bonhote, P.; Dias, A.; Papageorgiou, N.; Kalyanasundaram, K.; Graetzel, M. Hydrophobic, Highly Conductive Ambient-Temperature Molten Salts. *Inorg. Chem.* **1996**, *35*, 1168-1178.
- (148) Moon, H.; Wheeler, A. R.; Garrell, R. L.; Loo, J. A.; Kim, C. An integrated digital microfluidic chip for multiplexed proteomic sample preparation and analysis by MALDI-MS. *Lab Chip* **2006**, *6*, 1213-1219.
- (149) Pollack, M. G.; Fair, R. B.; Shenderov, A. D. Electrowetting-based actuation of liquid droplets for microfluidic applications. *Appl. Phys. Lett.* **2000**, *77*, 1725-1726.
- (150) Wheeler, A. R.; Moon, H.; Kim, C.; Loo, J. A.; Garrell, R. L. Electrowetting-Based Microfluidics for Analysis of Peptides and Proteins by Matrix-Assisted Laser Desorption/Ionization Mass Spectrometry. *Anal. Chem.* **2004**, *76*, 4833-4838.
- (151) Berge, B.; Peseux, J. Variable focal lens controlled by an external voltage: an application of electrowetting. *Eur. Phys. J. E* **2000**, *3*, 159-163.
- (152) Hayes, R. A.; Feenstra, B. J. Video-speed electronic paper based on electrowetting. *Nature (London, U. K.)* **2003**, *425*, 383-385.
- (153) Dubois, P.; Marchand, G.; Fouillet, Y.; Berthier, J.; Douki, T.; Hassine, F.; Gmouh, S.; Vaultier, M. Ionic Liquid Droplet as e-Microreactor. *Anal. Chem.* **2006**, *78*, 4909-4917.

- (154) Chatterjee, D.; Hetayothin, B.; Wheeler, A. R.; King, D. J.; Garrell, R. L. Droplet-based microfluidics with nonaqueous solvents and solutions. *Lab Chip* **2006**, *6*, 199-206.
- (155) Wijethunga, P. A. L.; Nanayakkara, Y. S.; Kunchala, P.; Armstrong, D. W.; Moon, H. On-chip drop-to-drop liquid microextraction coupled with real-time concentration monitoring technique. *Anal. Chem.* **2011**, *83*, 1658-1664.
- (156) Catalan, J.; Claramunt, R. M.; Elguero, J.; Laynez, J.; Menendez, M.; Anvia, F.; Quian, J. H.; Taagepera, M.; Taft, R. W. Basicity and acidity of azoles: the annelation effect in azoles. *J. Am. Chem. Soc.* **1988**, *110*, 4105-4111.
- (157) Abramowitz, R.; Yalkowsky, S. H. Melting point, boiling point, and symmetry. *Pharm Res* **1990**, *7*, 942-947.
- (158) Zhou, Z.; Matsumoto, H.; Tatsumi, K. Structure and properties of new ionic liquids based on alkyl- and alkenyltrifluoroborates. *ChemPhysChem* **2005**, *6*, 1324-1332.
- (159) Zhou, Z.; Matsumoto, H.; Tatsumi, K. Structure and properties of new ionic liquids based on alkyl- and alkenyltrifluoroborates. *ChemPhysChem* **2005**, *6*, 1324-1332.
- (160) Sheldon, R. Catalytic reactions in ionic liquids. *Chem Commun* **2001**, 2399-2407.
- (161) Visser, A. E.; Swatloski, R. P.; Rogers, R. D. pH-Dependent partitioning in room temperature ionic liquids. *Green Chem.* **2000**, *2*, 1-4.
- (162) Bradaric, C. J.; Downard, A.; Kennedy, C.; Robertson, A. J.; Zhou, Y. Industrial preparation of phosphonium ionic liquids. *Green Chem.* **2003**, *5*, 143-152.
- (163) Han, X.; Armstrong, D. W. Using Geminal Dicationic Ionic Liquids as Solvents for High-Temperature Organic Reactions. *Org. Lett.* **2005**, *7*, 4205-4208.
- (164) Gordon, C. M. New developments in catalysis using ionic liquids. *Appl. Catal., A* **2001**, *222*, 101-117.
- (165) Abramowitz, R.; Yalkowsky, S. H. Melting point, boiling point, and symmetry. *Pharm. Res.* **1990**, *7*, 942-947.
- (166) Zhu, Y.; Rosen, M. J.; Morrall, S. W. Chemical structure/property relationships in surfactants. 17. N-Substituted-N-acyl glycinate in pure and synthetic hard river water. *J. Surfactants Deterg.* **1998**, *1*, 1-9.
- (167) Armstrong, D. W.; Tang, Y.; Zukowski, J. Resolution of enantiomeric hydrocarbon biomarkers of geochemical importance. *Anal. Chem.* **1991**, *63*, 2858-2861.
- (168) Huang, K.; Armstrong, D. W. GC-MS analysis of crocetane, phytane and some of their stereoisomers using cyclodextrin-based stationary phases. *Org. Geochem.* **2009**, *40*, 283-286.

- (169) Huang, K.; Breitbach, Z. S.; Armstrong, D. W. Enantiomeric impurities in chiral synthons, catalysts, and auxiliaries: Part 3. *Tetrahedron: Asymmetry* **2006**, *17*, 2821-2832.
- (170) Armstrong, D. W.; DeMond, W. Cyclodextrin bonded phases for the liquid chromatographic separation of optical, geometrical, and structural isomers. *J. Chromatogr. Sci.* **1984**, *22*, 411-415.
- (171) Gratz, S. R.; Stalcup, A. M. Enantiomeric separations of terbutaline by CE with a sulfated beta-cyclodextrin chiral selector: a quantitative binding study. *Anal Chem* **1998**, *70*, 5166-5171.
- (172) Armstrong, D. W.; Li, W. Y.; Pitha, J. Reversing enantioselectivity in capillary gas chromatography with polar and nonpolar cyclodextrin derivative phases. *Anal Chem* **1990**, *62*, 214-217.
- (173) Bao, Y.; Yue, D.; Della Ca, N.; Larock, R. C.; Armstrong, D. W. Enantiomeric separation of isochromene derivatives by cyclodextrin-modified micellar capillary electrophoresis. *J. Liq. Chromatogr. Relat. Technol.* **2008**, *31*, 2035-2052.
- (174) Jiang, C.; Armstrong, D. W.; Peter, A.; Fulop, F. Enantiomeric separation of a series of β -lactams using capillary zone electrophoresis. *J. Liq. Chromatogr. Relat. Technol.* **2007**, *30*, 1709-1721.
- (175) Schurig, V.; Nowotny, H. P.; Schmalzing, D. Gas chromatographic enantiomer separation of unfunctionalized cycloalkanes on permethylated β -cyclodextrin. *Angew. Chem.* **1989**, *101*, 785-786.
- (176) Koenig, W. A.; Lutz, S.; Wenz, G.; Von der Bey, E. Cyclodextrins as chiral stationary phases in capillary gas chromatography. Part II: heptakis(3-O-acetyl-2,6-di-O-pentyl)- β -cyclodextrin. *HRC CC, J. High Resolut. Chromatogr. Chromatogr. Commun.* **1988**, *11*, 506-509.
- (177) Schurig, V.; Nowotny, H. P. Gas-chromatographic separation of enantiomers on stationary phases without metal complexes. 2. Gas-chromatographic separation of enantiomers on cyclodextrin derivatives. *Angew. Chem.* **1990**, *102*, 969-986.
- (178) Schurig, V.; Nowotny, H. P. Separation of enantiomers on diluted permethylated β -cyclodextrin by high-resolution gas chromatography. *J. Chromatogr.* **1988**, *441*, 155-163.
- (179) Dietrich, A.; Maas, B.; Mosandl, A. Diluted modified cyclodextrins as chiral stationary phases-influence of the polysiloxane solvent: heptakis(2,3-di-O-acetyl-6-O-tert-butyl-dimethylsilyl)- β -cyclodextrin. *J. High Resolut. Chromatogr.* **1995**, *18*, 152-156.
- (180) Jing, P.; Fu, R. N.; Dai, R. J.; Ge, J. L.; Gu, J. L.; Huang, Z.; Chen, Y. Consequence of diluting modified β -cyclodextrins in a side-chain crown ether polysiloxane and in a side-chain liquid-crystalline polysiloxane-containing crown ether as stationary phases in capillary gas chromatography. *Chromatographia* **1996**, *43*, 546-550.

- (181) Alexander, G.; Juvancz, Z.; Szejtli, J. Cyclodextrins and their derivatives as stationary phases in GC capillary columns. *HRC CC, J. High Resolut. Chromatogr. Chromatogr. Commun.* **1988**, *11*, 110-113.
- (182) Grisales, J. O.; Lebed, P. J.; Keunchkarian, S.; Gonzalez, F. R.; Castells, C. B. Permethylated β -cyclodextrin in liquid poly(oxyethylene) as a stationary phase for capillary gas chromatography. *J. Chromatogr. , A* **2009**, *1216*, 6844-6851.
- (183) Anderson, J. L.; Ding, R.; Ellern, A.; Armstrong, D. W. Structure and Properties of High Stability Geminal Dicationic Ionic Liquids. *J. Am. Chem. Soc.* **2005**, *127*, 593-604.
- (184) Anderson, J. L.; Armstrong, D. W. High-stability ionic liquids. A new class of stationary phases for gas chromatography. *Anal. Chem.* **2003**, *75*, 4851-4858.
- (185) Huang, K.; Han, X.; Zhang, X.; Armstrong, D. W. PEG-linked geminal dicationic ionic liquids as selective, high-stability gas chromatographic stationary phases. *Anal. Bioanal. Chem.* **2007**, *389*, 2265-2275.
- (186) Payagala, T.; Zhang, Y.; Wanigasekara, E.; Huang, K.; Breitbach, Z. S.; Sharma, P. S.; Sidisky, L. M.; Armstrong, D. W. Trigonal tricationic ionic liquids: A generation of gas chromatographic stationary phases. *Anal. Chem.* **2009**, *81*, 160-173.
- (187) Breitbach, Z. S.; Armstrong, D. W. Characterization of phosphonium ionic liquids through a linear solvation energy relationship and their use as GLC stationary phases. *Anal. Bioanal. Chem.* **2008**, *390*, 1605-1617.
- (188) Poole, S. K.; Poole, C. F. Experimental protocol for the assessment of solvent strength and selectivity of liquid phases used in gas chromatography. *J. Chromatogr.* **1990**, *500*, 329-348.
- (189) Berthod, A.; Carda-Broch, S. Uses of ionic liquids in chemical analysis. *Actual. Chim.* **2004**, 24-30.
- (190) Poole, C. F. Chromatographic and spectroscopic methods for the determination of solvent properties of room temperature ionic liquids. *J. Chromatogr. , A* **2004**, *1037*, 49-82.
- (191) Poole, C. F. Applications of ionic liquids in extraction, chromatography, and electrophoresis. *Adv. Chromatogr.* **2007**, *45*, 89-124.
- (192) Berthod, A.; He, L.; Armstrong, D. W. Ionic liquids as stationary phase solvents for methylated cyclodextrins in gas chromatography. *Chromatographia* **2001**, *53*, 63-68.
- (193) Tran, C. D.; De Paoli Lacerda, S. H. Determination of Binding Constants of Cyclodextrins in Room-Temperature Ionic Liquids by Near-Infrared Spectrometry. *Anal. Chem.* **2002**, *74*, 5337-5341.
- (194) He, Y.; Chen, Q.; Xu, C.; Zhang, J.; Shen, X. Interaction between Ionic Liquids and β -Cyclodextrin: A Discussion of Association Pattern. *J. Phys. Chem. B* **2009**, *113*, 231-238.

- (195) Berthod, A.; Li, W.; Armstrong, D. W. Multiple enantioselective retention mechanisms on derivatized cyclodextrin gas chromatographic chiral stationary phases. *Anal. Chem.* **1992**, *64*, 873-879.
- (196) Ding, J.; Welton, T.; Armstrong, D. W. Chiral ionic liquids as stationary phases in gas chromatography. *Anal. Chem.* **2004**, *76*, 6819-6822.
- (197) Armstrong, D. W.; Chang, L. W.; Chang, S. S. Mechanism of capillary electrophoresis enantioseparations using a combination of an achiral crown ether plus cyclodextrins. *J Chromatogr A* **1998**, *793*, 115-134.
- (198) Cai, H.; Nguyen, T. V.; Vigh, G. A Family of Single-Isomer Chiral Resolving Agents for Capillary Electrophoresis. 3. Heptakis(2,3-dimethyl-6-sulfato)- β -cyclodextrin. *Anal. Chem.* **1998**, *70*, 580-589.
- (199) Ong, T.; Tang, W.; Muderawan, W.; Ng, S.; Chan, H. S. O. Synthesis and application of single-isomer 6-mono(alkylimidazolium)- β -cyclodextrins as chiral selectors in chiral capillary electrophoresis. *Electrophoresis* **2005**, *26*, 3839-3848.
- (200) Tang, W.; Ng, S. Synthesis of cationic single-isomer cyclodextrins for the chiral separation of amino acids and anionic pharmaceuticals. *Nat. Protoc.* **2007**, *2*, 3195-3200.
- (201) Ciucanu, I.; Kerek, F. A simple and rapid method for the permethylation of carbohydrates. *Carbohydr. Res.* **1984**, *131*, 209-217.
- (202) Anonymous ChiralDex handbook, 6th edition. **2002**.
- (203) Liu, J.; Jonsson, J. A.; Jiang, G. Application of ionic liquids in analytical chemistry. *TrAC, Trends Anal. Chem.* **2005**, *24*, 20-27.

BIOGRAPHICAL INFORMATION

Xiaotong Zhang obtained his Bachelor degree in chemistry from Fudan university in shanghai china in 2004. He joined Dr Daniel W. Armstrong's group in Iowa State University in 2005 and followed him to the University of Texas at Arlington in 2006. He earned his Doctor of Philosophy in May 2011 working on research in areas such as development of chiral stationary phases and ionic liquids in analytical chemistry.